

Department of Mechanical Engineering

University of Canterbury

Te Whare Wānanga o Waitaha

Private Bag 4800

Christchurch 8020, New Zealand

Telephone: +64-3-366 7001

Facsimile: +64-3-364 2078

Website: www.mech.canterbury.ac.nz



MASTER OF ENGINEERING THESIS

MODELLING A NOVEL ORBITAL IC ENGINE TO AID FURTHER DESIGN

By Lindsay Muir BE (Hons)

31 August 2014

Requirements for the degree of

MASTER OF ENGINEERING IN MECHANICAL ENGINEERING

Approved by:

Dr Dirk Pons, Project Supervisor

COPYRIGHT
LINDSAY MUIR
24/10/2015

TABLE OF CONTENTS

1	INTRODUCTION	11
1.1	Scenario.....	11
1.2	Purpose.....	13
1.3	Scope	14
2	BACKGROUND.....	15
2.1	The Radial and Rotary engine.....	15
2.1.1	History.....	15
2.1.2	Multi-row radials.....	18
2.1.3	Diesel radials	19
2.2	General Engine Operating Principles.....	20
2.2.1	Advantages of the Engine.....	26
2.2.2	The operating principles for the 4 stroke engine (1st Prototype).....	27
2.2.3	Second Generation, 2 Stroke Prototype	28
2.3	Risk analysis	36
2.4	Research.....	37
2.4.1	IC Engines used for Power Generation.....	37
2.4.2	Fuels	38
2.4.3	IC Engine Fundamentals	39
2.4.4	Engine Development Strategies	49
2.4.5	IC Engine Modelling.....	50
2.5	Modelling	57
2.5.1	Ricardo Wavebuild.....	58
2.5.2	Model Setup.....	59
3	METHODOLOGY	62
3.1	Objectives.....	62
3.2	Modelling of Four Stroke Prototype	64
3.2.1	Manipulating WAVE for alternative configuration.....	64
3.2.2	Main Screen Showing General Model Layout.....	64
3.2.3	Constants Table.....	69
3.2.4	Engine General Panel.....	71
3.2.5	Friction and Dynamic Factors	73
3.2.6	Heat Transfer and Conduction.....	74
3.2.7	Combustion.....	75
3.2.8	Fuel Delivery.....	76
3.2.9	Valves	79
3.2.10	Tuning.....	83
3.2.11	Output calibration.....	84

3.2.12	Validation	87
3.3	Modelling of Two Stroke Prototype Stroke Engine	88
3.3.1	Combustion.....	90
3.3.2	Crankcase and Valves	91
3.3.3	Scavenging	92
3.3.4	Sensitivity and parameter Analysis	92
3.3.5	Gas Compressibility.....	93
3.3.6	Squish.....	93
3.3.7	Upstream breathing restriction investigation	94
3.3.8	Uniflow Scavenging	94
3.3.9	Ignition timing, Combustion and Fuel Analysis	95
4	RESULTS	98
4.1	4 Stroke Performance	98
4.1.1	Validation	99
4.2	2 Stroke Base Prediction	100
4.2.1	Validation	102
4.3	Investigation and optimization for performance predicting.....	103
4.3.1	Valve Sizing	104
4.3.2	Compression Ratio (CR) and Crankcase Ratio (CCR)	105
4.3.3	Figure: Fixing CCR at 2. CR changing:.....	106
4.3.4	Dwell	108
4.3.5	TDC Dwell investigation.....	109
4.3.6	Optimization of dwell.....	116
4.4	Optimizing 2 Stroke Engine	124
4.4.1	Comparing To ICE Engine	126
4.5	Performance prediction model	129
4.5.1	Validation	130
5	DISCUSSION.....	131
6	CONCLUSIONS	135
6.1	Recommendations	135
6.2	Technological Developments	136
6.3	Commercial Developments	137
6.4	System Developments.....	138
6.5	Future Work.....	138

APPENDICES

Appendix A – Project Milestones

Appendix B – 4 Stroke Property Constants Table

Appendix C – 2 Stroke Property Constants Table

Appendix D – Additional 4 Stroke Model Information

Appendix E - Additional 4 Stroke Model Information

Appendix F – Dynamometer Results of Original Prototype

Appendix G – Piston Profile and Valve Timing Tables

ANNEXES

Annex A - Risk and Reliability Engineering, Application in Engine Design

FIGURES

Figure 1 - Picture of Original Prototype	11
Figure 2 – Components that make up engine.	20
Figure 3 – Typical ICE Slider Crank Mechanism	21
Figure 4 – Lever dimensions on 2 stroke variant.	21
Figure 5 – Force and reaction path from combustion to the cam configuration for 2 stroke design	22
Figure 6 – Force Body Diagram of System	23
Figure 7 – Cam Detail of 2nd Prototype showing Maximum and Minimum Diameters	23
Figure 8 - Relative phase of each cylinder as it rotates.	27
Figure 9 – Angles of linkages on engine rotation for the 2 stroke prototype	32
Figure 10 – Exhaust, transfer and intake geometries on 2 stroke cylinder head.	33
Figure 12 – Comparison between the Otto cycle and Wiebe curve considering fuel combustion as the crankshaft rotates.	55
Figure 13 – Simplified Model Setup Procedure, (Dan Cordon, Charles Dean, Judith Steciak and Steven Beyerlein, 2007)	60
Figure 14 – Original Prototype Ricardo Model Overview (GUI)	65
Figure 15 – Duct Panel Geometry Panel	66
Figure 16 – Duct Panel Initial Conditions	67
Figure 17 – Complex Junction Panel	68
Figure 18 – Complex Y Junction Geometry Panel showing intake manifold for prototype engine	68
Figure 19 – Constants table	70
Figure 20 – General Engine Property Panel	72
Figure 21 – Piston Trajectory Profile (Found in 'Imposed Piston Motion' Tab shown on previous Figure.) This is the default design profile	72
Figure 22 – Combustion Curve relative to crank angle	75
Figure 23 – Carburetor sub screen	77
Figure 24 – Butterfly valve simulating throttle	77
Figure 25 – Fuel injector properties	78
Figure 26 – Injector Sub-screen properties	78
Figure 27 – Cylinder head panel	79
Figure 28 – Intake Valve Panel	80
Figure 29 – Swirl coefficient profile editor for intake valve	81
Figure 30 – Inlet valve lift profile in relation to phase	81
Figure 31 – Flow coefficient profile for inlet valve	82
Figure 32 – Exhaust valve lift profile in relation to phase	82
Figure 33 – Flow coefficient profile for Exhaust valve	83
Figure 34 – Results page, showing various properties that can be extracted from a simulation	83
Figure 35 – GUI Panel for 2 Stroke Engine	88
Figure 36 – General Engine Panel for 2 stroke prototype	89
Figure 37 – Combustion (Wiebe) Curve relative to crank position	90

Figure 38 – Crankcase Panel	91
Figure 39 – Tested Combustion Models	96
Figure 40 – Output Comparison for Fuel Types.	96
Figure 40 – Combustion (Wiebe) Curve relative to crank position used for investigation	97
Figure 41 – 1 st Prototype (2 cylinder, 250cc) Torque Curves	98
Figure 42 – 1st Prototype (2 cylinder, 250cc) Power Curves	99
Figure 43 - 2 nd Prototype Prediction, Basic Engine Parameters	100
Figure 44 –2nd Prototype (2 cylinder, 28L) Torque Curve Prediction	101
Figure 45 –2 nd Prototype (2 cylinder, 28L) Power Curve Prediction	102
Figure 46 – 2nd Prototype Valve Sizing Investigation, displayed as a percentage of the original design values	104
Figure 47 – Comparison of Torque Curve with varying compression ratio	105
Figure 48 – Comparison of Torque Curve with varying crank case ratio using a CR of 10.	106
Figure 49 – Comparison of Torque Curve with varying crank case ratio using a CR of 14	107
Figure 50 – Comparison of Torque Curve with varying crank case ratio using a CR of 18	107
Figure 50 – Piston Stroke Trajectories relative to engine rotation, varying dwell on compression	112
Figure 52 – Piston Stroke Trajectories relative to engine rotation, varying dwell on expansion	113
Figure 53 – Piston Stroke Trajectories relative to engine rotation, varying dwell on expansion and compression	114
Figure 54 – Torque curve comparison between varying piston trajectories	115
Figure 55 – Piston Stroke Trajectories relative to engine rotation, optimizing dwell at TDC and BDC	117
Figure 56 – Torque curve comparison between varying levels of TDC and BDC dwell piston trajectories	119
Figure 57 – Piston Stroke Trajectories relative to engine rotation, optimizing dwell at BDC	120
Figure 58 –Torque curve comparison between varying levels of BDC dwell piston trajectories	121
Figure 59 – Piston Stroke Trajectories relative to engine rotation, optimizing dwell at TDC	122
Figure 60 –Torque curve comparison between varying levels of TDC dwell piston trajectories	123
Figure 62 – Results of parameter investigation	125
Figure 63 – Engine Panel for Equivalent IC Pushrod Engine	126
Figure 64 – Power Output (hp) for Equivalent Pushrod engine	127
Figure 65 – Torque (Nm) Output for Equivalent Pushrod engine	127
Figure 66 – Comparing the orbital engine to a geared engine of equal displacement, valve configuration	128
Figure 67 – Output screen for Excel performance prediction calculator based on findings of modeling outputs	129

TABLES

Table 1 - Relative phase of each cylinder as it rotates.	28
Table 2 - Angles of linkages on engine rotation	32
Table 3 - Relative phase of each cylinder as it rotates.	35
Table 4 – Combustion Constants for Fuel Types.	95
Table 5 – Engine rotation degrees relative to valve positioning	111
Table 6 - Valve Action Relative to Engine rotation for dwell varied on compression piston trajectories	112
Table 7 - Valve Action Relative to Engine rotation for dwell varied on expansion piston trajectories	113
Table 8 –Valve Action Relative to Engine rotation for symmetric piston trajectories	114
Table 9 - Valve Action Relative to Engine rotation for optimized dwell at TDC and BDC piston trajectories	117
Table 10 - Valve Action Relative to Engine rotation for optimized dwell at BDC piston trajectories	120
Table 11 - Valve Action Relative to Engine rotation for optimized dwell at TDC piston trajectories	122

ACKNOWLEDGEMENTS

Dr Dirk Pons was my supervisor and has provided guidance in choosing an appropriate topic, narrow the scope of my research and given direction to the project.

Bill White, for his astonishing knowledge of the internal combustion engine and his contribution and assistance to data collection.

Graham Harris, for his ongoing support, industry contacts and resources. Also thanks for his willingness to continue the research into this engine's development.

Also a big thanks to all in their persistence in getting me to submit this thesis.

ABSTRACT

This project was aimed at developing an orbital internal combustion engine (ICE) technology that is able to combust a wide range of fuels that can be converted into useable energy that currently are not being utilized. The key difference that sets this engine apart from all other internal combustion engine's is that the combustion chambers themselves rotate with the output shaft around a fixed cam.

Similar orbital engine's were used earlier in the 20th century predominantly in aircrafts. These engine's faded out of production in the 1950's due to high maintenance demands due to worn cams and lubrication issues. With the today's technologic improvements, the shortfalls of the engine can now be mitigated with advances in material science lubricants and manufacturing. These engine's offer comparatively high outputs and never before have they been modeled to explore their true potential.

The concept engine being investigated operates at a very slow speed and has the advantage of being able to alter the piston trajectory by altering the cam geometry. This level of customization is impossible in traditional crank slider configurations. The slower rpm allows the combustion of very low grade fuels that are currently not being utilized commercially as an energy source while producing good output when compared to current internal combustion technologies.

Conventional engine simulation software was used to explore the performance potential for this engine configuration. An initial simulation model was verified against an existing prototype and a second model was created to aid in a second generation engine that is currently being developed. These models were used to explore the engine's capability and optimal configuration.

The results of a multitude of simulations were used to create a calculator for industry that uses Microsoft excel to access and interpolate from the data to predict performance for possible variants and to aid in future prototype designs without the need for the software package.

The primary focus of the research was to investigate how engine performance was affected by manipulating the piston trajectory, velocity and dwell time near TDC and BDC by adjusting the cam profile. This has proven to have very large implications concerning the engine's output.

It was discovered that by prolonging the time the piston spent at the extremities of its stroke (relative to crank rotation, or in this case, engine rotation) greatly improved combustion and engine performance. Prolonging the time the piston spends near bottom dead centre (BDC) allowed more time for air and fuel to enter the combustion chamber. With the addition of a highly pressurized crankcase, this proved to be highly successful in improving performance at higher RPM.

Prolonging the time the piston spends near top dead centre (TDC) after ignition leads to much higher pressure being developed during the power stroke, which is advantageous for volumetric efficiency and combusting slower burning fuels. Increasing the dwell time at TDC had the most benefit to performance predominantly at lower RPM. These tuning capabilities make the engine very versatile and highly desirable.

The results of tuning the piston trajectories using Ricardo Wave software have led to a potential 60% increase in peak torque on the engine as well as raising the torque delivery over the entire RPM spectrum. This analysis also provided critical information to aid in the development of the 2nd generation engine in respect to breathing and the forces acting on each of the engine components.

This research into the influence of dwell and how it can be manipulated to improve the efficiency of combustion is likely to have influences in other ICE applications and development and help push the envelope for better efficiencies and the use of alternative fuels.

NOMENCLATURE

Expression	Explanation
BDC	Bottom dead centre, when a piston is at the lowest point in its trajectory, when the volume of the combustion chamber is the greatest.
TDC	Top dead centre, when a piston is at the lowest point in its trajectory, when the volume of the combustion chamber is the greatest.
CAD	Computational Assisted Design.
CFD ANSYS and FEM	Mesh based simulation packages.
CR	Compression Ratio, the volume of the combustion chamber when the piston is at Top dead centre over the volume of the combustion chamber when the piston is at bottom dead centre.
CCR	Crankcase volume to combustion chamber volume ratio, typically between 1:1.1 and 1:1.5.
ICE or IC	Internal Combustion Engine
Reed valve	A one way valve used to let air and fuel mixture into the crankcase. The reed valve used is shown in Annex D
Transfer ports	Connection between the crank case and the combustion chamber, where the opening and closing is controlled by the piston moving in front the outlet of the transfer.
Up	Defined as piston move toward cylinder head and down as it moves away.
WAVE / RICARDO – 1D	Simulation software used to model an engine.
WOT	Wide open throttle position.
2 stroke	Referring to the 2nd prototype that includes a crankcase and transfer port rather than an inlet valve. Where the power and compression are carried simultaneously on the same stroke as well as intake and exhaust on the opposing stroke.
4 stroke	Referring to engine that consists of power exhaust intake and compression in a single cycle. A cylinder with an inlet and exhaust valve per cylinder.
Prototype	Referring to as the subject engine, either the 2 or 4 stroke.

1 INTRODUCTION

1.1 SCENARIO

The first working prototype of the engine has already been built and tested by WL White, a New Zealand firm based in Christchurch, specializing in motor development. The 250cc displacement 4 stroke engine produced 62Nm of torque at 390rpm while running on very low quality methane without the need for gearing. A second generation, 2 stroke prototype with a much larger displacement and is currently under development using the results gained from this research.

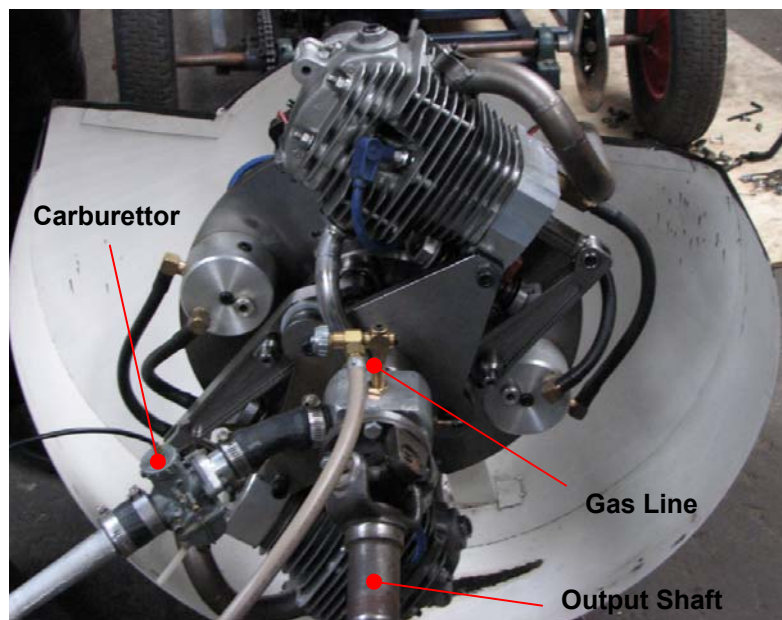


Figure 1 - Picture of Original Prototype

Essentially, the technology is a novel internal combustion engine that can be described as orbital as the entire engine rotates around a fixed cam. It is able to run on very low grade, waste product fuels that are not currently being utilized as an energy source because of its slower piston velocity and combustion frequency (compared to other IC engines).

This engine has almost unlimited potential in a multitude of applications, especially in the coming few decades where the search for alternative fuels is becoming increasingly important.

As well as advantages in its versatility of fuel options, this configuration allows a high level of customization in dwell parameters which are not available in traditional slider crank IC engines. It also offers a very high torsional output compared to other IC engines of similar displacement.

Hopeful areas of applications include:

- Energy generation – Running generators in remote location running on waste fuels. An example would be providing power to a coal mine running on the waste methane that is currently being vented straight into the atmosphere.
- Marine applications: The large inertial energy that this engine carries while running could be utilized for gyroscopic stabilization in large ships as well as propulsion.
- Anywhere there is a demand for an exceptionally high torsional output and there is a gaseous waste product available, this technology will be suited

This research will demonstrate that this engine configuration shows definite promise and warrants further research.

1.2 PURPOSE

Currently, IC engines are modified to be fit for purpose, predominantly used in the automotive industry. Pushing for higher efficiencies has led to the utilization of software to avoid costly prototype manufacturing processes.

The dynamics and combustion characteristics of the engine were not previously fully understood and by adding intellectual input from an in depth analysis, considerable value was added to the engine and will help it become a success. This analysis allowed the computer simulation to predict the performance of future prototypes and help configure them to perform the best of their ability.

Since this engine type is one of a kind, a thorough investigation into its capabilities and limits was required. Because producing multiple prototypes is an extremely expensive process, 1D modeling computer simulation software was used to explore a family of variants for this type of engine configuration. The results of this will provide an invaluable design aid.

The development of a computer simulation model for this engine configuration will allow exploration into the limits and possible spectrum of variants for this technology. This method is much faster as well as a cheaper way to explore the engine's capabilities. Other benefits that are expected from this project are insights into the engine's complex dynamics and combustion characteristics that differ greatly from a conventional IC Engine. The use of the software also allows a more in depth investigation into the exploration of alternative fuels and therefore of applications to a variety of power generation/propulsion systems. It will also permit the exploration of key geometries such as the internal linkage geometry so that they can be optimized for other performance outcomes that would otherwise be unobtainable by conventional mechanisms.

1.3 SCOPE

This research will use 1D software to model an existing prototype engine. Once this is verified against the 1st prototypes dynamometer torque vs rpm data, a 2nd model will be created to assist in the development of the 2nd generation engine. A design for the 2nd prototype has largely been finalized. The second prototype will be developed with a two stroke configuration with the addition of a crankcase, a larger displacement with the aim for a higher specific output and eliminate the need for additional valve /cam mechanisms on the cylinder heads. Both the original prototype and the design of the 2 stroke variant had their geometries modeled using 3D CAD software, Solidworks (Version 2010). The 1D software simulation models of both 4 stroke and 2 stroke models will be configured to test a range of parameters to explore the possibilities and limitations of this concept. The results of the simulations will be used to construct a excel calculator that can estimate outputs for a family a variants for the engine for future developments without the need for time consuming simulations or access to Ricardo.

Rather than tuning the 1st and 2nd prototype engine's by adjusting parameters like exhaust systems, breathing etc, the main goal will be to explore the primary capabilities and advantages that this engine has over its other IC counterparts. Specifically what will be looked at is how changing the piston trajectory influences performance output. The knowledge gained from this investigation will aid in the tuning process and future development of this engine.

2 BACKGROUND

2.1 THE RADIAL AND ROTARY ENGINE

The radial engine is a reciprocating type internal combustion engine configuration in which the cylinders "radiate" outward from a central crankcase like the spokes of a wheel. It resembles a stylized star when viewed from the front, and is called a "star engine" The radial configuration was very commonly used for aircraft engines before turbine engines became predominant.

The radial engine normally uses fewer cams compared to other types. Most radial engines use overhead poppet valves driven by pushrods and lifters on a cam plate which is concentric with the crankshaft.

2.1.1 HISTORY

In 1901, C. M. Manly constructed the first water-cooled five-cylinder radial engine converted from one of Stephen Balzer's rotary engines, producing 52 hp (39 kW) at 950 rpm.

In 1903–1904 Jacob Ellehammer used his experience constructing motorcycles to build the world's first air-cooled radial engine, a three-cylinder engine which he used as the basis for a more powerful five-cylinder model in 1907. This was installed in a triplane.

From 1909 to 1919 the radial engine was overshadowed by its close relative, the rotary engine— which differed from the so-called "stationary" radial in that the crankcase and cylinders revolved with the propeller. Mechanically it was identical in concept to the later radial except that the propeller was bolted to the engine, and the crankshaft to the airframe. The radial had an advantage by generating its own cooling airflow, which was a problem for the rotary engine.

By the early 1920s, however, the inherent limitations of this type of engine had rendered it obsolete for aircraft use, with the power output increasingly going into

overcoming the air-resistance of the spinning engine itself. The rotating mass of the engine also caused significant stability and control problems.

In 1925, the American rival firm to Wright's radial engine production efforts, Pratt & Whitney, was founded. The P & W firm's initial offering, the Pratt & Whitney R-1340 Wasp, test run later that year, began the evolution of the many models of Pratt & Whitney radial engines that were to appear during the second quarter of the 20th century, among them the 14-cylinder, twin-row Pratt & Whitney R-1830 Twin Wasp, the most-produced aviation engine of any single design, with a total production quantity of nearly 175,000 engines.

Pratt & Whitney Canada put these orbital engines into DC 1, DC 2s DC 3 and DC 5 aircrafts.

Advantages

- Weight: Liquid-cooled inline engines often weigh more than equivalent air-cooled radial engines.
- Damage tolerance: Liquid cooling systems are generally more vulnerable to battle damage. Minor shrapnel damage easily results in a loss of coolant and consequent engine seizure, while an air-cooled radial might be largely unaffected by small damage.
- Reliability: The shorter crankshaft also produces less vibration and hence higher reliability through reduced wear and fatigue.
- Smooth running: It is typically easier to achieve smooth running with a radial engine.

Disadvantages

- **Cooling:** While a single bank radial permits all cylinders to be cooled equally, the same is not true for multi-row engines where the rear cylinders can be affected by the heat coming off the front row, and air flow being masked.
- **Drag:** Having all the cylinders exposed to the airflow increases drag considerably, adding turbulence that can destroy the laminar airflow if used on an aircraft.
- **Power:** Because each cylinder on a radial engine has its own head, it is impractical to use a multivalve valvetrain on a radial engine. Therefore, almost all radial engines use a two valve pushrod-type valvetrain which may result in less power for a given displacement than multi-valve inline engines.
- **Size:** Radial engines are typically very bulky and when installed on an aircraft, can cause visibility issues.
- **Installation:** The designer can be limited in engine placement, having to ensure adequate cooling air.

The answer to some of the drag issues was the addition of specially designed cowlings with baffles to force the air over the cylinders. While inline liquid-cooled engines continued to be common in new designs until late in World War II, radial engines dominated afterwards until overtaken by jet engines, with the late-war Hawker Sea Fury and Grumman Bearcat, two of the fastest production piston-engined aircraft ever built, using radial engines. Factors influencing the choice of radial over inline were reliability and simplicity in maintenance.

2.1.2 MULTI-ROW RADIALS

Originally radial engines had one row of cylinders, but as engine sizes increased it became necessary to add extra rows. The first known radial-configuration engine to ever use a twin-row design was the 14-cylinder twin-row 160 hp Gnome "Double Lambda" rotary engine of 1912. Most stationary radial engines did not exceed two rows due to cooling issues of subsequent rows but the largest displacement mass-produced aircraft radial engine, the R-4360, with cylinders in corn-cob configuration, was a 28-cylinder 4-row radial engine used in a number of large American aircrafts in the post-World War II period. The Soviet Union built a limited number of 'Zvezda' engines with 56 cylinders but aircraft engines of this size, power and complexity were made obsolete by large turboprop engines which easily exceeded them in power without the weight or complexity. Large radials continued to be built for other uses though, as 112-cylinder diesel boat engines with 16 rows of 7 cylinders each displacing 383 liters (23,931 in³) and producing 10,000 hp (7,500 kW).

A number of companies continue to build radials today. Vedeneyev produces the M-14P radial of 360–450 hp (270–340 kW) as used on Yakovlev and Sukhoi aerobatic aircraft.

2.1.3 DIESEL RADIALS

While most radial engines have been produced for gasoline, there have been diesel radial engines. Two major advantages favour diesel engines — lower fuel consumption and reduced fire risk.

In 1931, a 9-cylinder 980 cubic inch displacement diesel radial aircraft engine was developed. It had 225 horsepower (168 kW) DR-980 and in a Bellanca CH-300, with 481 gallons of fuel, set a record for staying aloft for 84 hours and 32 minutes without being refueled. This record stood for 55 years.

A French company, Clerget developed the 14D, a 14-cylinder two-stroke diesel radial engine which by 1938 produced 520 hp (390 kW) at 1910 rpm cruise power, with a power-to-weight ratio near that of contemporary gasoline engines and a specific fuel consumption of roughly 80% that for an equivalent gasoline engine. During WWII the research continued, but no mass-production occurred because of the Nazi occupation. By 1943 the engine had grown to produce over 1,000 hp (750 kW) with a turbocharger. After the war, the Clerget company was integrated in the SNECMA company and had plans for a 32-cylinder diesel engine of 4,000 hp (3,000 kW), but in 1947 the company abandoned piston engine development in favour of the emerging turbine engines.

The Nordberg Manufacturing Company of the United States developed and produced a series of large two-stroke radial diesel engines from the late 1940s for electrical production, primarily at aluminum smelters and for pumping water. They differed from most radials in that they had an even number of cylinders in a single bank (or row) and an unusual double master connecting rod. Variants were built that could be run on either diesel oil or gasoline or mixtures of both.

2.2 GENERAL ENGINE OPERATING PRINCIPLES

The operating principle of this novel internal combustion engine is that the combustion chambers themselves rotate with the output shaft. The power of the combustion causes tangential forces, driving the rotation of the engine, and provides the torque to the output shaft attached to the centre of the flywheel.

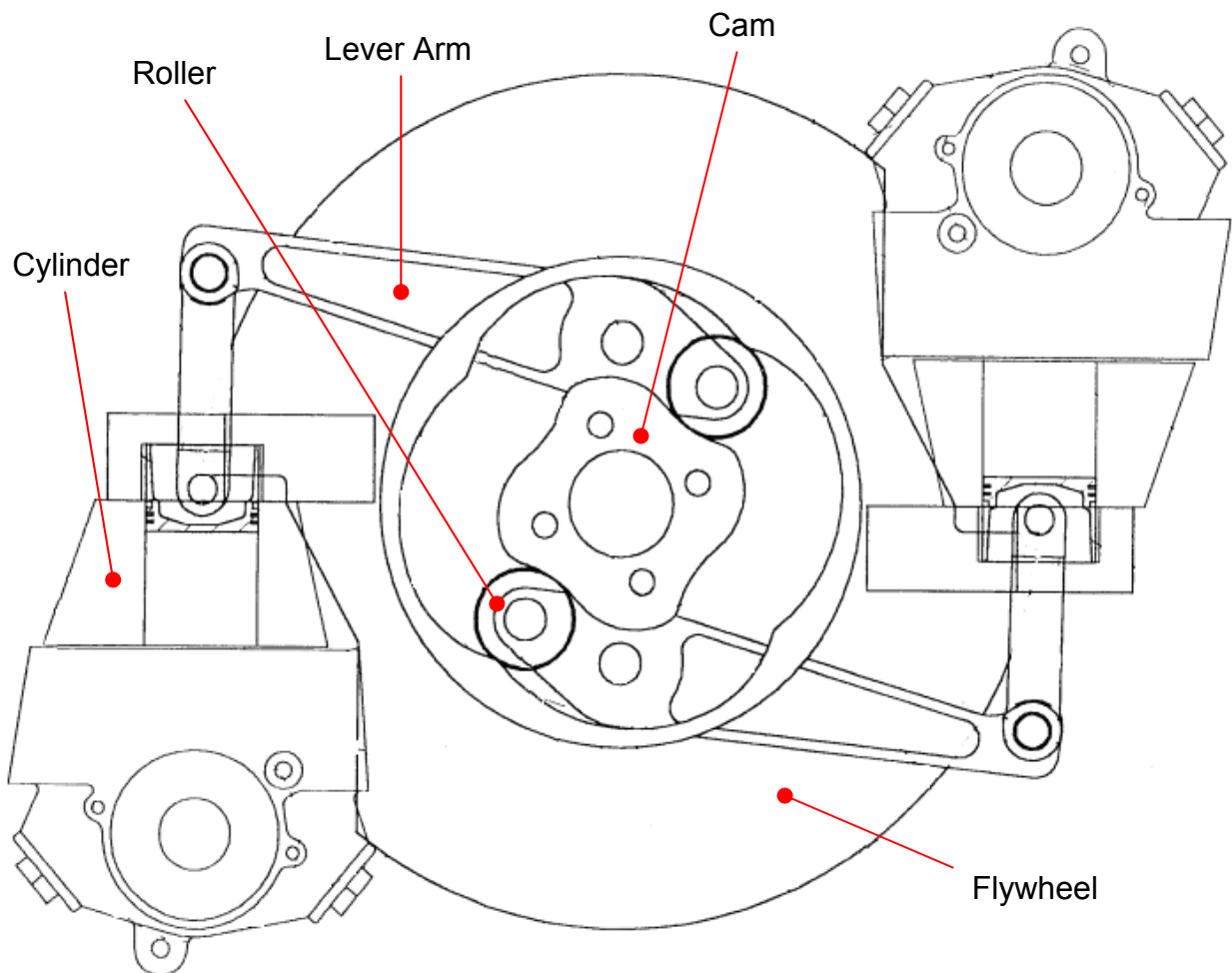


Figure 2 – Components that make up engine.

The engine consists of two main parts: The flywheel with two engine bores and the output shaft. The cam and housing fixed to a stationary frame.

The link between the cam and the roller limits the stroke of the piston and defines the cycle of the engine (Inlet, compression, power, exhaust). Since even without gearing, the output speed can be low (few hundred revolution per minute) the dynamics and the combustion processes are different compared to a conventional IC Engine.

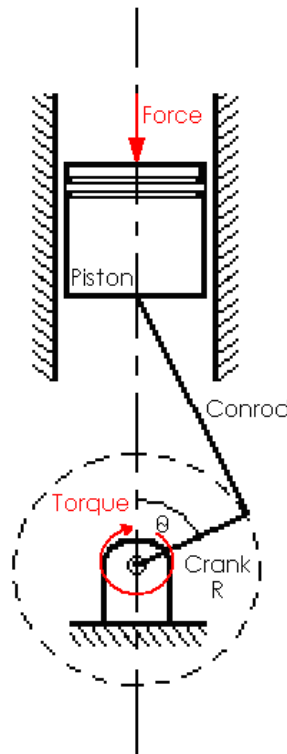


Figure 3 – Typical ICE Slider Crank Mechanism

For a slider crank configuration, the force created in the combustion chamber is transferred into rotation by use of the crank. The torque applied is a function of the Force times the length of the crank. Figure 4 shows the lever identified in Figure 2.

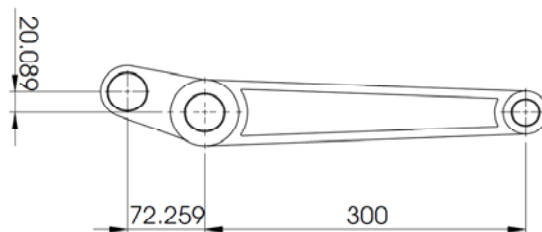


Figure 4 – Lever dimensions for 2 stroke variant under development (mm)

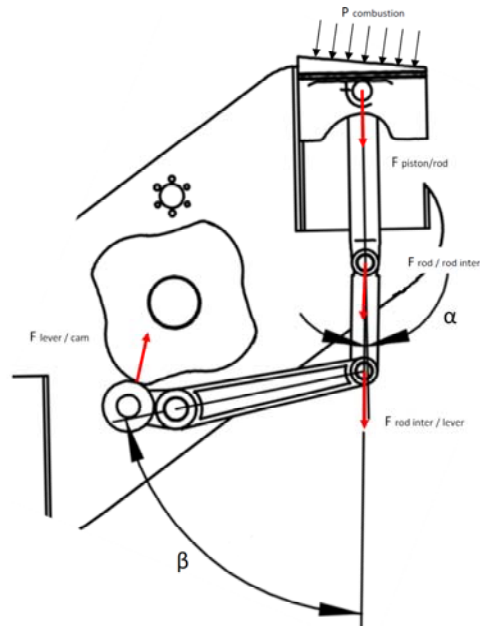


Figure 5 – Force and reaction path from combustion to the cam configuration for 2 stroke design

Figure 5 shows the forces acting on the different components at the beginning of the power stroke. The piston is on its upper most position and the combustion pressure is applying on the piston. What else can be noted from the Figure is that the conrod in the 2 stroke design has an additional linkage. This does not fluctuate more than 2 degrees during the power stroke. Therefore it is assumed that the conrod and additional linkage can be treated as a single member.

Figure 6 illustrates how this engine converts the force of combustion into torque. Unlike the slider crank configuration, the entire system rotates around the centre.

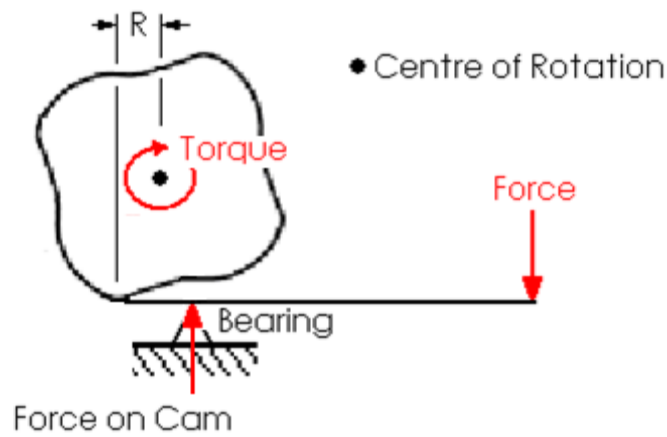


Figure 6 – Force Body Diagram of System

The difference in force between the bearing reaction and the pistons down force drives the cam upwards. The offset from the centre of rotation, where the cam makes contact with the roller is what drives the engines rotation. By pushing on the cam, the entire system rotates. The offset distance “R” is generally shorter than the crank would be for an engine of similar displacement but the loss in leverage is compensated by the increase in force generated by the lever arm.

The cam causes fluctuations in radius but during the power stroke, this radius changes by a fixed amount. As shown in Figure 7.

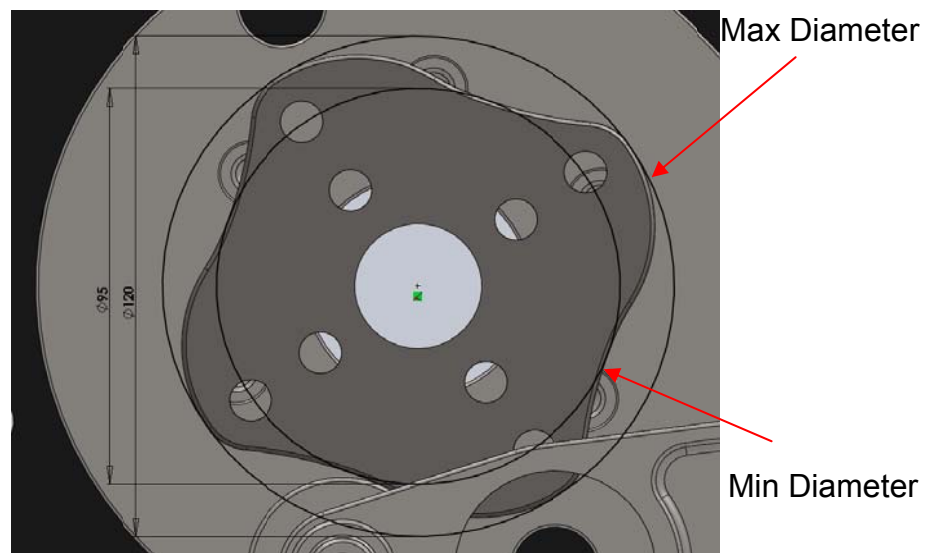


Figure 7 – Cam Detail of 2nd Prototype showing Maximum and Minimum Diameters

As can be seen by Figure 7 the cam radius varies slightly through rotation. Shown is the cam configuration design for the 2nd prototype. Using the 3D CAD model, the average offset “R” was 21.25mm. This value has a large influence on the magnitude of the torsion that the engine generates.

To demonstrate the forces on the components at the peak of combustion, the following example is used show using the 2nd prototype design values;

An approximate peak combustion pressure can be calculated using the ideal gas equation.

$$PV = nRT$$

Where

$$R = 8.314 \text{ kJ/mol K (universal gas constant)}$$

$$V = \text{Volume of combustion chamber at (or near) TDC.}$$

The volume is calculated from the bore, stroke and compression ratio of the cylinder.

$$\text{Bore} = 200 \text{ mm}$$

$$A_{\text{piston}} = \pi(\text{Bore}/2)^2 = 0.0314 \text{ m}^2$$

$$\text{Volume} = A_{\text{piston}} \times \text{stroke} = 0.0314 \text{ m}^2 \times 0.112 = 0.00352 \text{ m}^3 \text{ (at BDC)}$$

$$V = \text{Volume at BDC} / \text{Compression Ratio} = 0.00352 / 14 = 2.51 \times 10^{-4} \text{ m}^3$$

$$n = \text{number of mols}$$

For the fuel / air mixture, prior to combustion, take the molar volume to be similar to that of water vapour in ambient conditions 22 L / mol. In a volume of 3.5L (volume at BDC) equates to;

$$n = 3.5 / 22 = 0.16 \text{ mol}$$

$$T = \text{temperature in Kelvin,} = 1000 \text{ K (estimated upon combustion)}$$

Therefore, the pressure in the combustion chamber upon ignition is approximately;

$$P = nRT / V = 0.16 \times 8.314 \times 1000 / 0.000251 = 5.3 \text{ MPA} \sim 50 \text{ bar}$$

This corresponds to a normal expected peak pressure in traditional engine.

Forces applying on the piston:

$$A_{\text{piston}} = 0.0314 \text{ m}^2$$

$$\text{Force on Lever} = P \times A_{\text{piston}} = 5.3 \times 10^7 \text{ Pa} \times 0.0314 \text{ m}^2 = 157,081 \text{ N}$$

Using summary of moments around the bearing using the lever dimensions shown in Figure 6.

$$\text{Force on Cam} = (300 / 72) \times 157,081 \text{ N} = 654,504 \text{ N}$$

The offset for the 2 stroke design is currently 21 mm

$$\text{Instantaneous Torque Generated} = 652,149 \times 0.021 = \underline{13,744 \text{ Nm}}$$

This of course is an instantaneous torque, not sustained and does not take into account any friction etc. It also assumes that the bearing is fixed.

Compare this value to a traditional slider crank, where the crank length is equal to half the stroke. Using the 2nd prototype stroke current design, 112mm, (the 2 stroke current design) the torque produced for the same pressure;

$$\text{Instantaneous Torque Generated} = 157081 \times (0.112 / 2) = \underline{8,797 \text{ Nm}}$$

As can be seen, orbital engine generates 56% more instantaneous torque produced than the conventional slider crank configuration for the same combustion pressure.

Also to be considered is the reaction forces that are required by the bearing to withstand the leverage.

Summarizing the forces, the resulting force on the bearing is:

Using summary of forces in the vertical direction as shown in Figure 6;

$$\textit{Reaction on Bearing} = \textit{Force on Cam} + \textit{Force on Lever}$$

$$\textit{Reaction on Bearing} = 654,504 + 157,081 = \underline{809,230 N}$$

This is force that would be reacted on the bearing if the engine was unable to rotate, which equates to 82.5 tonnes.

Since the engine is free to rotate, the force acting on the bearing would be from any reaction forces opposing rotation. Sources of reaction forces include air friction, friction in the rollers and bearings, friction on the cam and piston wall friction. This frictional force can be measured by turning the engine when it is not operating to evaluate the reaction forces that will be acting on the bearing (excluding air friction).

As can be seen, this leverage may provide exceptional torsional output but imparts forces high enough to cause damage to the linkages, bearings, cam and cam housing.

2.2.1 ADVANTAGES OF THE ENGINE

The exhaust is attached to the rotating heads but the intake is carbureted and stationary. Fuel and air is fed to the cylinder heads centrifugally from a central shaft which encases the output shaft. Centripetal forces aid in feeding fuel and induce a small amount of forced induction.

The lever arm is what allows the engine to deliver such high output potential but is also the limiting factor due to the large forces it imparts on the moving components.

The main advantage that this engine has over others and that most of the analysis was the influence of dwell times at TDC and BDC by altering the geometry of the cam profile.

2.2.2 THE OPERATING PRINCIPLES FOR THE 4 STROKE ENGINE (1ST PROTOTYPE)

The first prototype was constructed from two Honda 125cc single cylinder motorcycle engines, mounted to a large flywheel. The two symmetrical engines operate in opposing stroke. When one is in its power stroke, the other is in its inlet phase. This eliminates negative strokes as found in traditional engines. Each cylinder completes two power strokes per revolution. A modest 5:1 compression ratio was used and this engine has been tested and torque and power data was collected on a dynamometer as seen at the end of Annex E.

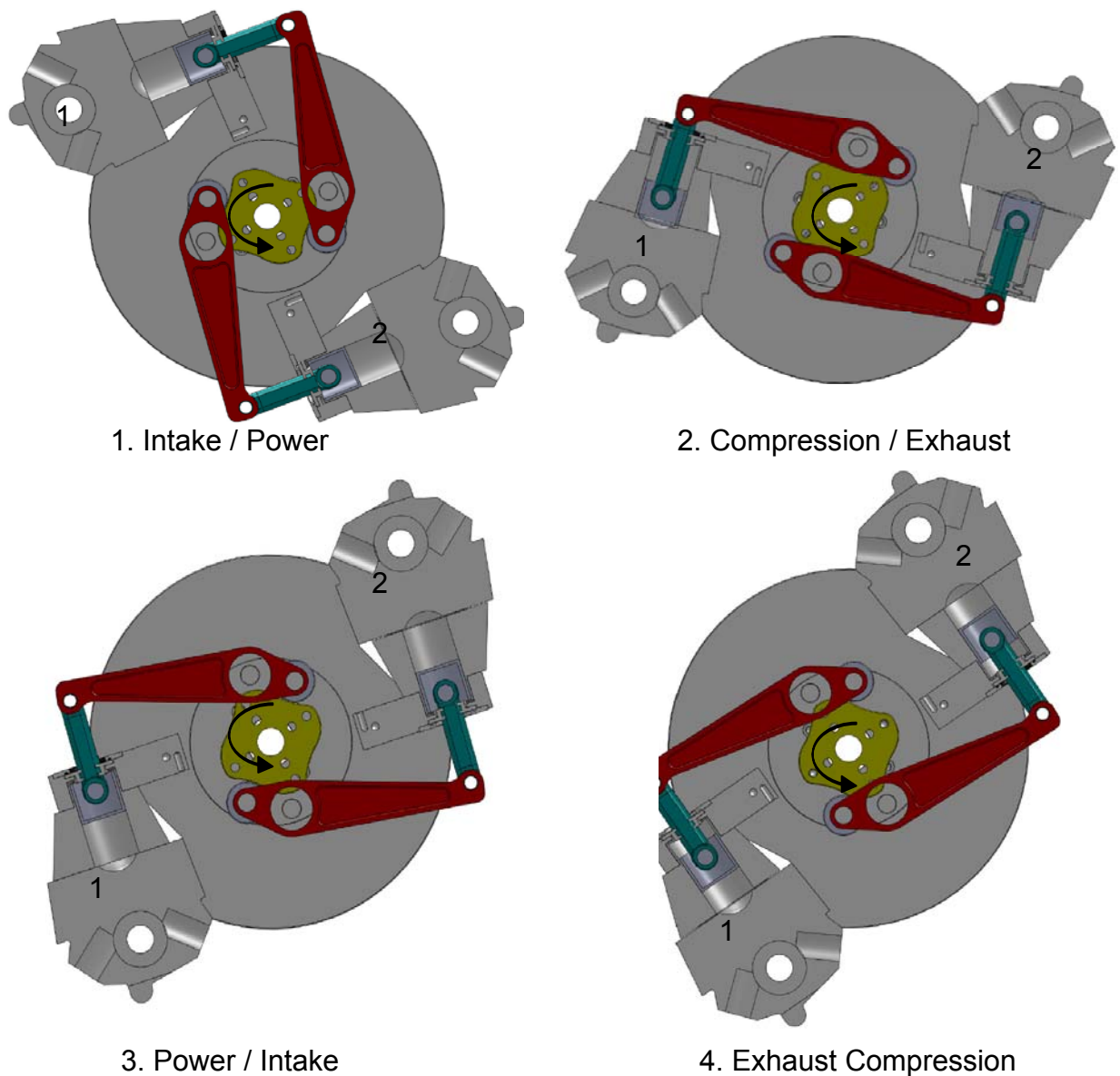


Figure 8 - Relative phase of each cylinder as it rotates.

<i>Prototype Engine Cycle</i>									
<i>Cylinder 1 Phase</i>	Power	Exhaust	Intake	Comp	Power	Exhst	Intake	Comp	Power
<i>Cylinder 2 Phase</i>	Intake	Comprssn	Power	Exhaust	Intake	Comprssn	Power	Exhaust	Intake
<i>Output Shaft Rotation (degrees) from TDC</i>	0	51	90	141	180	231	270	321	360

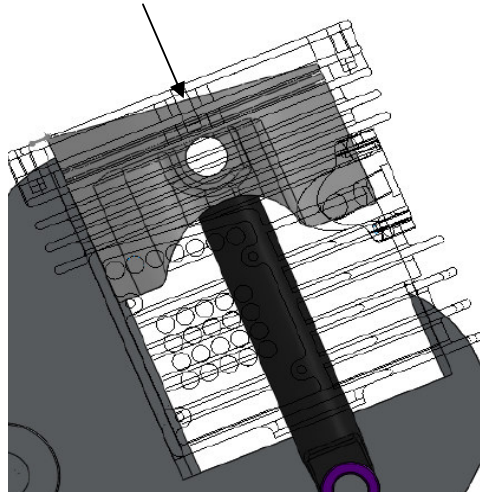
Table 1 - Relative phase of each cylinder as it rotates.

The engine's force path is defined as an action reaction through the centre of piston, ignoring pressure distributions on piston head. For the four stroke prototype with a symmetric and relatively small combustion chamber, this is a fair assumption.

2.2.3 SECOND GENERATION, 2 STROKE PROTOTYPE

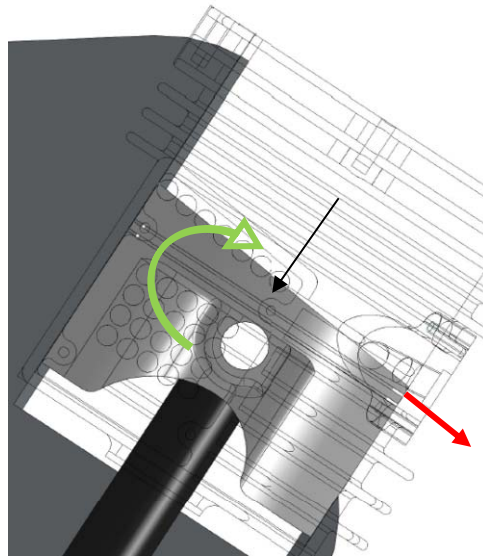
To optimize the design of this novel engine, WL White Ltd would like to develop a two stroke prototype. The reason behind developing a 2 stroke is because methane is a very clean burning hydrocarbon, reducing emissions. Also, a 2 stroke variant should deliver higher specific power. Methane is also a very abundant resource and can be stored relatively easily. Additionally, the porting arrangement for a two stroke configuration is much easier to manufacture than a four stroke. This is why two stroke engines are more common in chainsaws.

Although a two-stroke engine has less moving parts than a four-stroke engine, a two-stroke is still complex because it relies on gas dynamics. There are different phases taking place in the crankcase and in the cylinder bore at the same time. A traditional 2 stroke engine is explained below.



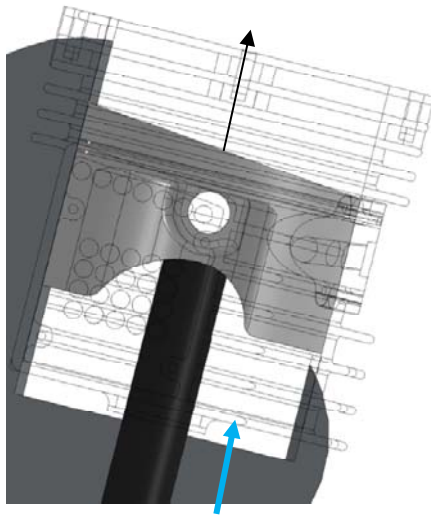
Power Stroke

- Starting with the piston at top dead centre (TDC 0 degrees) ignition has occurred and the gasses in the combustion chamber are expanding and pushing the piston down. This pressurizes the crankcase causing the reed valve to close. At about 90 degrees after TDC the exhaust port opens ending the power stroke. A pressure wave of hot expanding gasses flows down the exhaust pipe. The blow-down phase has started and will end when the transfer ports open. The pressure in the cylinder must blow-down to below the pressure in the crankcase in order for the unburned mixture gasses to flow out the transfer ports during the scavenging phase.



Transfer /Exhaust

- Now the transfer ports are uncovered at about 120 degrees after TDC. The scavenging phase has begun. Meaning that the unburned mixture gasses are flowing out of the transfers and merge with the last of the escaping exhaust gases. It is critical that the burnt gasses are scavenged from the combustion chamber, in order to make room for as much unburned gasses as possible. That is the key to making more power in a two-stroke engine. The more unburned gasses compressed into the combustion chamber, the more power the engine will produce. Now unburned mixture gasses have travelled into the exhaust pipe's header section. The gasses aren't lost because a compression pressure wave has reflected from the end of the exhaust pipe, to pack the unburned gasses back into the cylinder before the piston closes off the port. This is the unique super-charging effect of two-stroke engines. The main advantage of two-stroke engines is that they can combust more volume of fuel/air mixture than the swept volume of the engine. An example of this is a 125cc four-stroke engine combusts about 110cc of gasses but a 125cc two-stroke engine combusts about 180cc of gasses.



Compression

- Now the crankshaft has rotated past bottom dead centre (BDC 180 degrees) and the piston is on the upstroke. The compression wave reflected from the exhaust pipe is packing the unburned gasses back in through the exhaust port as the piston closes off the port the start the compression phase. In the crankcase the pressure is below atmospheric producing a vacuum and a fresh charge of unburned mixture gasses is flowing through the reed valve into the crankcase.
- The unburned mixture gasses are compresses and just before the piston reaches TDC, the ignition system discharges a spark causing the gasses to ignite and start the process all over again.

The 2nd generation engine consists of two cylinders, each with a bore diameter of 200 mm set up in a 2 stroke configuration. The stroke of the piston is 112mm. The engine has been designed with a compression ratio of 14:1 and a 2:1 crankcase ratio to encourage turbulence, swirl and maximize combustion.

Unlike the four stroke, there is less degree of symmetry in the combustion chamber as it has an angled piston head and a pentagonal squish region.

Force is still directly down the conrod and side forces can be neglected because this variant has been designed with a the high compression ratio (CR), crankcase ratio (CCR) and intake configuration that will cause a highly turbulent situation upon ignition, improving uniformity of pressure on the piston head acting along connecting members. To further ensure uniform and complete combustion, multiple (six) sparkplugs were to be installed into each combustion chamber.

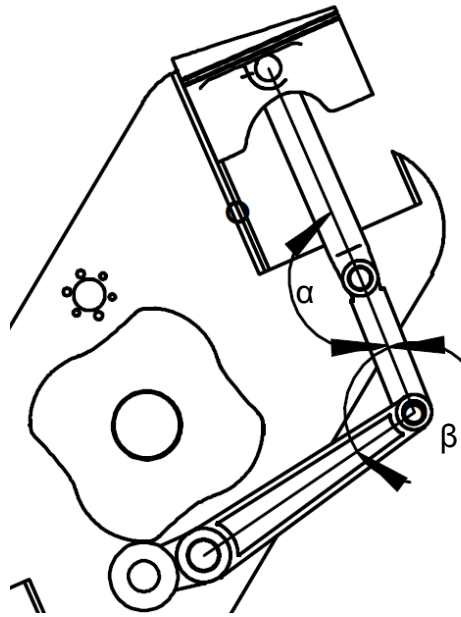


Figure 9 – Angles of linkages on engine rotation for the 2 stroke prototype

Table 2 presents the measurements between the two rods and the lever (α and β) depending on the position of the engine.

Event	Engine angles (deg)	Angles α Rod / Rod int (deg)	Angles β Rod int / Lever (deg)
TDC	0	178.32	102.25
	5	178.5	101.48
	10	179.15	98.45
	15	179.86	93.57
	20	179.97	87.89
	25	179.41	84.19
E0	26.78	179.9	92
BDC	38.11	178.14	80.73

Table 2 - Angles of linkages on engine rotation

It can be seen that angle “ α ” stays relatively straight and can be assumed to be fixed using the simulation analysis.

Engine dimension

Shown below is the engine bore and ports dimensions for the 2nd prototype.

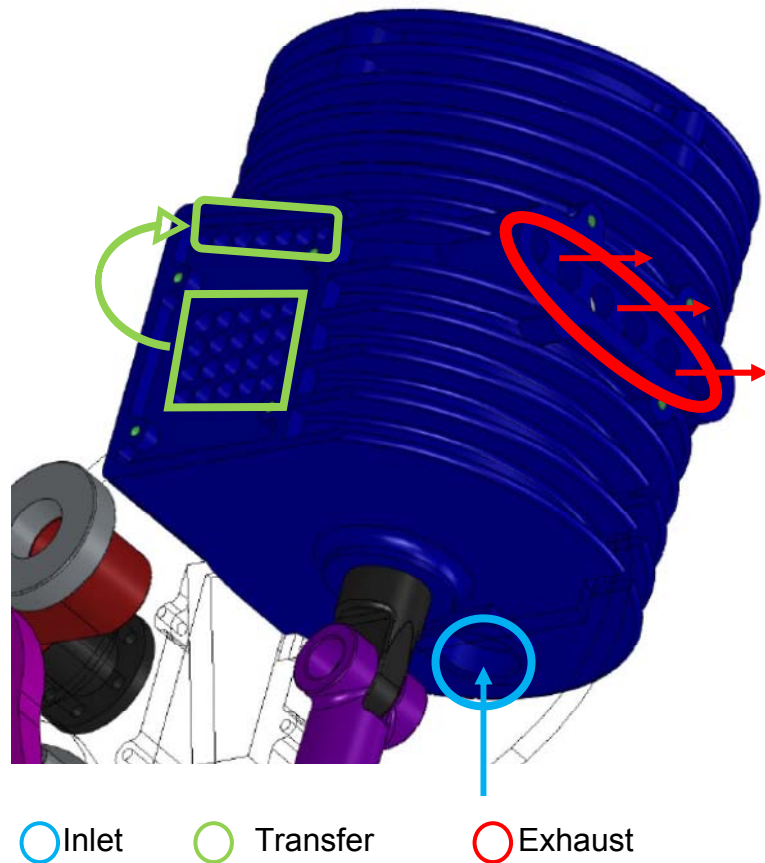


Figure 10 – Exhaust, transfer and intake geometries on 2 stroke cylinder head.

- Inlet ports: 1 hole $\text{\O} 45\text{mm}$. A flexible nose joins this hole to the air box. The volume of the mixture in this flexible is equal to the volume under the piston at TDC.
- Transfer ports: 4 x 5 holes $\text{\O} 13\text{mm}$ and 6 holes $\text{\O} 13\text{mm}$ for transfer the mixture from the bottom chambers to the combustion chambers.
- Exhaust ports: 6 holes $\text{\O} 18\text{mm}$

For simplification, each orifice had their respective areas summed into a single value, instead of incorporating the multiple holes that makes up each port. This will reduce the realistic amount of turbulence due to the increased obstacle to flow. This loss in turbulence is compensated for in the model by increasing swirl and turbulence factors at the matching locations.

The top of the piston is on a slant to introduce swirl as the transfer port opens. The 2:1 crankcase ration builds significant charge pressure in the hope that turbulence prior to combustion is maximized.

Opening ports area

A detailed 3D CAD model of the engine was constructed for both the original 4 stroke prototype and the 2 stroke variant. The following measurements were taken from the CAD model for the simulation analysis to verify the models accuracy.

The first point of these measures is the piston at top dead centre (TDC).

To verify the CAD model, the engine model was rotated and the transfer and exhaust areas were measured as the piston moved. This was to ensure that the CAD model reflected the design and was geometrically correct.

Angles (deg)	Event	Area transfers (mm2)	Area Exhaust (mm2)	Stroke
0	Top Up piston	0	0	1.03
46.48	Exhaust open	0	0	
48.89	Transfer open	0		
49.39		83.3		
50.17		312.76		
51		591.64		
51.82	Top Down piston	743.274		112.74
52.14		741.02		
53		721.91		
54		679.56		
55		613.62		
56.25		464.562		
57.5		321.104		
58.7		143.36		
59.94	Transfer close	0		
63.15	Exhaust close	0	0	
89.93	Top up piston	0	0	
133.71	Exhaust open	0	0	
136.22	Transfer open	0		
141.11	Top down piston	777.504		113.17
149.48	Transfer close	0		
152.66	Exhaust close	0	0	
180.13	top up piston	0	0	1.03
226.15	Exhaust open	0	0	
228.64	Transfer open	0		
231.6	Top down piston	743.82		112.74
239.95	Transfer close	0		
243.21	Exhaust close	0	0	
269.57	top up piston	0	0	
316.91	Exhaust open	0	0	
319.33	Transfer open	0		
322.3	Top down piston	743.82		112.74
330.56	Transfer close	0		
333.76	Exhaust close	0	0	
360.01	top up piston	0	0	

Table 3 - Relative phase of each cylinder as it rotates.

As can be seen from Table 3, there is a slight variation in stroke. The dimensions of the 2 stroke can be found in Appendix D. The design stroke of the piston is 112 mm and the cam should give 112mm of stroke at every BDC. The source of in discrepancy is the geometry of the cam. This 1% indiscrepancy was deemed acceptable for the purpose of this research.

2.3 RISK ANALYSIS

A FMEA style risk assessment study has been done to identify the most prominent mechanical failure modes in the engine so that they can be mitigated to assist in the development of the 2nd generation engine. This outlined all possible failure modes and which of those modes are more susceptible to failure. The most susceptible failure modes found were the cam and rollers, the frame and supports of the engine, the air cooling system and finally the seals and hoses. Fuel explosion was also had a large risk associated to it, mainly because of the large consequence in the event of this failure mode but, statistically, the likelihood of this happening was low. This analysis is attached in Appendix A.

2.4 RESEARCH

2.4.1 IC ENGINES USED FOR POWER GENERATION.

This technology would be particularly useful in NZ because of the abundance of coal mines where there is a supply of wasted methane gas. Coal mining releases large quantities of methane gas that must be ventilated or removed for the safety of the miners. Using waste methane was commercially proven at the Nelms No. 1 Mine, Ohio, USA and at the Appin and Tower Collieries, New South Wales, Australia. They found the following advantages as well as generating useable energy:

- Reduces emissions of coal mine methane, a greenhouse gas
- Improves safety for the miners by removing methane
- IC engines operate on gas at atmospheric pressure; they do not require compressed fuels like gas turbines.

Appin power project use 54 engines that each directly drives one 415 volt 1 megawatt generator. Fuel gas composition varies from 50 - 85% methane, 0-5% CO₂, and up to 50% air. This concept engine is capable of running on much lower methane concentrations.

Methane recovery operations already exist abroad to be injected into pipelines and sold to utility companies. Only methane concentrations of over 90% methane from vertically drilled holes are recovered. Lower quality gas containing 30-80% methane drained from gob wells are wasted and released into the atmosphere because it requires enrichment prior to pipeline injection.

2.4.2 FUELS

According to Maher A.R. Sadiq Al-Baghdadi , Haroun A.K. Shahad Al-Janabi (2003), the criterion for any fuel to be considered as an alternative fuel is;

- Availability: The fuel has to be in abundant supply or, preferably, derived from renewable sources,
- High specific energy content,
- Easy transportation and storage,
- Minimum environmental pollution and resource depletion,
- Good safety and handling properties.

Heather L. MacLean and Lester B (2002) investigated fuel efficiency of a multitude of fuels. They measured efficiency as the amount of energy in the fuel delivered to the consumer divided by the total amount of energy inputs to produce and deliver the fuel. They found that from well to tank 83-91% efficiencies can be achieved with CNG whereas currently, gasoline 80 - 87% and Diesel 83% 90%. Much lower Greenhouse emissions as a measure of grams per MJ of fuel can be achieved with CNG compared to diesel and gasoline.

Compared to other hydrocarbon fuels, burning methane produces less carbon dioxide for each unit of heat released. At about 891 kJ/mol, methane's heat of combustion is lower than any other hydrocarbon but the ratio of the heat of combustion (891 kJ/mol) to the molecular mass (16.0 g/mol, of which 12.0 g/mol is carbon) shows that methane, being the simplest hydrocarbon, produces more heat per mass unit (55.7 kJ/g) than other complex hydrocarbons.

When considering potential fuels that are likely to continue to be used for energy and propulsion into the future it was found that in particular, gasoline or diesel in an internal combustion engine (ICE) is currently the cheapest and will continue to be through to 2020. These vehicles will continue to evolve with improvements in performance, safety, fuel economy, and lower pollution emissions. However, if society desires a more sustainable system or one that

emits significantly less greenhouse gases, consumers will have to pay more for an alternative fuel or propulsion system.

Using a fuel with higher hydrogen to carbon ratio (H/C), improving fuel economy or using a renewable fuel can all reduce CO₂ emissions from engines. Also, natural gas has a relatively wide flammability limit. Accordingly, natural gas engines using high compression ratio, lean burn mixture or high exhaust gas recirculation would be expected to outperform gasoline engines in torque, power and can allow a remarkable reduction in pollutant emissions and an improvement in thermal efficiency. In the meantime, natural gas engines can achieve CO₂ levels below those of Diesel engines at the same air–fuel ratio, while keeping almost the same thermal efficiency under very lean conditions. CO₂ emissions of natural gas engines can be reduced by more than 20% compared with gasoline engines at equal power. This is why methane has been chosen as the preferred fuel option but is still able to run on gasoline to aid in startup and allows flexibility.

2.4.3 IC ENGINE FUNDAMENTALS

Cylinder Characteristics

The cylinder ports are designed to produce a certain power characteristic over a fairly narrow rpm band. Altering the timing, area size, and angles of the ports will directly adjust the power band to better suit demands. Cylinder heads can be reshaped to change the power band.

Effects of the Ignition Timing

To explain the influence of ignition timing on power band in an IC engine, a dirt bike example will be used. Advancing the timing will make the power band hit harder in the mid range but fall flat on top end. Advancing the timing gives the flame front in the combustion chamber, adequate time to travel across the chamber to form a great pressure rise. The rapid pressure rise contributes to a power band's "Hit". In some cases the pressure rise can be so great that it causes

an audible pinging noise from the engine. As the engine rpm increases, the pressure in the cylinder becomes so great that pumping losses occur to the piston. That is why engines with too much spark advance or too high of a compression ratio, run flat at high rpm.

Retarding the timing will make the power band smoother in the mid-range and give more top end over rev. When the spark fires closer to TDC, the pressure rise in the cylinder isn't as high. Gaining more degrees of retard at high rpm is of more benefit because this causes a shift of the heat from the cylinder to the pipe. This can prevent the piston from melting at high rpm, but the biggest benefit is when the temperature rises, the velocity of the pressure waves in the pipe increases. At high rpm this can cause a closer synchronization between the returning compression wave and the piston speed.

Crankcase compression

Primary compression or CCR is defined as the displacement volume of the piston plus the volume of the case divided by the volume of the case.

Having a higher crankcase compression ratio lets more air in during the intake phase, and creates higher pressure pushing that air through the transfers. Using the ideal gas law, if the volume of an area is decreased, the pressure or temperature must increase to compensate. In the very short time that the piston is moving between BDC and TDC, the gas does not have time to absorb enough energy to increase the temperature by a significant amount. Therefore a change in volume will directly relate to a change in pressure.

The higher pressure from a smaller final volume will push the air through the transfer ports at a higher velocity, improving scavenging, and transferring more air in the very short time the ports are open. This is why it is important to maximize the vacuum to get air to transfer as quickly as possible to maximizing the fuel / air mixture entering the combustion chamber. The time the piston is going up is limited by the engine RPM and the amount of air that can transfer is limited by the pressure, restrictions in the intake, and time. Therefore, the more pressure can be

achieved by improving the vacuum as well as a high CCR, the more air is forced into case on each stroke, which means more air and fuel into the cylinder.

Friction

Friction is a major source of lost energy in an IC engine. Grant Smedley, (2002) said that friction consumes between 4-15% of the total kinetic energy produced by an engine and that 40-55% of these losses is found in the power cylinder. Around half of the power cylinder friction losses can be attributed to the piston rings.

Knock

Knocking is a common problem encountered with IC engines. This happens when the peak of the combustion process no longer occurs at the optimum moment. The shock wave creates the characteristic metallic "pinging" sound, and cylinder pressure increases dramatically. Effects of engine knocking range from inconsequential to completely destructive. Eric Tribbett, Ed Froehlich, Lex Bayer (2005) stated that "engine knock provides a practical limit to raising the compression ratio in typical IC engines." The optimization of valve duration and timing is an efficiency solution for controlling the knock limits and for improving thermal efficiency.

Effect of Compression Ratio

The compression ratio is defined as maximum combustion chamber volume (at BDC) final divided by minimal combustion chamber volume (at TDC). The current prototype has a relatively low compression ratio in comparison to modern IC engines, (5:1). In the 1930s, a typical compression ratio value for the spark ignition engine was 5:1 or 6:1, the same as the current prototype. Today, the conventional automobile engine has a typical compression ratio of 10:1.

G.H. Abd Alla (2002) investigated the relation between compression ratio and compression pressure. He found that the compression pressure virtually triples by doubling the compression ratio.

The increase in output at higher compression ratios overrides the additional required compression work.” (Eric Tribbett, Ed Froehlich, Lex Bayer)

Changing the compression ratio does not change the displacement volume, thus an appreciable change in volumetric efficiency would not be expected. The amount of residual gas in the cylinder may affect the volumetric efficiency somewhat but can be considered negligible.

One consequence of increasing the compression ratio in an IC engine is the affect on exhaust temperature and in-cylinder peak pressure. The amount of energy released by the fuel is constant and can contribute to work-out or to increasing the enthalpy of the exhaust gas. IMEP (work) increases with increasing compression ratio. If more energy is being converted to work, the enthalpy of the exhaust gas– and thus its temperature must decrease if energy is to be conserved.

J-J Zheng, J-H Wang, B Wang and Z-H Huang (2009) found that when they conducted a study on a natural-gas direct-injection spark ignition engine that the compression ratio has a large influence on the engine performance, combustion, and emissions. Some more findings when increasing compression ratio is that the maximum cylinder gas pressure and the maximum gas mean temperature increased and the flame development duration, the rapid combustion duration, and the total combustion duration decreased.

Another consequence was that exhaust carbon dioxide decreases while nitrous oxide increases. They suggested as result of their study that based on the comprehensive evaluation of engine performance and emissions, a compression ratio of 12 is suggested as the optimum value for the natural-gas direct-injection engine.

It is clear that there is an optimum CR for every engine at which the performance will peak. Unfortunately performance may have to be compromised to meet emission standards. To keep the output power and torque of natural gas engines

comparable to those of their gasoline or diesel counterparts, high boost pressure was recommended.

Turbulence

G.H. Abd Alla (2002) found that increased turbulence in the unburned mixture at the time of combustion increases the burning rate. Turbulence is usually increased by generating swirl during the induction process.

Another factor that shows promise in improving performance is the introduction of turbulence in the combustion chamber. A Das and HC Wilson investigated this with a fuel injected engine being modified to run on natural gas. Various mixtures and compression ratios were tested over a wide range of operating conditions. The combustion chamber was modified to increase turbulence through squish motion to improve performance. Thermal efficiency of over 40 per cent and peak torques were achieved in thermal efficiencies that exceeded the petrol equivalent, with only 65% of the carbon dioxide emitted.

Turbulence within the combustion chamber is important because it allows better mixing and distribution of fuel and air before ignition. Recent research indicates that the type of turbulence within the cylinder is also important and that tumble is superior to swirl. The reason for this is because the tumble vortex stores energy until late in the compression stroke and when it breaks up it produces a high level of turbulence to result higher flame speed and combustion rate requiring smaller MBT (minimum advance for best torque) whereas swirl energy is continuously dissipated. The introduction of turbulence can improve cyclic combustion stability and the extension of the lean operating limit, particularly under part load conditions.

Increasing compression ratio and cylinder turbulence allowed burning of lean natural gas and air without combustion knock. Increasing turbulence through tumble and swirl mechanisms were at the expense of flow rate. The efficiency of the gas mixing is highly sensitive to the point of delivery of the gas. Poor gas mixing and unequal charge distribution led to decreased volumetric efficiencies

and cause flow unsteadiness. Higher thermal efficiency attained at higher compression ratio was found to lower HC emissions. High compression ratios decreased the CO₂ emissions.

Stroke Configuration

Since the second generation engine is a 2 stroke variant, the latest developments in 2 stroke variants were investigated. A study by P R Hooper, T Al-Shemmeri and M J Goodwin (2011) investigated future prospects for 2 stroke engines. 2 strokes provide in general higher performance per litre than 4 stroke variants and it is due to high maintenance and reliability issues that have caused a reduction in production. There is also a requirement for a high oil level for lubrication and excess fuel are used for cooling to extend the life but as a result 2 Strokes struggle to meet emission registration standards so 4 stroke configurations are preferred despite the reduction in performance.

An orbital, 2 stroke, three-cylinder 1.2 litre engine attracted the attention of major automotive manufacturers including Ford, Jaguar, Fiat, General Motors in the early nineties. It uses a fuel injector for fuel metering and with the addition of solenoid-controlled high-pressure compressed air, a highly atomized fuel–air mixture is propelled directly into the combustion chamber.

It was developed by Schlunke in 1989 and Smith and Ahern and automotive manufacturers were particularly interested in the very low emission characteristics, the high specific performance, and the flat torque output of the two stroke engine. Unfortunately further development was abandoned due to poor durability characteristics. While the two-stroke engine offers high-power-density and low-cost advantages, greater complexity in gas dynamics and hence increased unit cost is inevitable in order to meet ever more stringent emission standards. By application of direct-injection systems, high-speed poppet valve actuation, and active exhaust gas recirculation control to enable a wide range of operation, and variable-compression-ratio technology, the two-stroke engine still has the potential to provide competitive low-emission power train solutions.

Emissions are not as important in this situation, since methane will be used, instead of higher carbon emitting hydrocarbons. This is why the higher power density of the 2 stroke engine is more desirable. The simple, robust nature of this engine technology and low rpm should mitigate any reliability and durability issues.

Equivalence Ratio

The air-fuel ratio is simply the ratio between the mass of air per second and the mass of fuel per second in equation form, $\text{Air-Fuel Ratio} = \dot{M}_a / \dot{M}_f$

The air-fuel ratio is very important when designing an engine as to lean or rich a mixture will result in poor performance and/or damage to the engine.

The fuel power is calculated on the assumption that all combustible products meet with oxygen during the combustion process. This is not the case normally and uncombusted fuel will normally remain after the cycle. Hence the use of superchargers, intercoolers and turbochargers are used to either compress the air at intake or cool it to increase the volume available.

Eric Tribbett, Ed Froehlich, Lex Bayer (2005) also explored how varying the equivalence ratio effects performance with their research engine. They varied the air-fuel ratio which corresponds to varying the equivalence ratio. This was accomplished by changing the fuel rate at constant airflow. The compression ratio and spark advance were held constant.

At very low equivalence ratios the combustion process is limited by the available fuel so maximum performance is expected to be on the rich side of stoichiometric. At equivalence ratios that are too high the combustion process is limited by the availability of oxygen. At intermediate equivalence ratios the combustion process is limited, to a degree, by the ease of forming free radicals. Running slightly rich means that there is more fuel available to accomplish this. These factors combine to cause the observed maximum in the indicated mean effective pressure (IMEP) as a function of equivalence ratio.

Thermal efficiency tends to decrease and indicated specific fuel consumption tends to increase with equivalence ratio. Thermal efficiency is work-out divided by energy-in. In the case they studied, the energy-in was the product of the mass of fuel and the lower heating value. As the mixture is made richer a greater amount of the fuel does not burn. The energy contained in the bonds of this fuel is counted in the energy-in term but does not contribute to the work-out since it does not burn – thus the thermal efficiency decreases. At equivalence ratios that are too lean, the power output drops significantly causing the thermal efficiency to decrease.

These two factors cause there to be a maximum value of thermal efficiency at an intermediate equivalence ratio. Indicated specific fuel consumption (ISFC) is the mass flow rate of fuel divided by the power output. Very lean mixtures have a low mass flow rate of fuel but also have low power output. Very rich mixtures have a greater mass flow rate of fuel but the additional fuel does not contribute to power output. These two factors cause there to be a minimum in ISFC at an intermediate equivalence ratio. The minimum value of ISFC appears to occur at an equivalence ratio slightly greater than one.

They found that there appears to be no correlation between volumetric efficiency and equivalence ratio.

At very lean conditions there is very little fuel in the mixture. This means that the cylinder takes in a greater amount of air for a given amount of mixture. At very high equivalence ratios the effects of charge cooling may be significant. This decrease in temperature increases the density of the mixture, thus increasing volumetric efficiency.

Spark Timing

G.H. Abd Alla (2002) looked at retarding timing in engines with lower compression ratios to control nitrous oxide emission and to avoid knock. He found that the exhaust temperature increases as a result of retarding timing and both engine efficiency and heat loss to the combustion chamber walls decrease. Retarding timing is sometimes used to reduce hydrocarbon emissions by increasing the fraction oxidized during expansion and exhaust due to the higher burned gas temperatures that result.

An engine was developed with Eric Tribbett, Ed Froehlich, Lex Bayer (2005) explored how varying spark timing, compression ratio and equivalence ratio effects performance and how they interacted in a novel engine design. They found that the mean effective pressure (IMEP) tends to increase with spark advance. This is expected to a point, where it should drop off. Best performance is achieved when the greatest portion of the combustion takes place near top dead center. If the spark is not advanced enough, the piston will already be moving down when much of the combustion takes place, losing the ability to expand this portion of the gas through the full range, decreasing performance. If the spark is too advanced, too much of the gas will burn while the piston is still rising. The work that must be done to compress this gas will decrease the net work produced. These competing effects cause there to be a maximum in the mean effective pressure as a function of spark advance.

The peak pressure increases with increasing spark advance. Maximum pressure would be reached if all of the gas were burned by the time the piston reached TDC. With less advanced spark timing the gas does not burn completely until the piston is on its way down on the expansion stroke.

The exhaust temperature decreases with increasing spark timing. This is interesting when related to the mean effective pressure over this range. The mean effective pressure represents the work done on the piston. The exhaust gas temperature represents the enthalpy of the exhaust gas since for ideal gases the enthalpy is a function of temperature only. The energy released by the combustion of the fuel must go into expansion work or the enthalpy of the exhaust gas. Since

the pressure (work) increases over the range studied, the temperature of the exhaust gas (enthalpy) must decrease if energy is to be conserved.

Squish

Squish is the term used to describe that aspect of the combustion process where the gases within the combustion chamber are squashed or extruded due to the movement of the piston. This effectively magnifies the compression of fuel / air mixture prior to ignition, increasing the pressure acting on the piston head. The downside can be that it distorts the flame propagation within the combustion area and reduces combustion efficiency.

Performance Indicators

Indicated mean effective pressure (IMEP) is a better indicator of performance than torque since it is a direct measure of the combustions effectiveness, rather than how that energy is converted. Unfortunately, in cylinder pressure sensors are required in order to extract this data from a prototype. Although, like power and torque, it is expected that IMEP would tend to decrease after reaching a maximum due to increasing heat losses through the cylinder walls. As the surface area-to-volume ratio increases, greater amounts of heat are conducted out of the cylinder. The loss of this thermal energy decreases the amount of work that can be extracted from the system. This is how the simulation produces a torque output.

Torque Calculations

Since the torque production is not measured directly it must be estimated. The torque production is nonlinear and can be comprised of many variables such as fuel mass in cylinder, air/fuel ratio, engine speed, ignition, injection timing and exhaust gas regulation. Guzzella and Onder (2004) use a Willan's approximation to estimate engine torque. The Willan's approximation assumes that at constant speed the engine torque is a function of the brake mean effective pressure (IMEP)

and cylinder volume. Fuel mean effective pressure is also used in the calculation. The fuel mean effective pressure is a function of the lower heating value of the fuel, burnt per combustion cycle mass and volume displacement.

The Willan's approximation notes that there is a simple relationship between mean fuel pressure and mean effective pressure that approximates real engine behavior very well.

Another, simpler method is an instantaneous combustion torque model which considers the first law of thermodynamics and crank geometry. Where A is the area of the piston, p is the in-cylinder pressure, p_a is the ambient air pressure, r is the radius of the crank, L is the length of the connecting rod and θ is the crank angle in units of radians. The work output can then be found.

2.4.4 ENGINE DEVELOPMENT STRATEGIES

Virtual engine development appears to be the main driver in remaining competitive in the engine design industry. When looking into the modern design of diesel engines, Pavel Novotný and Václav Píšťek (2006) looked into dealing with fundamental problems such as crank dynamics, acoustics and fatigue using finite element method (FEM) and multi-body system (MBS).

The process is started with CAD, giving basic geometric information. FEM is good at modal analysis and harmonic analysis, but not for the durability calculations. Frequently these models have been simplified to remove the details such as holes and fillets which carry introduce stress concentrations that play an important role in the durability of a product.

3D Model software that relies on mesh generation makes a very powerful design tool. CFD is used to attempt to simulate the flow and combustion in IC engines. This step is quite slow due to the complexity of the models. Fatigue analysis can also be incorporated into the ANSYS and FEM models. This approach overcomes the historic "build-test-redesign" problems but its accuracy is limited to the input data and is also highly time consuming to construct accurate predictions.

The problem with mesh generation for IC engines is that they have very complex geometry with moving boundaries. Also different loads and speeds with different configurations of inlet manifold are the reason that setting up simulations is so difficult and simulation times can run for days and in some cases, weeks. Some ideas being developed to speed up simulations are auto mesh generators, parallel running computer simulations and auto post processors.

It appears that virtual engine development, although cheaper and traditionally faster than prototyping a multitude of complex parts, is still a lengthy iterative process. I looked into ways of speeding up the process.

3D virtual processes would be far too time consuming for the investigation. The use of one-dimensional computation fluid dynamic (1D CFD) engine simulation software is widespread throughout the engine development industry. This simulation method allows for characterizing engine operation without the need for high-end processing and time-intensive computations.

2.4.5 IC ENGINE MODELLING

Because this is an original concept, with only one existing prototype, there has never been an attempt to simulate this engine type with a computer model. Traditional IC engine software development packages assume a reciprocating piston engine model. Because of the deviation from a typical crank slider setup, current engine modeling software is not compatible with this configuration. Also, because of the geometry and cycle timing, the virtual model will need to be adapted to accommodate the difference from traditional IC setups. Another difference to traditional development methods is that not only is the engine's performance being optimized but the client wishes to upscale the engine displacement as well as change the piston cylinder from a 4 stroke set up to a 2 stroke configuration. Such a change makes predicting performance difficult.

Other areas of attention are;

- How each element interacts with each other.
- Force paths and what are the critical components that weather these forces.
- Scrutinizing the dynamic characteristics since even without gearing, the output speed can be low (few hundred revolutions per minute).
- Upper and lower geometrical and mechanical limits and how adjustments in cam profile, dwell parameters, valve timing and piston timing affect performance will need to be investigated.
- The slow combustion of methane and other low quality fuels, especially at such low rpm.
- Fluid dynamics and thermodynamics are also areas of interest. This will be predominantly how it effects cooling through conduction at different rpm.

The model will also be capable of producing detailed analysis on emissions, mass flows, pressure, temperatures and so much more.

Combustion

Because the intention is that this engine will run on methane, several characteristics concerning combustion need to be considered. With efficiency in mind, the goal will be to run the engine on the lean side of stoichiometric. There is limited information on lean burn gas engines and in most cases engines and operating conditions are too different from one to another to allow any pertinent comparison.

A mixture of methane and air has low burning velocity compared with that of gasoline and air, (approximately 30% slower burn rate). Homogeneous lean burn mixtures result in lower flame propagation, occurrence of miss-fire, low mixture distribution quality in multi-cylinder engines and high unburned HC emissions in the exhaust. The reason the flame speed of natural gas mixtures is lower than that

of other hydrocarbon fueled engines is due to its lower activation energy. This is most significant under lean conditions. This is why typically; natural gas produces approximately 16% less power than its gasoline counterparts, (assuming the same fuel conversion efficiency and operating conditions) due to the displacement of air by the fuel in the induced cylinder air mixture.

A lean burn strategy should result in minimum exhaust emissions and maximum thermal efficiency. A high compression ratio, a high energy ignition system (multiple spark plugs), as well as maximizing swirl and turbulence at the end of the compression was employed to achieve this lean burn strategy.

By increasing charge turbulence and charge density, a sufficiently rapid enough burn rate can be induced to compensate for the low density nature of natural gas. Johansson found that combustion chambers with a square cross section in the piston bowl resulted in the fastest combustion of natural gas. This has been implemented on the 2nd prototype squish area at the top of the combustion chamber.

Other points of interest that were integrated into the combustion model;

- The combustion duration lasts the longest at the peak rpm.
- Typical gasoline burntime – 30 degrees. 50% burn point around 9 degrees.
- Amount of burn duration variation in a typical IC engine is 3 – 5 degrees of crank rotation.
- 50% burn point reduces as rpm increases. This varies 0.5 – 2 degrees.
- The lower the compression ratio the longer the burn duration.
- The maximum burn time relative to crank position is 90 degrees.

With high centrifugal forces acting on the gas, prior to ignition, the fuel/air mixture is forced outwards to the sides of the piston. The use of squish and relative slow rotation of the engine compared to the piston velocity should mean that centripetal forces on the gas will not have a significant influence on combustion.

Otto Cycle

The Otto cycle is a standard rating cycle or an air standard cycle for conventional four stroke SI engine theoretical cycles. These are shown below:

- Isentropic compression
- Constant volume heating process
- Isentropic expansion process
- The constant volume heat release process

To simplify the engine modeling process, the following common conditions and assumptions can be implemented to estimate the behavior theoretical cycles of reciprocating engines:

- The operating fuel and air mixture is regarded as an ideal gas.
- The specific heat is considered to be constant.
- The compression and expansion processes of the ICE are isentropic processes.
- The combustion process is regarded as a heating process or a constant volume burning process.
- The heat release of the engine exhaust is regarded as a constant volume heat release process.
- All cyclical processes are reversible.

Wiebe Curve Combustion compared with Otto

The Wiebe function shown below is most often used to represent the mass fraction burned versus crank angle curve.

$$x_b(\theta) = 1 - \exp\{-a[(\theta - \theta_0)/\Delta\theta]^{m+1}\}$$

θ is the crank angle, θ_0 is the start of combustion, $\Delta\theta$ is the total combustion duration, while 'a' and 'm' are adjustable parameters. Varying 'a' and 'm' changes the shape of the mass fraction burned curves.

This was used to find the indicated work done from cylinder pressure. Other factors such as heat transfer from the cylinder, friction and pumping losses were taken into account to predict the brake mean efficiency pressure, brake thermal efficiency and brake specific fuel consumption.

Otto cycle is ineffective in simulating combustion in a spark ignition engine, compared to data measured in a real engine. The Otto cycle demands that the heating and cooling processes have constant volume during the combustion process. The problem is simply that an engine cannot conduct combustion at constant volume, because a real burning process takes time, the piston keeps moving and the cylinder volume changes. Another problem with the Otto cycle is that the combustion cycle is assumed to be instantaneous as illustrated in Figure 11.

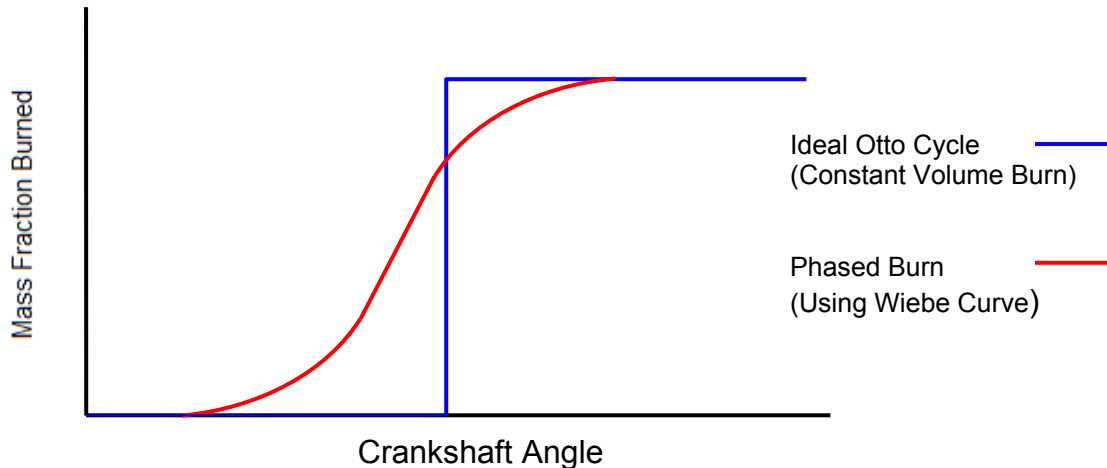


Figure 11 – Comparison between the Otto cycle and Wiebe curve considering fuel combustion as the crankshaft rotates.

The most influential parameters in the Wiebe function are; fuel, trapped overall mass, ignition delay, compression ratio and other parameters such as temperatures showed significant crank-angle-resolved sensitivities for predicted cylinder pressures.

Many variables including engine speed and cylinder wall temperature do not yield significant values for sensitivities. It is important to consider uncertainties in both predicted and measured cylinder pressures and heat release rates while validating any engine combustion model.

H. Cho, S. R. Krishnan, R. Luck and K. Srinivasan (2003) believed the Wiebe function based combustion model with a quadratic interpolation as a function of gas temperature and appropriate Wiebe parameters provide reasonable predictions of cylinder pressure, mass burned fraction, and heat release for most applications.

The Wiebe combustion curve is the closest combustion model that would yield the most reliable results.

Natural Gas combustion using Wiebe Curve

Limited data exists concerning lean combustion in gas engines in terms of ignition delay, combustion duration and combustion rate. This data is necessary when using thermodynamic models to predict energy and environmental performance and is quite useful to the Ricardo model being developed. S Rousseau, B Lemoult and M Tazerout looked into the combustion characteristics of natural gas in lean spark-ignition engines using the Wiebe function. By analyzing measured cylinder pressures cycles with a heat release analysis model they obtained the parameters used in the Wiebe function. The model they used takes into account heat transfer to the chamber walls and leakage.

Although they did produce form factors for the Wiebe function for natural gas engines, they found that in several cases the Wiebe function fails at the beginning and end of combustion. They recommended that in order best to reproduce the mass fraction burned, particularly at the beginning and end of combustion, further studies should test mathematical functions other than the Wiebe function, or a phenomenological model of combustion using the flame speed and the flame front geometry.

2.5 MODELLING

The development of a computer simulation model for this engine configuration will allow exploration into the limits and possible spectrum of variants for this technology. This method is much faster and economical method instead of building a multitude of prototypes to explore the engine's capabilities. Other benefits that are expected from this project are insights into the engine's complex dynamics and combustion characteristics that differ greatly from a conventional IC Engine. These areas are not fully understood and an in depth analysis in order to construct a simulation model will contribute to better understanding the thermodynamics and mechanics of this class of engine. Use of the software also allows a more in depth investigation into the exploration of alternative fuels and therefore of applications to a variety of power generation/propulsion systems. It will also permit the exploration of key geometries such as the internal linkage geometry so that they can be optimized for other performance outcomes that would otherwise be unobtainable by conventional mechanisms.

For this investigation, Ricardo WaveBuild, Version 8.3, 1D modeling software was used. The problem is that this software is suited to slider crank configuration internal combustion engines, not rotating engines with variable cycle times. To mitigate this problem, an equivalent engine will be created to evaluate and predict performance in different environments.

Initially, a virtual version of the current working prototype was created and was verified by comparing output performances of the virtual model with the actual dynamometer results of the prototype. The prototype model was then optimized and used as a basis to create the 2nd generation 2 stroke version model.

Modeling in Ricardo will be used to help produce an effective 2nd generation engine that will be appropriate for market introduction.

Because this is an original concept, with only one existing prototype, there has never been an attempt to simulate this engine with a computer model. Because of the incompatibility with the geometry and cycle timing of the current engine

modeling software is not compatible with this configuration; the virtual model will need to be adapted to accommodate the difference from traditional IC setups.

2.5.1 RICARDO WAVEBUILD

There are two primary engine simulation software packages used in the industry today: Ricardo WAVE and GT-Power. Both software packages are similar in purpose and functionality.

Ricardo WAVE is more than just an engine simulation program. It is an engineering code designed to analyze the dynamics of pressure waves, mass flows, energy losses in ducts, plenums, and the manifolds of various systems and machines. When further-detailed analysis is desired, WAVE can be coupled with various industry-standard software packages such as CFD analysis programs and statistical analysis software.

Ricardo Wavebuild, Version 8.3 is highly customizable combustion capabilities and incorporates geometric factors and follows similar calculations as developed by Heywood 1988. Unlike 3D packages, simulation time requires a fraction of time and provides a simpler overview of the entire engine cycle. Some manipulation of Ricardo's software will be required to accommodate the unusual dynamics of the prototype engine. I then looked at similar projects where this has been done. One is where the Wankel rotary engine. Phillip Stott, (2002) at Canterbury University, Mechanical Engineering department, constructed an accurate model of the Wankel Rotary engine. This engine differs in cycle time from traditional crank slider configurations much like the prototype engine that will be examined and modelled for this project. He found that by rating the rpm by amount of thermodynamic cycles rather than physical rotations of the crank, the correct power and torque curve can be found for engines with orbital engines. He also described how correction factors were used to adjust the Wavebuild calculations since it assumes a reciprocating piston engine model.

Being that all engine components work together as a system, it is advantageous to model the entire engine system rather than individual subsystems. Ricardo WAVE

is more than just an engine simulation program. It is an engineering code designed to analyze the dynamics of pressure waves, mass flows, energy losses in ducts, plenums, and the manifolds of various systems and machines. When further-detailed analysis is desired, WAVE can be coupled with various industry-standard software packages such as CFD analysis programs and statistical analysis software. The basic operation of the WAVE code analyzes flow networks composed of ducts, junctions, and orifices. Within this network of plumbing, engine cylinders, turbochargers / superchargers, compressors, and pumps can be inserted. WAVE can simulate internal combustion engines as well as other compressible-fluid flow systems. Once a simulation has completed, the post-processing program, WavePost, allows for detailed analysis of the simulated engine operation.

The overall capabilities of WAVE extend beyond the simulation of engine operation. The software bundle has a program specifically dedicated to acoustic and noise analysis. Other secondary software uses include: Hybrid 1D/3D CFD engine simulation, thermal analysis, controls systems, and combustion and emissions simulation.

2.5.2 MODEL SETUP

The engine model is setup by defining some relatively basic inputs and then some more advanced inputs that require some engine testing. The basic inputs are composed of engine geometry and boundary conditions. Therefore, all dimensions from the intake and exhaust ducting must be measured and put in the model. Likewise, manufacturer specifications for internal engine geometry such as bore, stroke, connector rod length, wrist-pin offset and compression ratio must be input. Initial conditions such as exhaust temperatures, intake temperatures, and wall temperatures need to be input as reasonable values. These can be modified later to higher accuracy once actual engine measurements become available. A general flow diagram for the development of a model is shown in Figure 12.

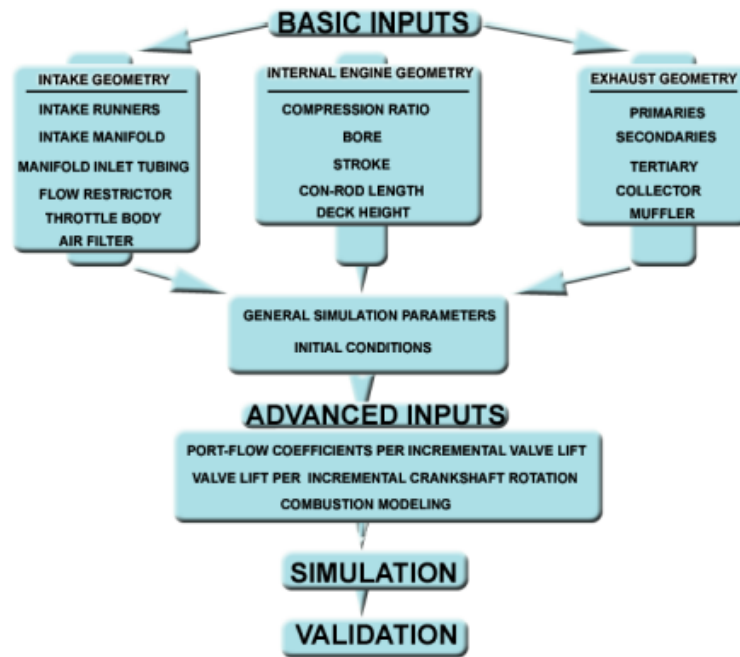


Figure 12 – Simplified Model Setup Procedure, (Dan Cordon, Charles Dean, Judith Steciak and Steven Beyerlein, 2007)

Without in-cylinder pressure measurements, the combustion model had to be predicted based on typical forced induction Wiebe function parameters. WAVE allows for three parameters in the Wiebe correlation to be input: 10-90 percent burn duration, 50 percent burn point, and the Wiebe exponent.

Ricardo has provided a very comprehensive set of input parameters that allow users to highly customize any flow model. One such limitation comes into play when trying to model ducts that have significant geometric changes over very small length increments. An example of such geometry is the bell-mouth of an intake runner. The 3-D flow phenomenon that occurs in such geometry cannot be accurately modelled by 1D code. In this case, discharge coefficients can be used based on published findings for bell-mouth discharge coefficients. So, essentially flow losses can be imposed on geometric instances that can't be accurately modelled with 1D code. Furthermore, when modeling tapered ducts, it is recommended to keep angles smaller than 7 degrees. This is due to the fact that flow separation, a phenomena not modelled in 1D code, typically occurs at flow

angles of 7 degrees or more. One such instance that was encountered in this research was in the modeling of the flow restrictor that had a converging angle of over 20 degrees. If the restrictor is modelled exactly from its physical geometry, WAVE will over-predict power output due to the inability to calculate flow losses due to flow separation.

Wave utilizes a system of PDE's (Partial Differential Equations) to model engine performance. These equations address the two fundamental aspects of engine operation, thermodynamics and gas dynamics.

The simulation process involves the engine being divided up or "discretised" and boundary conditions defined for the resulting finite volumes. The discretions of the governing physical equations result in a set of ODE's (Ordinary Differential Equations) (which defines engine performance. Within these volumes the resulting effects of such processes as heat transfer and fluid dynamics are computed. Time steps are then taken through the process from one volume to the next until convergence is obtained for a given engine speed. This procedure is then repeated for a variety of engine speeds. The greater the number of volumes that the engine components are divided into, the greater the number of time steps required. This resulted in an increased simulation accuracy (to a certain extent) and increasing computing time to analyse the process. Various parameters are specified such as duct initial conditions and general engine operating conditions for the simulation. If these parameters are known (e.g. from test data) rather than estimated, the convergence of the program will be faster and be more accurate. Such parameters include: inlet charge composition, temperature, pressure, size of inlet and exhaust duct along with valve and cylinder geometry

3 METHODOLOGY

3.1 OBJECTIVES

The objective is to build a reliable model in Ricardo Wavebuild of the 1st prototype and verify this model against the test data. This will be then be modified to construct a 2nd Ricardo model of the 2nd two stroke prototype currently under development, using known values corresponding to the current design. This second model will be used as a way of predicting the output and helping its development through optimizing engine parameters. This model will be used to test the theoretical potential of this design configuration. The primary parameter being assessed is the piston motion profile (dwell), which is controlled by the geometry of the cam.

Both models are constructed using 3D CAD model data and physical measurements. Refinement of parameters and inputs will be adjusted once the simulation is producing reasonable results. Parameters for refinement include:

- Thermal conductivity constants.
- Initial conditions.
- Boundary conditions.
- Air to fuel ratio at different throttle positions.
- Combustion constants in relation to RPM.

Ricardo simulation outputs provide information on everything from cylinder pressures and temperatures to fuel consumption and exhaust emissions. These outputs are displayed in plots and were often exported to excel for easier presentation and comparison of the data.

It was recommended that initial validation and calibration of the model should be performed by comparing predicted volumetric efficiency to that measured on the dynamometer. In order to obtain volumetric efficiency calculations, an accurate air-mass flow sensor must be interfaced with the engine and dynamometer data

acquisition but this was not available. Instead, torque output was the parameter used to validate the model. While volumetric efficiency validation is recommended, torque validation could be considered the next best method. Torque output validation is performed by comparing torque output measured on a dynamometer to predicted torque output.

Once the model has been validated to an acceptable degree of accuracy (i.e. +/- 5%), the model can be used with a greater level of confidence to construct the next generation engine.

Again, geometric data from the 3D CAD model was used to capture known geometries of the 2nd generation engine. Parameters are modelled based on the refining results found in the first prototype and a baseline torque and power prediction is produced by the simulation software.

These two models are now both used to investigate and optimize both variants by adjusting different parameters and engine characteristics. The parameters that will be investigated are

- Valve timing and areas.
- Displacement – stroke and bore.
- Crankcase ratio.
- Compression ratio.
- Piston profile – dwell time near TBC and BDC by altered the cam profile.

Optimal engine performance can be very subjective so the objective was achieving highest torque possible at a sustainable rpm that would burn methane efficiently unaided by additional fuel sources. Once the engine parameters have been optimized, other properties can be included such as the lever ratio, forces on cam and linkages using the output torque.

3.2 MODELLING OF FOUR STROKE PROTOTYPE

3.2.1 MANIPULATING WAVE FOR ALTERNATIVE CONFIGURATION.

The main issue with using Ricardo is that Wave simulation software is not compatible with this type of engine. To overcome this problem, the same methodology used for the modeling a Wankel rotary engine performance in Wave was utilized. To model this engine, it is necessary to create an equivalent reciprocating engine. Both the four stroke and two stroke variants are modelled so that they complete the equivalent amount of thermodynamic cycles per rpm. Therefore the output RPM is out by a factor of four since there are four times more thermodynamic cycles (i.e. induction, compression, combustion and exhaust) for each revolution of the crank in this engine configuration. Because WAVE assumes a reciprocating piston engine model, it is therefore necessary to apply a correction factor to the engine speed. So for the 2 cylinder engine, 8 cylinders were modelled to achieve equivalence as shown in Figure 13 and Figure 19 for the 4 stroke configuration) and Figure 35 and Figure 36 for the 2 stroke configuration.

For the unusual piston profile, a customized position vs crank array was created and integrated into the model. The original design piston profile is shown in Figure 20.

3.2.2 MAIN SCREEN SHOWING GENERAL MODEL LAYOUT

A screen-capture of the WAVE graphical user interface (GUI) is presented in Figure 13. This shows the basic cylinder layout comprised of (from left to right) ambient conditions, inlet duct, duct injection, inlet duct with fuel injector, combustion chambers with one inlet and one exhaust valve, exhaust duct, and finally ambient conditions once again. Figure 14 through Figure 38 and shown in Appendix D and E illustrate these elements that make up the models. Tabs within each of these window allow for data input associated with engine geometry, operating parameters, heat transfer, scavenge (where applicable) combustion and conduction to be altered.

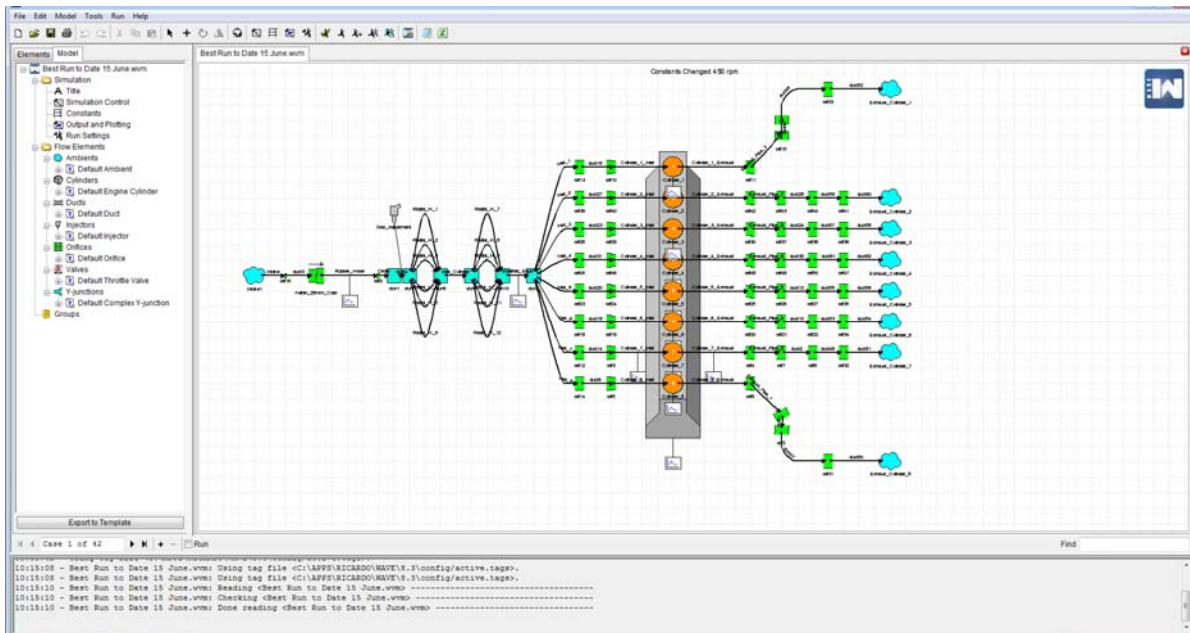


Figure 13 – Original Prototype Ricardo Model Overview (GUI)

The right side of the screen is the visual portrayal of the engine model layout in which all parameters can be modified.

Certain wave data input values are mandatory for a simulation to run while other inputs are optional. Wave also contains default values for some inputs based on typical piston engines which can either be left or overwritten. Once the engine model has been created, a simulation can be run. This take up to 30 hours to run depending on the model complexity, (8GB Ram on simulation computer).

The left portion of the screen lists the elements available to be inserted into the model such as engine cylinders, ducts, and orifices. Each element has a large amount of customizability. An example of typical elements are shown in the Figures below and in Appendix C and D.

Figure 14 shows one section of the intake flumes. This panel allows adjustment to pressure to accommodate forced induction (increasing initial conditions on pressure and temperatures based on measurements). Since the engine is rotating, gathering real data from these flumes is difficult so for the intakes, the air / fuel mixtures are assumed to be ambient which should be close to actual since the point that the air enters the intake manifold is stationary. The small amount of

centripetally forced induction caused by the engine's rotation is included by increasing the average air velocities in each section of moving duct calculated from the RPM and distance from the centre of location.

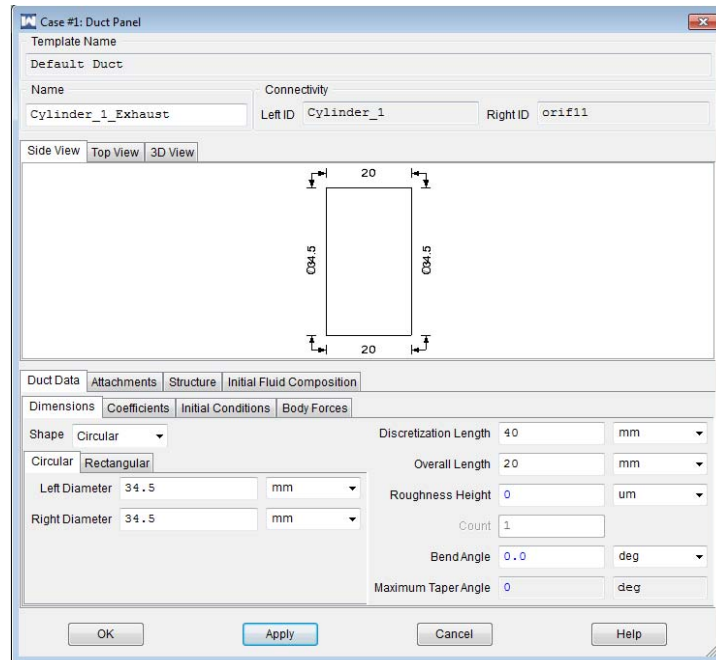


Figure 14 – Duct Panel Geometry Panel

The sections of duct, especially those in close proximity to the combustion chambers have their wall and gas temperatures altered. These temperatures are based on conduction and convection calculations on the duct surfaces based on their geometry and composition and the air / fuel / exhaust gas temperatures were established by iterative simulations until they remained constant (within 1%).

Additional inputs are wall friction coefficients, forces as well as details on fluids initial and dynamic conditions. More duct examples are shown in Appendix D (4 stroke) and E (2 stroke).

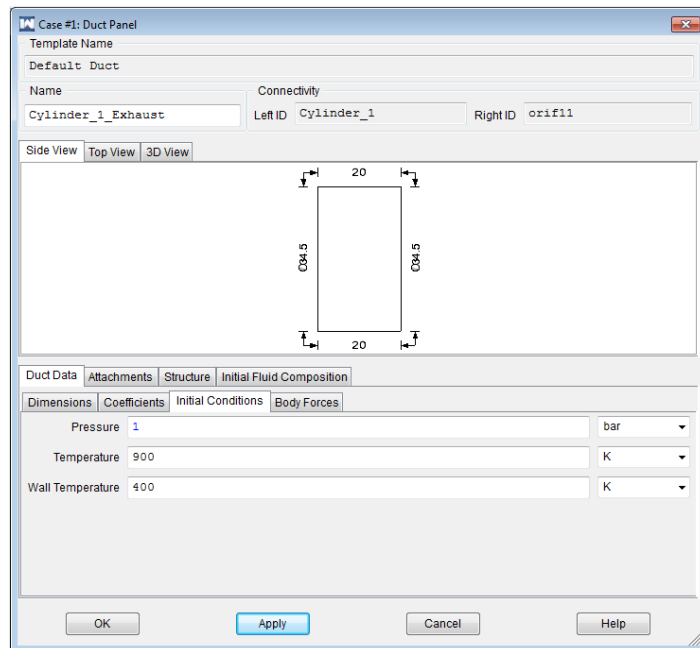


Figure 15 – Duct Panel Initial Conditions

Orifices are used to link the duct sections. They are defined as a mass-less and zero-length junction used to directly connect two ducts. The diameter of the orifice defaults to match the connecting ducts but can be input independently when necessary. This exhaust duct has the temperature of the exhaust gas (approximated from combustion temp of methane in this case) and the inner wall temp based on the inside gas temp and external forced cooling, calculated from the duct thickness and the rate of heat lost by conduction through the pipe wall.

A more complex region can be modelled using complex Y junctions to model the manifold geometries just beyond the fuel injection region. This is shown in Figure 16 and Figure 17:

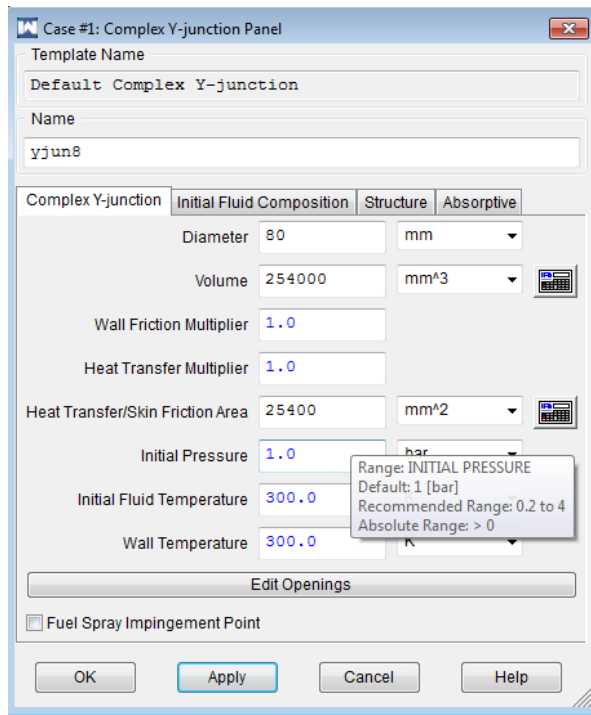


Figure 16 – Complex Junction Panel

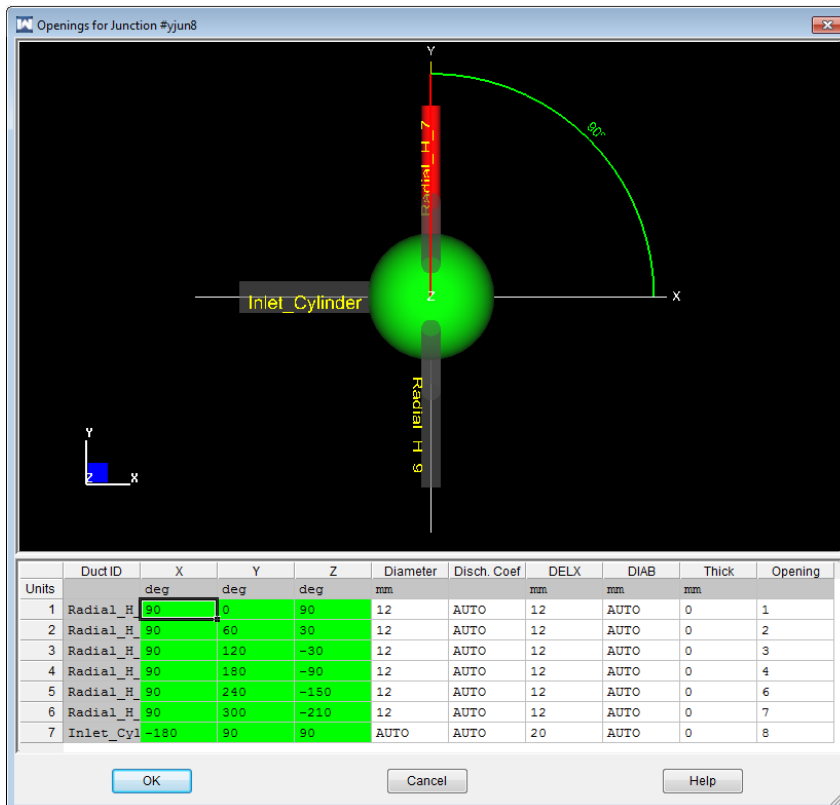


Figure 17 – Complex Y Junction Geometry Panel showing intake manifold for prototype engine

The intake manifold had a number of complex junctions that had to be accurately modelled. The volume and area were calculated from physical measurements and the ambient conditions for the intake were assumed constant (20°C, 100kPa). The exhaust duct temp and pressure was calculated based on rpm (air cooling) combustion temp and pressure. All initial values and inputs assume steady state conditions.

A Y-Junction is a junction that contains more than two openings or other geometries that cannot be adequately modelled with ducts and orifices. Used to model complex geometries such as intake manifolds, mufflers, air filters, and exhaust collectors.

Figure 16 shows the customization panel for the intake manifold junction. Y junctions should be used anytime that a desired geometry cannot be achieved through the use of ducts and orifices. Any flow junction that has a branched flow. (I.e. manifold), must be modelled with Y junctions. Complex Y junctions are represented by an arbitrary shaped volume. A three dimensional view allows for the arrangement of ducts relative to the junction to be modeled shown in Figure 17. Additionally length properties from the duct opening to the back wall of the volume, discharge coefficients and area change parameters can be modified.

For this reason, WaveBuild allows complex geometries to be imported into the model from 3D CAD files using a program called WaveMesher.

3.2.3 CONSTANTS TABLE

Inputs can be entered as a set value or replaced by a value that varies for different cases. I set up an array of cases for RPM 5 apart since most parameters vary depending on engine speed. Variables in the Constants Table (shown in Appendix B) can replace any inputs or values input into the model. This is particularly useful for when variables are RPM dependent, (temperatures due to increased convection, temperature increasing with more combustions occurring etc).

Status	Name	Units	Case 7	Case 8	Case 9	Case 10
1	A_F		28	24.1	22.2	20.8
2	BDUR	deg	43.931	45.426	46.308	47.082
3	CA50	deg	21.6360175	22.826565	23.61708	24.3060825
4	EV_TEMP	K	648	661	664	668
5	HEAD_TEMP	K	518	505	501	496
6	IV_TEMP	K	633	644	647	650
7	LINER_TEMP	K	525	516	513	509
8	PISTON_TEMP	K	562	564	564	564
9	SPEED	rpm	420	415	410	405
10	THERMAL_COND_HEAD	W/m.K	44.5935	44.8075	45.075	45.182
11	THERMAL_COND_LINER	W/m.K	42.6675	42.3465	41.758	41.5975
12	THERMAL_COND_PISTON	W/m.K	44.861	45.075	45.289	45.3425
13	THROTTLE_ANGLE	deg	81.7	81.7	81.7	81.7

Figure 18 – Constants table

Figure 18 shows all the adjustable properties as shown in Appendix B. By replacing properties with an array of different properties sourced from the input table, an array of values can be evaluated.

- Air to fuel ratio (shown as A_F). This varies over the RPM range and is determined predominantly by the carburetion system. It will be closest to stoichiometric (ideal mixture for complete combustion) around the peak engine performance. Prior to peak in power, the mixture will tend to be rich (with throttle fully open) and become lean beyond peak power. Since the simulations were run at full open throttle, the air to fuel ratio was modelled to match this pattern. The stoichiometric mix for methane is around 17:1. The ratio was adjusted during the validation process on the four stroke and was duplicated for the 2nd generation engine.
- Burn duration (BDUR), 50% burn point (CA50).

- Exhaust and inlet valve temperature (EV_TEMP & IV_TEMP). This increase as the rpm increases with the increase in combustion cycles. Values for these were sourced from default data for the combustion of methane and relative RPM.
- Head, Liner and Piston Temperatures as well as the thermal conductivity constants which vary with RPM due to the increase in forced conduction due the rotation of the engine. These were calculated based on the conduction through the engine block (steel conduction coefficient varies depending on temperature. Forced conduction increase with RPM was modelled by increasing the air convection coefficient.
- The throttle angle in the carburettor was also included to accommodate throttle changes during dynamometer runs. WOT was assumed otherwise.

3.2.4 ENGINE GENERAL PANEL

The the general engine panel shown in Figure 19 is the primary input screen. This represents the engine block and contains displacement, clearance height, compression ratio, bowl geometries and firing order, as well as typical friction correlations can be entered. Of particular use is the customizable piston motion. The default assumes sinusoidal motion. The firing order was set as 90 degrees apart in order to achieve the amount of thermodynamic cycles in a single revolution as explained in Section 3.2.1

Since the both prototypes are 2 cylinders, the 8 cylinders were modelled to make the power strokes per revolution equivalent. The intake manifold and exhausts are geometrically equivalent to the engine, taken from measurements of the engine itself and CAD data. The exhaust is a single pipe with a 90 degree turn. Although this is not shown visually for all cylinders, the properties and simulations reflect this.

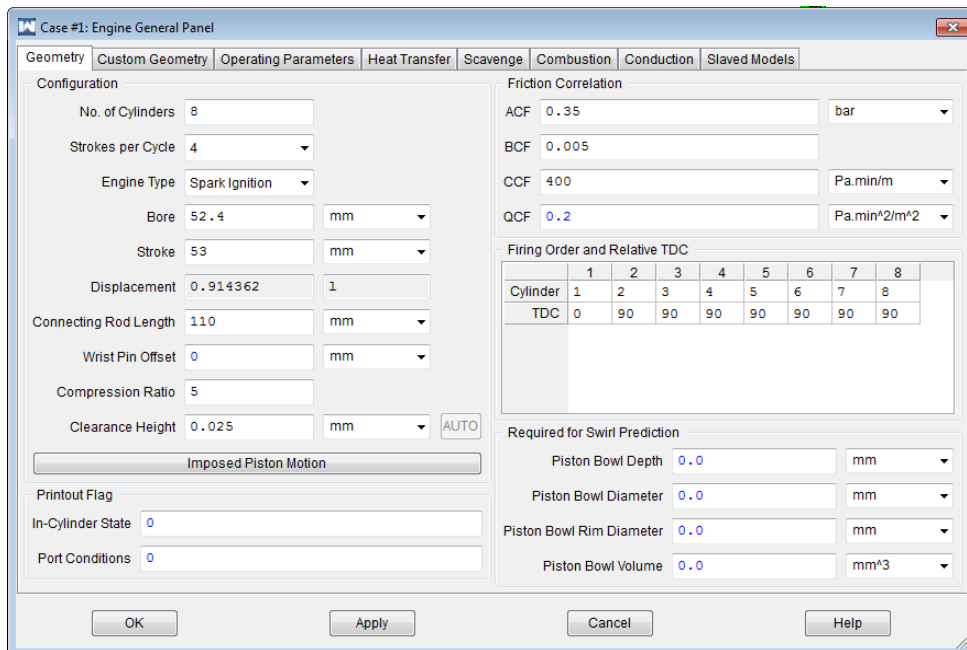


Figure 19 – General Engine Property Panel

What also can be noticed is the imposed Piston motion which allows deviations from the slider crank configuration. Valve settings need to be manually updated to match the piston trajectory.

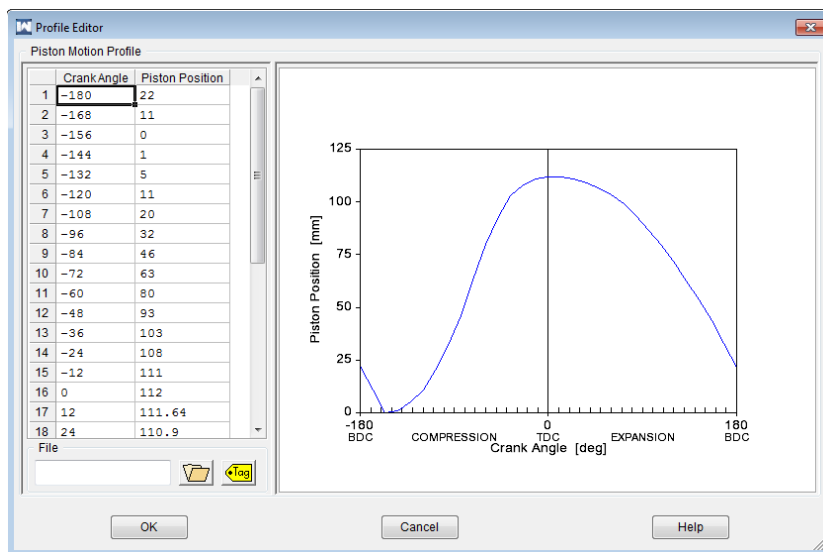


Figure 20 – Piston Trajectory Profile (Found in 'Imposed Piston Motion' Tab shown in Figure 19.) This is the original design piston trajectory profile

3.2.5 FRICTION AND DYNAMIC FACTORS

This panel also allows friction to be calculated. The four defaulted constants are modified from the Chen-Flyn correlation, based on higher friction due to the friction on the rollers compared to a traditional IC engine. For a reciprocating engine, the typical friction per cylinder based on wall friction, piston velocity and linkage losses is around 15%, based on the research done by Grant Smedley. Wave utilized the Chen-Flynn friction correlation model and allows this to be manipulated for a specific simulation. The constants of the friction model are identified within WAVE and related so that

Friction Mean Effective Pressure (FMEP);

$$FMEP = ACF + BCF \times P_{max} + CCF \times (rpm \times stroke/2) + QCF \times (rpm \times stroke /2)^2$$

Units and typical values are :

ACF – bar or psia - .5 bar, 7.35 psia

BCF – dimensionless – 0.006

CCF – Pa/min / m for both SI and BR units - 600

QCF - Pa min²/ m² – 0.2

In the absence of specific test data, a given FMEP value can be estimated and imposed by setting ACF to the FMEP value desired and the rest to 0.

Since the aim of this simulation was to find the power produced from the cylinders and the actual engine output is calculated from this, the default in cylinder frictional settings were used.

Another factor that had to be considered was inertial effects. Since the entire engine rotates, this was incorporated into the model by adding a rotational mass equivalent to a large flywheel attached to the engine.

3.2.6 HEAT TRANSFER AND CONDUCTION

The heat transfer tab allows surface areas and temperatures for the different components. It is these tabs that the inputs from the constant tables can be input so that the correct conductivity constants and relative temperatures are drawn for the respective RPM.

For the heat transfer model, there are several presets. A customized load compensating Woshini model was used. Load compensating adjusts temperature and friction for different RPM, reflecting the higher the opposing forces. Piston, head valve, liner temps vary over the RPM range and differ depending on their relative position relative to the combustion, intake and exhaust gases, for example, the intake is cooler than the exhaust temperature. These properties were calculated iteratively from simulations, until the resulting temps at diff rpm's matched those at steady state.

The cooling rates can be calculated and built into the model by entering the heat capacity of the components and the cooling system. The valves and pistons thermal properties are completely customizable. Dimensions are based on the actual sizes, other property were either based on typical IC engine values or calculated.

The conduction tab calculates heat mass transfer based on the thermal conductivity and cylinder geometric properties such as cylinder head, piston and liner thicknesses, volumes as well as heat capacities of the different parts, oil temperatures at different points, coolant temperatures which in this case was air and how much area is exposed to the areas. These were all calculated from the 3D CAD data.

Additionally, since the motor is air cooled, the rate of forced conduction increases as the RPM increases. This was calculated using the surface area of the cylinder head and calculating the airspeed which is dependent on the radius from the centre of rotation. This was reflected in the thermal conductivity coefficient in the input variable in Appendix C and D for the two stroke engine.

3.2.7 COMBUSTION

Combustion has a large influence on the engine output and a lot of research has gone into accurately modeling the combustion process. For this engine, the Wiebe combustion model shown in Figure 21 was used.

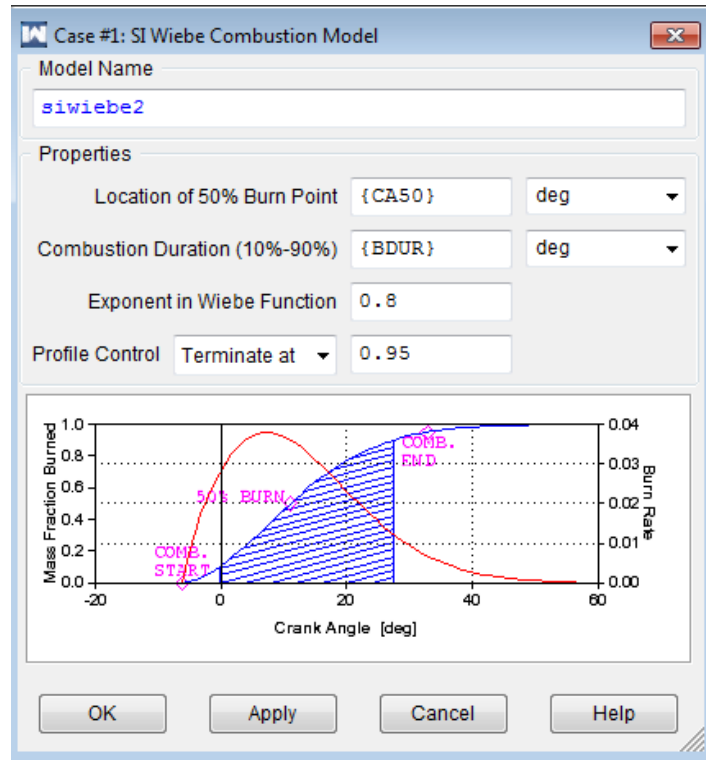


Figure 21 – Combustion Curve relative to crank angle

With reference to Figure 21, the Wiebe combustion model is defined by:

W = Cumulative mass fraction burned

$\Delta\theta$ = Crank degrees past start of combustion

$BDUR$ = User-entered 10-90 percent burn duration in crank angle degrees

$WEXP$ = User-entered Wiebe exponent

AWI = Internally calculated parameter to allow $BDUR$ to cover the 10-90 percent range

$CA50$ = User-entered 50 percent burn location in crank angle degrees after top-dead centre

The combustion duration and burn point have been left customizable, since these change over the RPM range. Without in-cylinder pressure measurements, the combustion model had to be predicted based on typical forced induction Wiebe function parameters. WAVE allows for three parameters in the Wiebe correlation to be input: 10-90 percent burn duration, 50 percent burn point, and the Wiebe exponent.

How the combustion used in the simulation effects the engine's performance was explored more in Section 2.4.5. See Annex B for details on what values were assigned to these values. A sensitivity analysis of the model showed that the dependency if the 50% burn point and burn duration did not have any significant effect on the model output. Reasons for this are that at steady state, the combustion temperatures remain constant and the increase in combustion frequency is balanced by the increased cooling due to the faster engine rotation. The components are assumed to have already reached a constant temperature and any variations would be relatively small.

For naturally aspirated engine the burn duration is relatively constant but does increase slightly with engine speed. Ignition timing advance increases with engine speed but the 50 percent burn location, CA50, remains relatively constant. Lastly, the Wiebe exponent, WEXP, tends to decrease with engine speed.

It was assumed that 95% of the fuel was successfully combusted.

3.2.8 FUEL DELIVERY

The four stroke had a 28 mm Kelhein carburetor which was modelled as a butterfly valve, that controls the amount of air enter the system. This is shown below in Figure 22 and Figure 23. The flow through the valve was assumed to be linear relationship depending on the angle of the throttle.

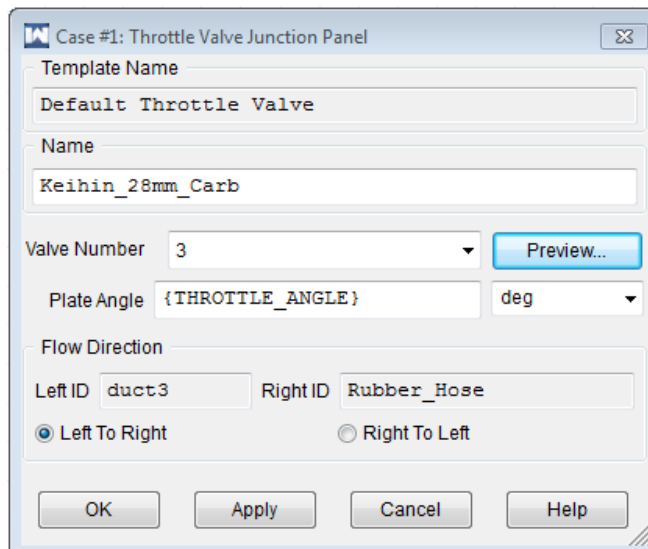


Figure 22 – Carburetor sub screen

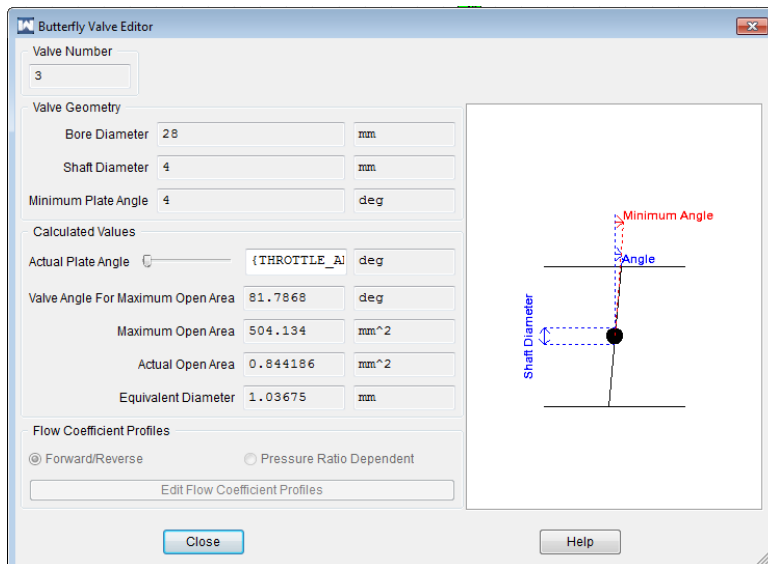


Figure 23 – Butterfly valve simulating throttle

Figure 23 shows the properties for the carburetor. The injection of fuel was simulated using an injector just prior to the carburetor (shown in Figure 24).

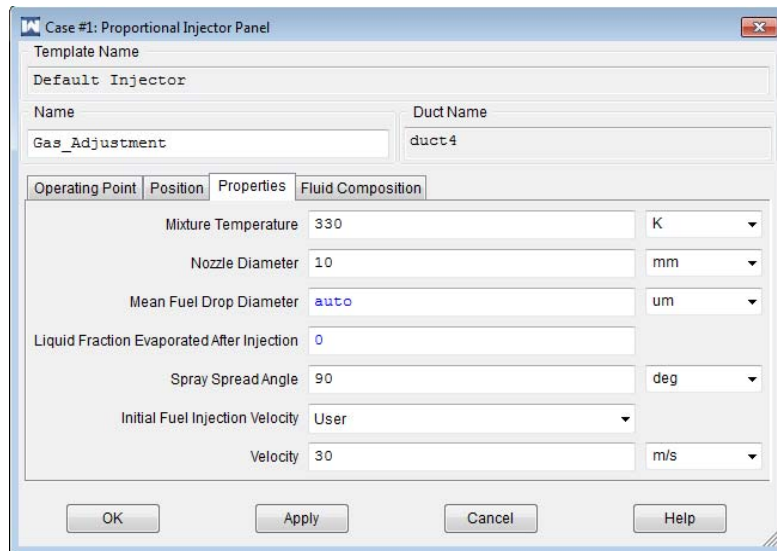


Figure 24 – Fuel injector properties

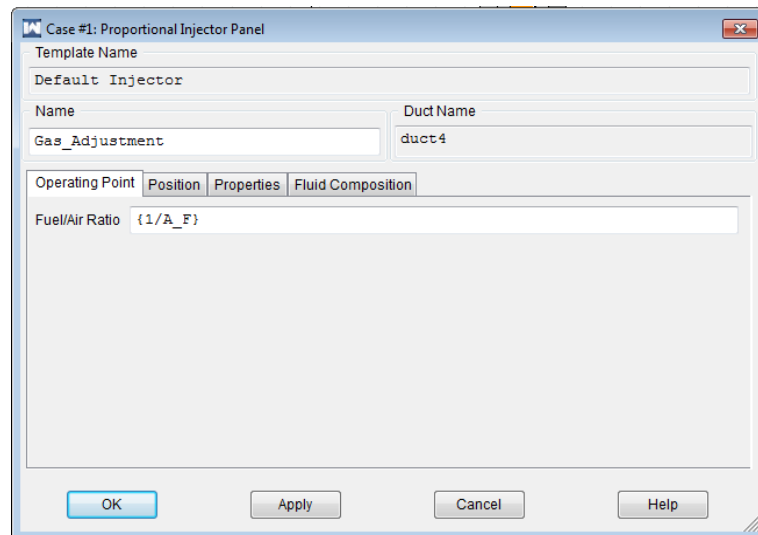


Figure 25 – Injector Sub-screen properties

This is the injection point of the gas / fuel modelled as an electronic injector. The values are based on a typical injector in a typical IC engine. This ensures perfect mixing prior to combustion, which is fair considering mostly gaseous injection and allows fair comparison between fuels, it also ensures that the fuel is completely vaporized so is suitable for gaseous or liquid fuel.

The fuel / air ratio is made adjustable by making it a function that can be entered into the properties for various RPM, shown in Appendix B.

Fuel delivery is achieved in WAVE by either entering a fuel rich ambient or using one of the many available fuel injectors. Internal dimensions of the venture duct were taken and entered into wave. A junction size is equal to the area in the carburetor at the throttle butterfly were entered to accommodate for the flow restriction at this point. A proportional fuel injector was used and the fuel /air ratio component was set as a variable in the constants table to allow this to be varied at each rpm increment in order to match the carburetor. The fuel air ratio was varied in wave to achieve a comparable temperature profile to the real engine data. This had a significant effect the performance. This variable was adjusted to reflect the amount of fuel consumed during dynamometer runs.

3.2.9 VALVES

The valves are critical influencing factors on engine performance because the flow through the engine is highly dependent on the flow through cylinder head port. The lift profile and flow coefficients were sourced from data found on the Honda 125 engines and entered into the model as shown in Figure 29 through to Figure 33.

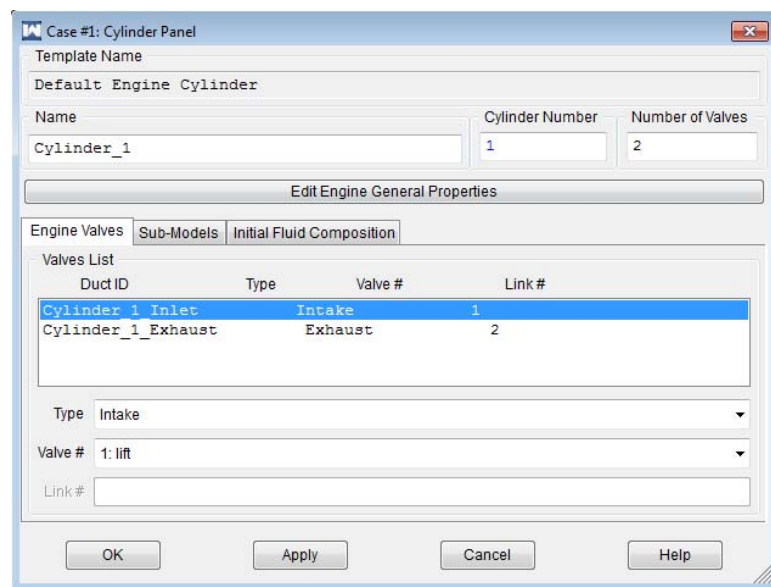


Figure 26 – Cylinder head panel

Figure 26 shows the inlet valve, allowing the adjustment of timing, flow coefficients and swirl.

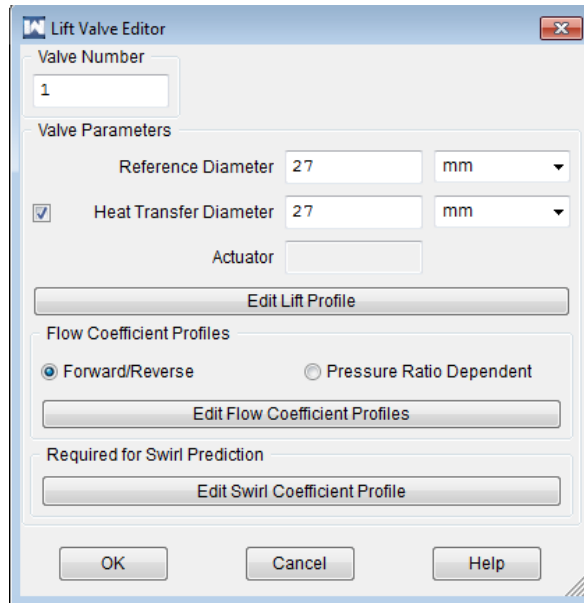


Figure 27 – Intake Valve Panel

Valve models are based on the thermodynamics and fluid dynamics of isentropic (i.e. ideal reversible) gas flow and principles of conservation of mass and energy. How valve settings affect the performance of this engine is explored in section 4.3.1. The simulation treats the valve area as a function of crank angle and assumes steady state flow. Wave accounts for gas flow interaction with various selectable valve configurations and provides for the fact the dynamic effects of the gas flow result in an “effective area” of the valve opening being less than the geometric area,

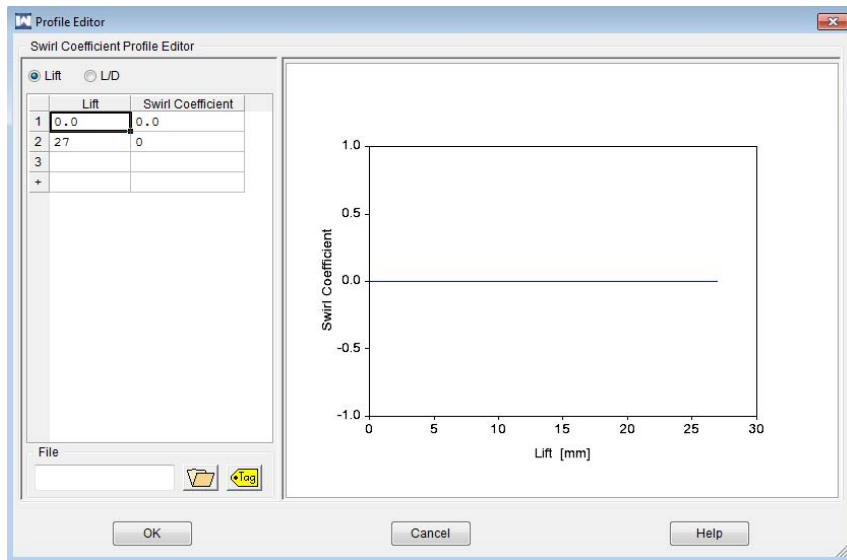


Figure 28 – Swirl coefficient profile editor for intake valve

Swirl was omitted from the 4 stroke model as the valves are not designed for swirl.

The second advanced input within the cylinder head is the valve lift per crankshaft rotation. The valve lift per camshaft rotation can be measured by incrementally rotating the camshaft and measuring valve lift. This was established for a 3D cad file of the two stroke and the four stroke were measured from an identical 125 motor.

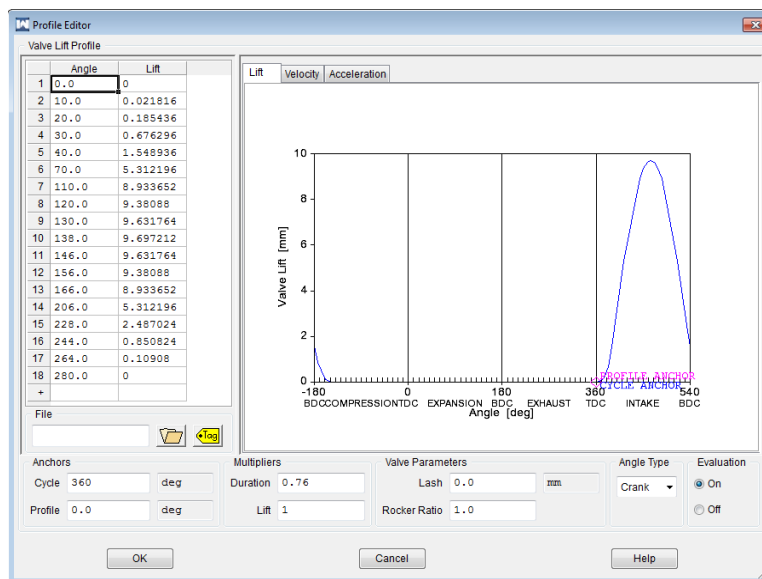


Figure 29 – Inlet valve lift profile in relation to phase

Figure 29 through to Figure 33 show the lift profile of the valves and the corresponding flow coefficient. This is typically found by flow bench data. Because the initial prototype was two Honda 125 engines, the flow bench data was easily acquired. The second prototype was scaled up and tweaked based on size, timing of engines of similar displacement.

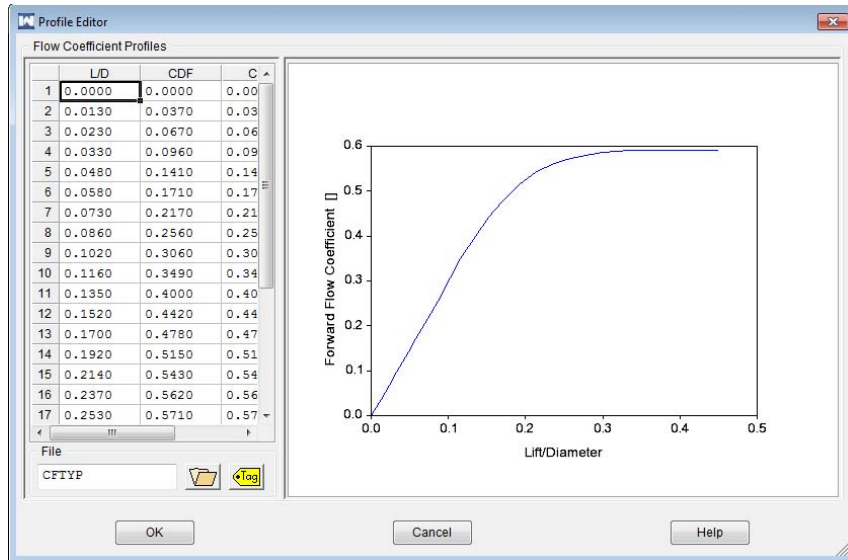


Figure 30 – Flow coefficient profile for inlet valve

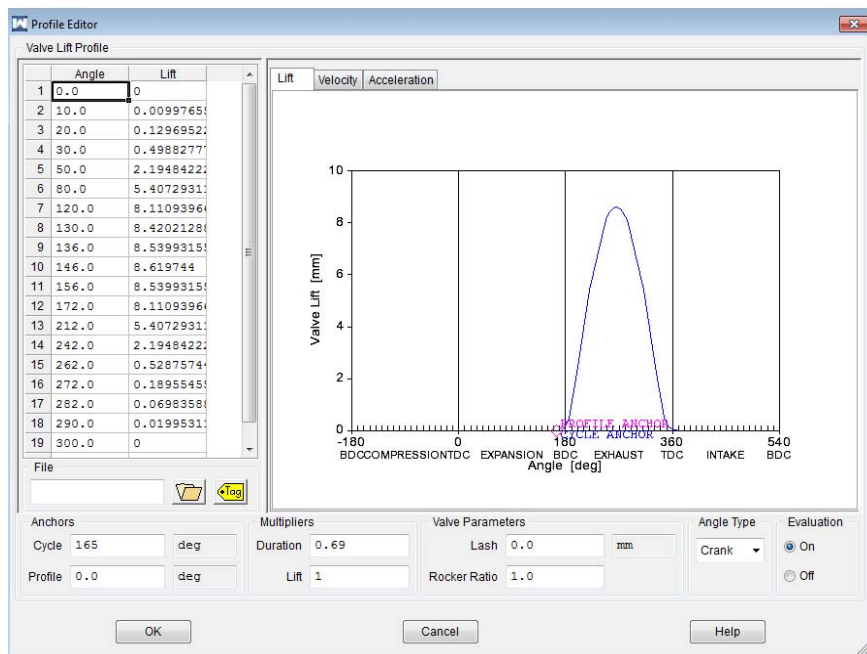


Figure 31 – Exhaust valve lift profile in relation to phase

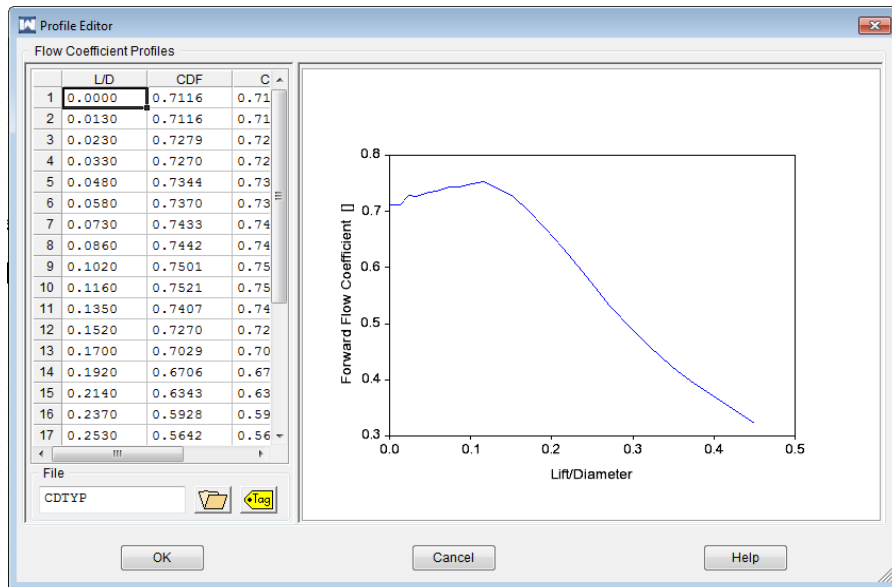


Figure 32 – Flow coefficient profile for exhaust valve

3.2.10 TUNING

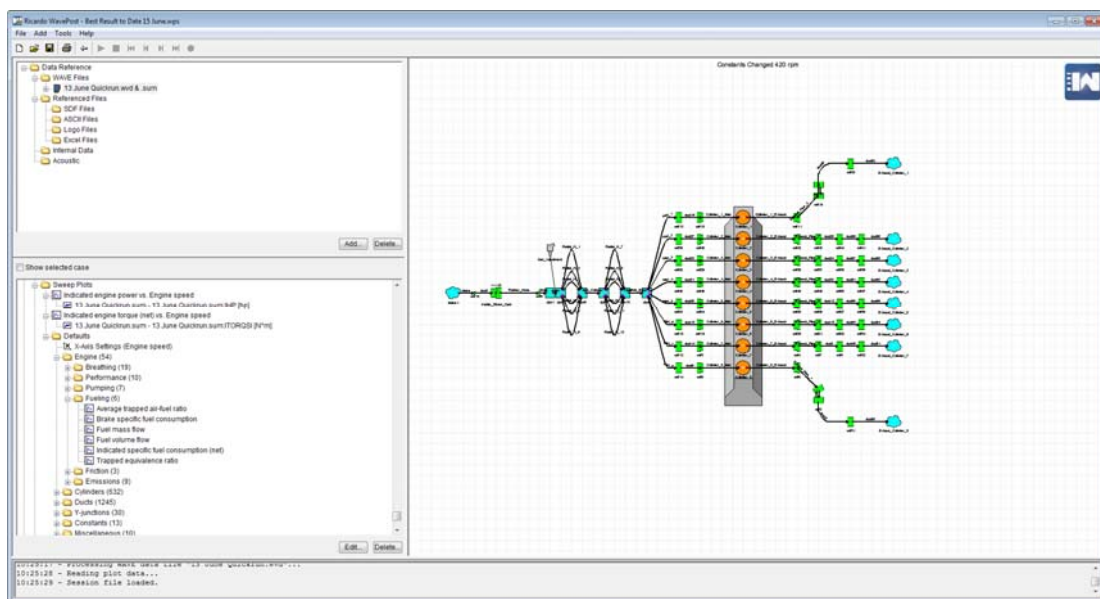


Figure 33 – Results page, showing various properties that can be extracted from a simulation

WAVE is the solver that performs all the calculations needed to simulate engine operation. It is a non-interactive program that runs in a DOS window while streaming certain output data and simulation progress. The output data shown during simulation runtime can be customized to show parameters of interest.

These parameters can be used as indicators to show whether or not the simulation is reducing reasonable results, allowing the simulation to be prematurely stopped if the model is not function properly. Once a simulation is finished, a large output file is created that contains all data needed to analyze the simulated engine operation. WavePost is the post-processor for WAVE simulations that allows interpretation of simulation results. It allows for the creation of: time plots, sweep plots, spatial plots (animated), and TCMAP plot

One of the obvious trends in almost all scenarios is the sudden drop off in power after certain point which suggests a restriction. This is the point in which the throttle is decreased as RPM above this point is thought to be impossible.

Manual convergence was used to reach many of the initial conditions.

3.2.11 OUTPUT CALIBRATION

Ricardo allows the outputs to be modified with the addition of multipliers. The multipliers required are outlined in Section 2.2 to convert the Ricardo torque output into the actual torque output. This is where the leverage advantage of the engine can be factored in.

Figure 34 compares how the subject engine and how a typical slider crank engine convert essentially the same combustion force (F_1) into useable torque.

With reference to configuration shown on the right side of Figure 34, the torque output calculated by Ricardo is as follows;

Downforce produced from combustion on the piston head = $F_{Combustion}$

Crank (Ricardo) = R_1 = Stroke / 2

Ricardo output Torque, $T_{Ricardo} = F_{combustion} \times R_1$ (1)

Therefore, the torque output from Ricardo needs to be modified by a factor to simulate the geometry of the subject engine configuration.

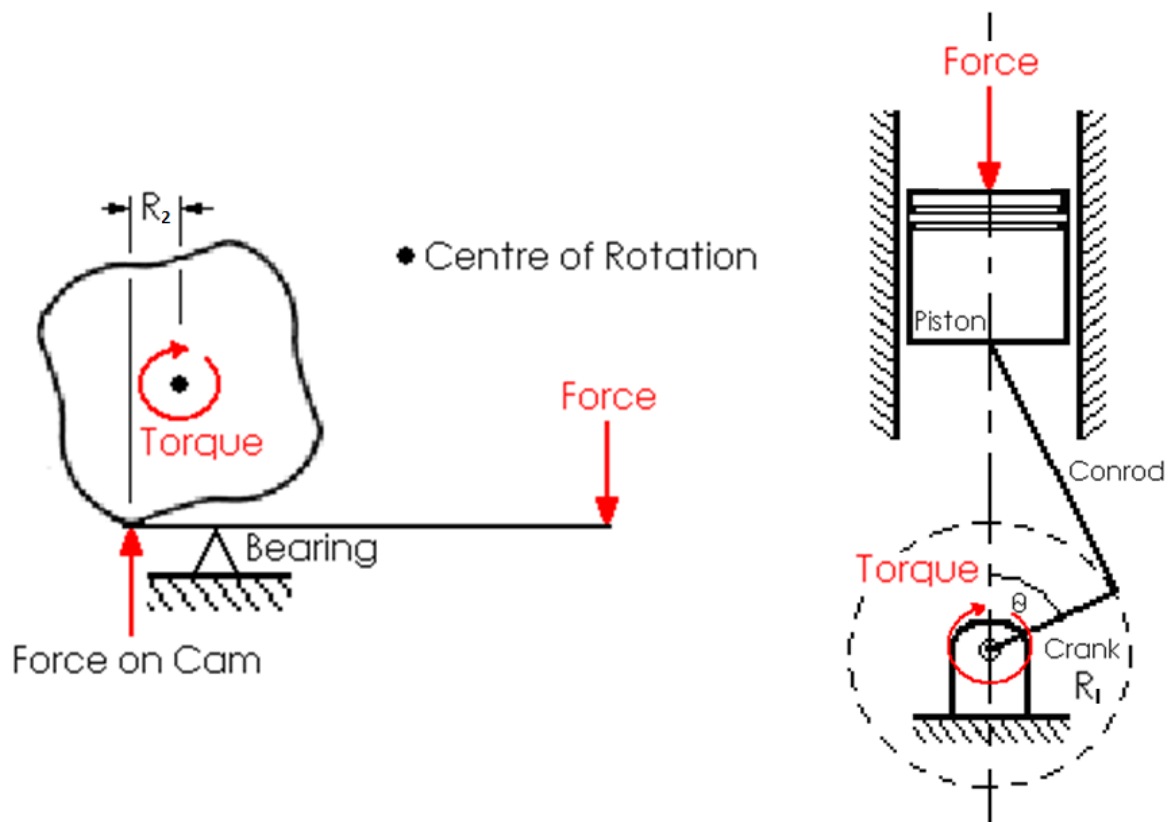


Figure 34 – Force Body Diagram of System compared to Typical ICE Slider Crank Mechanism

The force on the cam is the difference between the leveraged force on the bearing and the cam. A torque output value could determine how much force is imparted on the bearing. A strain gauge could be used to determine the exact force on the bearing. However, without data, it is assumed that the bearing imparts no upward force and acts as a fulcrum to determine the maximum possible force that this engine could impart without cam friction or resistance to engine rotation. It assumes that the engine is already in motion.

Referring to Figure 34, the modified torque output is calculated found as follows;

$$T_{Actual} = F_{Cam} \times R_2 \quad (2)$$

Therefore the factor 'X' that the torque output the 4 stroke Ricardo model needs to be modified by is as follows

$$T_{Actual} = X \times T_{Ricardo} \quad (3)$$

For the force on the cam, the leverage off the bearing needs to be factored against the combustion force. Using the FBD in Figure 4, the force on the cam is related to the combustion force by the taking moments around where the bearing supports the lever arm. The leverage is described by LR = longer length / shorter length of the lever arm.

$$F_{Cam} = LR \times F_{combustion} \quad (4)$$

Substituting equations (1) and (2) and (4) into (3) yields the following expression;

$$LR \times F_{combustion} \times R_2 = X \times F_{combustion} \times R_1$$

Solving for the multiplication factor, X;

$$X = LR \times R_2 \div R_1 \quad (5)$$

For the 4 stroke prototype;

$$\text{Lever arm Ratio, } LR = 200 \div 54 = 3.704$$

$$R_1 = \text{stroke} \div 2 = 53\text{mm} \div 2 = 26.5 \text{ mm}$$

$$\text{Roller, Cam Offset} = R_2 = 13.5\text{mm}$$

Using equation (3) and (5), the Ricardo output torque needs to be modified by the following magnitude;

$$X_{4 \text{ Stroke}} = 3.704 \times 13.5 / 26.5 = 1.89$$

$$T_{Actual \ 4 \ Stroke} = 1.89 \times T_{Ricardo \ 4 \ Stroke}$$

The 2nd prototype's output is modified in the same manner, with a stroke of 112mm, Roller / Cam offset of 21.25mm and the lever shown in Figure 4 and Figure 7. Lever arm Ratio, LR;

$$LR = 300 \div \sqrt{(72.3^2 + 20.1^2)} = 4.00 \quad (\text{Refer to Figure 4})$$

$$X_{2 \text{ Stroke}} = 4 \times 21.25 / 56 = 1.52$$

$$T_{Actual \ 2 \ Stroke} = 1.52 \times T_{Ricardo \ 2 \ Stroke}$$

3.2.12 VALIDATION

Dynamometer information was gathered although the throttle positions were not exact during run. The engine started to become unstable during the run, causing the operator (Bill) to button off. The instability was due to balancing, vibration and the forces on the linkages were overcoming the damping springs, causing the rollers to lift off the cam. The throttle position was approximated on best guess and by iterative simulations to gain more accurate combustion temps, the 4 stroke was finally successfully modelled.

3.3 MODELLING OF TWO STROKE PROTOTYPE STROKE ENGINE

Some of the 2nd generation engine design has already been finalized. This includes the bore sizes, piston head design, area transfers and geometry of the flywheel / cylinders. The intake system has been somewhat simplified. The carburetor was not finalized so the same fuel delivery system used in the 4 stroke version was scaled up. The heat transfer areas have been incorporated into the forced conduction calculations.

The GUI is the very similar, as shown in Figure 35.

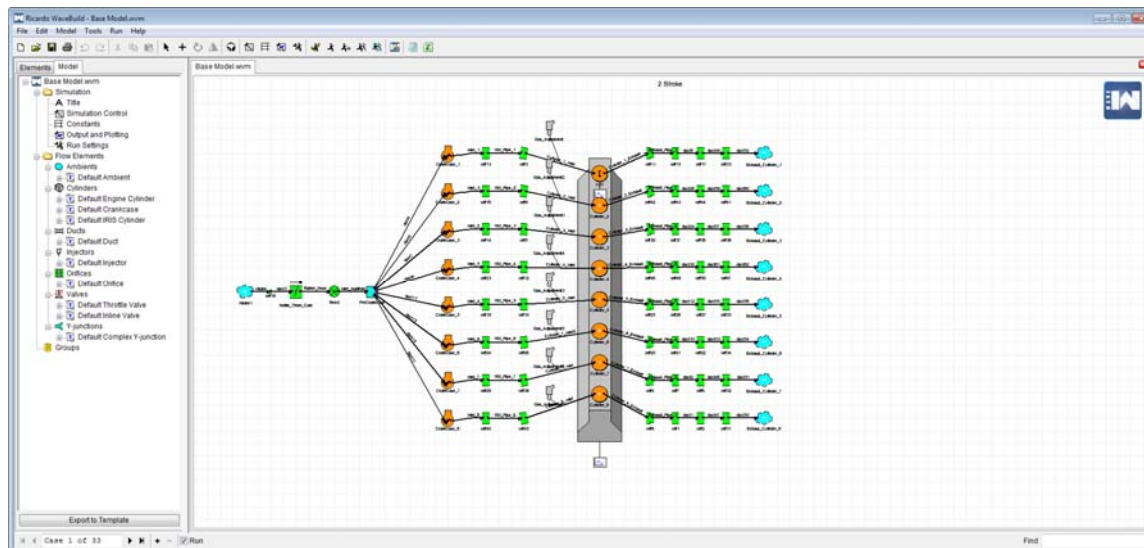


Figure 35 – GUI Panel for 2 Stroke Engine

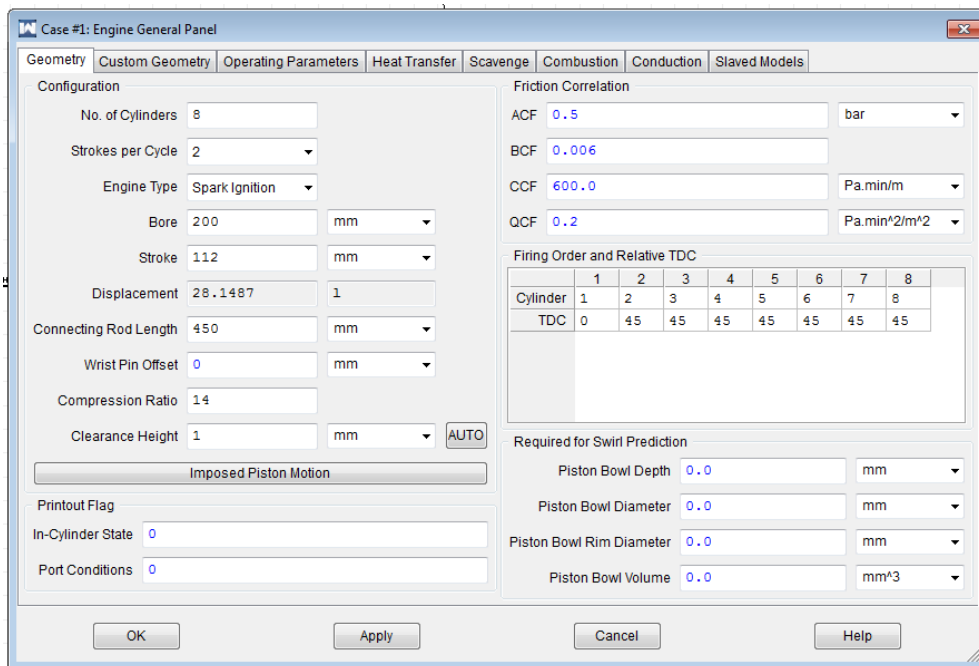


Figure 36 – General Engine Panel for 2 stroke prototype

Some changes from the 4 stroke model can be seen from Figure 36. The power strokes being reduced to 45 degrees apart as well as the changes in engine scale.

3.3.1 COMBUSTION

Based on the high amount of turbulence and squish, initial combustion was fast. Figure 37 illustrates the new combustion model.

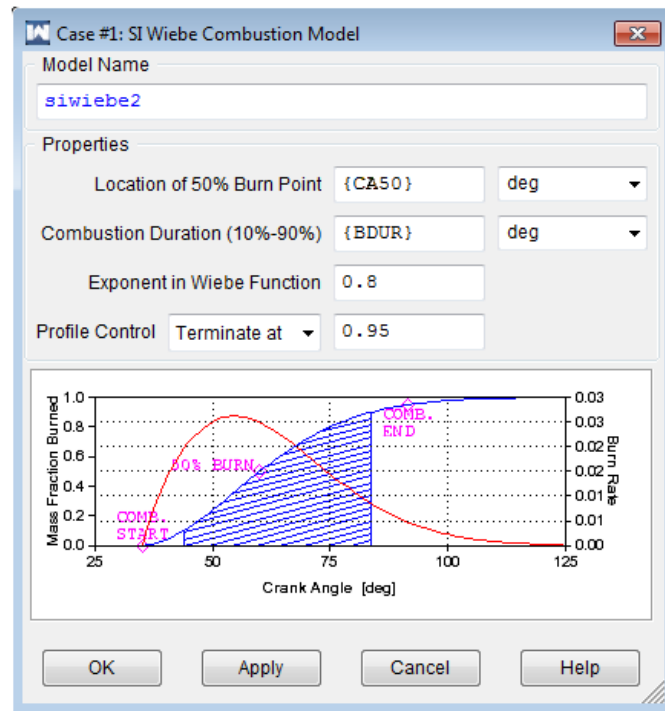


Figure 37 – Combustion (Wiebe) Curve relative to crank position

Combustion is assumed to be much more effective due to the much higher turbulence, effective use of swirl and squish and most importantly, multiple spark plugs that can be independently operated to ensure that the maximum amount of fuel is combusted. This will allow the use of very low quality fuel.

3.3.2 CRANKCASE AND VALVES

Another addition was the crankcase elements. These required the addition of reed valves for the intake. The transfer does not have a valve and is closed off by the piston but a valve is used to simulate the piston opening and closing the transfers.

An additional valve was included to model the reed valves and transfers ports which were modelled based on the physical geometries drawn from the CAD model.

Initially an orifice valve (open at all times) was used and a reed valve was modelled at the intake port. The flow coefficients for this are shown in Figure 38. The details of the Reed Valve used are shown at the end of Appendix D.

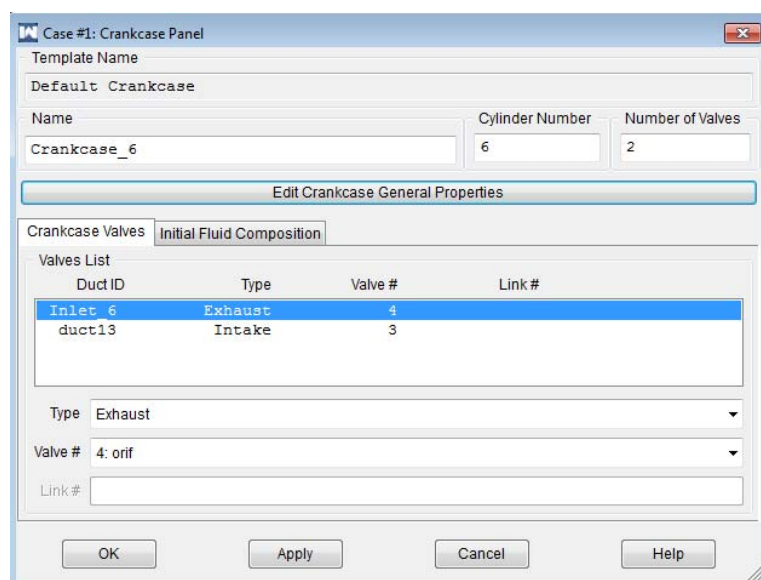


Figure 38 – Crankcase Panel

The 2 stroke variant did have the transfers and piston slope set up to encourage swirl and a conservative flat 0.5 swirl coefficient was assigned for all points of valve lift. There is a large degree of uncertainty associated with this quantity but a sensitivity analysis for the 2 stroke engine revealed that the influence of swirl was negligible compared to the effects of altering the compression ratio, crankcase compression ratio and squish area. The 0.5 linear flat swirl coefficient was therefore deemed acceptable for the investigation.

3.3.3 SCAVENGING

For the scavenging model, there are three scavenging models available in WAVE. The first is a mixed flow model, which assumes that the fresh intake charge instantaneous mixes with the spent exhaust gases in the combustion chamber to form a uniformly distributed 50-50 mix of exhaust and intake charge. The second is a cubic curve approximation and the third is user defined. Since no scavenging data was available, the first model was assumed.

3.3.4 SENSITIVITY AND PARAMETER ANALYSIS

Once the mode was predicting reasonable results, it was further refined. Boundary conditions and initial conditions were input to converge on actual temperatures and pressures measured at different junctions. This helps improve model accuracy and decreases computational time needed for convergence.

Air and fuel ratio ratios changes depending on throttle position. The Kelheim carb used on the 1st prototype engine was duplicated and upsized for the 2nd generation relative to the displacement increase.

Before attempting to optimize an entire package, general trends, sensitivities, and near-optimal values should be investigated.

A sensitivity analysis gives an indication to which parameters were most significant in the simulation. One parameter would be changed while the rest kept constant.

3.3.5 GAS COMPRESSIBILITY.

Ricardo allows to compressibility scenarios. Ideal gas and real gas scenarios were both entered into the simulator WAVE allows for both transient and steady-state engine simulations. While transient simulations can provided a more detailed representation of engine performance, steady-state simulations are better suited for simulations in their early stages of development for various reasons. A significant advantage of steady-state simulations is that parameters can be modified independently for each engine speed simulated.

A more in depth investigation can be conducted later with different configurations allows exploration of performance possibilities.

For the 4 stroke model, because of the relatively simple combustion chamber and intake system, there was no significant difference between using ideal or real gas for the simulations. Therefore, ideal gas was assumed for the remainder of simulations since this greatly reduced the simulation time.

The effect of upsizing the displacement of the engine was first investigated by altering the stroke and bore. First by keeping the relative ratios of bore and stroke, then the stroke and bore were altered independently to see how this influenced engine output.

3.3.6 SQUISH

Ricardo allows custom geometry for squish. Squish can have a high influence on combustion so was modelled from the CAD models and left. Varying the compression ratio has a similar effect on performance and was sufficient for this investigation.

3.3.7 UPSTREAM BREATHING RESTRICTION INVESTIGATION

The sensitivity of the intake and exhaust system was tested by widening and closing the intake geometries. Predictably, this had a large influence on the performance. The area was adjusted, keeping all other combustion properties and geometries constant until the optimal size for the intakes and exhaust for the engine's displacement and valve sizing was found through iterative simulations. These areas were used for all subsequent investigations into the 2 stroke design and were scaled relative to engine displacement.

3.3.8 UNIFLOW SCAVENGING

This property has a large influence, but since designing an appropriate exhaust and expansion chamber to capitalize on scavenging is out of scope, a standard Ricardo default scavenging model was assumed so that the 2 stroke performance could be explored although this property does warrant further investigation for a custom engine build as it can be altered to provide the desired performance. Perfect scavenging was not assumed since the crankcase compression ratio is being altered and has a high influence on scavenge. The higher the CCR, the higher the pressure the fresh mixture coming through the transfer is, reducing the amount of exhaust gases being scavenged.

3.3.9 IGNITION TIMING, COMBUSTION AND FUEL ANALYSIS

Methane is relatively slow burning compared to other hydrocarbons and this needed to be incorporated into the simulation. Three combustion curves were created to investigate the sensitivity and influence the fuel type has on input. The three types were;

- Standard petroleum, which is the Ricardo default for an IC engine.
- High Quality Methane, (30 - 80% methane concentration) Low quality methane, 50%

The variables are burn duration, peak and the exponent function which adjusts the ferocity of the ignition. These are shown on Table 4 below. The more refined the methane, the faster the combustion. The combustion goal for the engine is to achieve a lean burn using poor quality methane while retaining reasonable performance. This would give the engine a significant efficiency advantage over other IC technologies.

Combustion Model	Burn Duration	50% Burn Point	Exponent
Ricardo defaults	20	8	2
Natural gas engine 1*	26	14	2
Nat gas engine 2*	22	12	2
Lower Quality Methane	35	15	1.8

Table 4 – Combustion Constants for Fuel Types.

* S Rousseau, B Lemoult and M Tazerout tested several natural gas Wiebe curves, Natural gas engine 1 and Natural gas engine 2 are there two test cases.

The methane case shown in Figure 39 below was constructed using the values from two separate combustion studies shown in Table 4. Notice that ignition is advanced and burn duration is prolonged for the methane. Decreasing the exponent translates to a slower burn which is expected for the methane

combustion. The profile control determines what percent of the fuel is combusted. 90% is the default and for the lower quality, 80% combustion is assumed (using multiple ignition points).

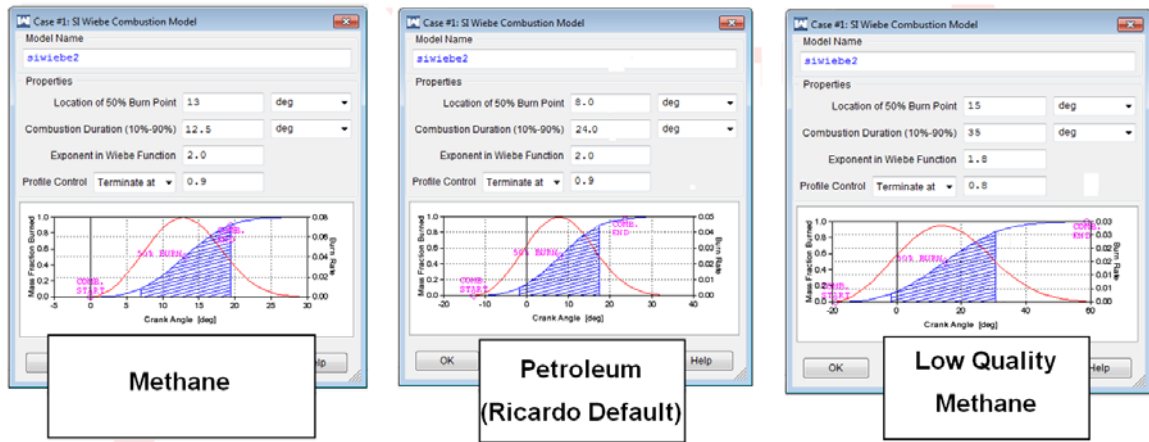


Figure 39 – Tested Combustion Models

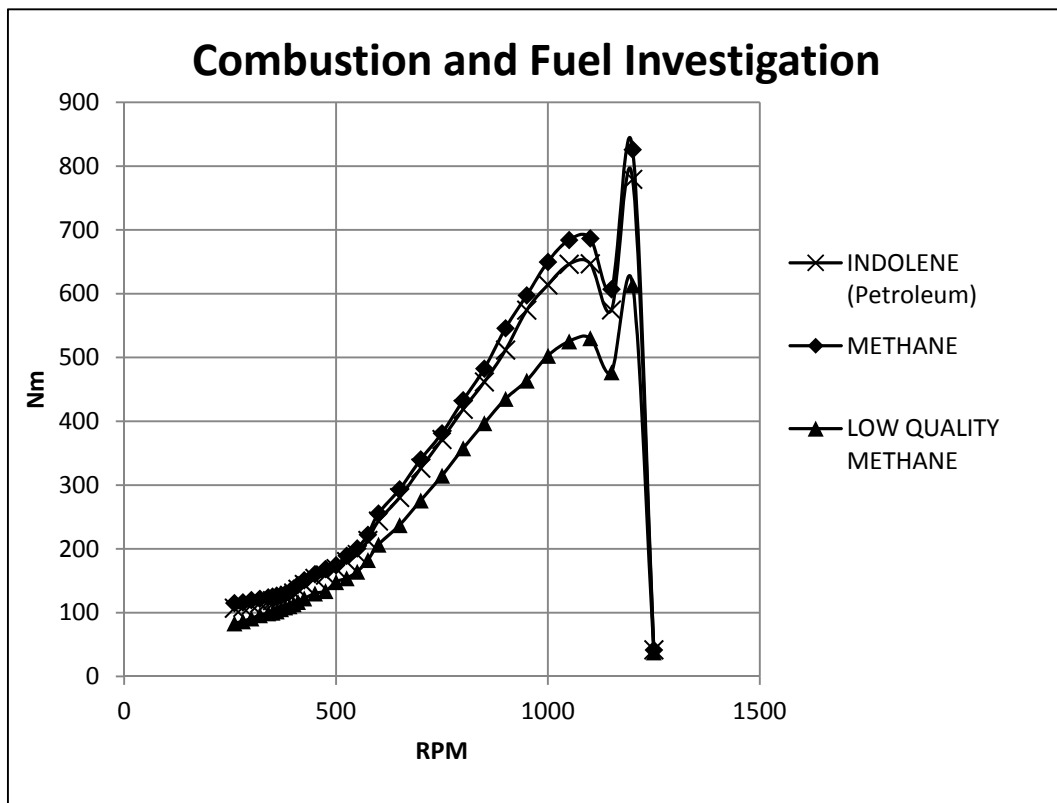


Figure 40 – Output Comparison for Fuel Types.

This showed that the combustion rate was not very sensitive for this displacement and running this slow. This showed that indolene and methane are offer similar output on this engine configuration and the lower quality fuel still follows the same approximate curve. Interestingly, the methane slightly outperformed petroleum using this engine configuration. The reason for this is because methane releases more heat per mass than indolene and each simulation were run assuming equivalent mass of fuel. The methane was selected to explore other performance characteristics since the shape of the output curve remained constant and only the magnitude was affected, therefore a fixed burn duration of 25 degrees and a 50% burn point of 13 degrees was selected based on the two natural gas studies under investigation as shown in Figure 41.

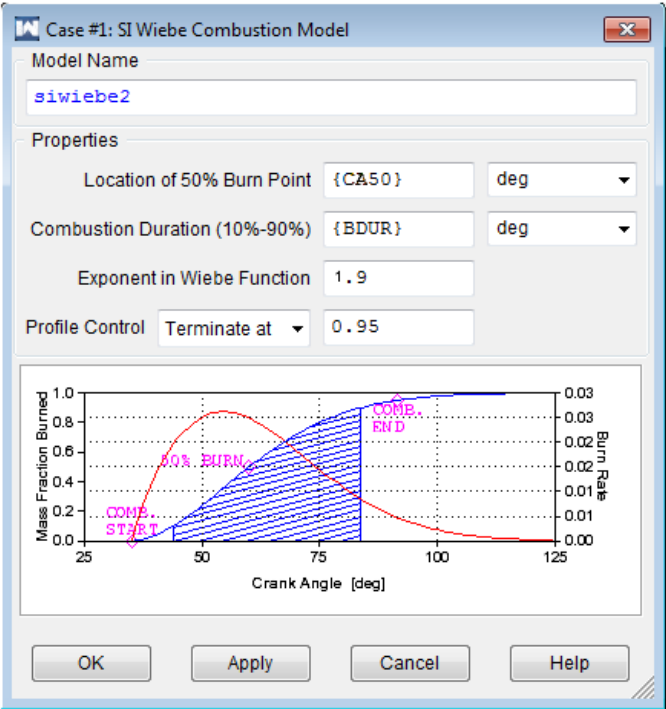


Figure 41 – Combustion (Wiebe) Curve relative to crank position used for investigation

4 RESULTS

4.1 4 STROKE PERFORMANCE

Shown in Figure 42 is the simulated torque predicted by the Ricardo Model, compared to the torque measured on the dynamometer for the 1st prototype that used two 125 cc 4 stroke honda engines.

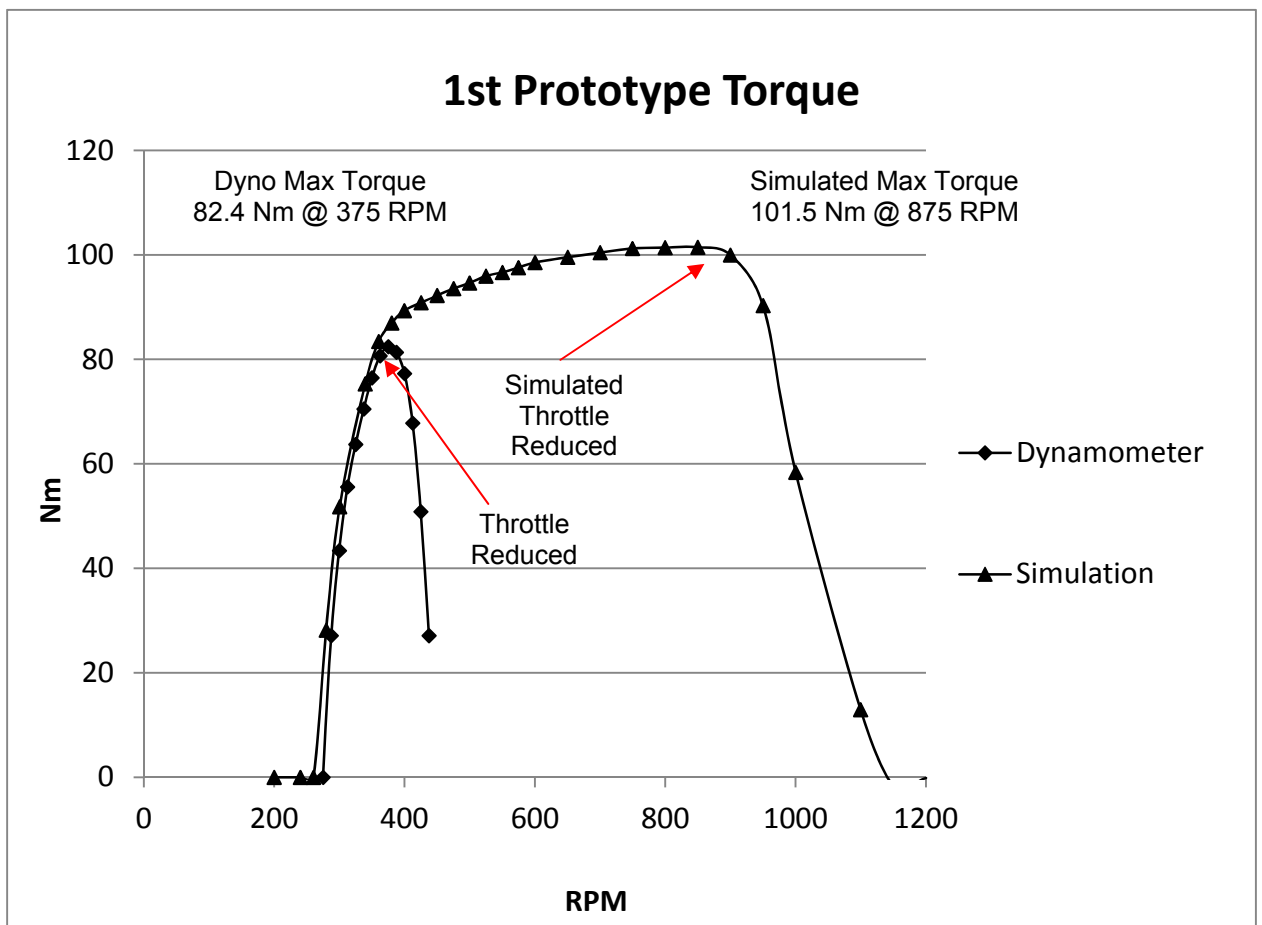


Figure 42 – 1st Prototype (2 cylinder, 250cc) Torque Curves

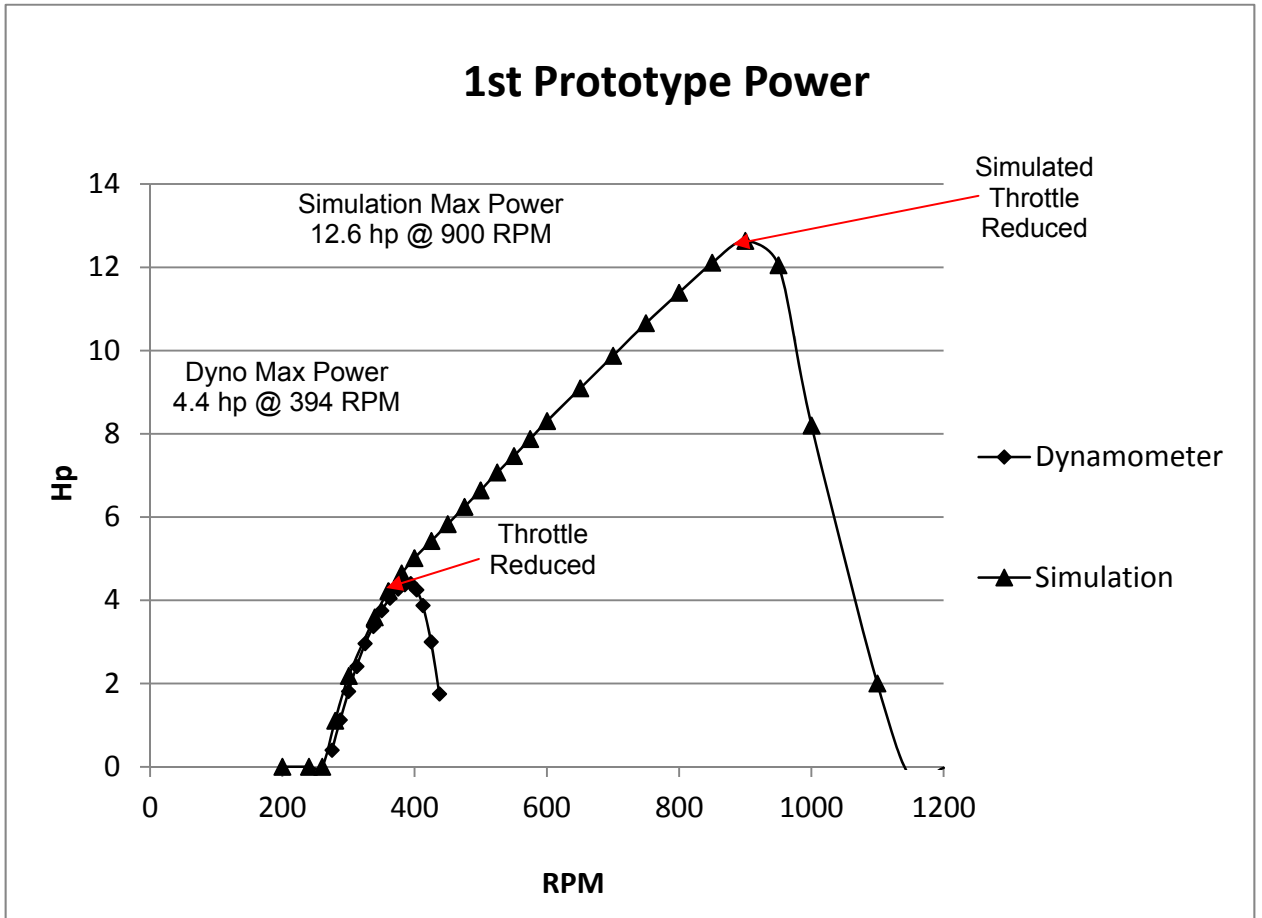


Figure 43 – 1st Prototype (2 cylinder, 250cc) Power Curves

4.1.1 VALIDATION

The model correlates well (within 5% for 200 – 400 RPM) but unfortunately the dyno run did not continue beyond 400 rpm. The simulated throttle reduced from 1000 RPM and was closed at 1200 rpm. The contrast between the simulated power and the actual measured power is expected since hp is a function of RPM and torque and since the torque curve is reasonably flat, then this explains the linear increase in power. The higher frictional forces and losses in the linkages experienced by the actual engine cause a lower output than what has been predicted.

4.2 2 STROKE BASE PREDICTION

Case #1: Engine General Panel

Geometry Custom Geometry Operating Parameters Heat Transfer Scavenge Combustion Conduction Slaved Models

Configuration

No. of Cylinders 8

Strokes per Cycle 2

Engine Type Spark Ignition

Bore 200 mm

Stroke 112 mm

Displacement 28.1487 1

Connecting Rod Length 450 mm

Wrist Pin Offset 0 mm

Compression Ratio 14

Clearance Height 1 mm AUTO

Imposed Piston Motion

Printout Flag

In-Cylinder State 0

Port Conditions 0

Friction Correlation

ACF 0.5 bar

BCF 0.006

CCF 600.0 Pa.min/m

QCF 0.2 Pa.min²/m²

Firing Order and Relative TDC

	1	2	3	4	5	6	7	8
Cylinder	1	2	3	4	5	6	7	8
TDC	0	45	45	45	45	45	45	45

Required for Swirl Prediction

Piston Bowl Depth 0.0 mm

Piston Bowl Diameter 0.0 mm

Piston Bowl Rim Diameter 0.0 mm

Piston Bowl Volume 0.0 mm³

OK Apply Cancel Help

Figure 44 - 2nd Prototype Prediction, Basic Engine Parameters

Figure 44 shows the engine parameters for the two stroke model. Note that the firing frequency is doubled .

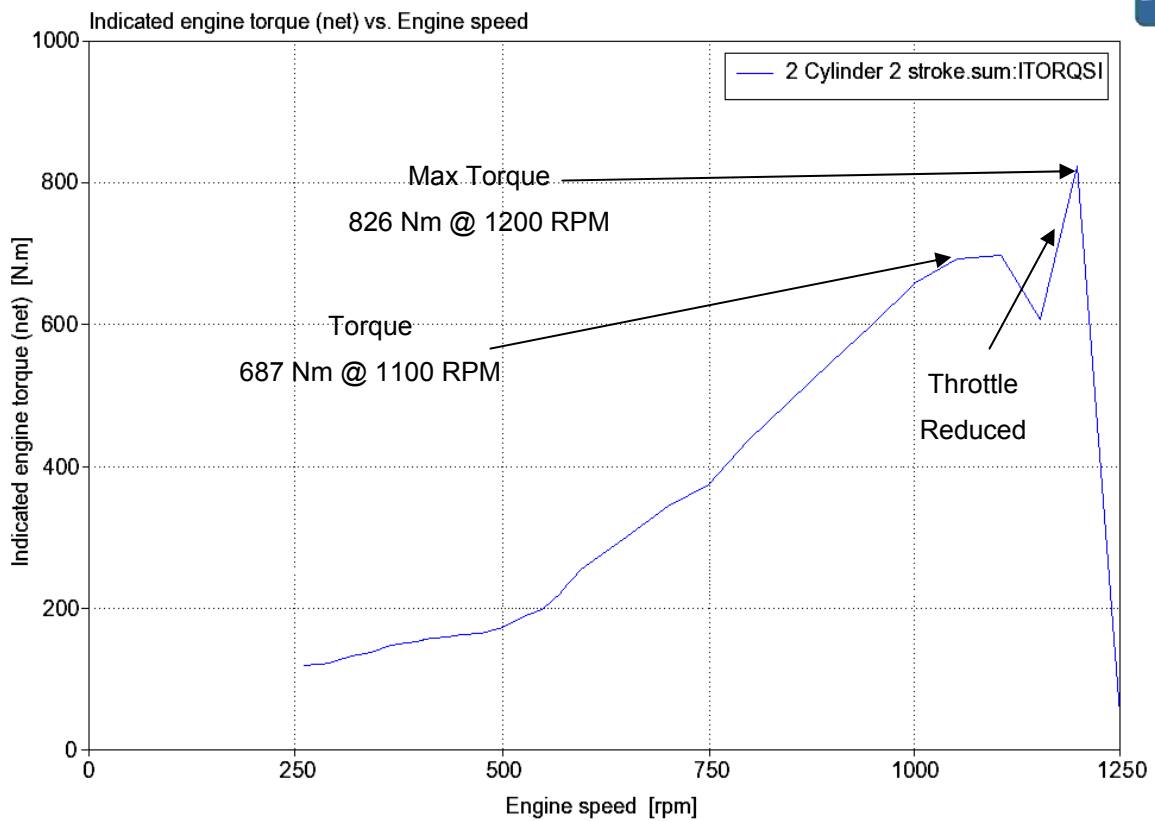


Figure 45 –2nd Prototype (2 cylinder, 28L) Torque Curve Prediction

The following properties have been scaled up from the initial prototype, proportionate to displacement;

- Intake geometry.
- Air to Fuel Ratio with RPM.
- Frictional Forces.
- Valve sizing, flow coefficients etc.
- Heat transfer and conduction.

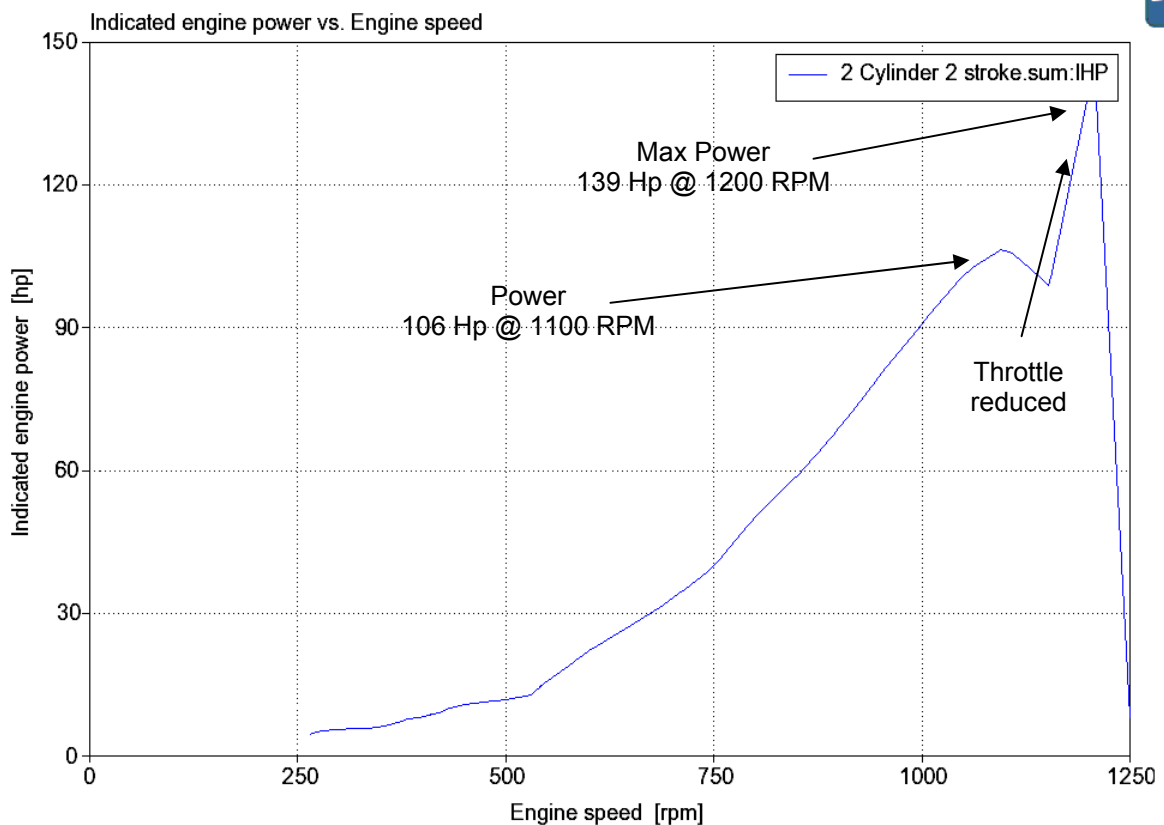


Figure 46 –2nd Prototype (2 cylinder, 28L) Power Curve Prediction

4.2.1 VALIDATION

The 2 stroke model is yet to be validated against the real engine as the bearings in the linkages failed when the engine was first started. This was likely due to the roller not moving fluently coupled with the use of large leverage and a large engine displacement. Validation will be required before the simulation can be used with confidence.

The peak can easily be identified around 1100rpm where the ports are operating most efficiently. The small drop after peak is expecting from as throttling begins to occur. The slow increase in torque at lower rpm was the lag caused by having to accelerate the large flywheel modelled to simulate the rotating mass of the engine. The sudden increase after the peak was not anticipated but since this is above the

peak and a useable RPM for the engine, this was considered an error, likely due to the scavenging model.

In the interim, this data will be used to for the investigation into exploring the theoretical performance potential of this engine by altering the piston trajectories and other characteristics.

4.3 INVESTIGATION AND OPTIMIZATION FOR PERFORMANCE PREDICTING

The following section explores the parameters that are known to have a large influence on engine performance. Specifically under observation is how the engine combusts methane when the piston trajectory is altered and how dwell at BDC and TDC affect performance.

Prior to altering the piston dwell geometry, other engine characteristics needed investigating to devolve an understanding for the engine's sensitivities. The sensitivity investigation also provides valuable data to assist in the prediction of performance for engine variants and explore the theoretical limits of this engine.

4.3.1 VALVE SIZING

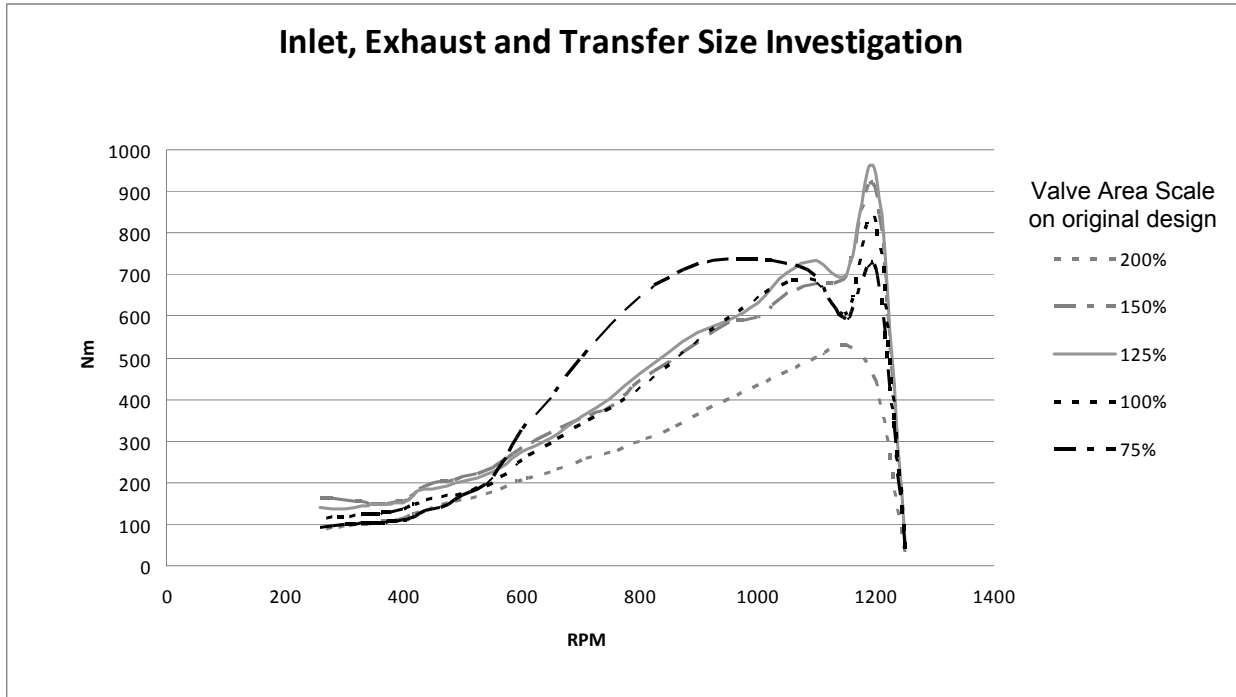


Figure 47 – 2nd Prototype Valve Sizing Investigation, displayed as a percentage of the original design values

Figure 47 shows the effect of increasing and decreasing the original design inlet, transfer and exhaust areas for the original displacement settings .

The valve sizes were scaled by the factors shown in Figure 47. As can be seen from the figure, there was a slight increase in power at the higher rpm when scaled up by 25% – 50%. Beyond this hurt the powerband across the spectrum because of the slower gas velocity and lessened compression and expansion volume due to the valves being exposed for longer periods. A slight decrease led to an increase in lower RPM power due to the higher gas velocity encouraged by the smaller areas. There will be a point where too small will constrict the fuel and air too much.

The relative ratio of inlet and exhaust valve were kept although the increased performance from the increase in gas velocity by reducing the valve size by 25% was noted, it was not implemented onto the 2nd prototype as the combustion chamber and valves had already been finalized.

4.3.2 COMPRESSION RATIO (CR) AND CRANKCASE RATIO (CCR)

The benefits of increasing the compression ratio are already well known as increasing the pressure of the fuel air mixture prior to ignition increases the fuel efficiency by improving combustion. The real life limits to increasing compression ratios is the ability of the combustion chamber to contain the combustion and the onset of knock. The CR was tested for ratios between 4:1 and 18:1, fixing the CCR at different values to establish values for performance prediction. The engine model has had all characteristics based on the current 2 stroke design.

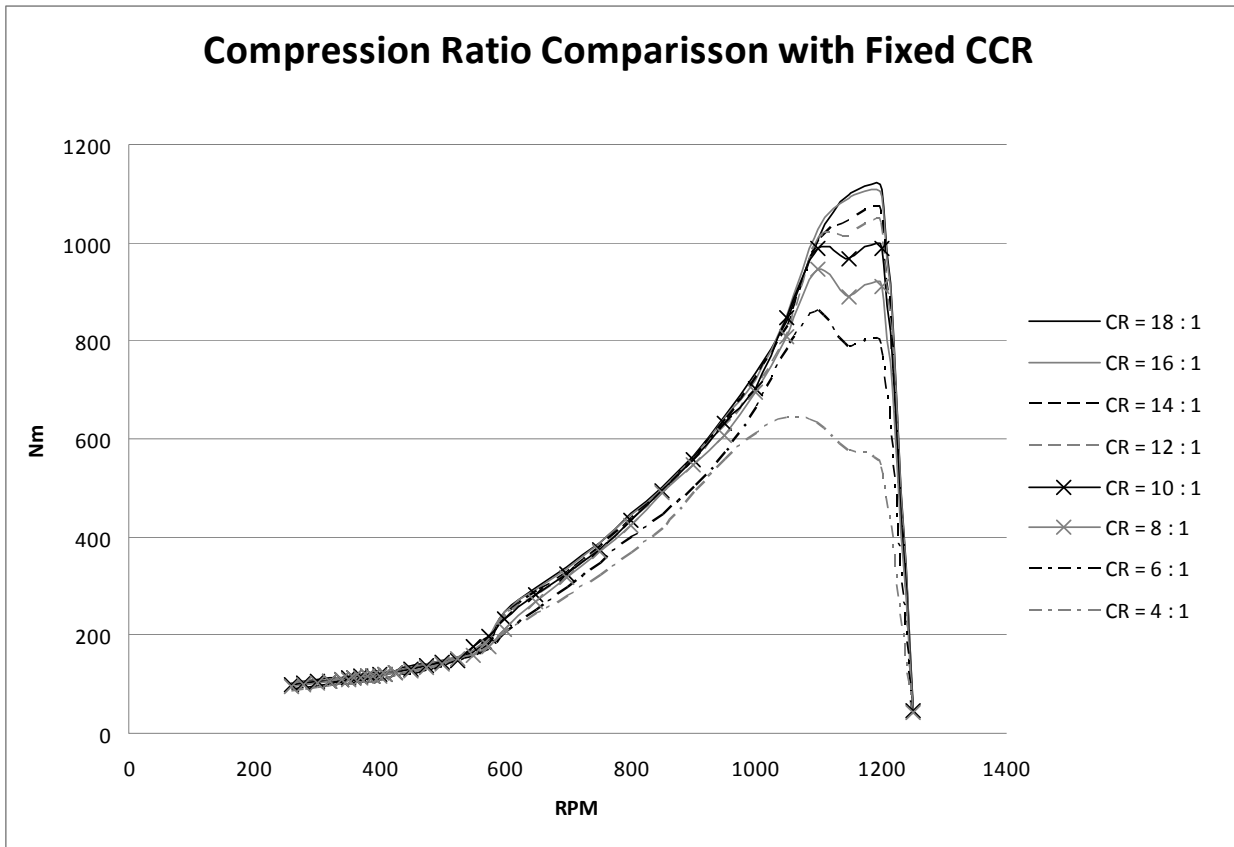


Figure 48 – Comparison of Torque Curve with varying compression ratio

As can be seen from Figure 48 for the set design values for the 2nd prototype, compression ratio becomes less influential on output when CR is raised beyond 14:1. The 18:1 and 16:1 CR produce almost identical results whereas raising the CR from 8:1 to 14:1 only affects the peak power. This suggests that a CR above

16 is sufficient for the complete combustion of the methane, and a CR above 14 will not provide any gainful improvements to torque with these design parameters and will likely cause the onset knock.

4.3.3 FIGURE: FIXING CCR AT 2. CR CHANGING:

In a typical 2 stroke configuration, 1.2 – 1.5 CCR Ratio is used. Because of the low quality fuel and lower RPM, a higher CCR was investigated to increase the air and fuel that could be pushed into the combustion chamber at greater velocity, encouraging swirl and turbulence to increase combustion. Initially, to establish a baseline, the CR was fixed at 10:1, 14:1 and 18:1 and a number of simulations were run for CRR values between 1:1 and 3:1. See Figure 49 through Figure 51.

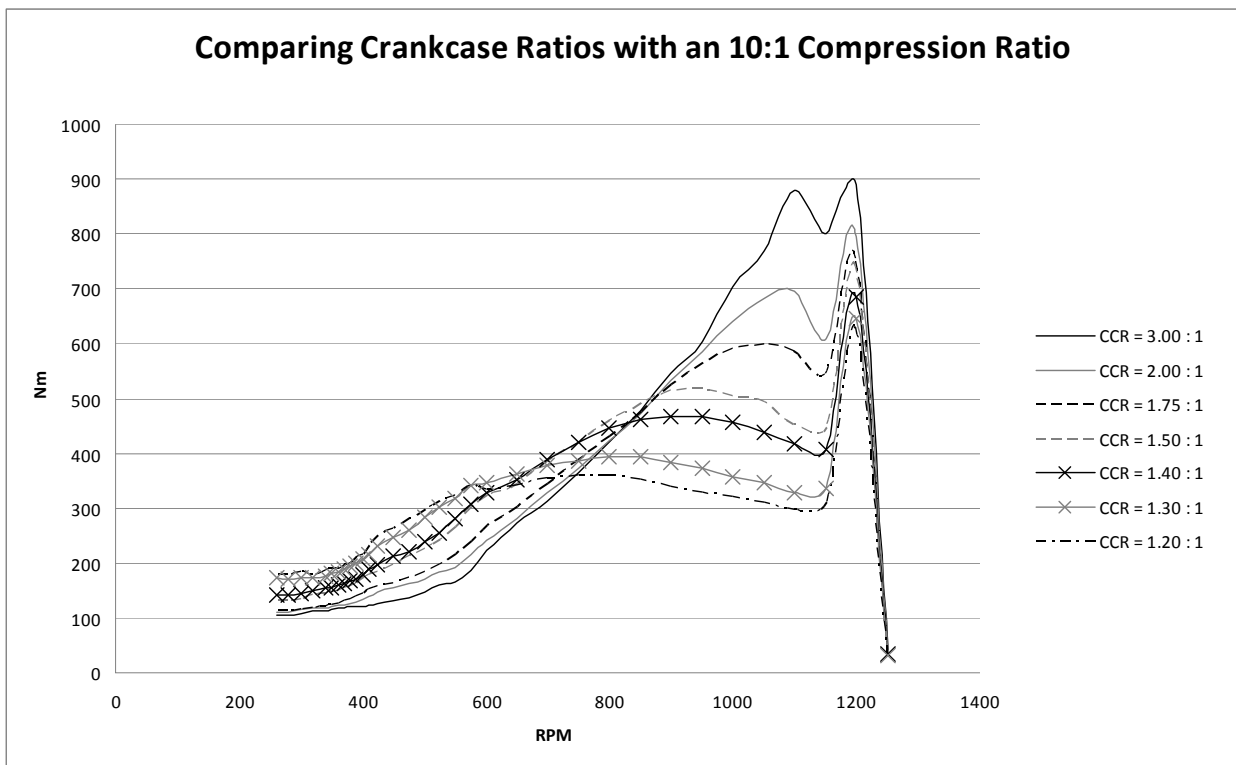


Figure 49 – Comparison of Torque Curve with varying crank case ratio using a CR of 10.

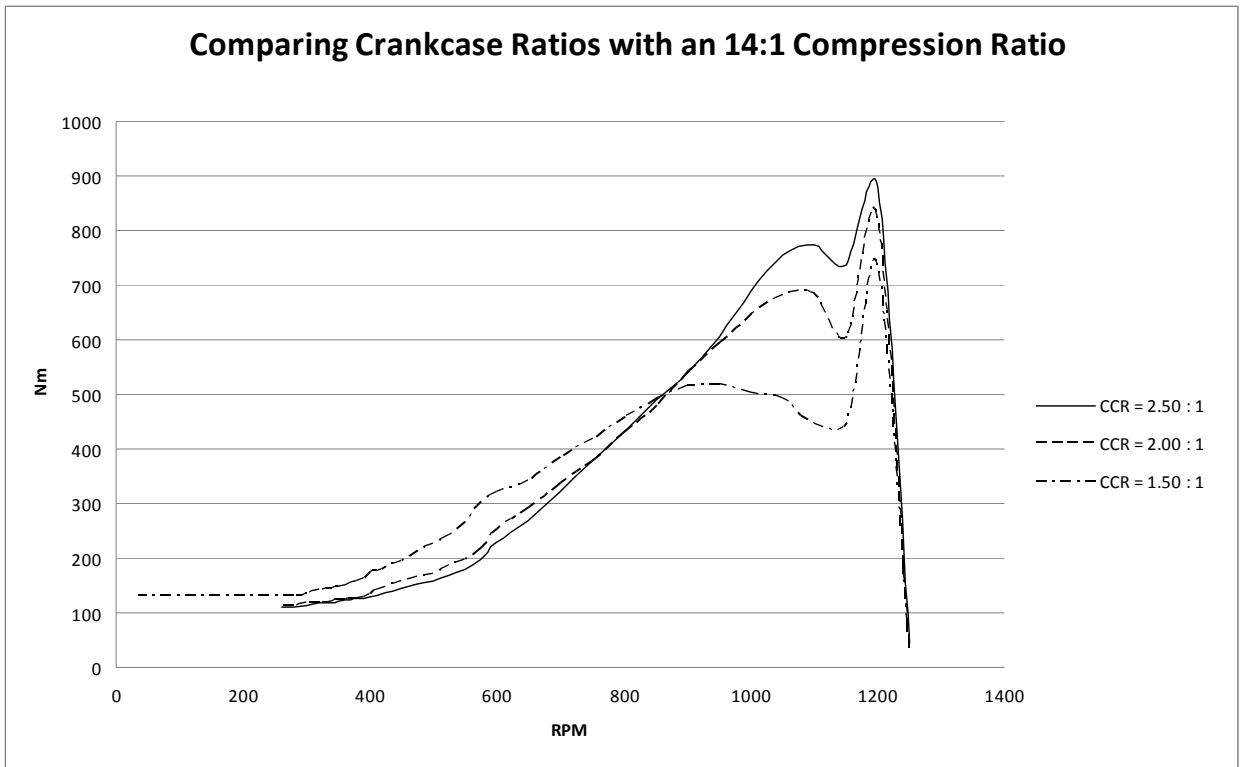


Figure 50 – Comparison of Torque Curve with varying crank case ratio using a CR of 14

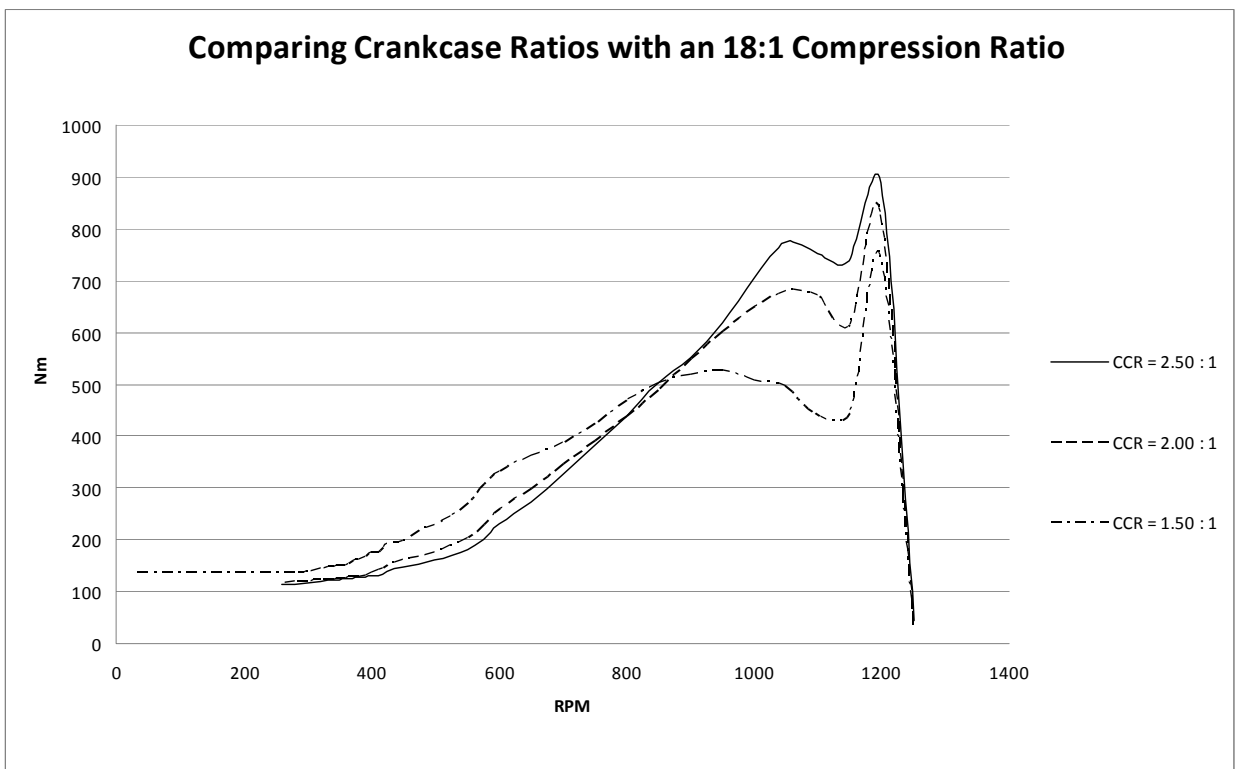


Figure 51 – Comparison of Torque Curve with varying crank case ratio using a CR of 18

As can be seen, like the compression ratio investigation, higher CCR ratios predominantly benefits top end power, a CCR of 1.5 outperformed a higher CCR value at lower rpm.

The upper limit for the crankcase is set by amount of air that can be stuffed into the volume of the combustion chamber, not the CCR. Increasing the crankcase compression ratio actually hurt the lower end of the power band because of the resistance to piston movement as the gas cannot pass through the transfer fast enough. Figure 49 shows that a CCR of 3 delivers the highest peak power. Unfortunately, this is at the expense of efficiency since even though theoretically, this allows the maximum amount of fresh air and fuel mixture into the combustion chamber it also overfills it, wasting fresh fuel and the extreme crankcase pressure eliminating the scavenging of hot exhaust gases.

The position of the transfers means that too higher CCR will result in increased wall friction and erosion of the piston

Therefore, the 2:1 CCR specified in the original design is deemed acceptable

4.3.4 DWELL

To investigate the influence on performance the dwell times at BDC and TDC, a range of different piston trajectory profiles were created The next section explores how the dwell times spent near the extremities influences engine performance.

To do this, all the baseline model parameters were fixed as the design was intended. The combustion model was simplified to simulate the slower combustion of methane under a 14:1 compression ratio. A Wiebe curve with a 26 degree burn time and 12.5 degree % 50 Burn point, and modifying factor of 2. The head was designed to improve turbulence and create high velocity flow and squish, combining a large compression ratio and 2:1 ratio to crankcase volume.

Each piston trajectory displays the piston position (relative to BDC) relative to the crank angle. Note that each 360 degree crank angle actually represents $\frac{1}{4}$ of actual engine RPM.

For each relative piston profile, the inlet and exhaust valve timing had to be adjusted to suit which was established from the 3D CAD model. Table 5 identifies the crank angle in which the respective valves open and close. Essentially, changing the piston trajectory had the same effect as the changing the valve timing. The points where the valves are exposed is indicated by the vertical lines on the Figures and the exact valve timings of each piston trajectory are shown in Annex E.

Symmetric and unsymmetrical profiles were investigated and for comparison included in the profiles is a traditional slider crank piston profile for (curve number 0) and the original design piston profile (curve number E2).

4.3.5 TDC DWELL INVESTIGATION

Initially, the dwell time at TDC was investigated before and after ignition as shown in Figure 52 through Figure 54. The piston trajectory around BDC was shaped similarly to ensure a smooth transition with the timing reflecting the original design profile.

- Figure 52 shows the piston trajectories, adjusting the dwell just prior to TDC ignition (see Section 3.3.9 for ignition details) during compression.
- Figure 53 shows the piston trajectories, adjusting the dwell just after TDC during expansion.
- Figure 54 shows the symmetrical piston trajectories, adjusting the extent of dwell on both on expansion and compression

S0 is a sinusoidal default motion found in slider crank IC engines. This is included as a baseline.

Note that E2 is the original design (alike the 4 stroke prototype) piston profile. The results of this investigation hope to improve the performance produced by this profile.

Exhaust Opening	37
Exhaust Fully Open	19
Transfer Opening	16
Transfer Fully Open	3
Transfer Closing	3
Transfer Fully Closed	16
Exhaust Closing	19
Exhaust Fully Closed	37

Table 5 – Engine rotation degrees relative to valve positioning

Curve Description	Curve Identifier (Figure 52)	Degrees Transfer Open	Degrees Exhaust Open
Sinusoidal	S 0	90	140
Original Design	1 (E2)	59	102
Minor increase on Dwell at TDC	C1	69	120
	C2	44	93
	C3	55	85
	C4	45	73
Maximum Dwell at TDC	C5	52	78

Table 6 - Valve Action Relative to Engine rotation for dwell varied on compression piston trajectories

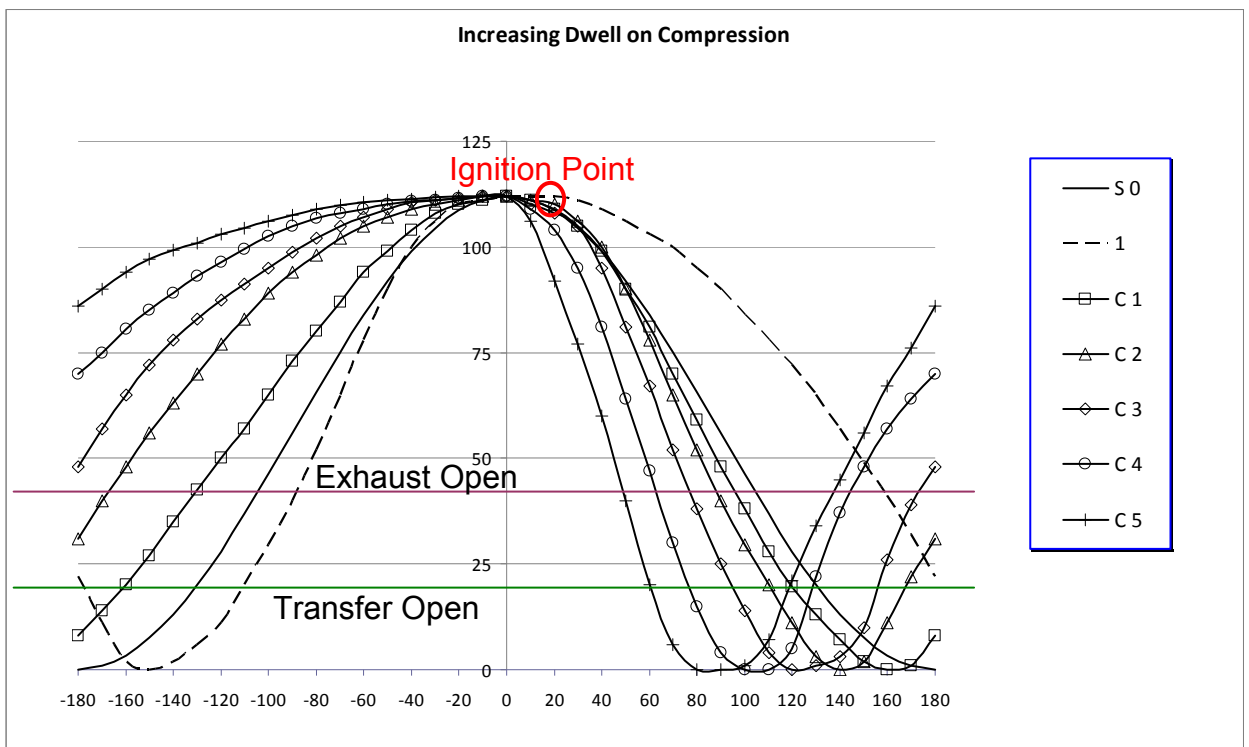


Figure 52 – Piston Stroke Trajectories relative to engine rotation, varying dwell on compression

Curve Description	Curve Identifier (Figure 53)	Degrees Transfer Open	Degrees Exhaust Open
Sinusoidal	S 0	90	140
Minor increase on Dwell at TDC	E1	68	121
Original Design	1 (E2)	59	102
	E3	55	86
Maximum Dwell at TDC	E4	55	82
	E5	52	80

Table 7 - Valve Action Relative to Engine rotation for dwell varied on expansion piston trajectories

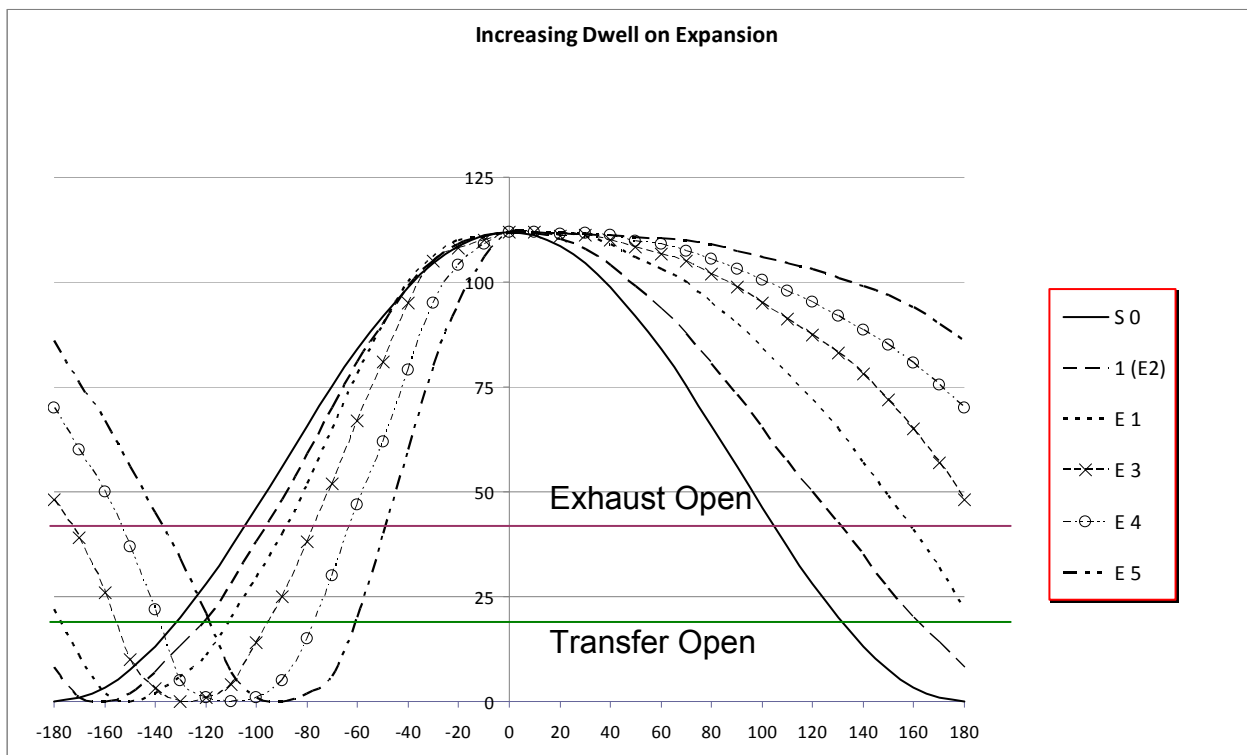


Figure 53 – Piston Stroke Trajectories relative to engine rotation, varying dwell on expansion

Curve Description	Curve Identifier (Figure 54)	Degrees Transfer Open	Degrees Exhaust Open
Maximum BDC Dwell	S -2	234	258
Longer Dwell at BDC	S -1	176	212
Equal Dwell at BDC and TDC (Sinusoidal)	S 0	90	140
Longer Dwell at TDC	S 1	80	124
Maximum TDC Dwell	S 2	72	104

Table 8 – Valve Action Relative to Engine rotation for symmetric piston trajectories

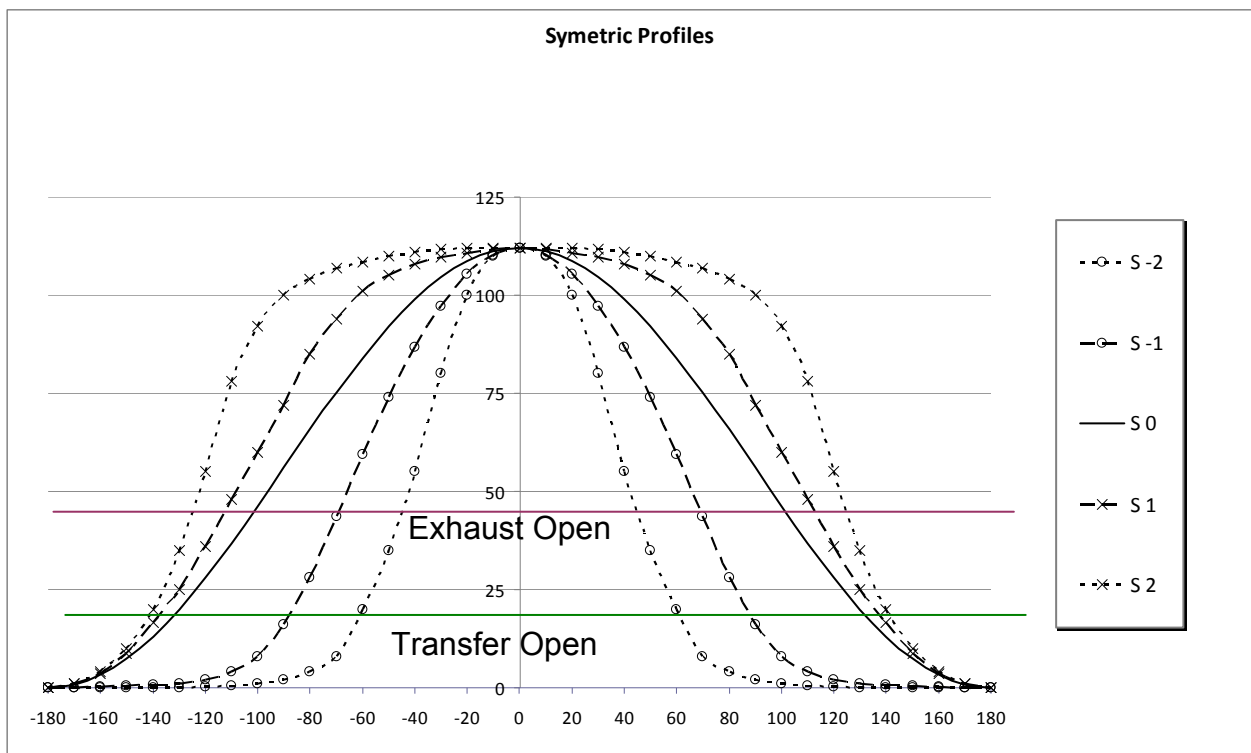


Figure 54 – Piston Stroke Trajectories relative to engine rotation, varying dwell on expansion and compression

Each piston trajectory configuration from Figure 52, Figure 53 and Figure 54 was simulated and Figure 55 shows the resulting engine output torque.

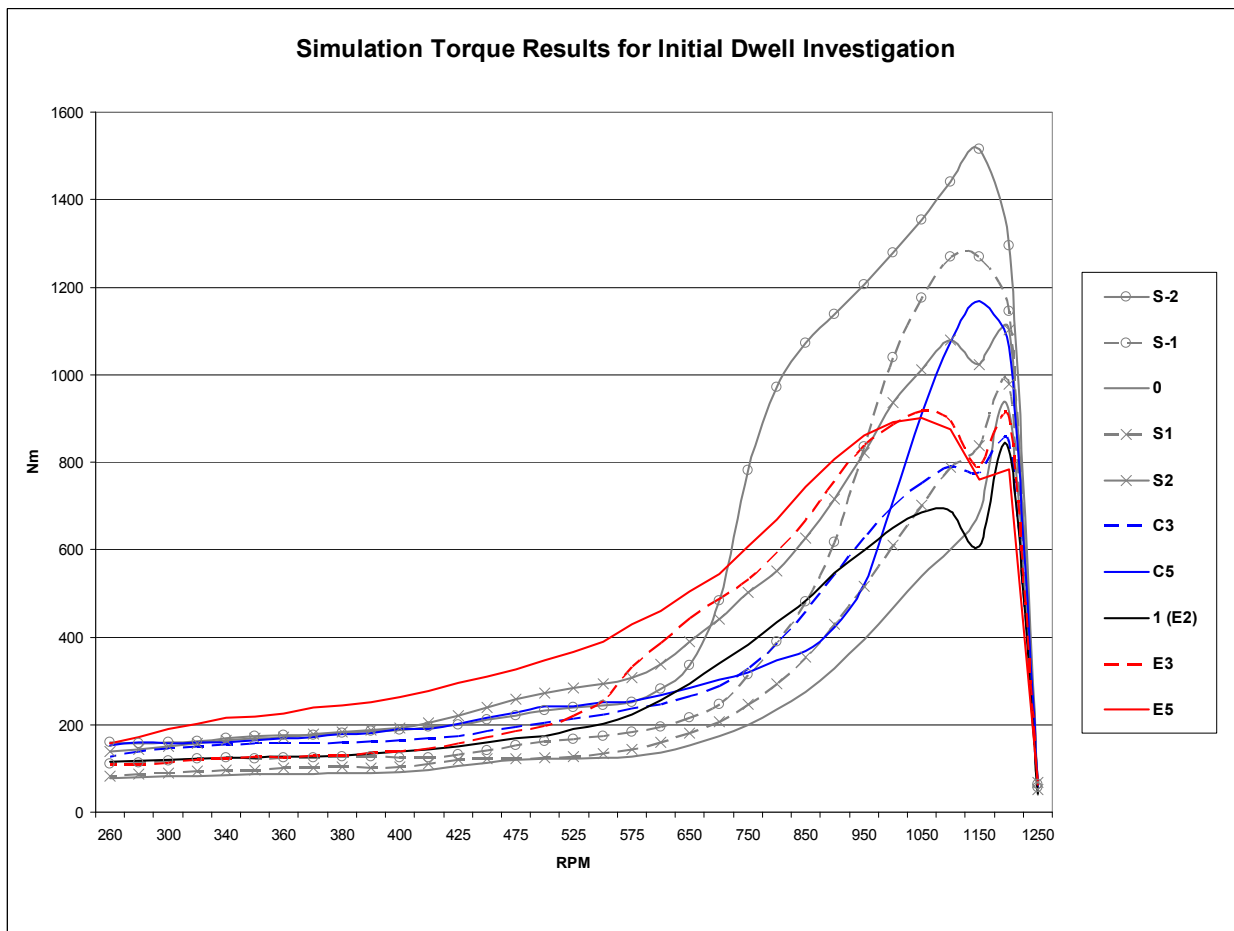


Figure 55 – Torque curve comparison between varying piston trajectories

Some results have been omitted for clarity since the resulting simulated torque fell between the output curves displayed in Figure 55. It appeared that dwell near TDC improved performance over the entire RPM range as shown in by the increased dwell on expansion curves, E3 and E5. E5 was the best performer over the range. Interestingly though, these curves did not deliver the highest peak figures. It was the symmetric curves that had the least time at TDC and the longest dwell time near BDC that produced significantly higher torque and power at elevated RPM.

The curves S-1 and S-2 both produced impressive peak numbers at peak rpm but performed poorly at lower rpm. What can be noticed from Table 8 is that the transfer ports and exhaust ports are open for significantly longer period than the other curves, explaining their impressive peak torque and power. The longer dwell at BDC allows more air and fuel to enter the transfers. It should be noted that a 2

stroke engine typically has an exhaust opening time of 180 degrees so it is not a surprise that as the longer these ports are open, the better the performance.

The increase in piston dwell time at TDC on the compression cycle resulted in higher output, as shown by the difference between C3 and C5.

The results of this dwell investigation warranted an additional refinement of piston profiles to capitalize on the strengths and weaknesses of dwell at TDC, BDC and by keeping symmetry.

4.3.6 OPTIMIZATION OF DWELL

To find the optimal dwell parameters, encompassing the peak by having long dwell at BDC as well as capitalizing on lower end power and torque provided by a longer dwell at TDC. Eight different piston profiles were developed varying from extreme to close to symmetric profile of which the performance is now known. These profiles are shown below in Figure 56.

Curve Description	Curve Identifier (Figure 56)	Degrees Transfer Open	Degrees Exhaust Open
Original Design	1	59	102
Minor increase on Dwell at BDC and TDC	O 1	160	180
	O 2	147	169
↓	O 3	108	154
Maximum Dwell at BDC and TDC	O 4	88	131
Original Design Output	E2	160	134

Table 9 - Valve Action Relative to Engine rotation for optimized dwell at TDC and BDC piston trajectories

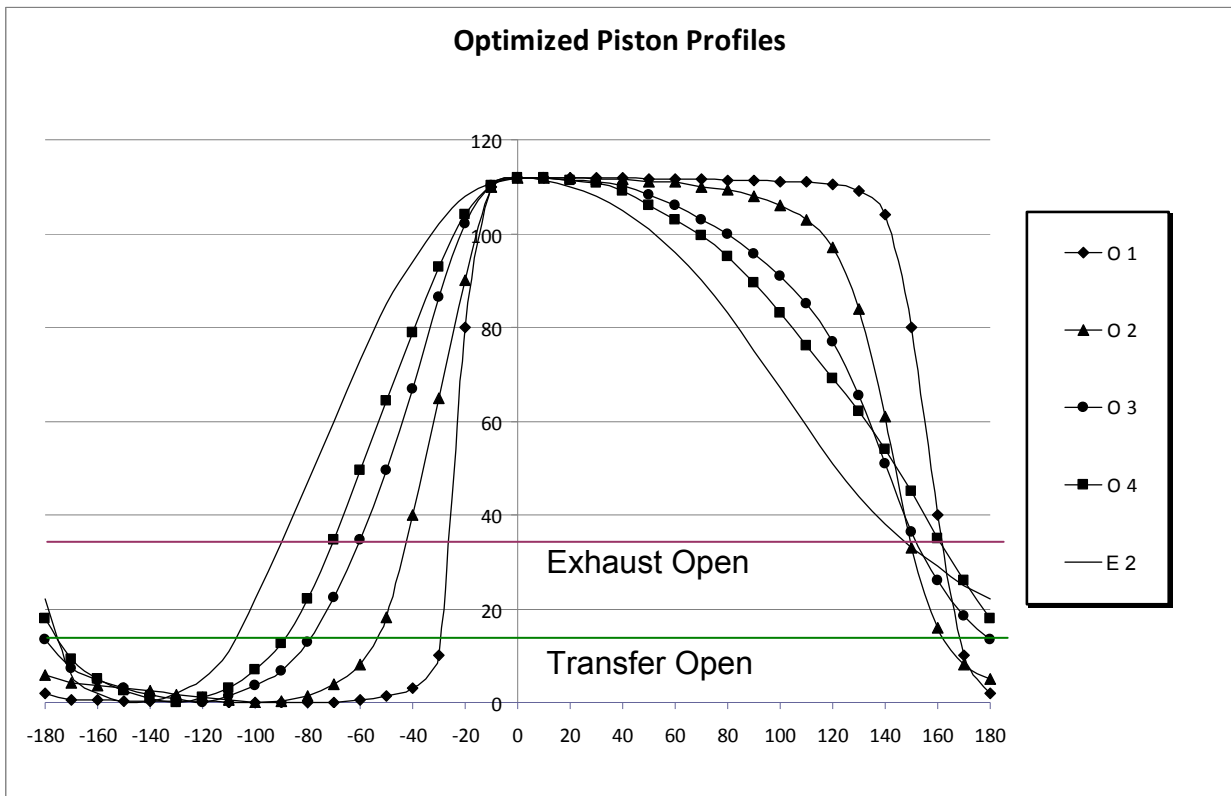


Figure 56 – Piston Stroke Trajectories relative to engine rotation, optimizing dwell at TDC and BDC

These were developed to see what effect altering both the dwell at BDC and TDC had on engine output torque. Again the valve timing was adjusted for these profiles. Curve O1 in Figure 56 had the longest dwell at BDC and TDC so the valves open the longest and takes advantage of the slower compression and expansion. The severity of this curve was lessened with each curve to number O4. For comparison, the original piston trajectory was left (E2). It was hypothesized that curve O1 would theoretically perform the best based on the findings of the first investigation. Results are shown below in Figure 57.

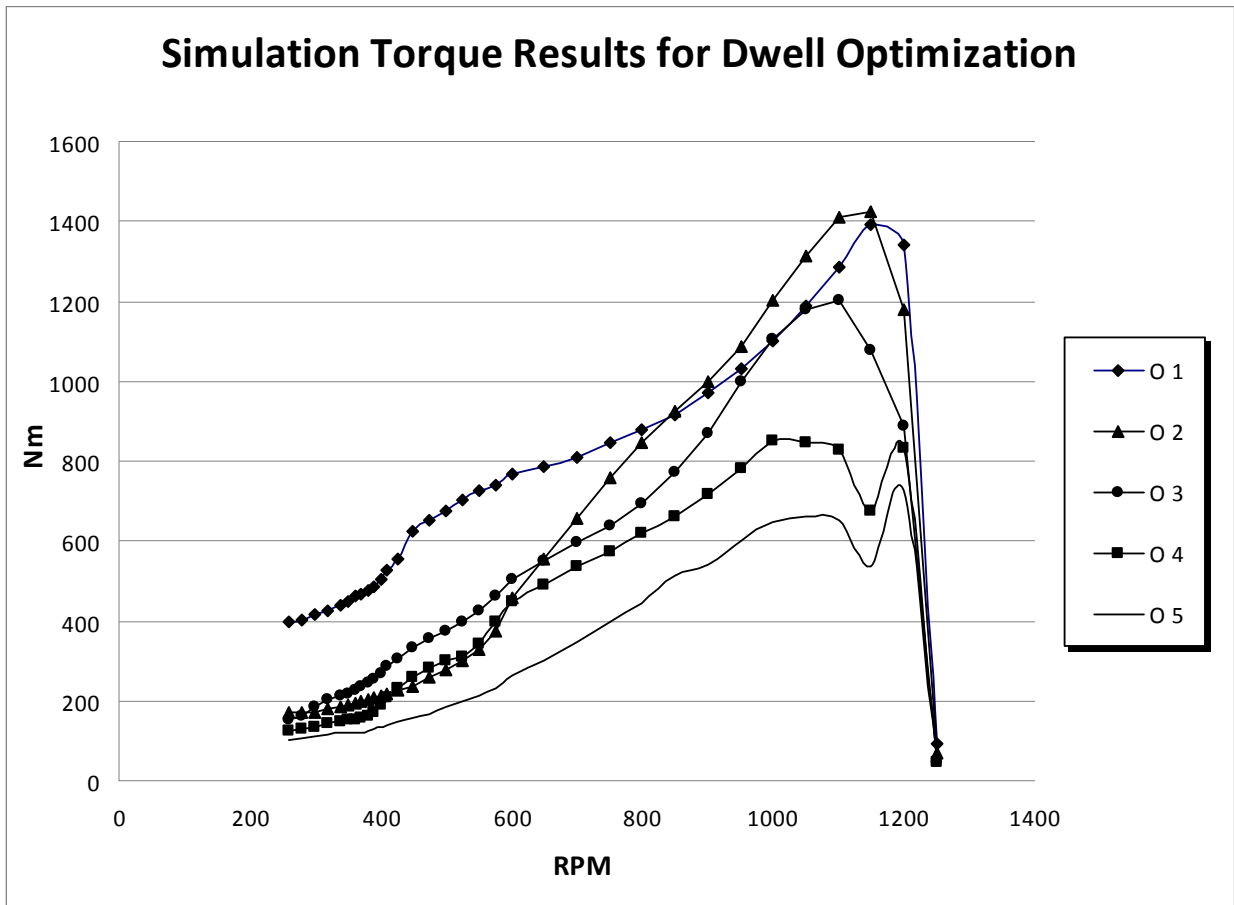


Figure 57 – Torque curve comparison between varying levels of TDC and BDC dwell piston trajectories

Predictably, the order of performance directly correlated to increasing dwell times at both extremes. O1 producing the best performance yet, more than doubling the potential output of the original design. Although it should be noted that O2 had comparably peak power. Finally, to find which was more beneficial, dwell at BDC or TDC needed to be investigated. B4 and A3 piston profiles were selected from the previous investigations as a middle of the range benchmark. Piston curves were developed for prior to ignition (profiles shown in Figure 58) and after (profiles shown in Figure 60).

Curve Description	Curve Identifier (Figure 58)	Degrees Transfer Open	Degrees Exhaust Open
Minor increase on Dwell at BDC and TDC	B 1	108	194
↓	B 2	143	174
	B 3	118	154
	B 4	74	144
Maximum Dwell at BDC and TDC	B 5	59	124

Table 10 - Valve Timing Relative to Engine rotation for optimized piston dwell prior to ignition (at BDC)

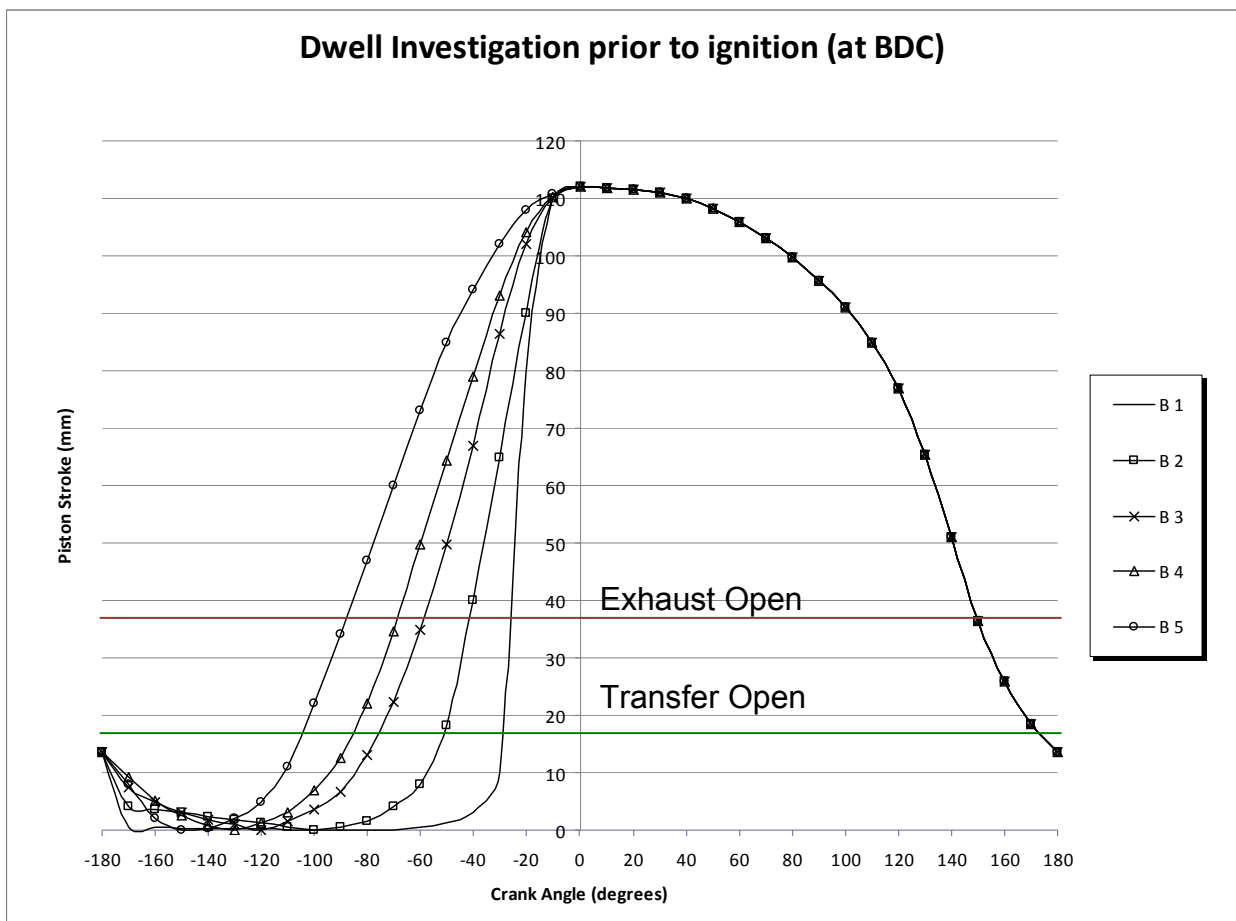


Figure 58 – Piston Stroke Trajectories relative to engine rotation, optimizing dwell at BDC

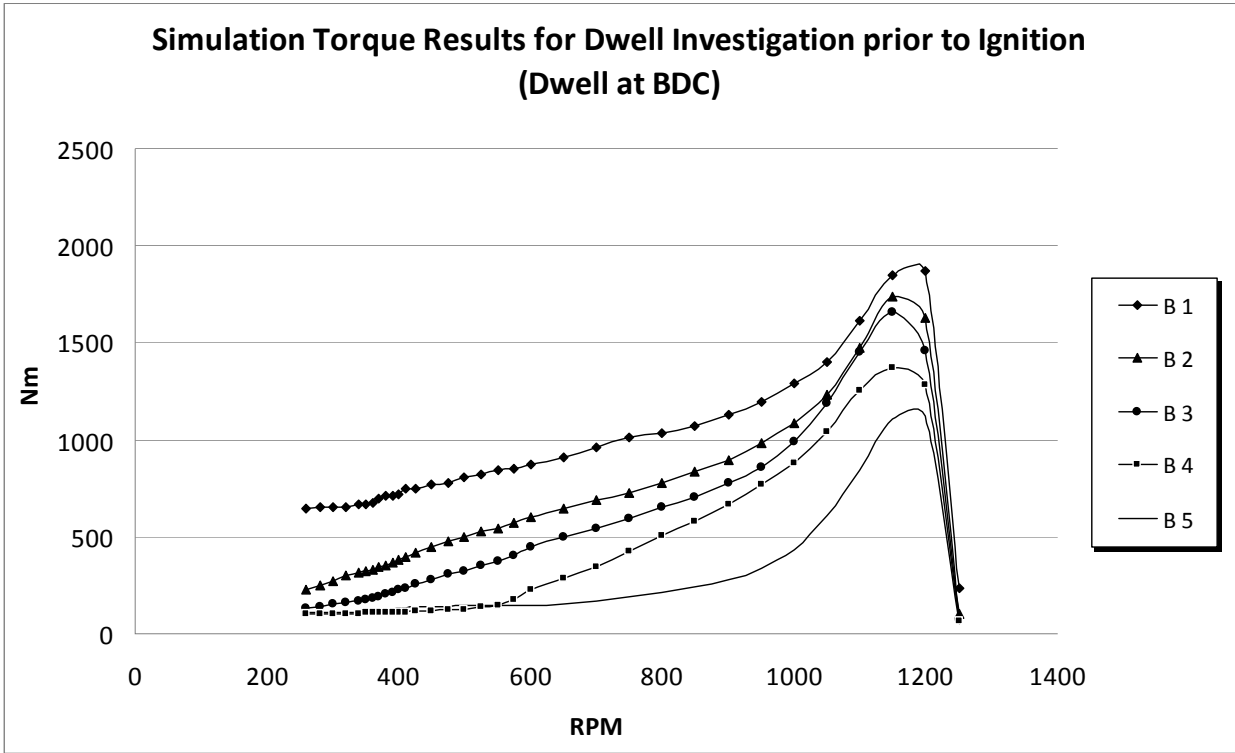


Figure 59 –Torque curve comparison between varying levels of BDC dwell piston trajectories

<i>Table of Valve Timing for Dwell after ignition (at TDC)</i>			
Curve Description	Curve Identifier (Figure 60)	Degrees Transfer Open	Degrees Exhaust Open
Minor increase on Dwell at BDC and TDC	A 1	97	126
↓	A 2	97	129
	A 3	97	137
	A 4	97	139
Maximum Dwell at BDC and TDC	A 5	97	141

Table 11 - Valve Timing Relative to Engine rotation for optimized piston dwell after ignition (at TDC).

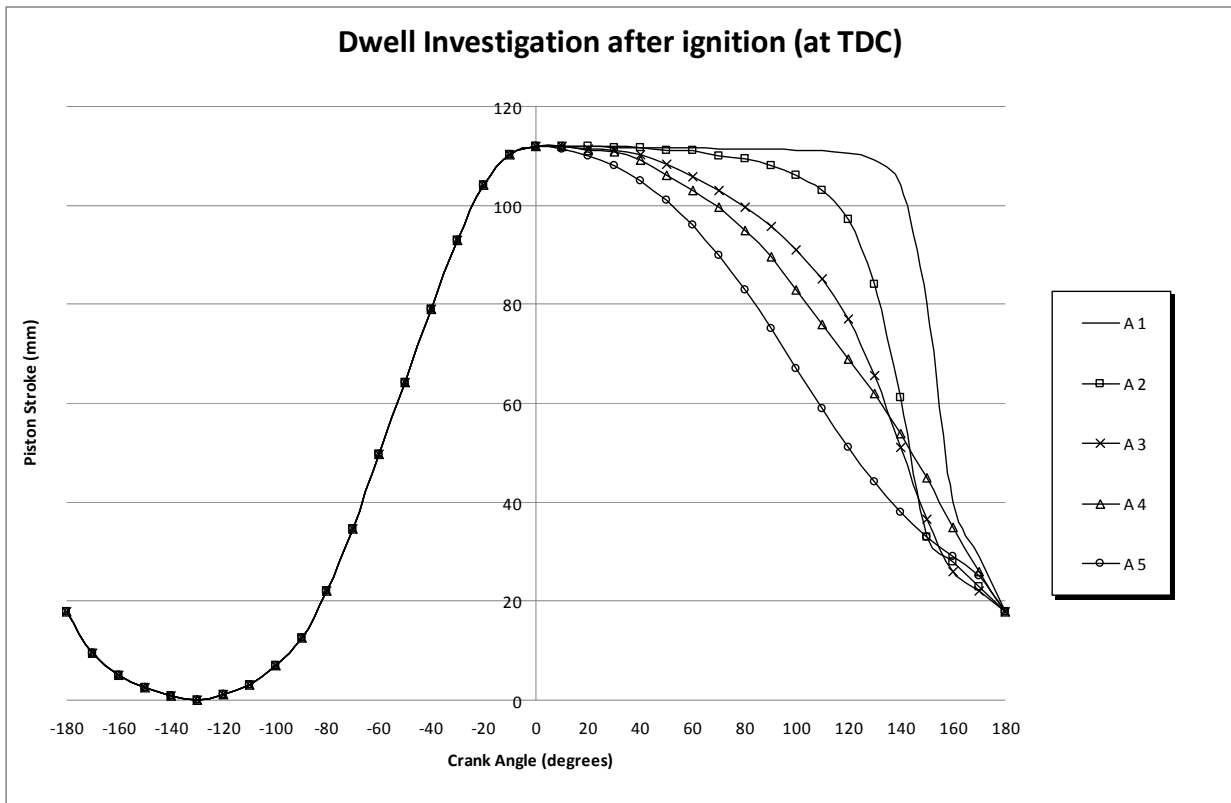


Figure 60 – Piston Stroke Trajectories relative to engine rotation, optimizing dwell at TDC

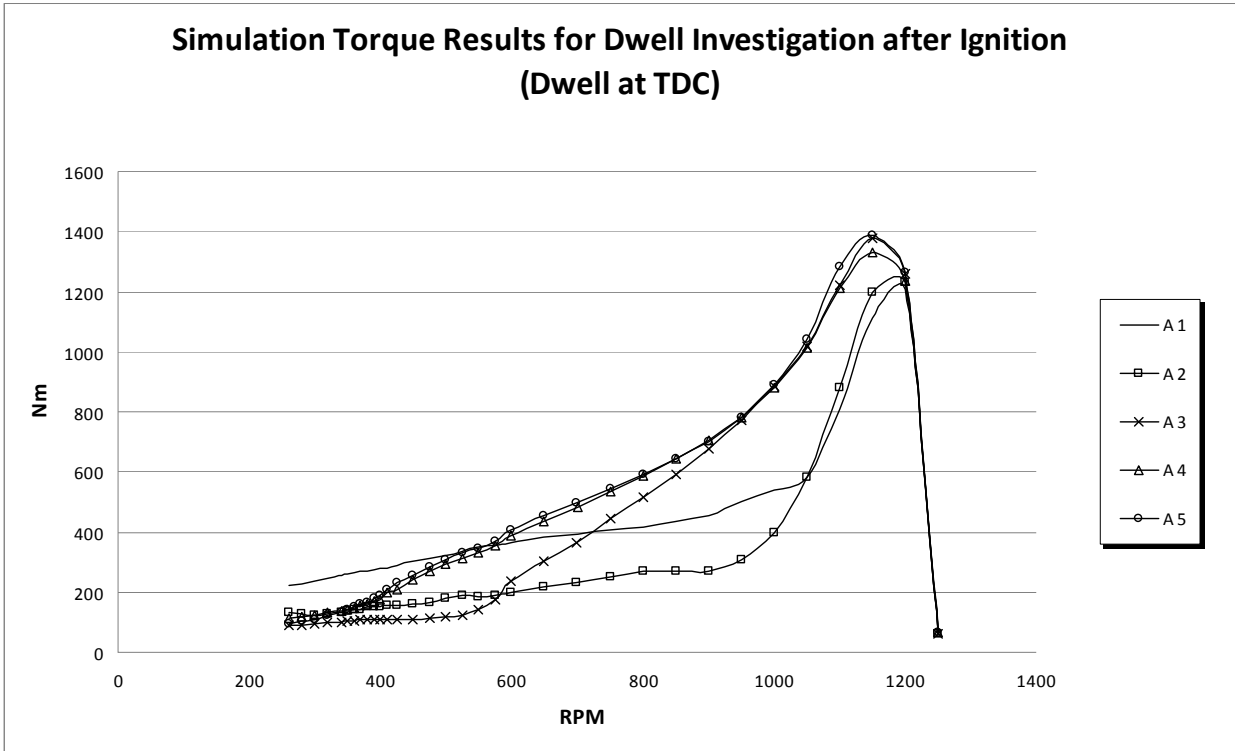


Figure 61 –Torque curve comparison between varying levels of TDC dwell piston trajectories

When comparing Figure 59 to Figure 61 that it was the dwell pattern at BDC that had a greater impact on influence. An extreme dwell at TDC can improve power at very low RPM due to an improvement in volumetric efficiency as can be seen by curve A1 in Figure 61. However, further increasing TDC dwell time did not further increase performance.

4.4 OPTIMIZING 2 STROKE ENGINE

Using the results found in the investigation, the following configurations were developed to find the optimal design for the 2 stroke prototype. Fuel efficiency was still deemed an important quality so driving up CRR to lead to waste was not employed. It should be noted that this engine is not designed to operate above 500 rpm but for interest, if engine stability was maintained and the components were capable of withstanding the forces involved, the theoretical limits for each was explored. The following characteristics were used for the following optimized engines:

Theoretical Limit (Peak Optimized Curve)

Using the extreme piston trajectories that maximized dwell times at BDC and TDC the theoretical limit for this engine configuration with a set displacement was investigated. This was coupled with a CR was set of 14:1, CRR as 2:1, inlet, exhaust and transfer size was scaled to 30% larger than the original design and swirl and turbulent coefficients were maximized.

Recommended Design

This uses the same CR and CRR as the peak optimized curve but uses less extreme, more practical dwell at BDC and TDC to lessen instability and the forces on the linkages on the components imparted by the abrupt changes in piston direction. The valve and transfers sizing was left as the original design value since this had already been manufactured. The gains at lower rpms are not worth the over engineering required to ensure that the components can sustain the forces involved. There is also a compromise in optimal power for reliability.

Flat Torque Design

Mostly the same as the recommended design, except using a slightly reduced dwell time near TDC and a 25% reduction in valve size to balance low down torque, sacrificing the top end output at higher rpm.

Figure 62 compares the torque outputs of the three engine configurations described, as well as the original design output.

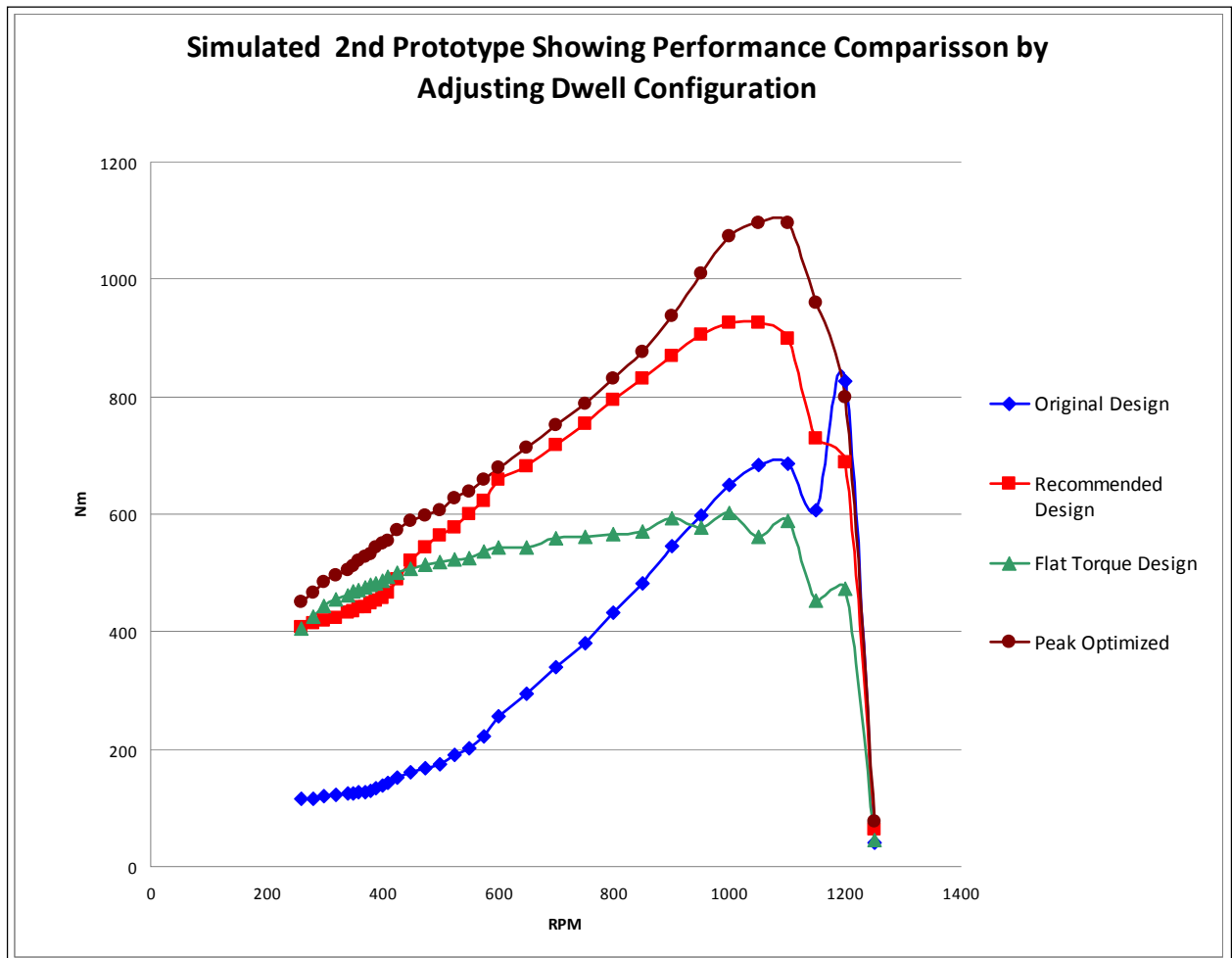


Figure 62 – Results of parameter investigation

4.4.1 COMPARING TO ICE ENGINE

To see how this engine compares to current IC technology, a model was built for a conventional petrol run 2 stroke, 2 cylinder engine of equivalent port size and displacement. This engine would rev to 3000 – 5000 rpm and was fitted with a gearbox to give the same output RPM. The engine’s breathing geometry was made geometrically identical as the recommended design illustrated in Figure 62 and Section 4.4.

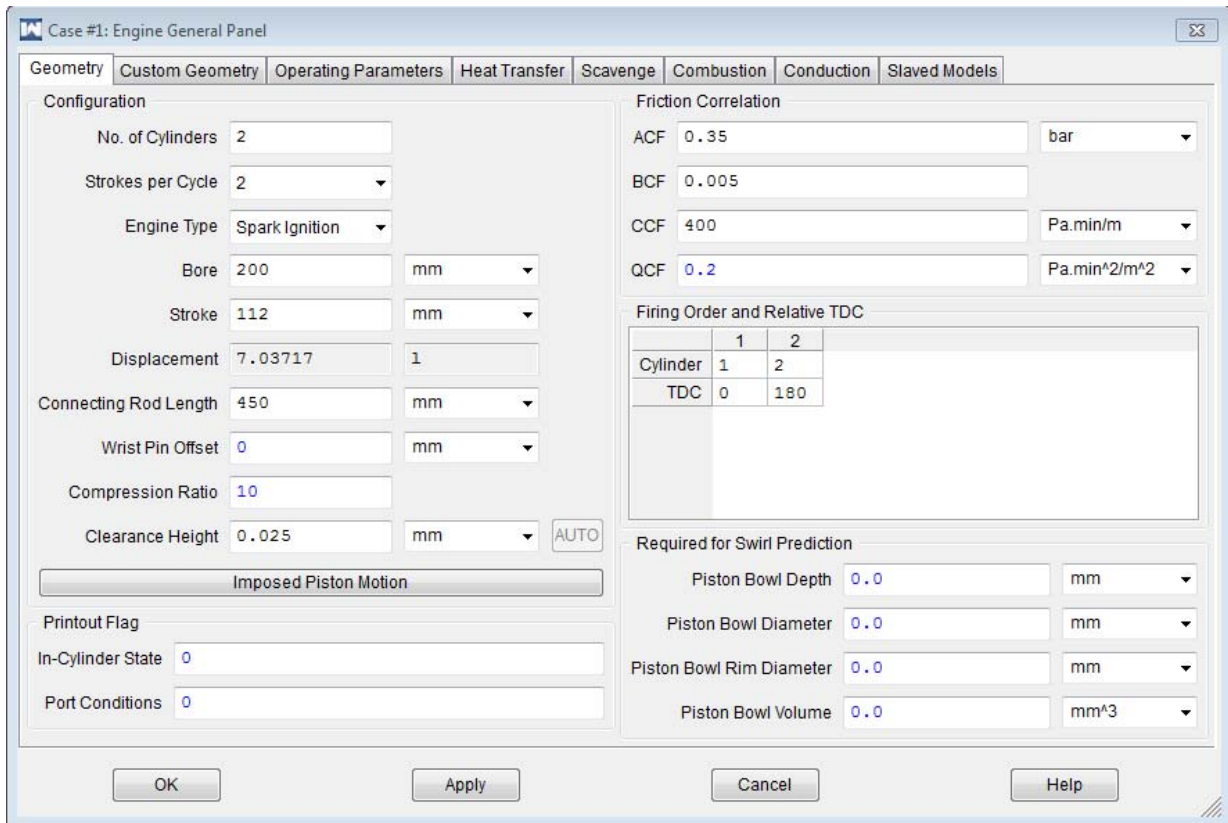


Figure 63 – Engine Panel for Equivalent IC Pushrod Engine

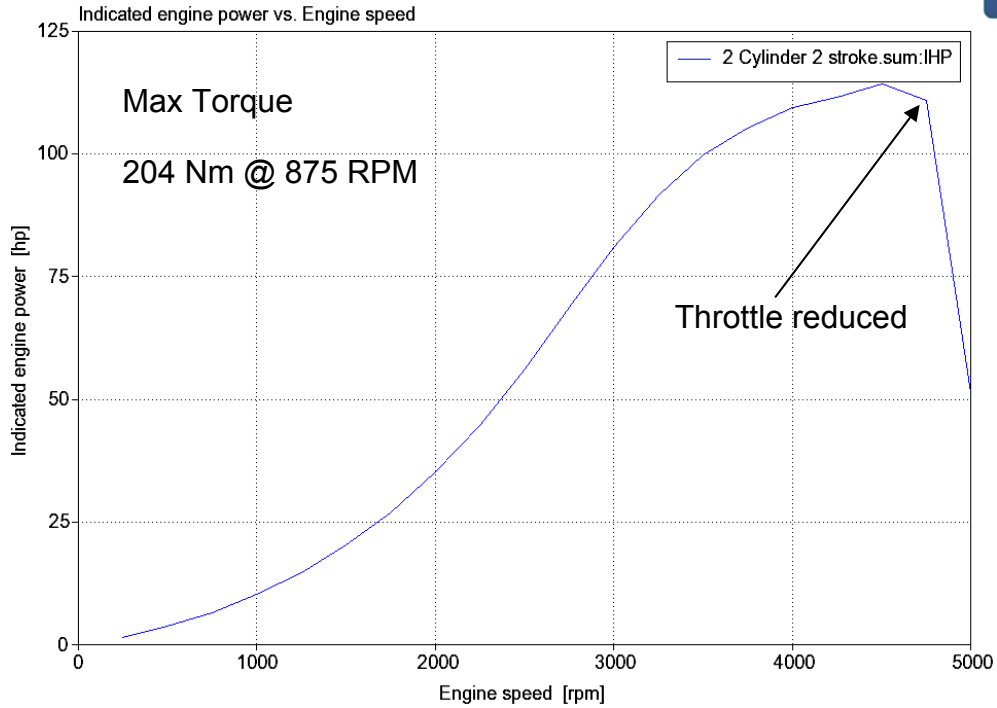


Figure 64 – Power Output (hp) for Equivalent Pushrod engine

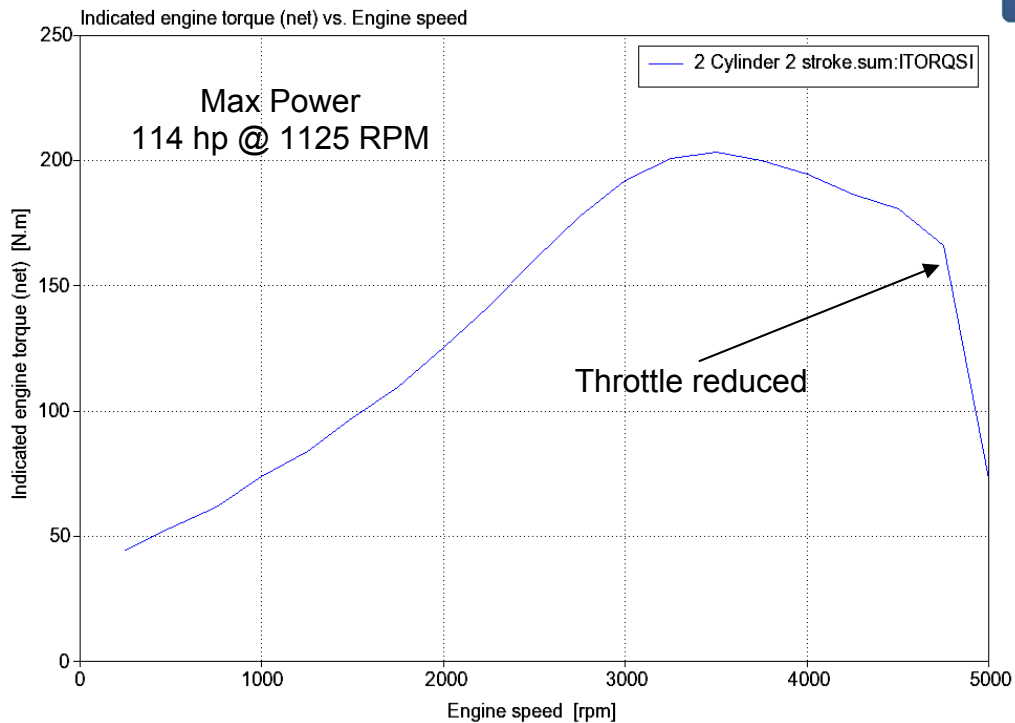


Figure 65 – Torque (Nm) Output for Equivalent Pushrod engine

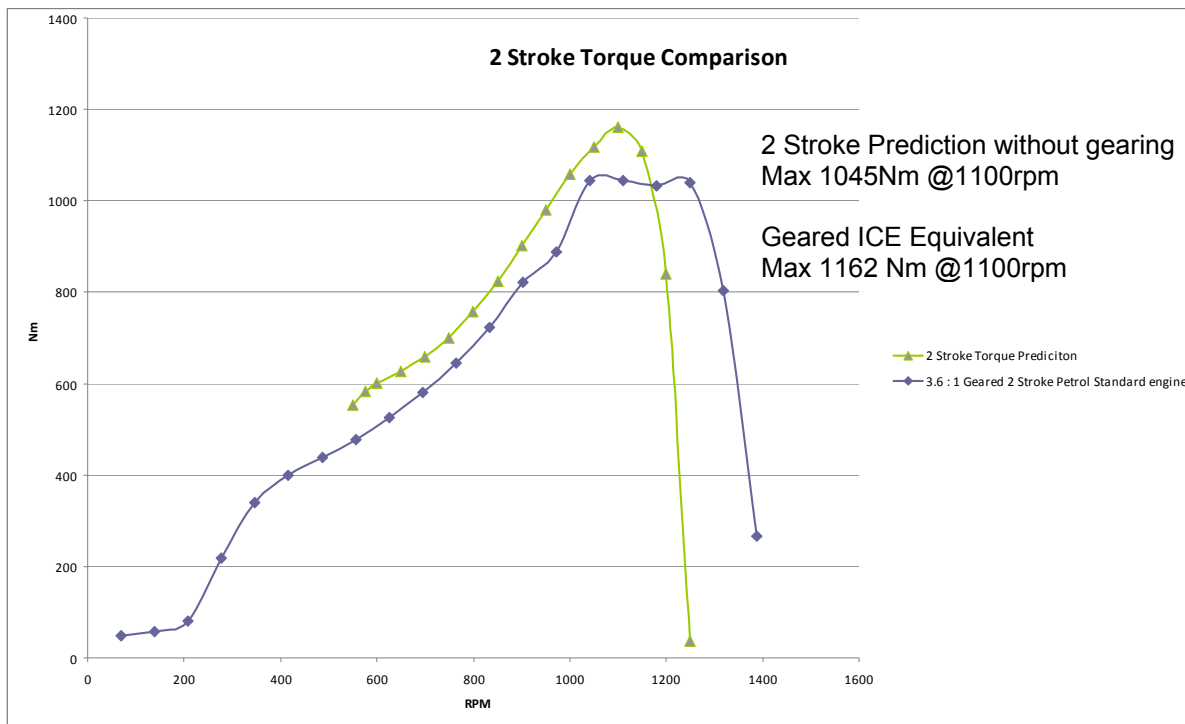


Figure 66 – Comparing the orbital engine to a geared engine of equal displacement, valve configuration

As can be seen the delivered power of the prototype is comparable to that of the IC engine, which is very surprising considering that petrol run engines typically outperform methane run engines by 16% as explained in Section 2.4.2

It should be noted that equivalent engine output shown does not include gearbox losses and the exhaust systems are identical and a generic WAVE scavenging model was applied.

4.5 PERFORMANCE PREDICTION MODEL

Using the now known influences of valve sizes, displacement and most importantly the influence of piston profile and dwell at BDC and TDC, using hundreds of simulation runs were conducted and a performance prediction calculator was generated by interpolating the data generated from the simulations using a Microsoft excel spreadsheet. This platform allows quick results to be generated without the need for use of the expensive software.

The overall influences of bore, stroke, compression and crankcase ratios, valve/port sizing, fuel type and piston trajectories were used and interpolated where necessary to construct a performance calculator for a range of variants so that the simulation was not necessary for a quick indication of performance for a set of variables. The input and output screen can be seen in Figure 67.

It was validated against the simulator and gave reasonable results to within 20% of the simulator estimated torque vs rpm curves over a modest displacement range. Since the simulator has only been verified against a single engine, a limited level of confidence can be given.

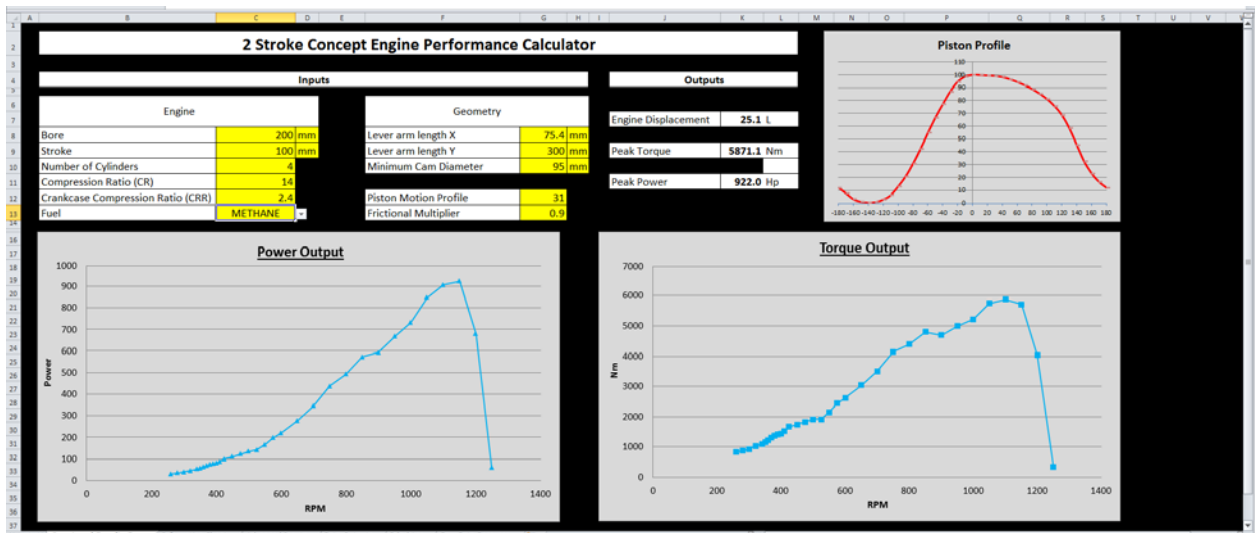


Figure 67 – Output screen for Excel performance prediction calculator based on findings of modeling outputs

Inputs are shown in yellow. When these are altered, the calculator displays peak power and torque as well the forces on the critical members. It also provides a power and torque curve in relationship to engine speed. The model is prebuilt with over 30 piston profiles adjustable to fit any configuration for the engine design.

4.5.1 VALIDATION

Until a prototype is built, these cannot be fully verified. But over a modest spread of displacement, the prediction model should have reasonable confidence in performance characteristics based on the combustion simulations.

5 DISCUSSION

A model is only as accurate as the input data. This is a principle that must always be kept in mind when attempting to validate a model. Likewise, it is important to recognize that 1D simulation is not a 100 percent accurate prediction of true gas dynamics. While good simulation results can be within 5 percent of actual performance, the amount of time spent troubleshooting a model while trying to perfectly match empirical data to simulation predictions should be limited.

One of the reasons why 1D simulation is the mainstream form of engine simulation is because it allows for rapid development whereas a full-blown 3D CFD simulation could take weeks to calculate engine operation at a single engine speed. Another thing that should be kept in mind is that two identical engines will exhibit slightly different performance due to different conditions such as: bearing wear, piston ring seal, valve seating, carbon build-up, and fuel composition.

These are all reasons why it is important to not expect perfect-matching predictions. What is more important is that the simulation accurately predicts the shape of the torque curve as opposed to the exact magnitudes.

Discrepancies between predictions and measurements can arise from several sources. For example, if the model is not accurately predicting the location of the pressure-wave-induced intake / exhaust torque peaks, then the dimensions of the intake / exhaust geometry and intake / exhaust valve opening inputs should be checked for accuracy. If the overall torque magnitude is offset a certain amount across the entire engine speed range, engine parameters such as the combustion model, heat transfer and friction correlations should be checked for accuracy. It should also be kept in mind when troubleshooting a model that the erroneous input is most often due to an input that was guessed due to a lack of data.

The most interesting development to arise from the optimization investigation was the influence of dwell. This characteristic has not been explored to the extent before. Implications are particularly of interest with a 2 stroke configuration

where piston motion controls the opening and closing of the inlet, transfer and exhaust valves.

The obvious improvement in peak torque by increasing piston dwell at BDC is caused by the longer duration that the transfer valve is open. Combined with a large CCR value allows more time for air and fuel into the combustion chamber, increasing the ferocity of combustion and flame speed.

By increasing the dwell at TDC, the smaller combustion volume is maintained for longer, leading to higher combustion pressure and impulse pushing on the piston head. Combined with the larger volume of fuel and air involved for the given displacement and a high CRR coupled with effective scavenging this engine should far exceed the performance limits of an engine of similar displacement and valve sizing running on indolene as shown in Section 4.4.1, where Figure 66 demonstrated higher performance, even when run on a methane.

Increased dwell at TDC with the smaller combustion volume has another advantage, utilizing the slower piston speed to allow the combustion of much slower burning combustibles. Higher peak pressures can be maintained compared to a slider crank configuration even with a much lower flame speed.

The improvements on performance by extending dwell at TDC is limited by the engine's displacement and valve sizing. Compression ratios above 14 for these settings has already show not to benefit and can lead to knock. And a high CCR can lead to hurting scavenging potential and fuel wastage.

Another consideration is that dwell times at both stroke extremities, BDC and TDC is that the longer the piston spends at either TDC or BDC, the faster it must accelerate and decelerate between these extremities. The higher the acceleration and deceleration of the piston, the higher the forces on the linkages, as well as problems on startup. The performance of this engine is limited by the amount of force on the linkages.

The forces that are induced onto the linkages can be estimated using the steps laid out in Section 2.2 and 3.2.11. Increasing the cam diameter increases the torsional output, alleviating forces on the bearing. The leverage assists in

increasing the power output but imparts a very large normal force on the cam, increasing the frictional opposition to rotation.

Dwell time at BDC and TDC should be maximized to what the cam geometry and linkages will physically allow. The other consideration is the severity of changing profile may influence system stability as at higher rpms, the more severe acceleration required may cause vibrational issues and excessive forces on linkages but if this can be mitigated effective material selection for critical components, then the real benefits of these findings can be capitalized on.

Further refinement of valve sizes and CCR in relation to displacement would be highly beneficial to finding the optimal performance. By employing a higher CCR and CR coupled with the increase in BDC and TDC dwell times, additional gains could be made by increasing the leverage and Cam Radius. Although, increasing the leverage also increases frictional forces. On selecting the bearing for the linkages, a very large safety factor should be applied since the load fluctuates between maximums at a rate proportionate to the RPM. To reduce the loading on the bearing, the frictional forces that oppose rotation need to be minimized, ensuring that the energy produced from the combustion is converted into rotation. Reducing the leverage will also help alleviate high forces on the cam. Even though this decreases the force acting on the cam to rotate the engine, this can be balanced by increasing the radius of the cam which has a proportionate influence to the output torque, as outlined in Section 2.3.

It can be noticed that a 'false peak' in power occurred for the 2 stroke engine, a drop off then it would spike. After this the throttle was pulled off as above 1250 RPM is thought to be far beyond the physical limits of the engine.

A smaller leverage ratio will decrease the overall output but refinement of the valve sizing and maximizing CCR and CR while increasing dwell times will lead to higher, more sustainable torque.

The performance calculator allows Bill to explore the influence of changing the piston profile and how this affects the torque curve.

By manipulating the piston trajectory and combustion, the torque curve can be flattened, providing much more consistent output over a wider range of RPM than a traditional IC engine.

Theoretically, more than 2 cylinders could be set up in series like previous orbital engines. If the combustion sequence is timed right, could lead to improved dynamic stability.

Extreme limits of dwell would make start up difficult,

The findings for the dwell configurations have wide implications for all IC engines. If increasing dwell time, increasing combustion pressure can be utilized, then this will improve performance. As can be seen from the investigation, almost all altered piston trajectories investigated outperformed the conventional sinusoidal piston trajectories.

6 CONCLUSIONS

6.1 RECOMMENDATIONS

The optimum parameters outlined in Section 4.4 should be used in conjunction with the performance calculator to assist in the development of the current and future prototypes to produce the desired output.

Since at the time of publishing, a lot of the parameters of the current engine design have been finalized, the following recommendations are made in respect the 2 stroke prototype currently under development;

- Retain inlet, exhaust and port sizes outlined in Section 3.3.2 and Annex D that reflects other 2 stroke configurations of similar displacement.
- In respect to the lobes on the cam, increase the maximum and minimum diameters to achieve the desired piston trajectory. The 3D CAD model easily converts cam geometry to a cam profile.
- Compression Ratio of 14:1. This delivers the best output without the risk of causing the onset of knock.
- Crankcase Ratio of 2:1. This is already considerably higher than other industry used two strokes and delivers very good charge pressure in conjunction with the valve geometries that are arranged for swirl production.

Validation of the performance prediction calculator against the 2 stroke prototype is highly recommended to assist in future development.

This investigation into this engine configuration has shown that this technology definitely has merit in producing useable energy from an abundant fuel source and warrants further research. The advantage of being able to alter piston trajectory has also proven a highly desirable tuning property and has shown that even when using a less potent fuel, can outperform its ICE counterparts.

6.2 TECHNOLOGICAL DEVELOPMENTS

Because the dynamics and combustion characteristics of this engine were relatively unknown, an in depth investigation into these area's will provide a better understanding led to a better design decisions and allowed steps towards optimizing this technology and improving its efficiency.

This analysis also provided practical limits in several areas that may have otherwise been overlooked. These areas include, fuel type, combustion, speed and dynamic limits, thermodynamic limits, as well as mechanical limits when considering subsequent forces and stresses on linkages, rollers etc. Better understanding of these limits allows better design decisions for future engines with this configuration.

This engine has almost unlimited potential in a multitude of applications, especially in the coming few decades where the search for alternative fuels is becoming increasingly important. Hopeful areas of applications include:

Energy generation – Running generators in remote location running on waste fuels. An example would be providing power to a coal mine running on the waste methane that is currently being vented straight into the atmosphere.

Marine applications: The large inertial energy that this engine carries while running could be utilized for gyroscopic stabilization in large ships as well as propelling the ship forward, instead of sacrificing engine power to run an additional gyroscope.

Other engine applications: The low speed output could eliminate the need for gearing in several areas, eliminating a source of lost energy.

6.3 COMMERCIAL DEVELOPMENTS

The use of Ricardo software to develop this easy to use design aid will save considerable costs in iterative prototyping. The material cost alone of building a single prototype depending on its scale is well into the thousands. Instead of building variations in this engine configuration, which can take months and even years at a time, the type of engine configuration can be entered in and an immediate prediction of performance can be obtained. The addition of this computer simulation package will save thousands of hours in time and tens of thousands in dollars that would have been spent on prototypes exploring the configurations capabilities.

Less time and money spent developing multiple variants of this prototype will mean time can be spent on other projects currently underway at WL White. More understanding of this engine equates to more informed decisions and a better end product to be introduced to the appropriate market.

An added bonus of benefit will be that these engines run on waste methane gas that can be used to run a generator that can provide electrically back into the national grid. At this stage, the interest of several Utility companies has been caught.

This is a very promising technology in an industry that is currently searching for cleaner, more efficient means of energy generation. This could potentially completely replace Diesel generators in the next decade. It's robust nature and high efficiency at constant rpm really promotes sustainable practices in an industry that currently relies on fossil fuels.

6.4 SYSTEM DEVELOPMENTS

The project had reasonable goals and even though the 2nd generation engine was not completed within the time scheduled, the primary goals were still achieved. (See Table 1 in Appendix C).

This sort of project is an exciting new technology that is being sought after more and more in the manufacturing industry and should be capitalized on. The time and money saved with the use of computer simulation packages to aid in design is becoming invaluable.

All future development work on this engine will be fast tracked with the use of the optimization and design tool developed with the aid of the computer simulation model developed through this project.

It should be noted that this project is ongoing through 2013. I have started employment with another company and am writing a thesis part time but am continuing support for this design aid tool and will until it can be verified against the 2nd generation engine to ensure of the projects continual success.

6.5 FUTURE WORK

An aspect that definitely requires further work now that the optimal configuration for producing the most power from methane is to mitigate the forces associated with pushing the acceleration of the pistons between TDC and BDC.

The two stroke configuration would benefit greatly from an expansion chamber on the exhaust, so development in this area could be of great benefit. The exhaust pipe of a two-stroke engine attempts to harness the energy of the pressure waves from combustion. The diameter and length of the five main sections of a pipe are critical to producing the desired power band. The five sections of the pipe are the head pipe, diffuser cone, dwell, baffle cone, and the stinger. In general, after market exhaust pipes shift the power band up the rpm scale.

Also the greatest power is achieved beyond the 1000rpm stage. Which considering the thermodynamic cycles per revolution. Unfortunately due to the extreme forces and centripetal acceleration of the components mean that significant work is needed for this engine to capitalize being able to run effectively at these speeds. Forces on the cam, linkages and bearings cause breakages.

REFERENCES

Graham Harlin. Rolls Royce Plc – Whole engine development, 2005 (VIVAE Forum, Warwick England).

P R Hooper, T Al-Shemmeri and M J Goodwin. Advanced modern low-emission two-stroke cycle engines 225: 1531 Proceedings of the Institution of Mechanical Engineers, Part D: Journal of Automobile Engineering, Aug 2011

Pavel Novotný, Václav Pištěk. Virtual development process of modern diesel engines - Dealing with the Research of Combustion Engines. KOKA 2006, XXXVII. International conference of Czech and Slovak Universities' Departments and Institutions

Jasak, J.Y. Luo, B. Kaludercic and A.D. Gosman. Rapid CFD Simulation of Internal Combustion Engines, Computational Dynamics Ltd. H. Echtele, Z. Liang and F. Wirb eleit Daimler-Benz AG M. Wierse SGI/Cray Research S. Rips and A. Werner University of Stuttgart G. Fernstrom and A.Karlsson AB Volvo Technological Development

Cory Griswold. Development of a high speed data acquisition system for spark ignition engine. Georgia Southern University, 2008

Environmental Protection Agency. (2008) Control of emissions from marine is and small is engines, vessels, and equipment final regulatory impact analysis. Retrieved from <http://www.epa.gov/oms/regs/nonroad/marinesi-equipld/420r08014.pdf>(EPA.gov)

Bosch. Wideband A/F Oxygen Sensors. Retrieved June 13, 2011, from <http://www.boschautoparts.com/OxygenSensors/Pages/WidebandOxygenSensors.aspx>

Grabner, P., Eichlseder, H., & Eckhard, G. (2010). Potential of E85 Direct Injection for Passenger Car Application (No. 2010-01-2086). Warrendale, PA: SAE International. Retrieved from <http://papers.sae.org/2010-01-2086/>

Greene, A. B., & Lucas, G. G. (1969). Testing of Internal Combustion Engines. Hodder & Stoughton Ltd.

Guzzella, L., & Onder, C. (2010). Introduction to Modeling and Control of Internal Combustion Engine Systems (1st ed.). Springer.

Hendricks, E., & Sorenson, S. C. (1990). Mean Value Modeling of Spark Ignition Engines (No. 900616). Warrendale, PA: SAE International. Retrieved from <http://papers.sae.org/900616/>

Herman, P., & Franchek, M. A. (2000). Engine idle speed control using actuator saturation. Control Systems Technology, IEEE Transactions on, 8(1), 192-199. doi:10.1109/87.817704

Heywood, J. (1988). Internal Combustion Engine Fundamentals (1st ed.). McGraw-Hill Science/Engineering/Math. 130

Jing Sun, Kolmanovsky, I., Cook, J. A., & Buckland, J. H. (2005). Modeling and control of automotive power train systems: a tutorial. American Control Conference, 2005. Proceedings of the 2005 (pp. 3271-3283 vol. 5). Presented at the American Control Conference, 2005. Proceedings of the 2005. doi:10.1109/ACC.2005.1470476

Kiencke, U., & Nielsen, L. (2010). Automotive Control Systems: For Engine, Driveline, and Vehicle (2nd ed.). Springer.

LSU42.pdf. (n.d.). Retrieved from <http://www.bosch-motorsport.com/pdf/sensors/lambda/LSU42.pdf>

National Institute of Standards and Technology. (1995). ITS-90 Thermocouple Database, Web Version 2.0. NIST ITS-90 Thermocouple Database. Retrieved June 13, 2011, from <http://srdata.nist.gov/its90/main/>

Rajamani, R. (2005). Vehicle Dynamics and Control (1st ed.). Springer.

Rajamani, R. (2006). Vehicle dynamics and control. Birkhäuser.

Varde, K. S., & Manoharan, N. K. (2009). Characterization of Exhaust Emissions in a SI Engine using E85 and Cooled EGR (No. 2009-01-1952). Warrendale, PA: SAE International. Retrieved from <http://papers.sae.org/2009-01-1952/>

Wu, Yuh-Yih, Chen, Bo-Chiuan, Hsieh, Feng-Chi, Huang, M.-L., & Wu, Y.-H. (2006). Development of Hardware-In-the-Loop Simulation for Scooter Engine Control (No. 2006-01-0614). Warrendale, PA: SAE International. Retrieved from <http://papers.sae.org/2006-01-0614/>

Eric Tribbett, Ed Froehlich, Lex Bayer. Effects of ignition timing, equivalence ratio and compression ratio on RDH Engine Performance. Mechanical Engineering Dept. Stanford University

A-P Qiao 1,2, Y-Q Li 1 , and F Gao 1. Improving the theoretical cycles of four-stroke internal combustion engines and their simulation calculations. 2 Beijing University of Aeronautics and Astronautics, Beijing, People's Republic of China, 2 Taiyuan University of Technology, Taiyuan, Shanxi Province, People's Republic of China September 2005. DOI: 10.1243/095440706X72646

G.H. Abd Alla . Computer simulation of a four stroke spark ignition engine Energy Conversion and Management 43 (2002) 1043–1061 Al-Ain Technical School, P.O. Box 17835, Al-Ain, United Arab Emirates April 2001

H Cho, S R Krishnan, R Luck and K K Srinivasan. Comprehensive uncertainty analysis of a Wiebe function-based combustion model for pilot-ignited natural gas engines. 223: 1481 Proceedings of the Institution of Mechanical Engineers, Part D: Journal of Automobile Engineering, 2009

Dan Cordon, Charles Dean, Judith Steciak and Steven Beyerlein, One dimensional engine modeling and validation using Ricardo. National Institute for Advanced Transportation Technology University of Idaho, September 2007

Clark Talkington, Dr. Pamela Franklin. Methane use in IC engines at coal mines. Environmental Protection Agency: Coal Methane Outreach Program

Technical Options Series, Coalbed Methane Outreach Program, U.S. EPA (6202J), Washington, DC 20460 USA, 2004.

Maher A.R. Sadiq Al-Baghdadi, Haroun A.K. Shahad Al-Janabi. A prediction study of a spark ignition supercharged hydrogen engine. Department of Mechanical Engineering, College of Engineering, University of Babylon, Babylon, Iraq. May 2003

Heather L. MacLean, Lester B. Lave. Evaluating automobile fuel/propulsion system technologies Department of Civil Engineering, University of Toronto, 35 St George Street, Toronto, Canada M5S 1A4 Graduate School of Industrial Administration, Carnegie Mellon University, Tech and Frew Sts, Pittsburgh, PA 15213-3890, USA. September 2002

S Rousseau, B Lemoult and M Tazerout; Combustion characterization of natural gas in a lean burn spark-ignition engine 1999 213: 481 Proceedings of the Institution of Mechanical Engineers, Part D: Journal of Automobile Engineering.

J-J Zheng, J-H Wang, B Wang and Z-H Huang. Effect of the compression ratio on the performance and combustion of a natural-gas direct-injection engine. 2009 223: 85 Proceedings of the Institution of Mechanical Engineers, Part D: Journal of Automobile Engineering

Haeng Muk Cho, Bang-Quan He. A review of spark ignition natural gas engines —Development of a natural gas SI engine for optimal performance. Division of Mechanical Engineering and Automotive Engineering, Kongju National Univeristy, 276, Budaе-Dong, Cheonan-City, Chungnam 330-717, Korea, State Key Laboratory of Engines, Tianjin University, 92, Weijin Road, Nankai District, Tianjin 300072, PR China. May 2006

K K Srinivasan, S R Krishnan, and K C Midkiff. Improving low load combustion, stability, and emissions in pilot-ignited natural gas engines. Department of Mechanical Engineering, University of Alabama, Tuscaloosa, Alabama, USA

A Das and HC Wilson. Development of a natural gas spark ignition engine for optimum performance by Department of Mechanical and Manufacturing Engineering, University of Melbourne, Australia

S Rousseau, B Lemoult and M Tazerout. Combustion characterization of natural gas in a lean burn spark-ignition engine. 1999 213: 481 Proceedings of the Institution of Mechanical Engineers, Part D: Journal of Automobile Engineering. 7: 131 International Journal of Engine Research. 2006

J Adair, D Olsen and A Kirkpatrick. Exhaust Tuning of Large-Bore, Multicylinder, Two-Stroke, Natural Gas Engines. Part D: Journal of Automobile, Proceedings of the Institution of Mechanical, <http://pid.sagepub.com/content/213/5/481>

Heywood, J. B. (1988). Internal combustion engine fundamentals / John B. Heywood. New York : McGraw-Hill Book Company. Retrieved from http://platon.serbi.ula.ve/librum/librum_ula/ver.php?ndoc=271732

Grant Smedley. Piston Ring Design for reduced friction in modern IC engines. Mechanical Engineering, McGill University. 2002.

L.S. Johansson¹, C. Tullin¹, B. Leckner², P. Sjövall². Particle emissions from biomass combustion in small combustors.

¹ SP Swedish National Testing and Research Institute, Department of Energy Technology, Box 857, Borås 50115, Sweden

² Chalmers University of Technology, Department of Energy Technology, Göteborg 41296, Sweden, 2003.

J Adair, D Olsen and A Kirkpatrick. Exhaust Tuning of Large-Bore, Multicylinder, Two-Stroke, Natural Gas Engines. Part D: Journal of Automobile, Proceedings of the Institution of Mechanical, 1999. <http://pid.sagepub.com/content/213/5/481>

G. Bourn, S. Stacy and J. Campbell (2011). A Case Study on Trapped Equivalence Ratio Control & Fuel Composition Effects. El Paso Pipeline Group case study.

APPENDIX A

PROJECT MILESTONES

Objective	Target Date	Status	Comments
Objective 1			
1.1 Analyze the current 4 stroke prototype	3rd March 2012	Completed 3rd March 2012	An in depth investigation identified the key elements of the engine and how they influence its performance.
1.2 Create 1D computer model of existing prototype	25 th May 2012	Completed 25 th May 2012	All elements were constructed and inputs adjusted as well as manipulating the software so that it could cope with an engine in this configuration.
1.3 Verify model against 4 stroke prototype performance	8 th June 2012	Completed 8 th June 2012	The engine performance calculated by the simulation built in Ricardo (Appendix A) was compared against the dynamometer results on the 1 st prototype and was found to be comparable.
Objective 2			
2.1 Create and upscale model to a 2 stroke variant	24 th August 2012	Completed 12 th October 2012	The model was recreated to predict the performance of the larger 2 stroke variant being developed.
2.2 Predict performance of the 2 stroke variant	31 st August 2012	Completed 12 th October 2012	A prediction was created by simulation. It's accuracy is based on the similarities to the verified first generation engine.
2.3 Validate model against 2 stroke test data performance	14 th September 2012	Ongoing	The 2 nd generation, 2 Stroke Engine still not ready for testing, as soon as test data is available, the model can be further validated. As of now, the single 4 stroke engine performance is the only form of validation.
Objective 3			
3.1 Critically evaluate model	30 th September 2012	Completed/ Ongoing	The model has been verified against a single set of real data and even though this matched extremely well, further verification is needed for confidence.
3.2 Refine model to more adequately follow empirical results	5 th October 2012	Ongoing	The model is continually being refined, improving usability and incorporating other areas that will aid in future design.
3.3 Apply both computer models to explore the family of variants	2 nd November 2012	Completed	Hundreds of simulations were completed using the Ricardo models and there is copious amounts of data stored within the calculator exploring a wide range of variants.
3.4 Develop an optimization and design tool model suitable for practitioners to use without the need of expensive software.	28 th December 2012	Completed/ ongoing	Current design tool that doesn't need any special software (only Microsoft Excel to run) is shown in Appendix B.

Table A1 – Milestones

APPENDIX B

ENGINE CONSTANTS TABLE FOR 2 STROKE AND 4 STROKE MODELS

Constant	Model Identifier	Unit	Value	Comment
Air / Fuel Ratio	A_F	-	17.2	Stoichiometric for Methane
Burn Duration	BDUR	deg	40	See section
50% Combustion Point	CA50	deg	60	
Exhaust Valve Temperature	EV_TEMP	K	625	Calculated based on proximity to, material thickness and temperature of combustion
Engine Head Temperature	HEAD_TEMP	K	435	Calculated based on proximity to, material thickness and temperature of combustion
Intake Valve Temperature	IV_TEMP	K	610	Calculated based on proximity to, material thickness and temperature of combustion
Liner Temperature	LINER_TEMP	K	460	Calculated based on proximity to, material thickness and temperature of combustion
Piston Temperature	PISTON_TEMP	K	520	Calculated based on proximity to, material thickness and temperature of combustion
Speed of Engine	SPEED	RPM	Varies	Increments of 25 RPM, Max 1200 RPM Min 0 RPM
Thermal Conductivity of Head, Liner and Piston	THERMAL_COND_	W/m. K	45	Same alloy assumed for Head, Liner and Piston.
Throttle Position	THROTTLE_ANGLE	deg	86	Wide open throttle position

Table B1 – Engine Constants for 2 Stroke and 4 Stroke Models

APPENDIX C

ADDITIONAL 4 STROKE MODEL INFORMATION

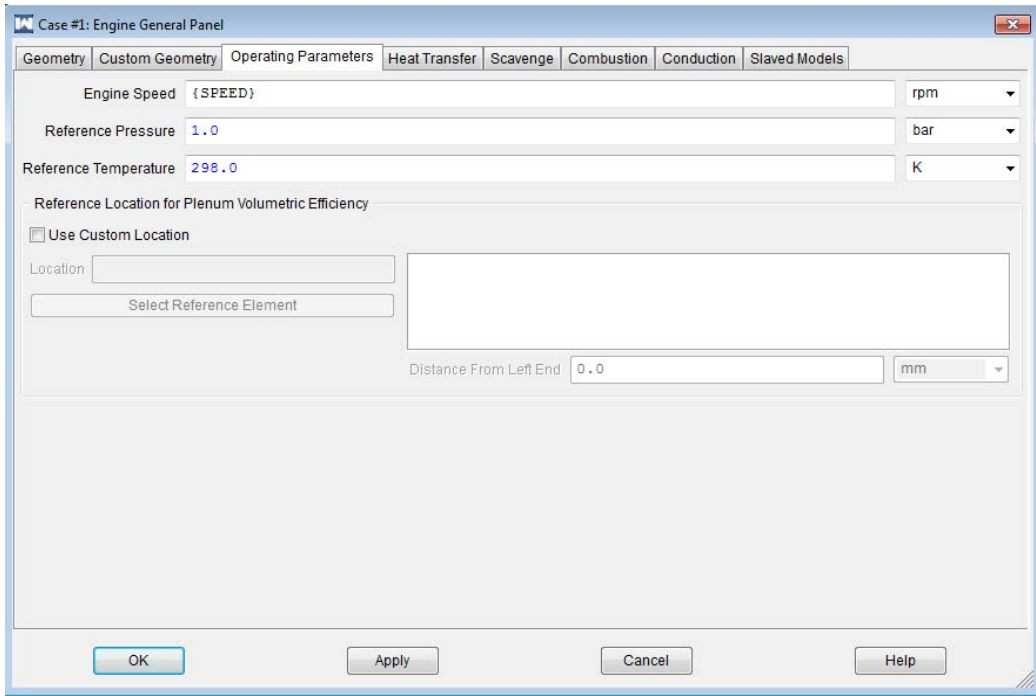


Figure C1 – Engine General Panel, Operating Parameters

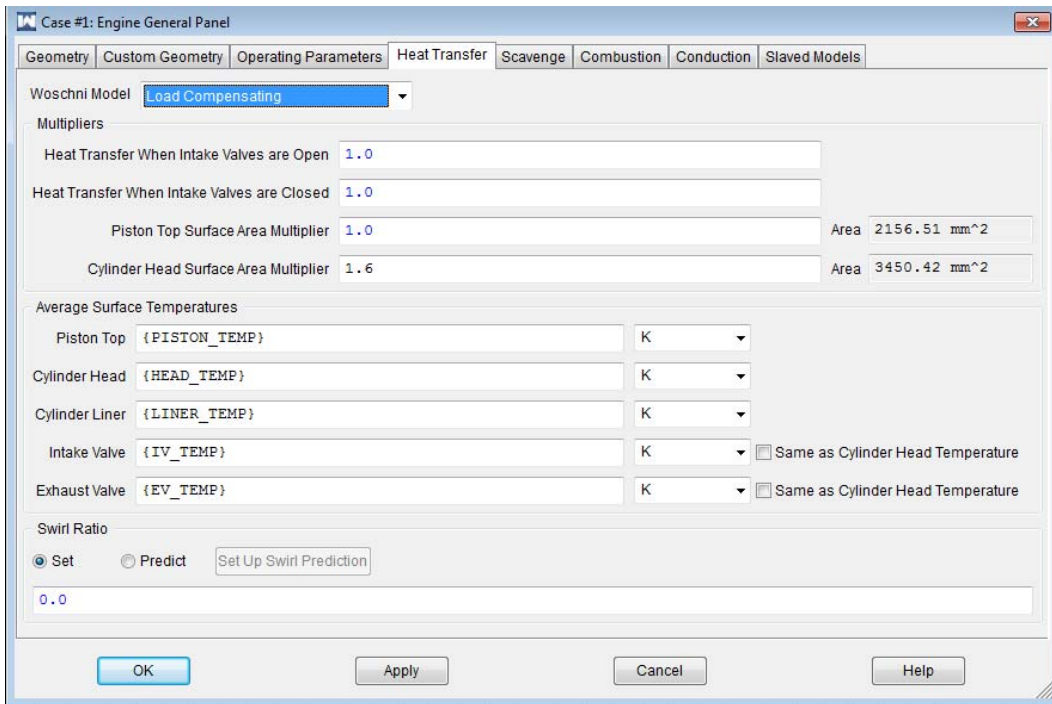


Figure C2 – Engine General Panel, Heat Transfer

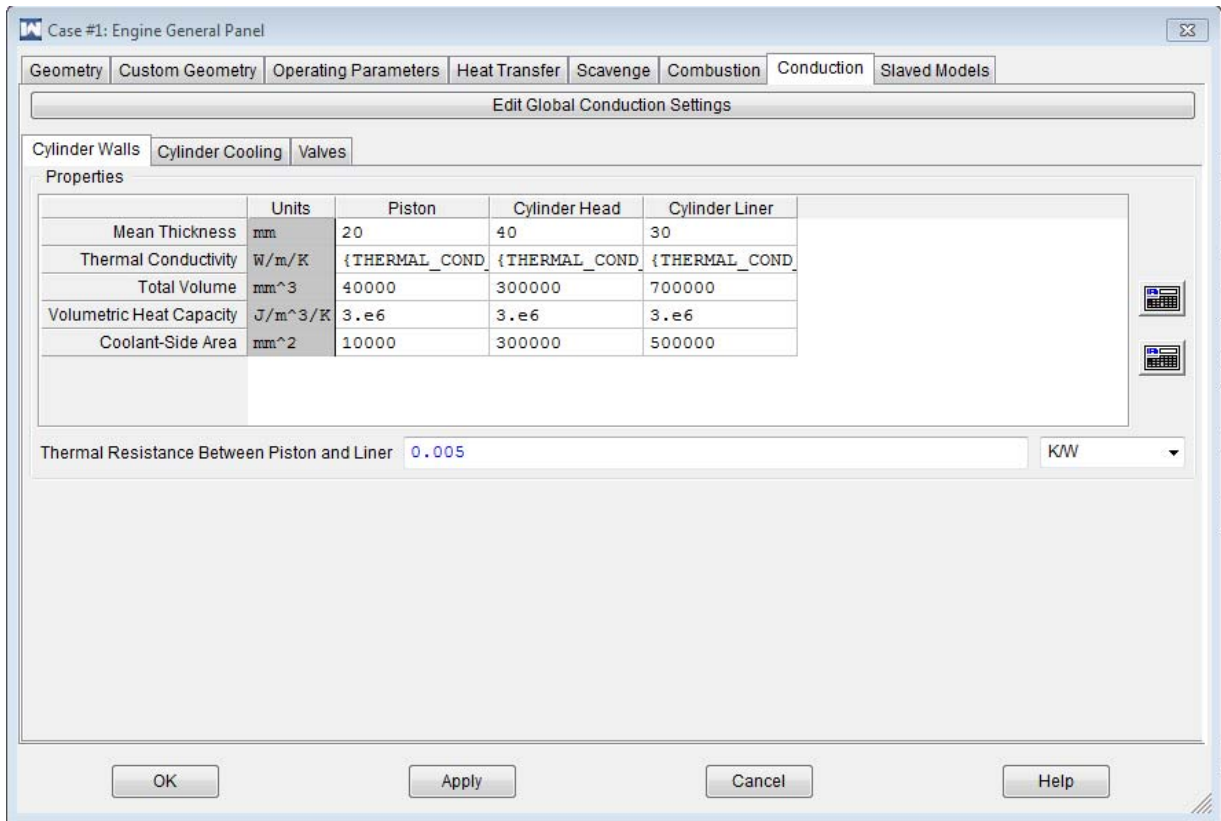


Figure C3 – Engine General Panel, Conduction Coefficients for Cylinder Walls

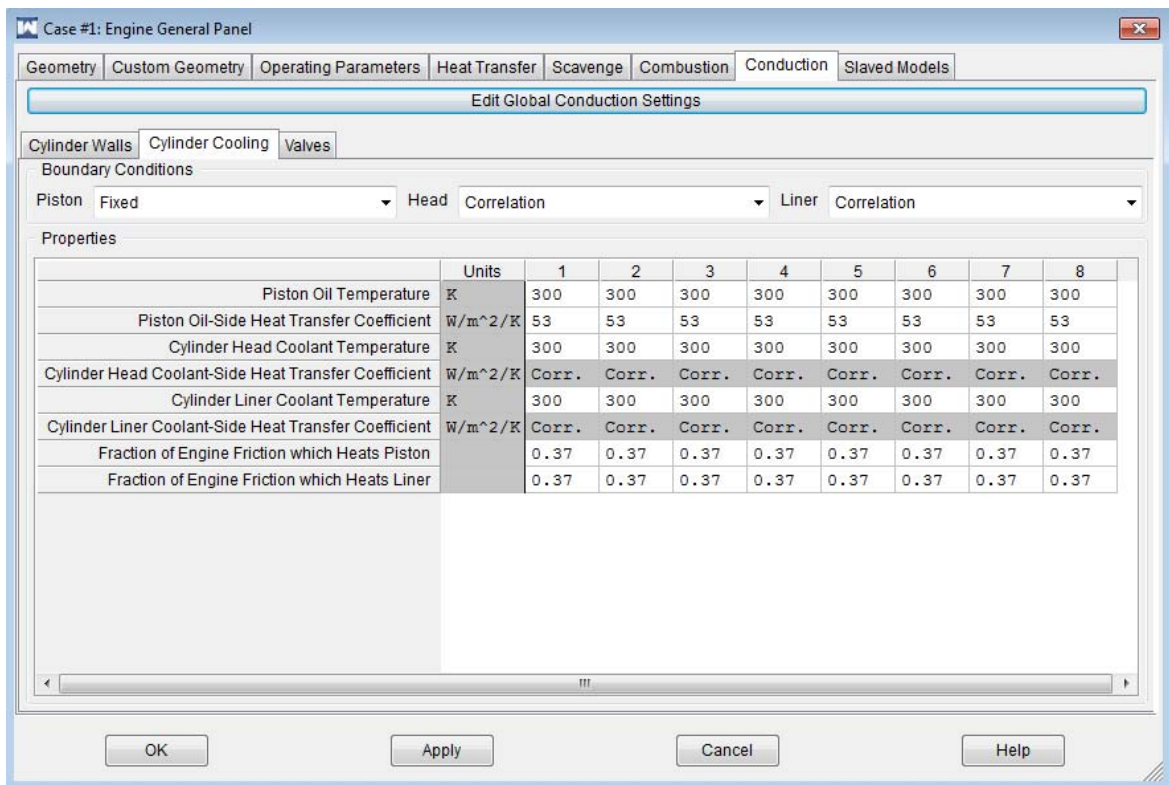


Figure C4 – Engine General Panel, Conduction Coefficients for Cylinder Cooling

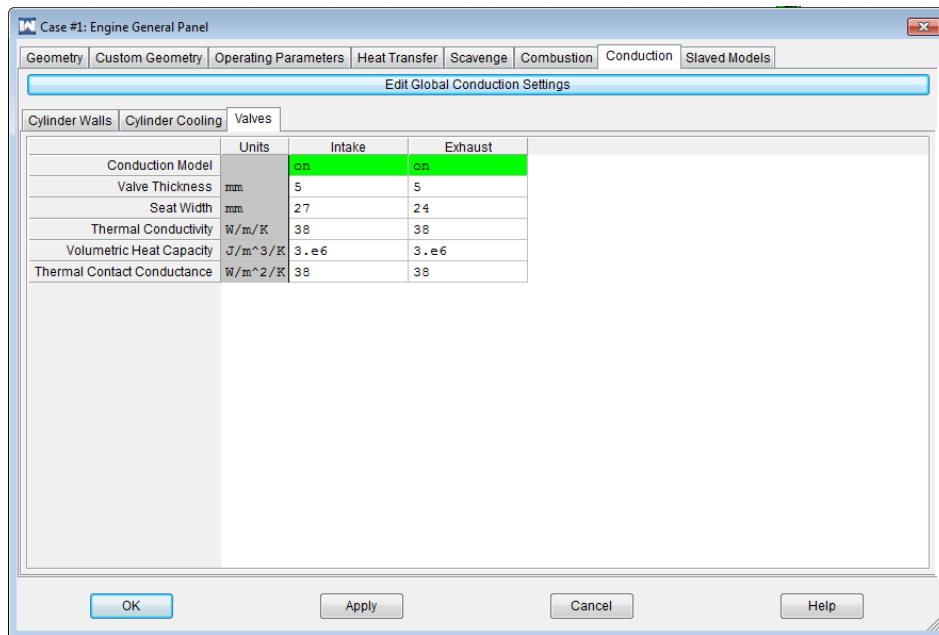


Figure C5 – Engine General Panel, Conduction Coefficients for Valves

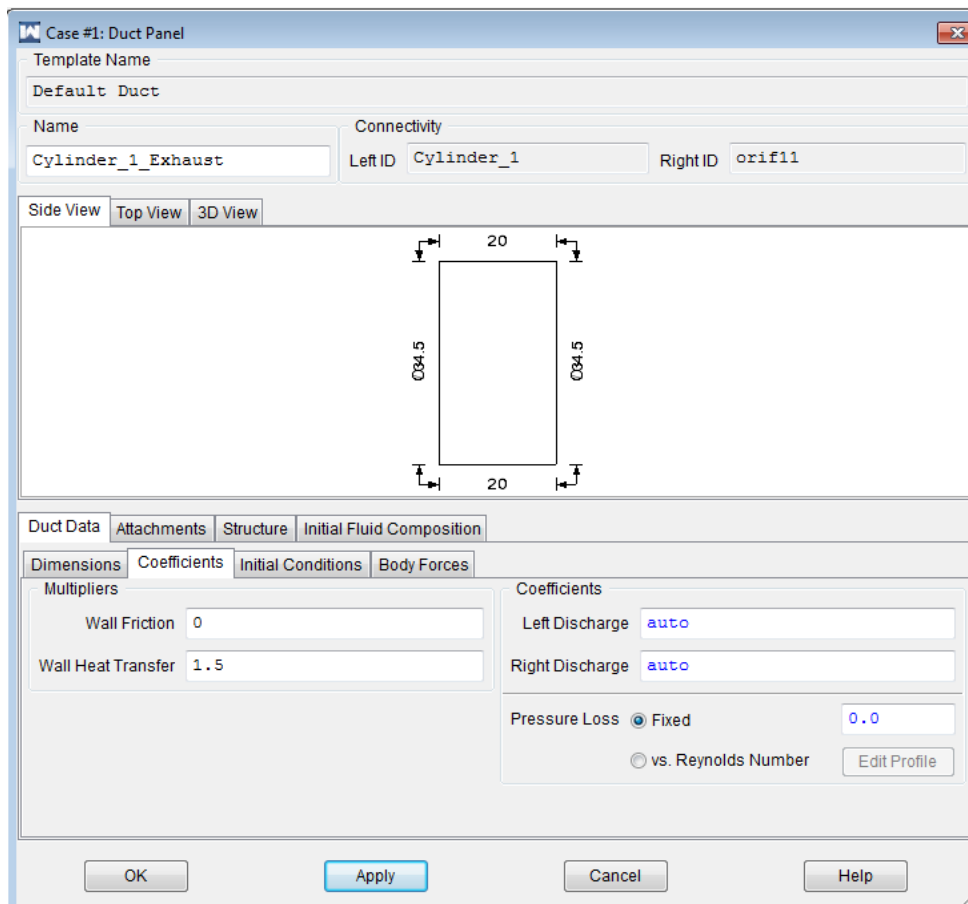


Figure C6 – Exhaust Ducting Profile

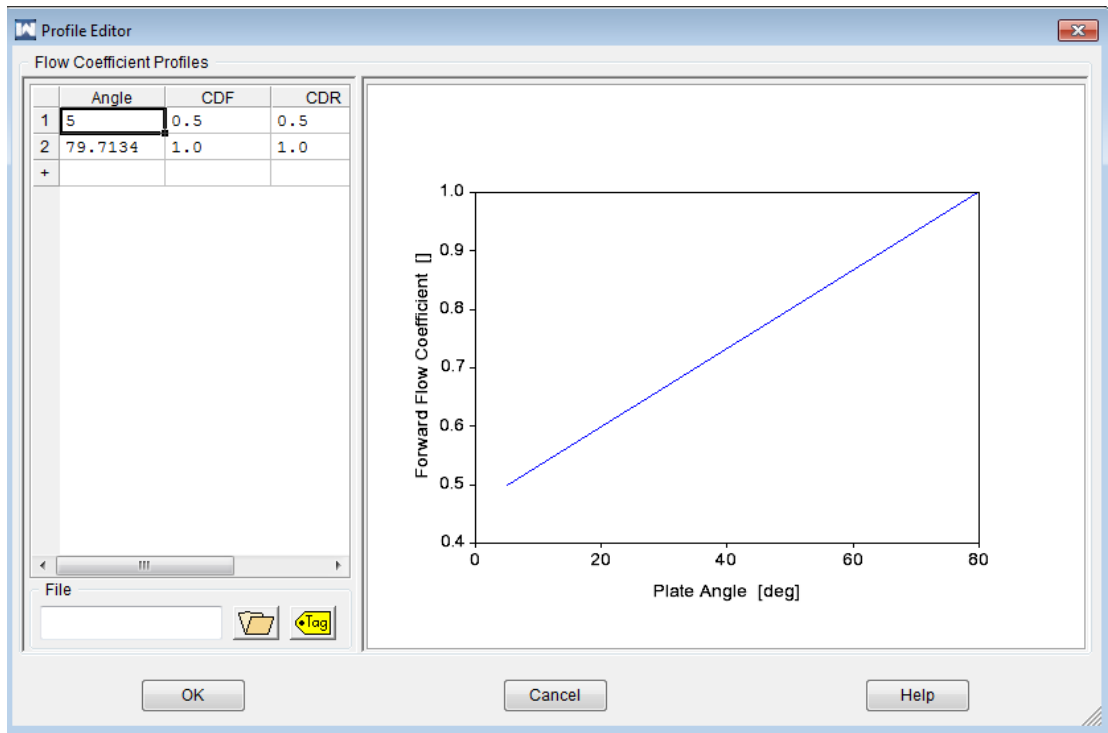


Figure C7 – Butterfly valve flow, assumed to be linear to WOT

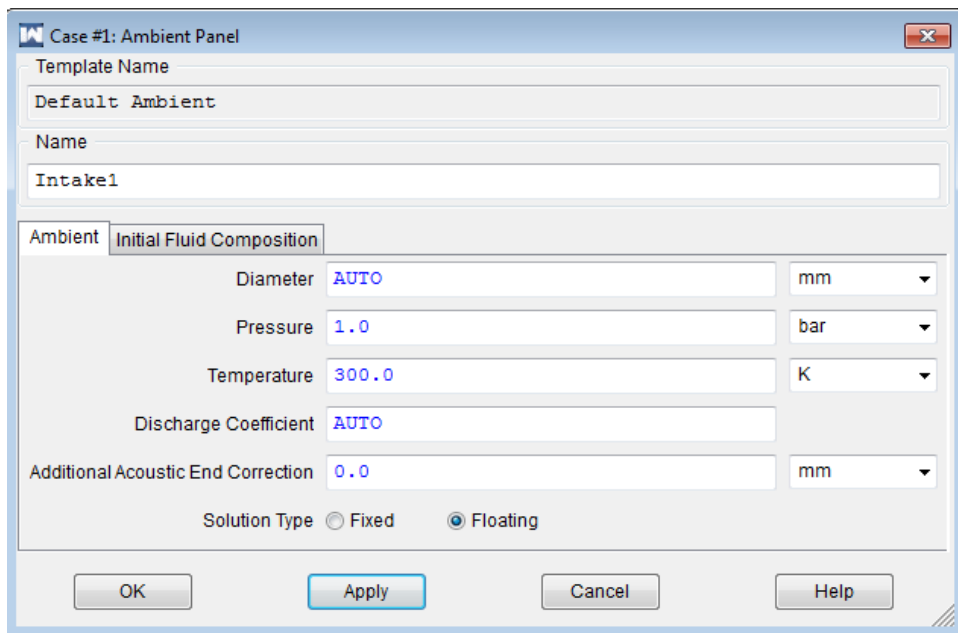


Figure C8 – Intake Flume

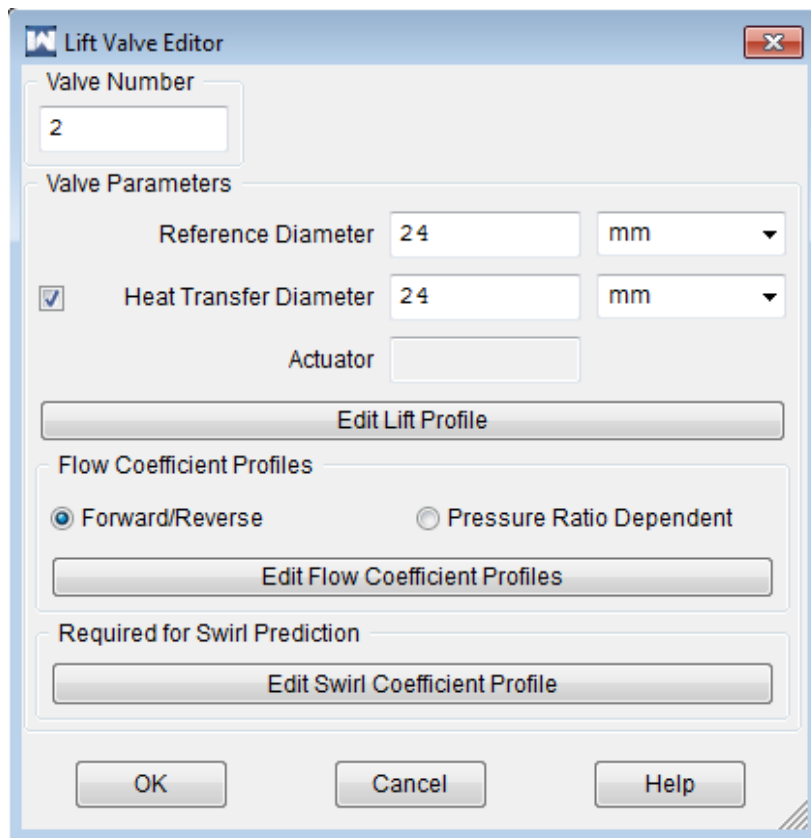


Figure C9 – Exhaust valve

APPENDIX D

ADDITIONAL MODEL INFORMATION 2 STROKE

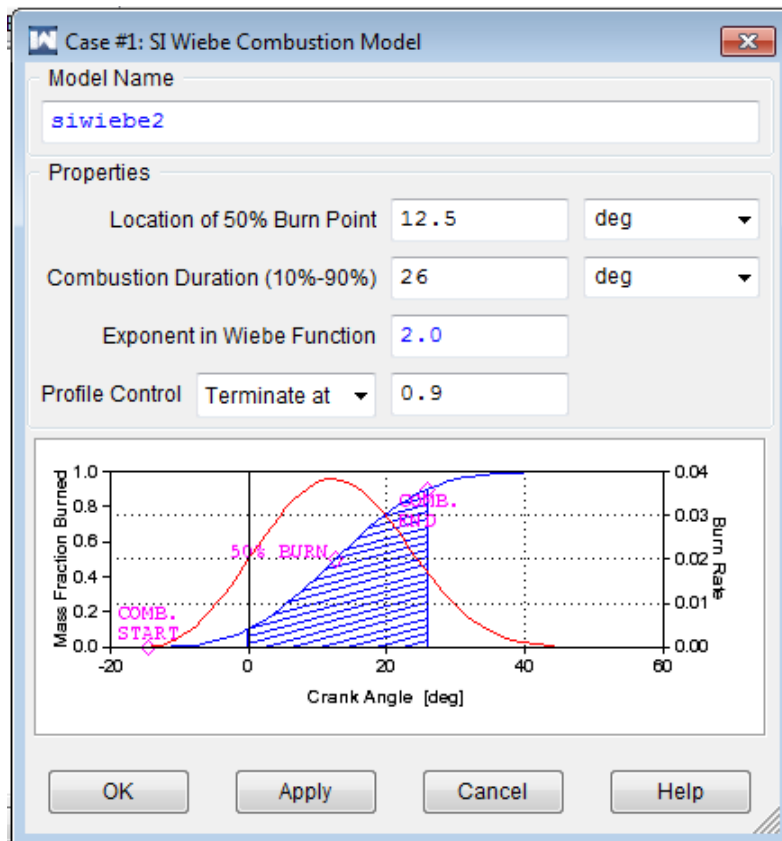


Figure D1 – 2 Stroke Wavebuild model Used Combustion

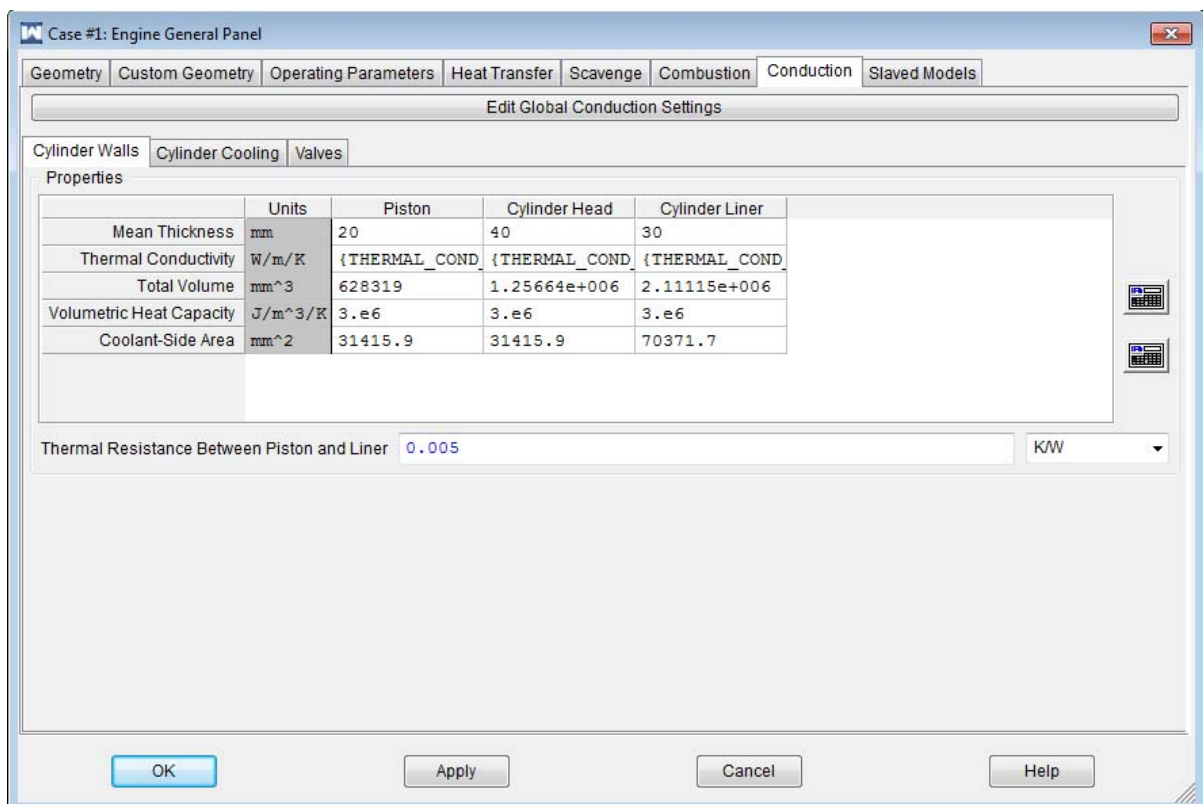


Figure D2 – Engine General Panel, Conduction Coefficients for Cylinder Walls

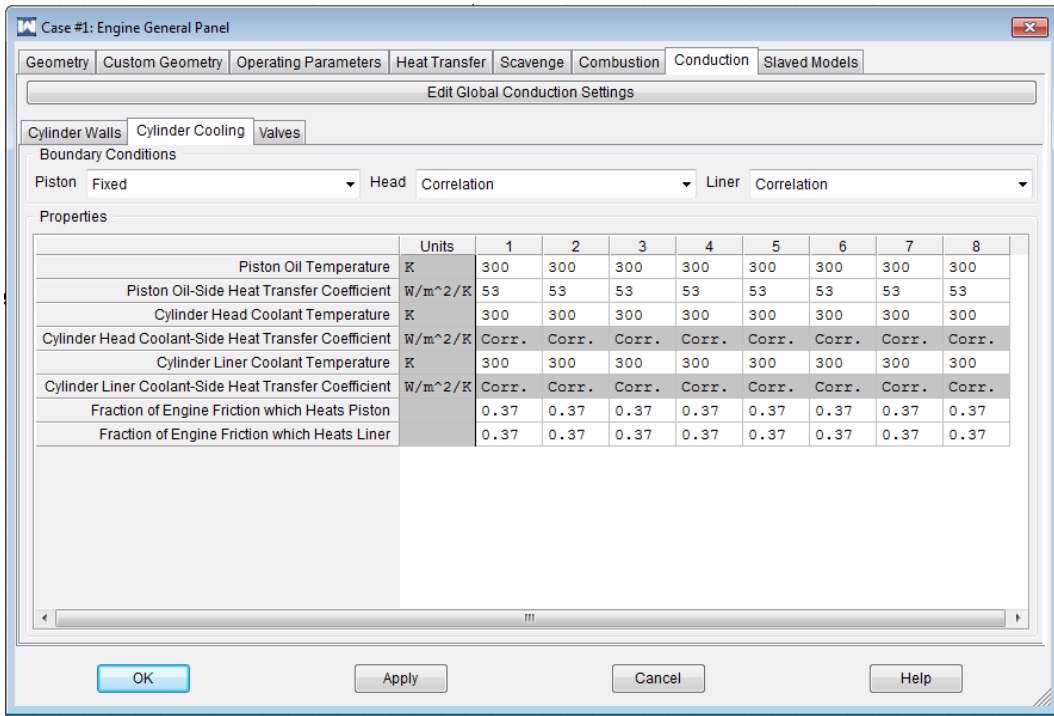


Figure D3 – Engine General Panel, Conduction Coefficients for Cylinder Cooling

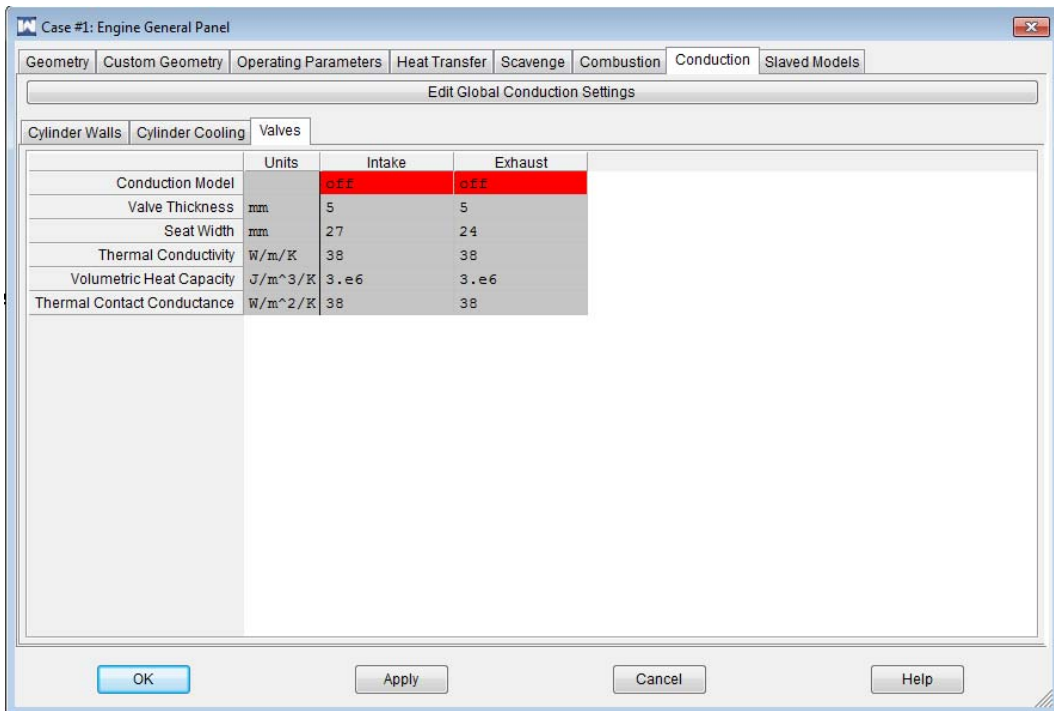


Figure D4 – Engine General Panel, Conduction Coefficients for Valves

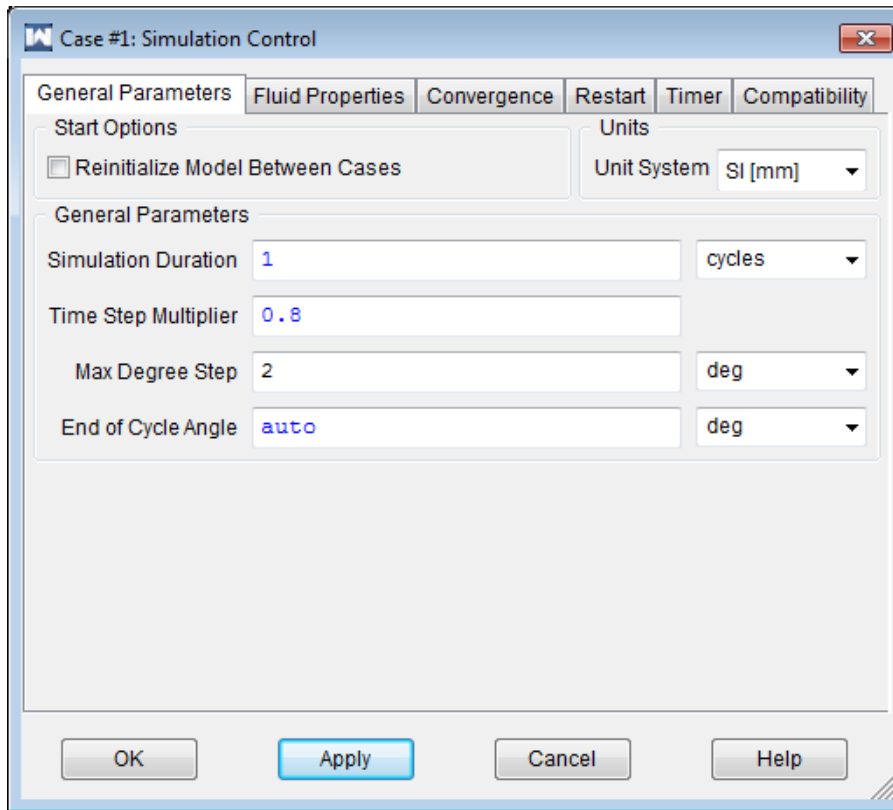


Figure D5 – Simulation Control, General

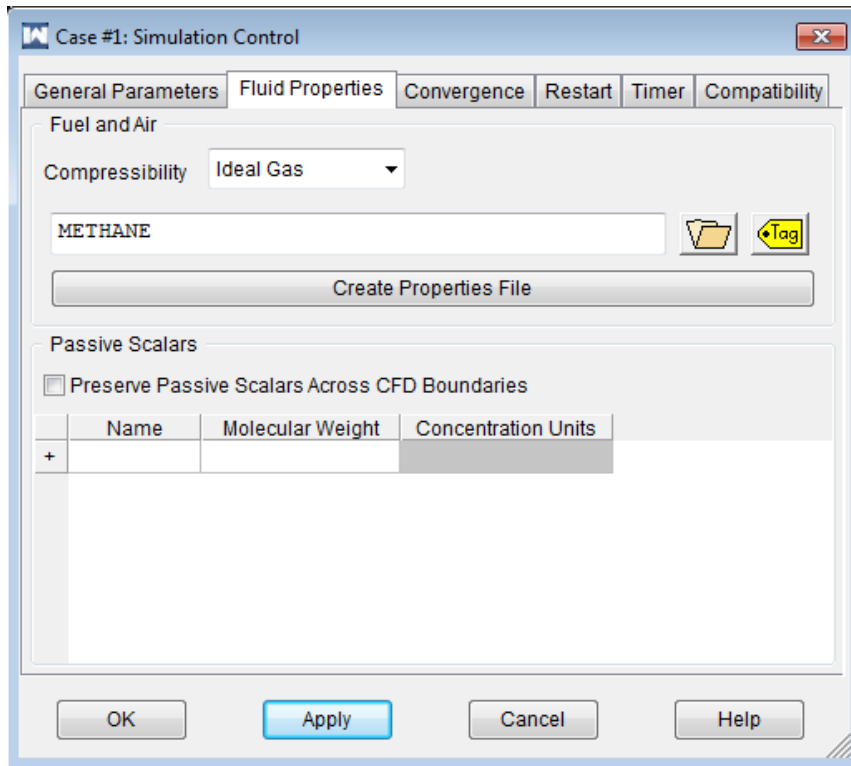


Figure D6 – Simulation Control, Fluid Properties

Constants

Constants Table Sweep Constants Dependent Constants External Constants

Status	Name	Units	Case 1	Case 2	Case 3	Case 4
			Run	Run	Run	Run
1	A F		17.2	17.2	17.2	17.2
2	BDUR	deg	40	40	40	40
3	CAS0	deg	60	60	60	60
4	EV_TEMP	K	625	625	625	625
5	HEAD_TEMP	K	435	435	435	435
6	IV_TEMP	K	610	610	610	610
7	LINER_TEMP	K	460	460	460	460
8	PISTON_TEMP	K	520	520	520	520
9	SPEED	rpm	1250	1200	1150	1100
10	THERMAL_COND_HEAD	W/m.K	45	45	45	45
11	THERMAL_COND_LINER	W/m.K	45	45	45	45
12	THERMAL_COND_PISTON	W/m.K	45	45	45	45
13	THROTTLE_ANGLE	deg	86	86	86	86
+						

Number of Cases 33 Import... Export... Display Profile... Catalog Usage...

OK Cancel Help

Figure D7 – Constants Table

Butterfly Valve Editor

Valve Number
1

Valve Geometry

Bore Diameter 75 mm

Shaft Diameter 5 mm

Minimum Plate Angle 4 deg

Calculated Values

Actual Plate Angle 4 deg

Valve Angle For Maximum Open Area 86.1774 deg

Maximum Open Area 4043.14 mm²

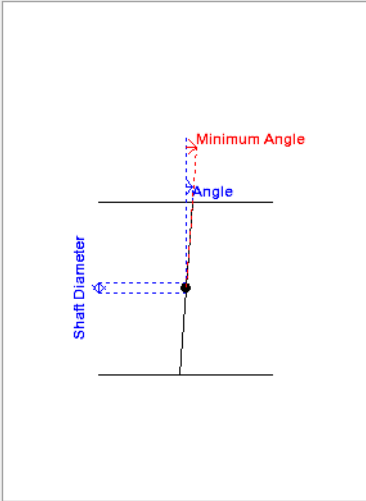
Actual Open Area 0 mm²

Equivalent Diameter 0 mm

Flow Coefficient Profiles

Forward/Reverse Pressure Ratio Dependent

Edit Flow Coefficient Profiles



The diagram shows a vertical shaft with a diameter of 5 mm. Two horizontal plates are attached to the shaft, forming a butterfly valve. The angle between the plates is labeled as 'Angle'. A red dashed line indicates the 'Minimum Angle' between the plates. The shaft diameter is labeled as 'Shaft Diameter'.

OK Cancel Help

Figure D8 – Butterfly Valve Editor

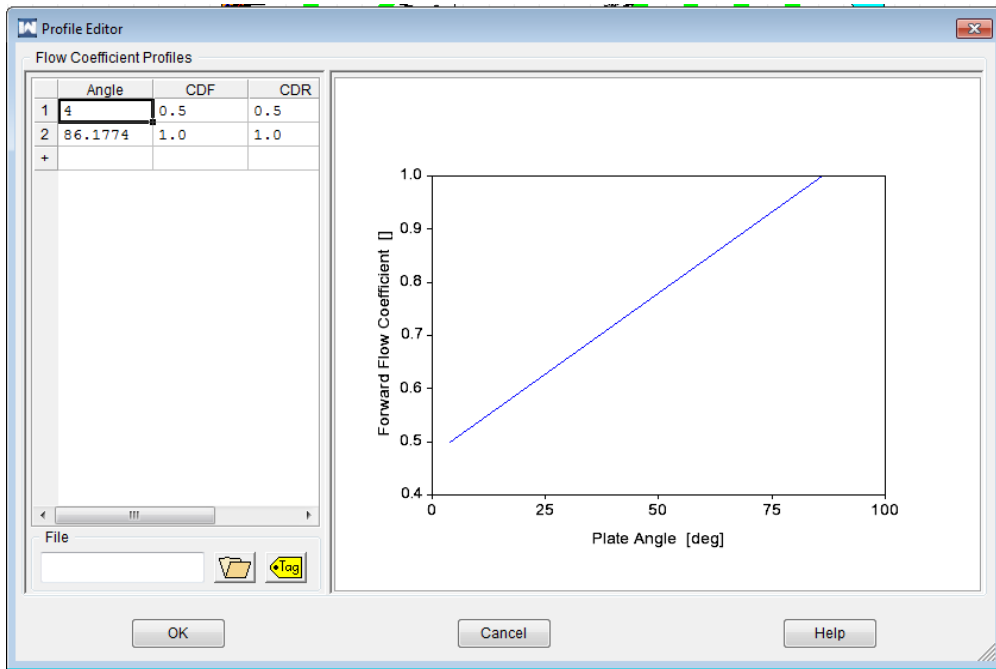


Figure D9 – Butterfly valve flow, assumed to be linear to WOT

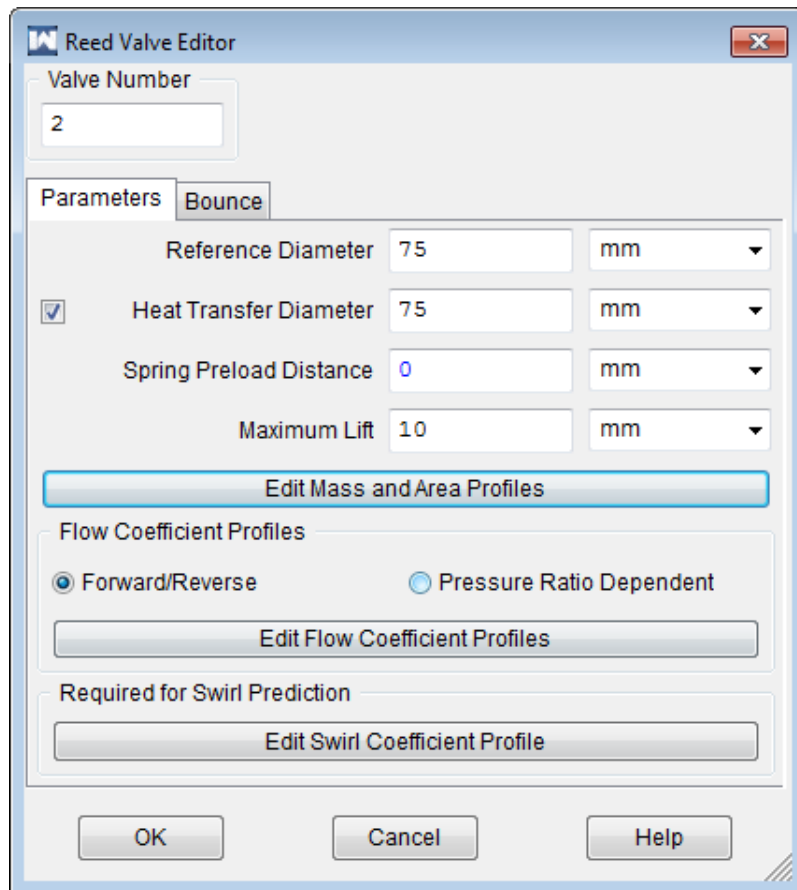


Figure D10 – Reed Valve Editor

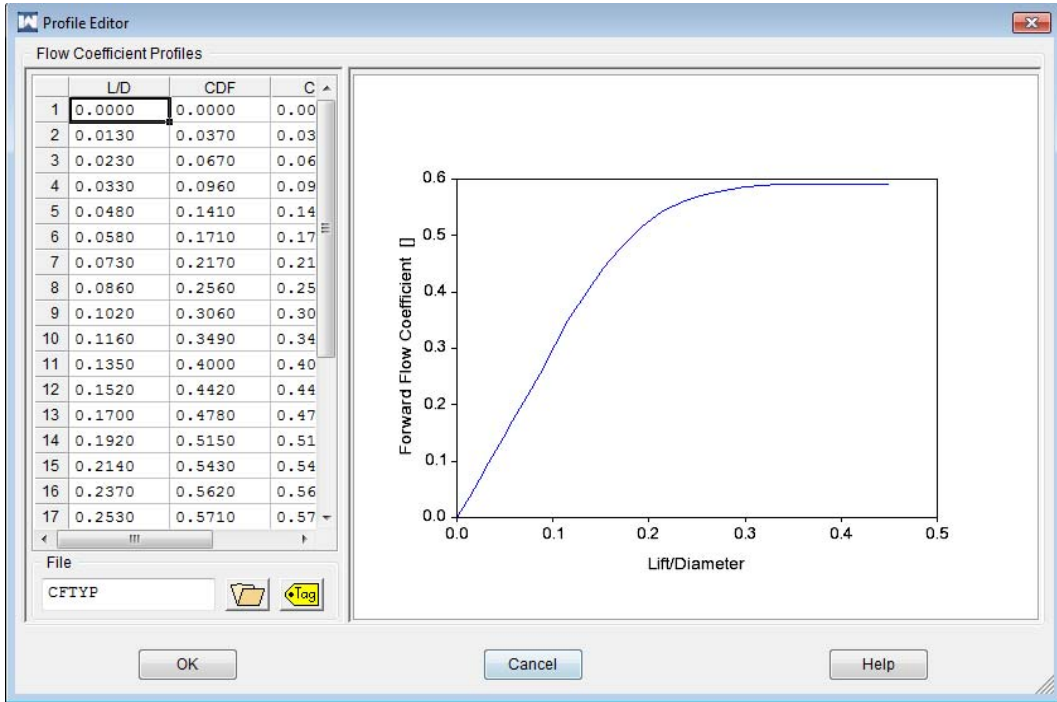


Figure D11 – Reed Valve Flow Coefficient Profile – see Figure D25

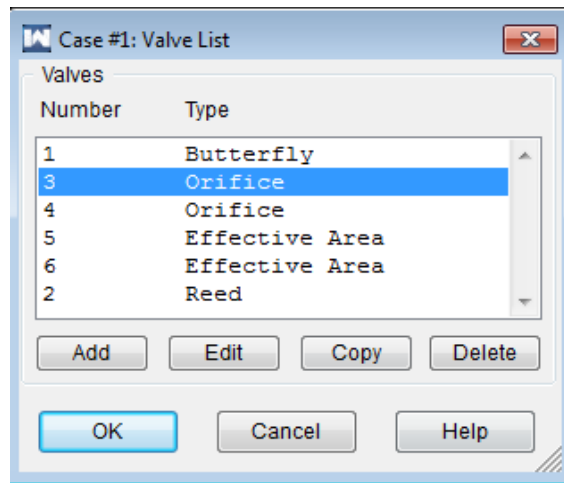


Figure D12 – List of Valves used on 2 stroke engine

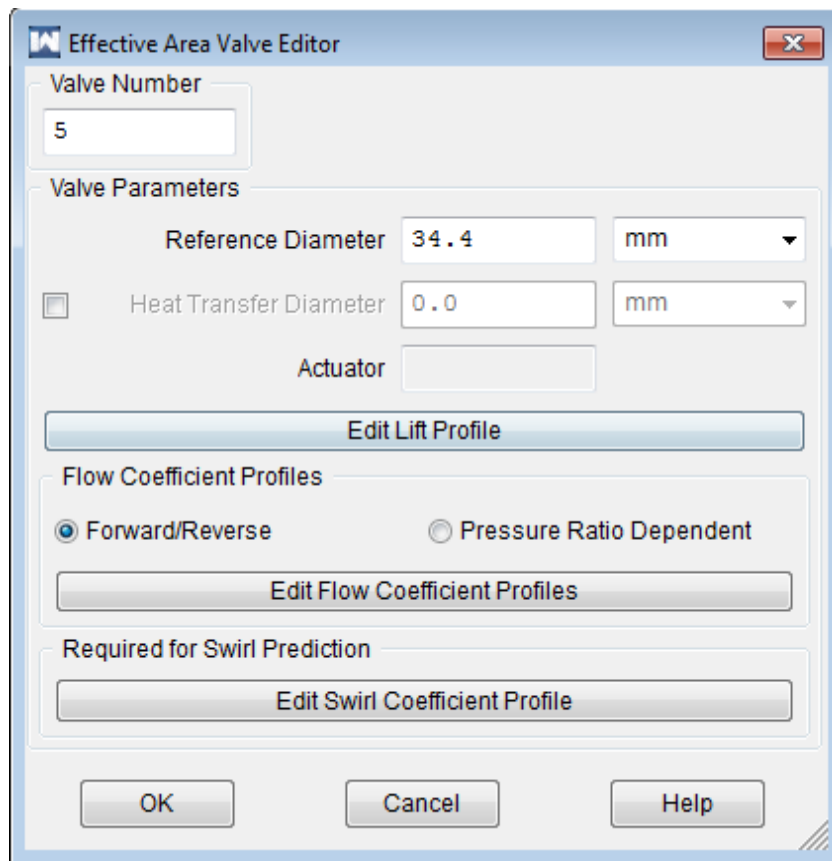


Figure D13 – Inlet Port (Cylinder Operated Effective area model)

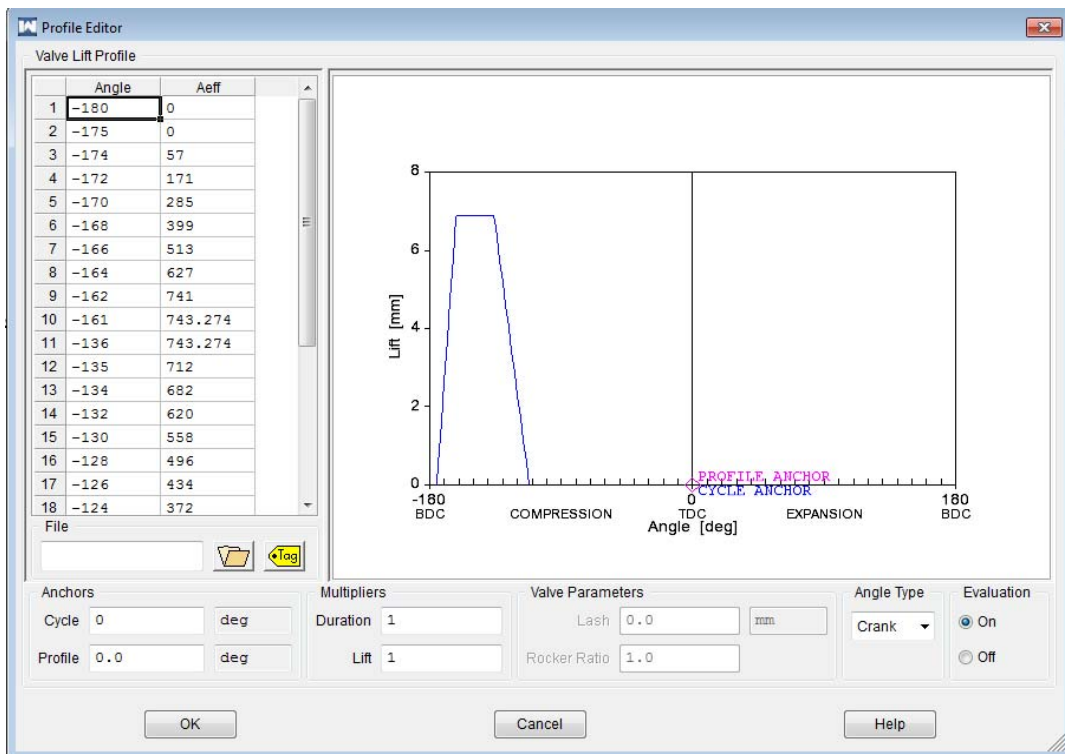


Figure D14 – Inlet Port Lift Profile (Cylinder Operated Effective area model)

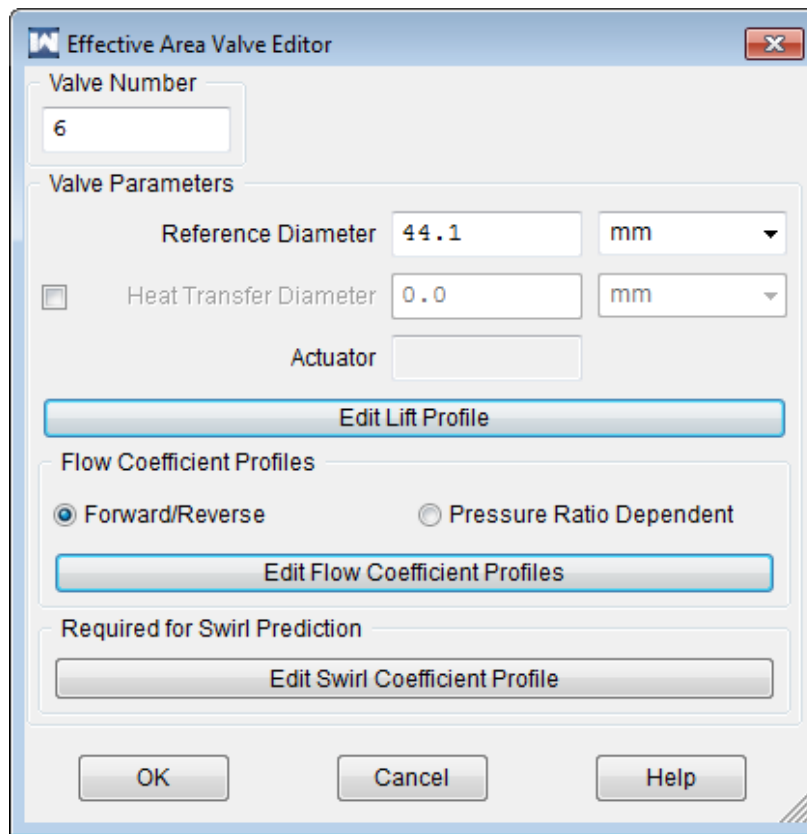


Figure D15 – Exhaust Port (Cylinder Operated Effective area model)

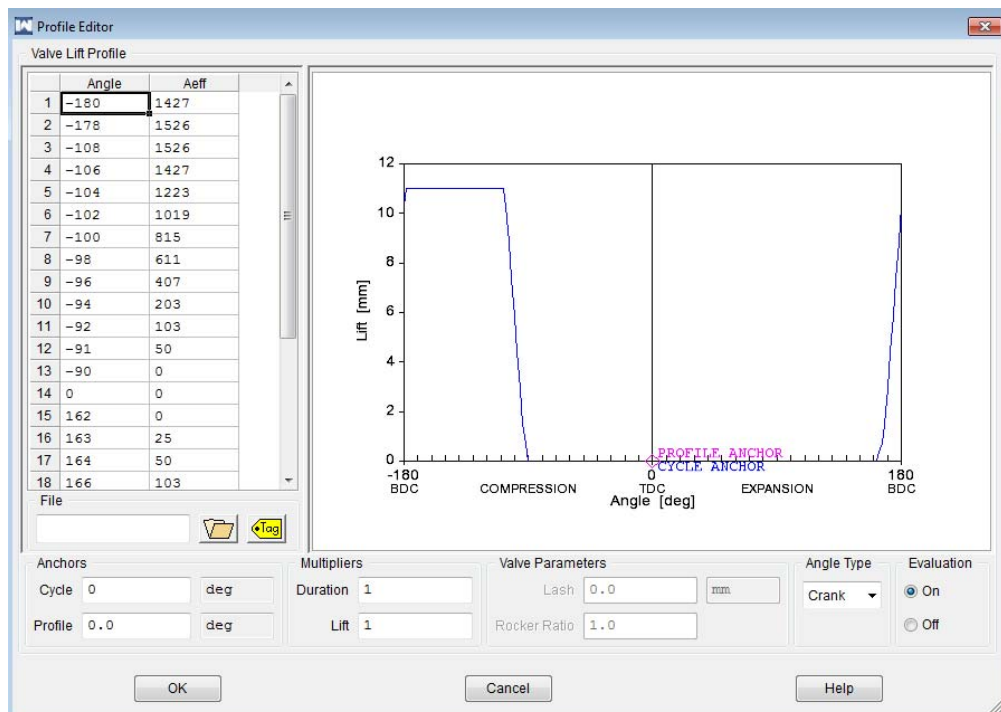


Figure D16 – Exhaust Port Lift Profile (Cylinder Operated Effective area model)

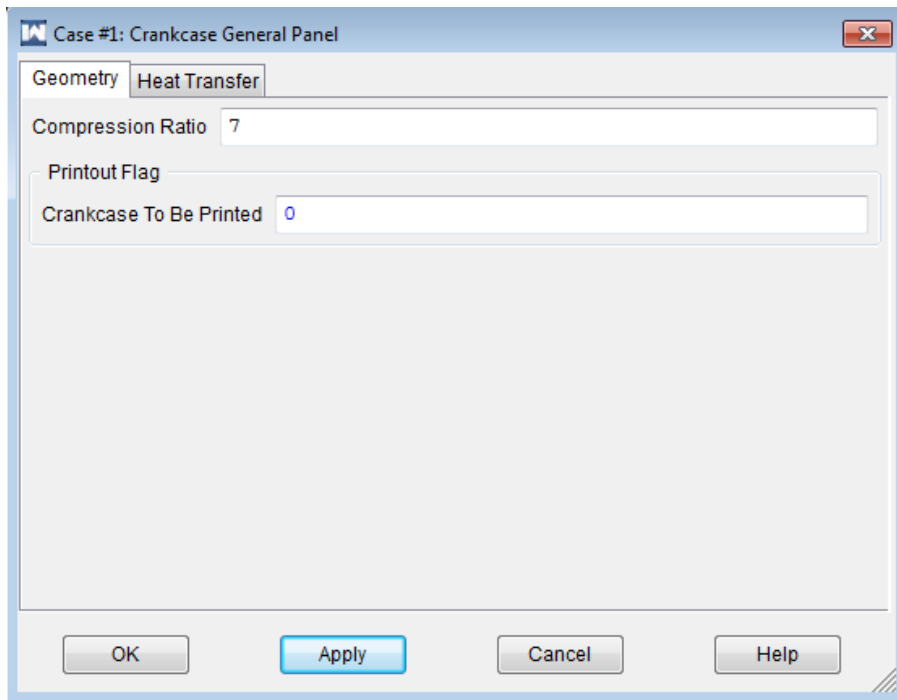


Figure D17 – Crankcase General Panel

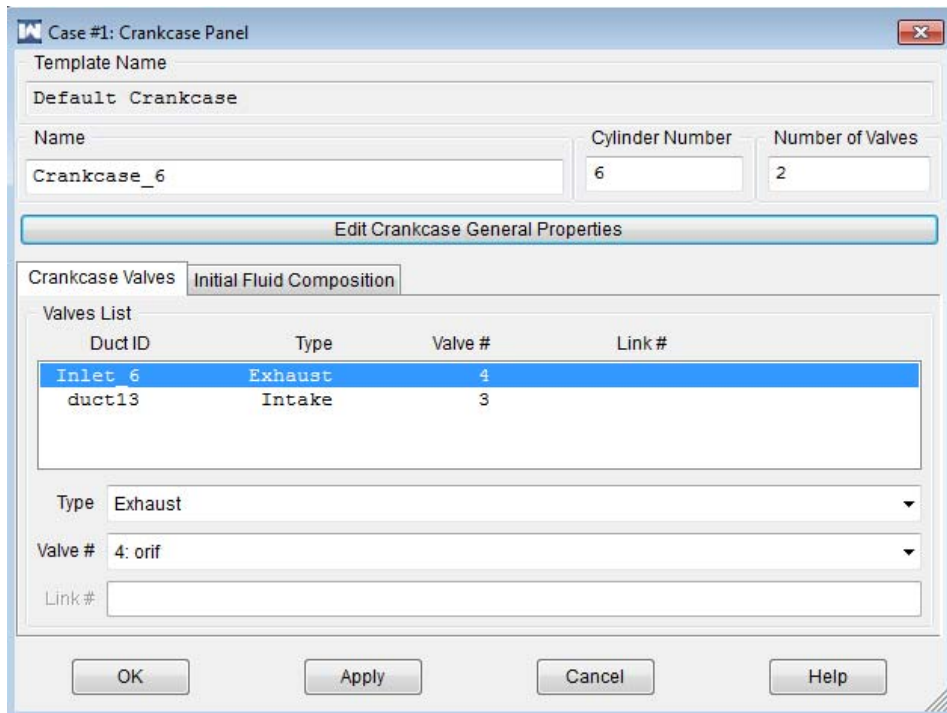


Figure D18 – Crank Case Valve Setup

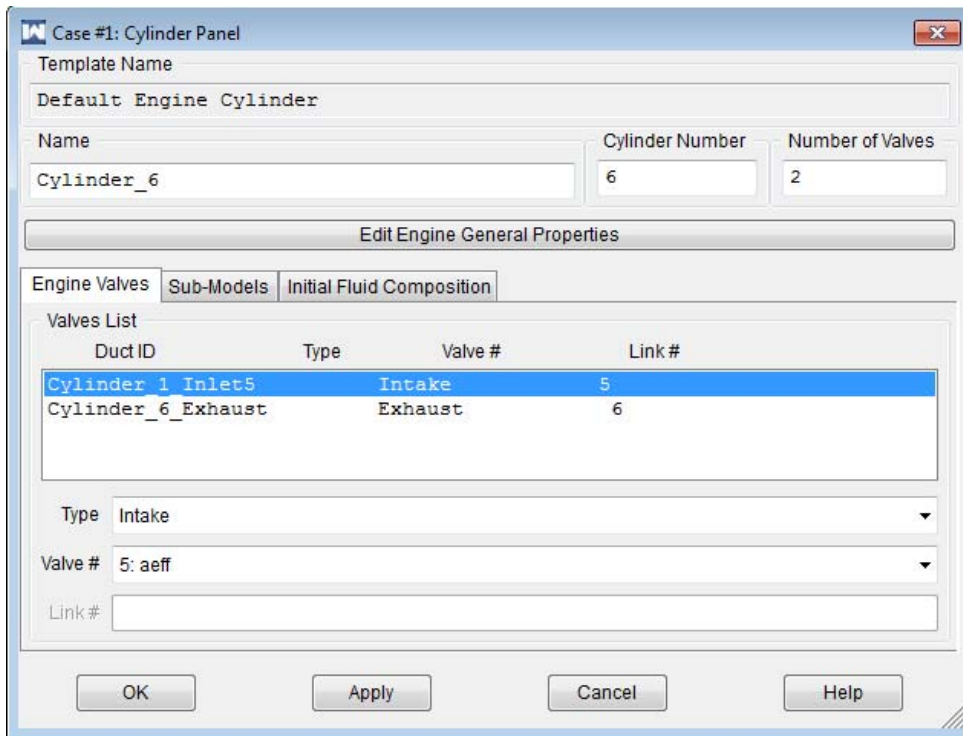


Figure D19 – Engine Cylinder Valve Setup

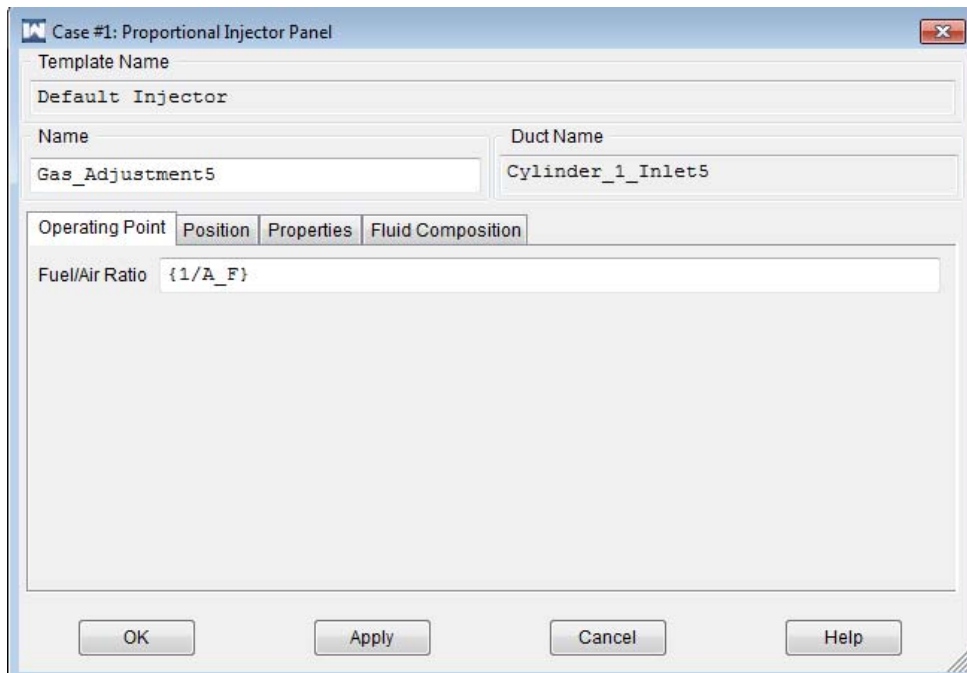


Figure D20 – Fuel Injector Panel, Operating Point

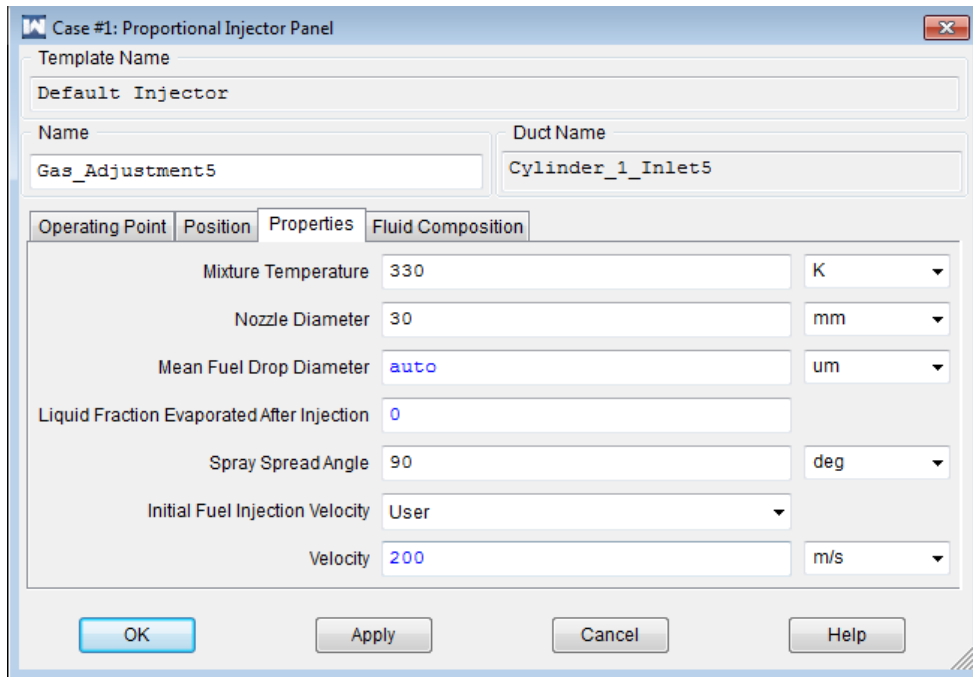


Figure D21 – Fuel Injector Properties

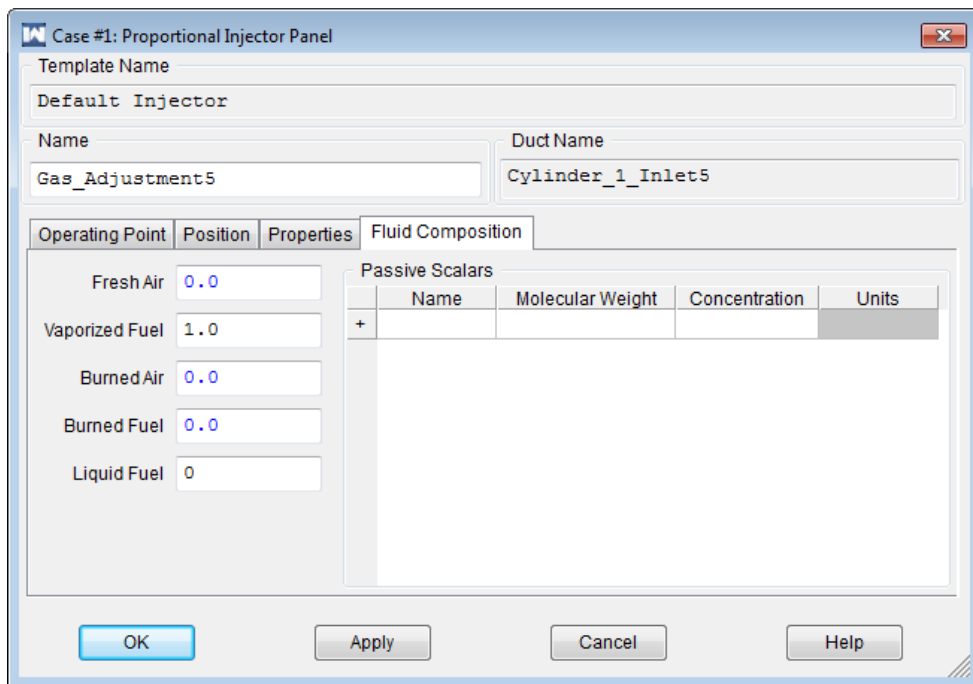


Figure D22 – Fuel Injector Properties of Fuel

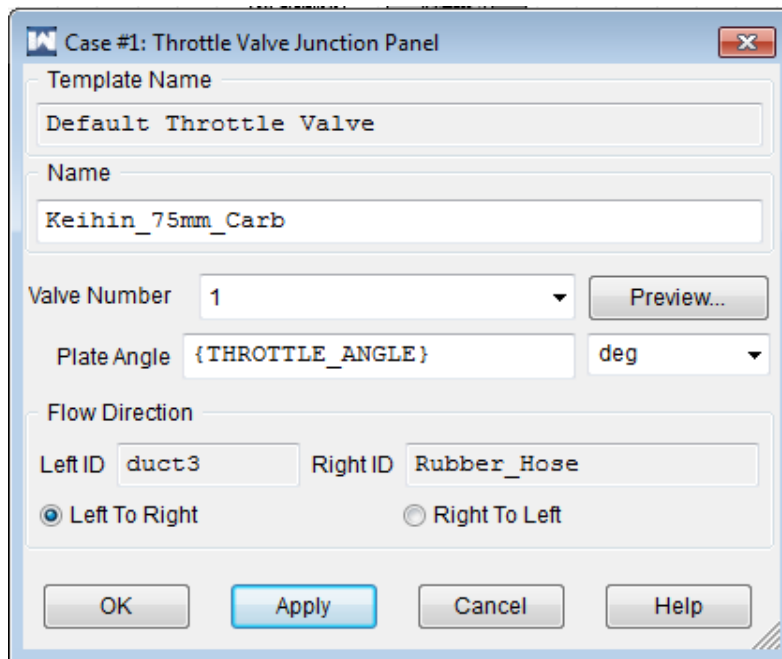


Figure D23 – Carburetor General Panel

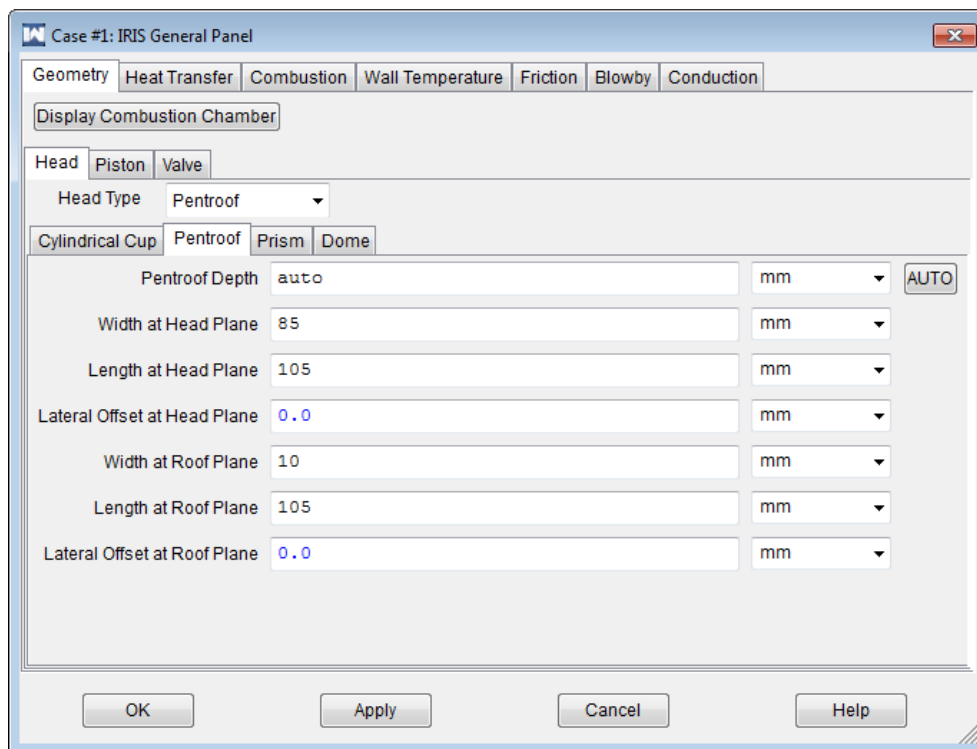
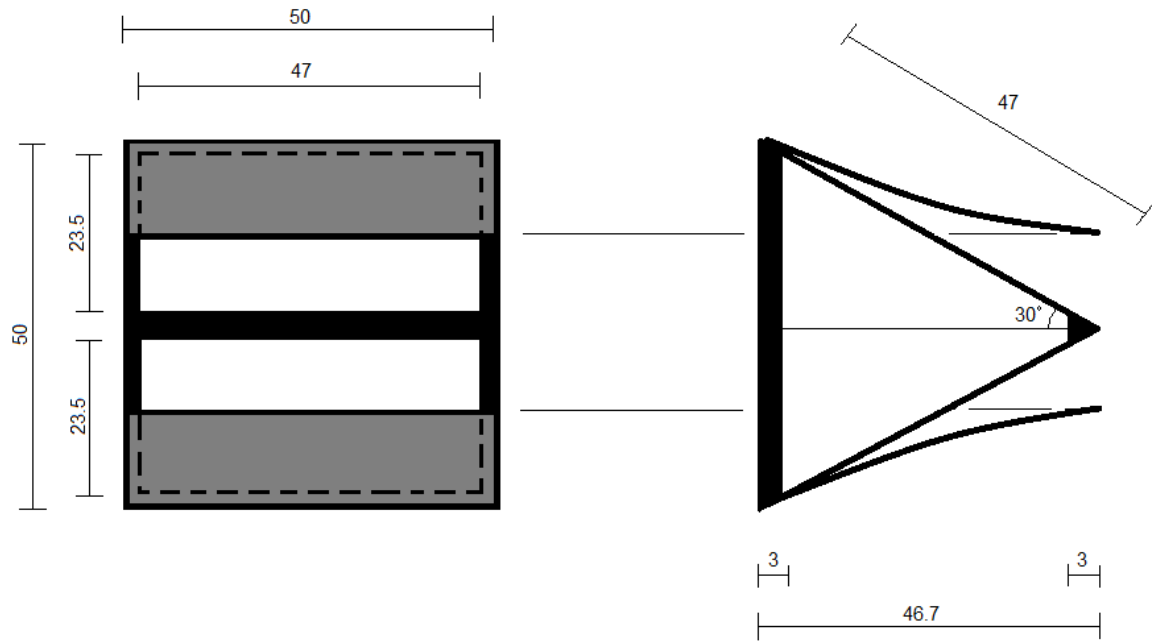
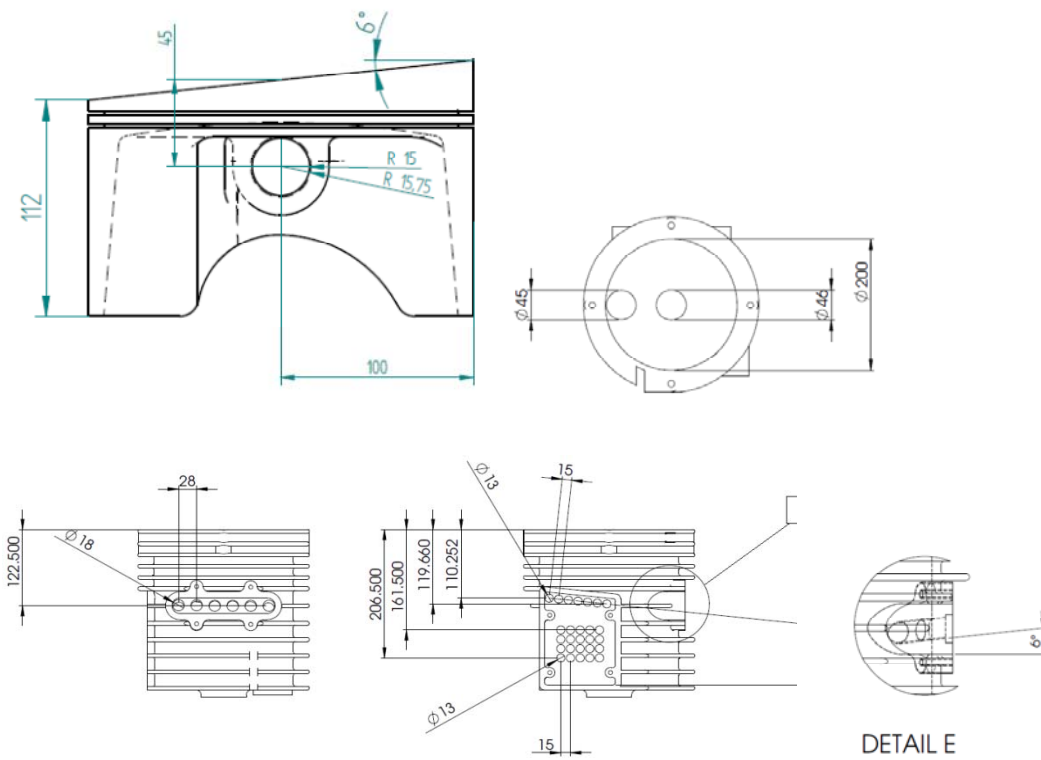


Figure D24 – Geometry of Squish Region on Piston Head



Number of reeds	1
Number of ports	1
Reed thickness	0.50
Reed width	47
Reed length	47
Reed material	Carbon Fibre
Reed block port width	50
Reed block port length	46.7
Reed block angle	30.0
Length from clamp	48.0
Stop plate radius	75
Reed natural frequency	7526
Reed exposed area	4418

Figure D25 – Reed Valve Details



Plan of Bore

Exhaust detail

Figure D26 – Key 2 stroke engine dimensions Details of 2nd Prototype Ports

APPENDIX E

DYNAMOMETER RESULTS OF ORIGINAL PROTOTYPE COMPARED TO RICARDO MODEL

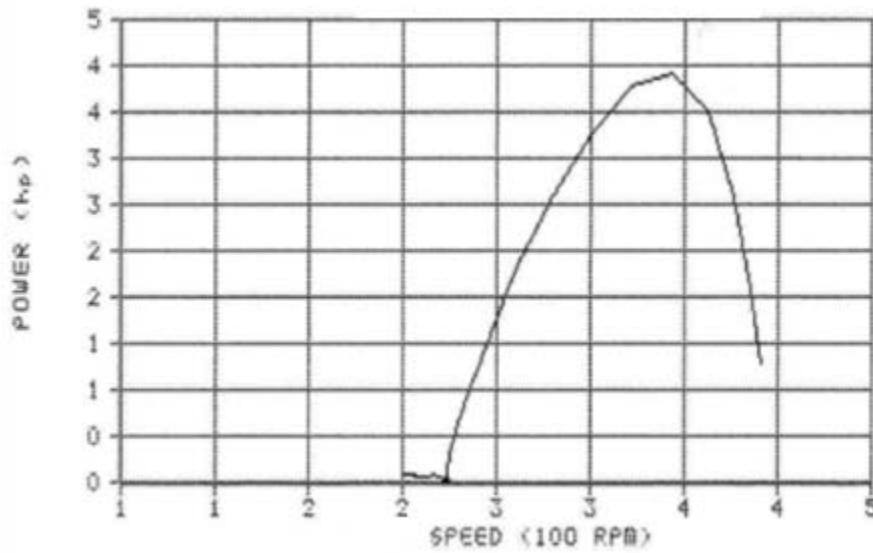


Figure E1 – Dynamometer Torque (Nm) Output for Stroke Prototype

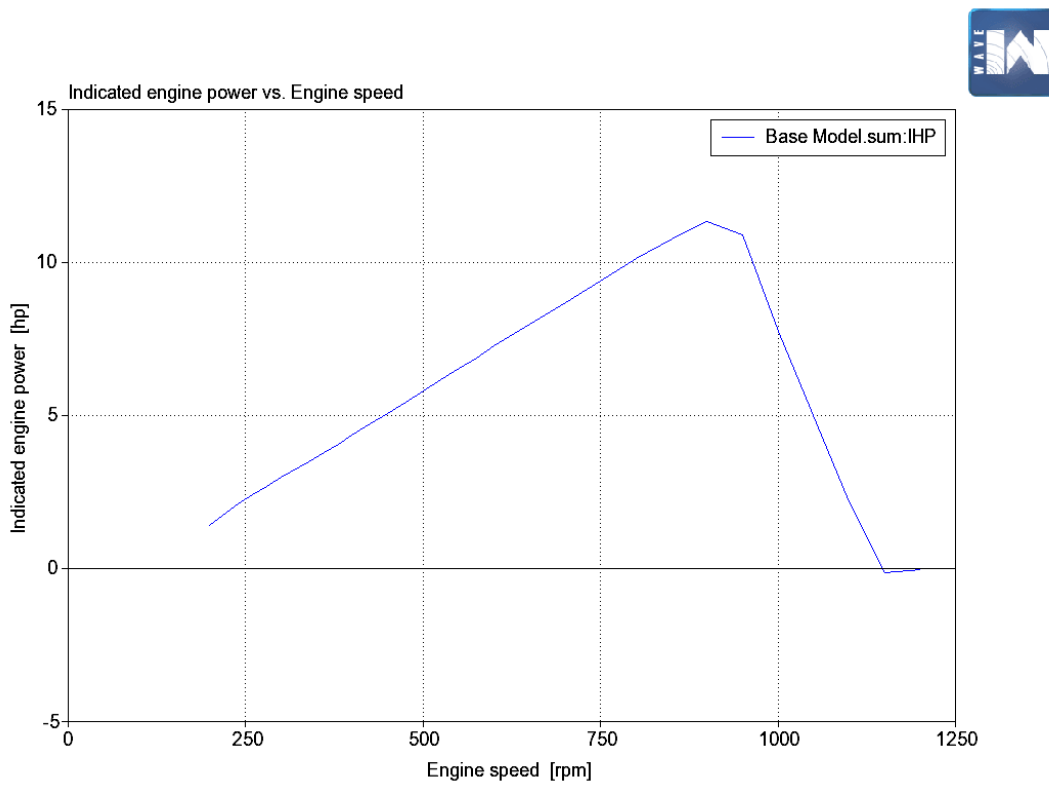


Figure E2 – Dynamometer Torque (Nm) Output for Stroke Prototype

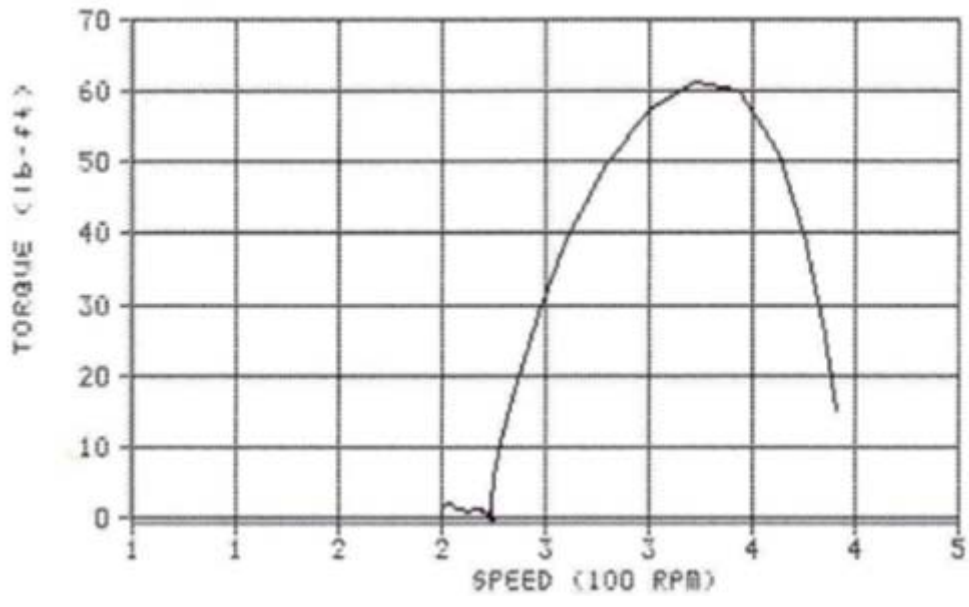


Figure E3 – Dynamometer Torque (Nm) Output for Stroke Prototype

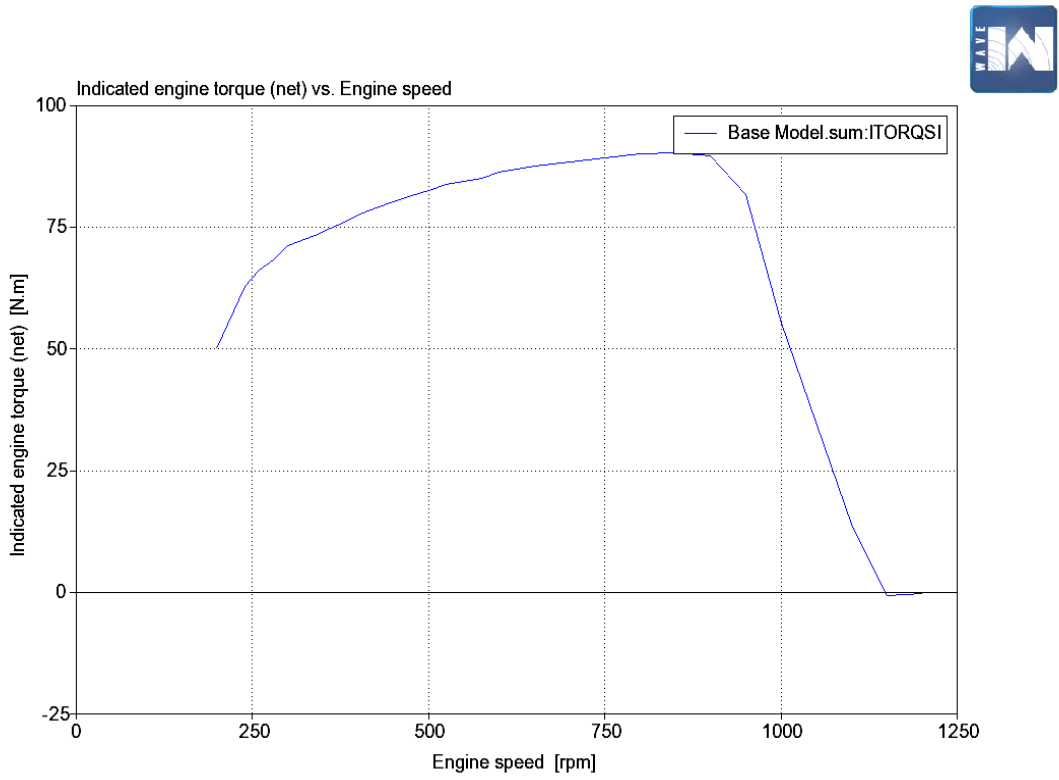


Figure E4 – Dynamometer Torque (Nm) Output for Stroke Prototype

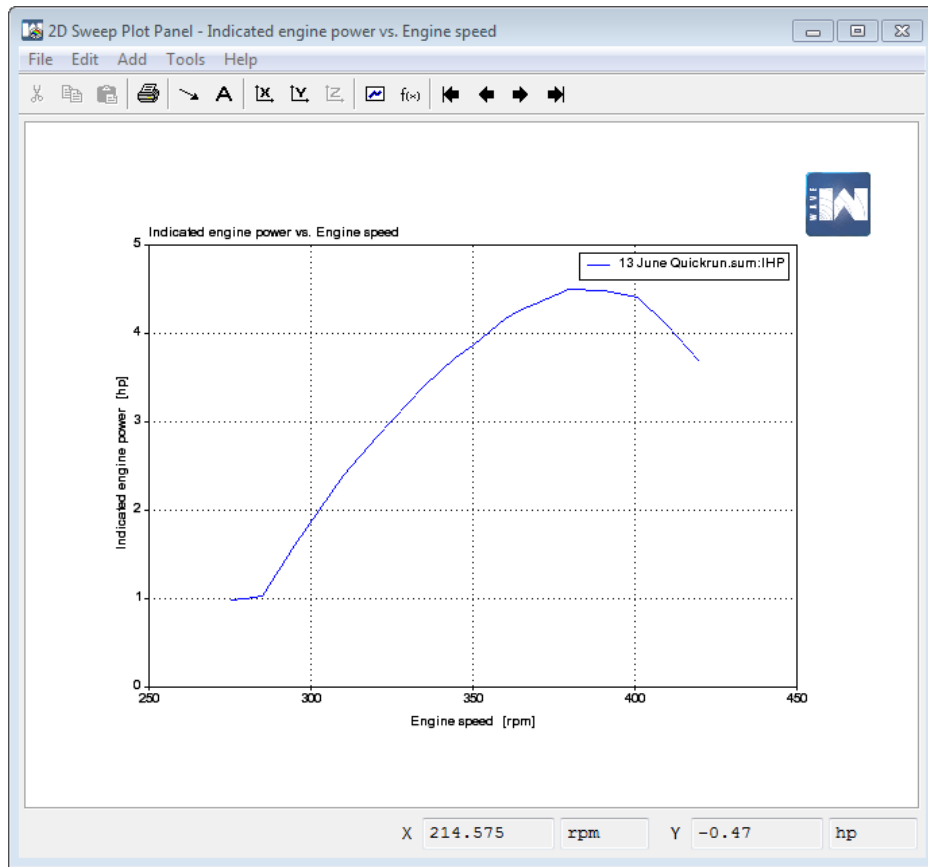


Figure E5 – Dynamometer Torque (Nm) Output for Stroke Prototype

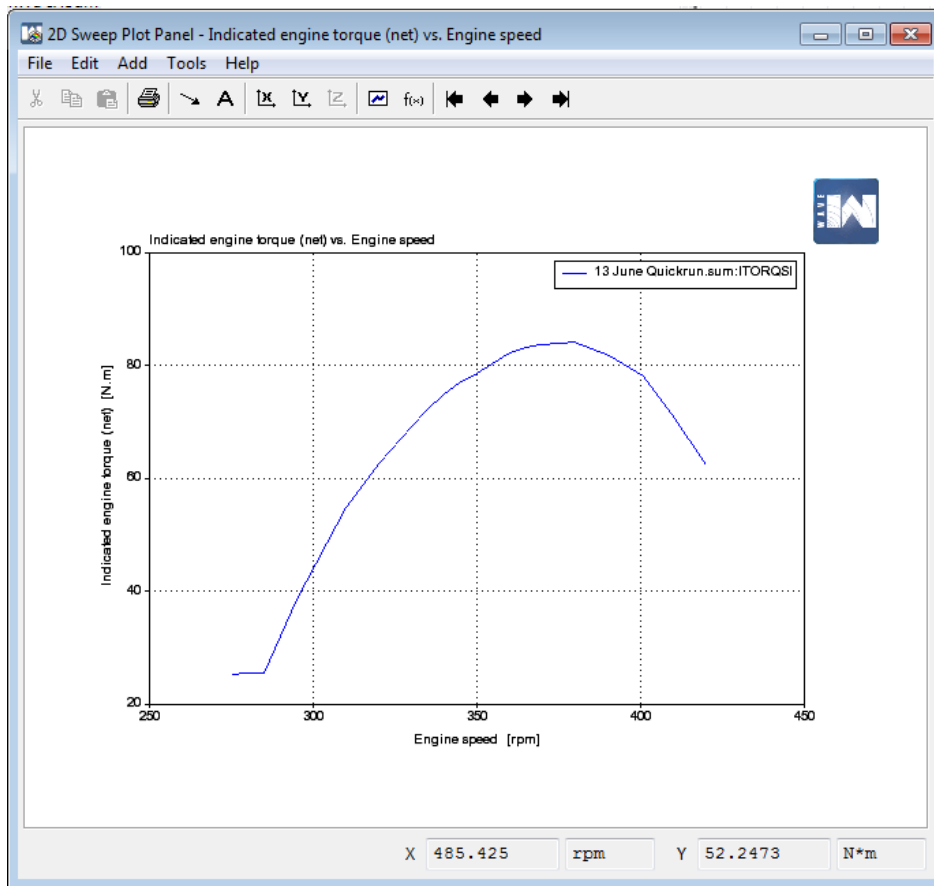


Figure E6 – Dynamometer Torque (Nm) Output for Stroke Prototype

APPENDIX F

PISTON PROFILE AND VALVE TIMING TABLES

	Piston Position from BDC (mm)	C1	C2	C3	C4	C5
Exhaust Valve Opening	37	103	94	82	66	52
Exhaust Fully Open	19	120	110	95	76	61
Transfer Opens	16	125	120	98	80	63
Transfer Fully Open	3	148	134	111	92	74
Transfer Closing	3	174	152	140	117	104
Transfer Closed	16	-166	164	153	125	115
Exhaust Closing	19	-160	167	155	127	118
Exhaust Closed	37	-137	-173	167	139	130

Table F1 – Valve Action Relative to Engine rotation for dwell varied on compression piston trajectories

	Piston Position from BDC (mm)	E1	1 (E2)	E3	E4	E5
Exhaust Valve Opening	37	137	164	-168	-148	-133
Exhaust Fully Open	19	160	-176	-155	-137	-118
Transfer Opens	16	166	-174	-153	-135	-116
Transfer Fully Open	3	-174	-163	-140	-126	-105
Transfer Closing	3	-149	-140	-113	-95	-83
Transfer Closed	16	-126	-115	-98	-80	-64
Exhaust Closing	19	-120	-112	-96	-77	-62
Exhaust Closed	37	-102	-94	-82	-66	-53

Table F2 - Valve Action Relative to Engine rotation for dwell varied on expansion piston trajectories

	Piston Position from BDC (mm)	S2	S1	S 0	S-1	S-2
Exhaust Valve Opening	37	128	118	110	74	51
Exhaust Fully Open	19	140	138	130	87	61
Transfer Opens	16	144	140	135	92	63
Transfer Fully Open	3	160	160	160	111	80
Transfer Closing	3	-160	-160	-160	-111	80
Transfer Closed	16	-144	140	-135	-92	63
Exhaust Closing	19	-140	138	-130	-87	61
Exhaust Closed	37	-128	118	-110	-74	51

Table F3 - Symmetric Piston Curve Degrees Piston Stroke Trajectories relative to engine rotation, varying dwell on expansion and compression

	Piston Position from BDC (mm)	O 1	O 2	O 3	O 4	O 5	O 6	O 7	O 8
Exhaust Valve Opening	37	162	156	150	145	148	158	154	138
Exhaust Fully Open	19	166	158	158	157	169	178	180	-179
Transfer Opens	16	168	160	161	163	176	-176	-175	-172
Transfer Fully Open	3	180	-160	-155	-132	-143	-147	-155	-160
Transfer Closing	3	-40	-60	-75	-85	-105	-114	-123	-130
Transfer Closed	16	-32	-38	-52	-65	-78	-88	-99	-108
Exhaust Closing	19	-29	-35	-48	-61	-73	-82	-95	-103
Exhaust Closed	37	-26	-30	-41	-48	-58	-71	-80	-88

Table F4 - Piston Stroke Trajectories relative to engine rotation, optimizing dwell at TDC and BDC

	Piston Position from BDC (mm)	B 1	B 2	B 3	B 4	B 5
Exhaust Valve Opening	37	148	148	148	148	148
Exhaust Fully Open	19	169	169	169	169	169
Transfer Opens	16	176	176	176	176	176
Transfer Fully Open	3	-157	-150	-143	139	-132
Transfer Closing	3	-76	-90	-105	-110	-125
Transfer Closed	16	-29	-52	-78	-85	-103
Exhaust Closing	19	-22	-48	-73	-87	-102
Exhaust Closed	37	-18	-38	-58	-68	-88

Table F5 - Valve Timing Relative to Engine rotation for optimized piston dwell prior to ignition (at BDC)

	Piston Position from BDC (mm)	A 1	A 2	A 3	A 4	A 5
Exhaust Valve Opening	37	163	160	152	150	148
Exhaust Fully Open	19	179	179	178	178	177
Transfer Opens	16	-178	-178	-178	-178	-178
Transfer Fully Open	3	-151	-151	-151	-151	-151
Transfer Closing	3	-112	-112	-112	-112	-112
Transfer Closed	16	-87	-87	-87	-87	-87
Exhaust Closing	19	-84	-84	-84	-84	-84
Exhaust Closed	37	-71	-71	-71	-71	-71

Table F6 – Valve Timing Relative to Engine rotation for optimized piston dwell after ignition (at TDC)

ANNEX A

RISK ASSESSMENT AND RELIABILITY ENGINEERING APPLICATION IN ENGINE DESIGN

Department of Mechanical Engineering

ENME 627 – Risk and Reliability Engineering

University of Canterbury

Te Whare Wānanga o Waitaha

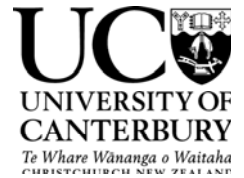
Private Bag 4800

Christchurch 8020, New Zealand

Telephone: +64-3-366 7001

Facsimile: +64-3-364 2078

Website: www.mech.canterbury.ac.nz



Risk Assessment and Reliability Engineering

Application in Engine Design

1st July 2011

EXECUTIVE SUMMARY

I am looking to optimize the design of a new internal combustion engine. Reliability is an important attribute of the engine but it is difficult to predict potential failure modes in such a complex system. This paper investigates some current industry risk assessment methodologies, particularly in engine applications and their failure modes. Each methodologies respective strengths and weaknesses are studied. An appropriate analysis was selected from the investigation and is modified to suit the case study.

The analysis chosen was a FMEA style with a risk rating system built into it to prioritize potential risk factors concerning the components in the engine design.

TABLE OF CONTENTS

EXECUTIVE SUMMARY	1
Introduction	3
Context.....	3
CASE STUDY	4
Project Scope	5
Risk Management Methodologies Relevant to Topic.....	5
DOCUMENT 1: FAILURE MODE & EFFECTS CRITICAL ANALYSIS	6
DOCUMENT 2: RISK ASSESSMENT METHOD FOR FRACTURE OF CRITICAL COMPONENTS	6
DOCUMENT 3: DESIGN REVIEW BASED ON FAILURE MODE	10
DOCUMENT 4: PRACTICAL APPLICATION OF DESIGN RISK ASSESSMENT MODELS	11
DOCUMENT 5: INDEPENDENT REVIEW OF THE FAILURE MODE OF THE F1 ENGINE AND PROPELLANT SYSTEM	11
DOCUMENT 6: INDEPENDENT ENGINE RELIABILITY MAINTENANCE	12
DOCUMENT 7: RELATIVE RELIABILITY RISK ASSESSMENT TO ORIGINAL DESIGNS AT CONCEPT STAGE & AHP	13
DOCUMENT 8: PROBABILISTIC RISK ASSESSMENT APPROACH; A PRACTICAL AND COST EFFECTIVE APPROACH	14
METHOD SELECTION FROM REVIEW	15
Risk Assessment Using FMECA	17
Assumptions.....	18
System Structure	19
Failure Mode Identification Table	21
Failure Mode Analysis	24
Failure Probability Tree	26
Risk Matrix.....	27
DISCUSSION	28
REFERENCES	29

INTRODUCTION

Context

In the automotive industry, the majority of new vehicles being developed must adhere to strict budget restrictions. As a result, compromises in design must be made to balance budget with sound design. For example, to create an invincible product would, in theory, have an infinite cost. Consumers understand that cheaper products are in general more likely to fail in use than a more expensive version. The reason it is more expensive is because more has been spent on increasing the quality of the product rather than keeping costs down. It is this balance that most industries battle with. It comes down to the goals of the company, whether they strive to make the most superior products on the market or provide the best value and leave it to the consumer to decide how higher quality they are willing to pay for.

This trend is seen throughout engineering industry. Reliability of a product can be predicted through approximation methods based on design and through subsequent testing. Companies gain a better reputation through quality products so it is in their best interest to produce the highest quality products possible with the economic and manufacturing resources available to them. Predicting reliability can be difficult when a substantial number of products are being produced. Exact prediction is impossible as failure occurs (depending on the product) according to a probability distribution. This distribution depends on the product and testing and comparison with other similar products is the only real way to accurately verify what distribution suits the failure point.

More complex designs with an intricacy of parts mean that there are generally multiple failure modes, some more prominent than others. Assessing the reliability of each part and its contribution to the reliability of the entire entity is necessary.

When applied to engine design, risk assessment is predominantly used when attempting to predict all failure modes, determining how likely they are to occur

and what the potential consequence of each failure mode. All this is summarizing the reliability of the product.

Risk assessment is started generally around the conceptual stage to assess whether it is worth investing in the development of a project. If it is deemed worthwhile, risk assessment continues concurrently with design all the way up to manufacturing stage and sometimes is ongoing into the products performance in the market to verify predictions for future risk assessments.

Risk and reliability engineering design particularly in the automotive industry has not been well documented since the 1970's due to a large liability case involving the Ford Pinto where the company was held liable for negligence in their fuel tank placement during design. It was discovered early in the design stages that placing the fuel tank behind the rear axle to gain more boot space increased the risk of the tank being pierced in a rear collision, causing the car to burst into flames and or explode. It was going to cost \$11 per vehicle to amend this design flaw by putting plastic guards between the rear axle and the tank to reduce this risk. A cost benefit analysis was done and the result was Ford decided that it was worth proceeding with the small risk that the cars would ignite upon rear impact rather than spending the extra money rectifying the flaw. This is illustrated in an extract from the Ford Motor Company Internal memorandum shown below in Figure 1.

BENEFITS
<i>Savings:</i> 180 burn deaths, 180 serious burn injuries, 2,100 burned vehicles.
<i>Unit Cost:</i> \$200,000 per death, \$67,000 per injury, \$700 per vehicle.
<i>Total Benefit:</i> $180 \times (\$200,000) + 180 \times (\$67,000) + 2,100 \times (\$700) = \mathbf{\$49.5 \text{ million.}}$
COSTS
<i>Sales:</i> 11 million cars, 1.5 million light trucks.
<i>Unit Cost:</i> \$11 per car, \$11 per truck.
<i>Total Cost:</i> $11,000,000 \times (\$11) + 1,500,000 \times (\$11) = \mathbf{\$137 \text{ million.}}$

Figure 1: Ford Motor Company Internal memorandum, "Fatalities Associated with Crash-Induced Fuel Leakage and Fires."

Unfortunately this system cost Lilly Gray her life and left 13 year old Richard Grimshaw badly burnt, and the ensuing lawsuit cost Ford compensatory [damages](#) of \$2.5 million and [punitive damages](#) of \$3.5 million.

Ford was found guilty of negligence whereas quality compromises for value in industry and assessing the potential risks against not increasing the quality of a final product is still practiced, even sometimes at the cost of safety. But as a result of the Pinto trial, risk benefit analysis in the automotive industry it is not well publicly documented.

In order to apply risk assessment techniques to engine design, I am looking for examples of assessments of other complex designs where the components are dependent on each other in order for the entire system to work.

I will explore the techniques used in complex designs to assess the overall risk of failure in service of a product and identify primary risks of a product to aid in the design process.

CASE STUDY

A risk assessment procedure will be applied to a novel internal combustion engine where the combustion chambers themselves rotate with the output shaft. The engine consists of two cylinders, two spark plugs and a simple centrifugal force fed fuel delivery system. Because the majority of the engine rotates around a fixed cam, it carries a large amount of momentum and energy. Although this is a risk to the user, this will not be considered in the investigation as it will be mitigated by use of a large guard to avoid injury if the product gets to market stage. The engine is also air cooled. The purpose of the engine is to provide adequate torque at constant rpm to a generator using low cost fuels.

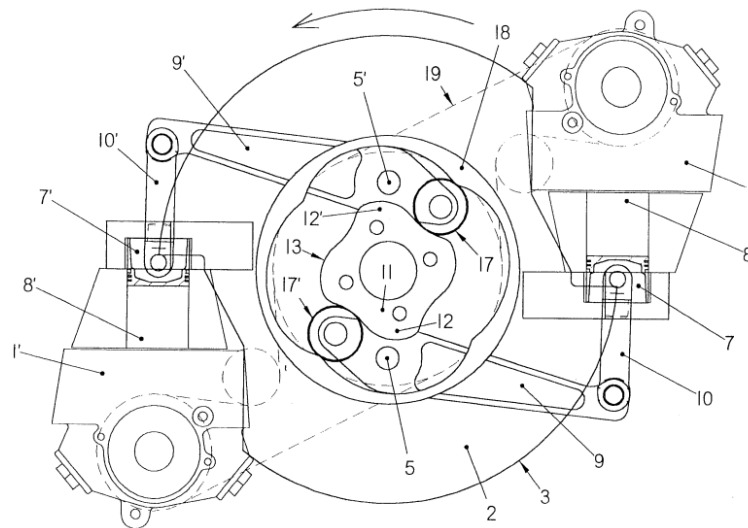


Figure 2 – Schematic of novel internal combustion engine used for case study.

Project Scope

I will be interested in identifying the most prominent mechanical failure modes in the engine so that they can be mitigated to assist in the development of the 2nd generation engine. Major health and safety aspects will only be considered as consequences of a mechanical failure mode. Environmental risks are not being taken into consideration. User friendliness is not considered also as this engine is being developed to test the performance limitations of the engine. Ergonomic and aesthetic considerations are out of scope of the case study. Broad economic risks in respect to the expense of components and their manufacturability will be incorporated but marketability and any post production expenses are left out of this investigation.

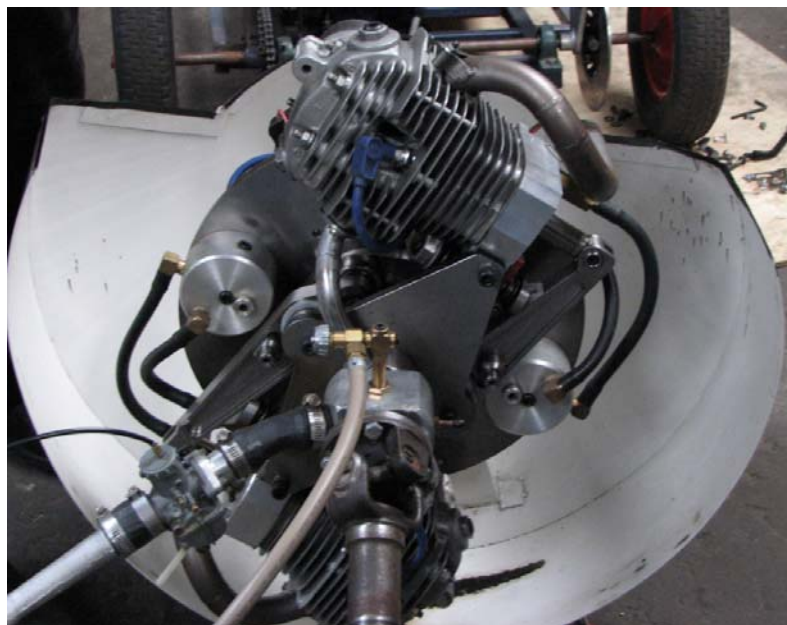


Figure 3 – *Picture of previous prototype showing main components.*

RISK MANAGEMENT METHODOLOGIES

RELEVANT TO TOPIC

Below is a summary of documents that explore several different methodologies approaching complex design risk assessments. I will discuss the merits and demerits of each method and after I have explored each will develop my own method to apply to the case study specified above.

Document 1:

Failure Modes and Effects Critical Analysis (FMECA)

This article was a step by step guide through a typical FMECA procedure used in industry to identify and mitigate problem areas of complex systems; it is very similar to FMEA, (Failure Modes and Effects Analysis).

The C in FMCEA indicates that the critical (or severity) of a risk that is considered and ranked. FMCEA is used for the selection of design alternatives to optimize reliability, particularly during the early design period. It explores all conceivable failure modes and their effects on the operational success of the system. The severity of these effects is also considered. It also provides a basis for maintenance and documentation for future reference to aid in failure analysis. The steps outlined are as follows.

First, each part of the system is analyzed to see how it could fail and what would cause this failure. The effects and possible detection modes are then explored. Mitigation steps are then provided to the design to compensate and avoid failures where possible.

There are two approaches to FMECA, one is the bottom up approach. This is usually performed on a system at conceptual stage. Each component is studied one by one, attributing all risks to one system model. This is the most complete analysis since it covers every component and is most useful when the concept is

mostly understood. The other approach is described as the top down approach where it is mostly function orientated. The top is the overall objective of the system and components are devised to achieve the desired function. Failure modes are used to devise new components to compensate for them. This system is more suited to an unknown concept where the required function of the system is the driving operator.

The first step in conducting FMECA is to construct a system structure. It is divided into manageable units and elements. The level of detail in the breakdown will depend on the objective of the analysis. A hierarchical tree diagram is often useful to illustrate this step.

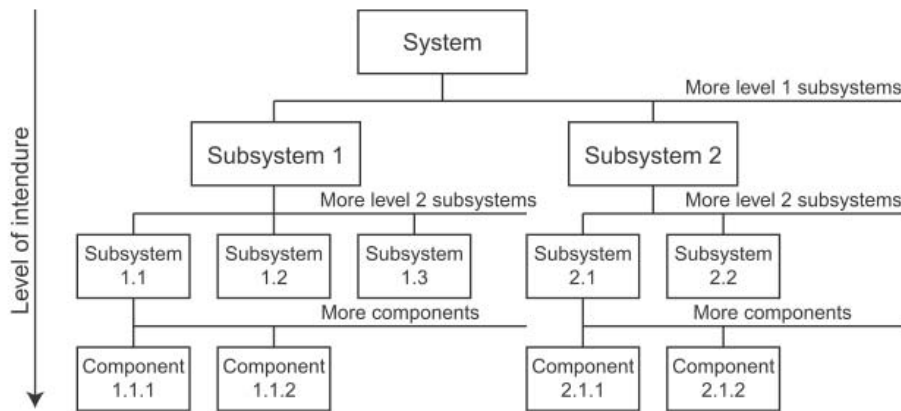


Figure 4 – System hierarchical tree diagram.

The analysis should be carried out on an as high level in the system tree as possible. If unacceptable consequences are discovered on this level of resolution then the particular element should be divided into further detail to identify failure modes and causes at a lower level. The higher the resolution, the more complete the analysis but only a certain amount of time and effort should be invested as a basic analysis is often much more cost effective.

The use of worksheets is used to further investigate failure modes. This is shown below in Figure 5.

System:

Performed by:

Ref. drawing no.:

Date:

Page: of

Description of unit			Description of failure			Effect of failure		Failure rate	Severity ranking	Risk reducing measures	Comments
Ref. no	Function	Operational mode	Failure mode	Failure cause or mechanism	Detection of failure	On the subsystem	On the system function				
(1)	(2)	(3)	(4)	(5)	(6)	(7)	(8)	(9)	(10)	(11)	(12)

Figure 5 - Example of a FMECA worksheet

The frequency column in Figure 5 is rated on a scale of 1 -5. Figure 6 illustrates what the scale indicates.

system.

Rank	Description	Frequency
1	Very unlikely	Once per 1000 years or more seldom
2	Remote	Once per 100 years
3	Occasional	Once per 10 years
4	Probable	Once per year
5	Frequent	Once per month or more often

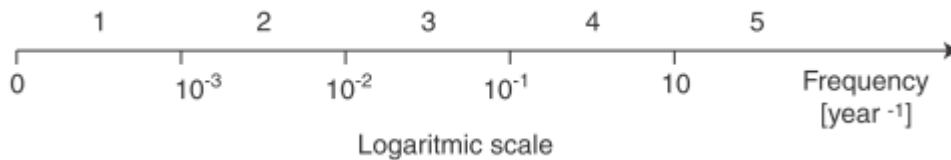


Table 1: Example of the Frequency Scale used for FMCEA with a complex mechanical

The severity is a measure of consequence of the failure. The consequence is dependent on the system goals and what is specified as a failure. Table 2 shows an example of severity to a system.

Rank	Severity Class	Description
10	Catastrophic	Failure results in major injury or death
7 - 9	Critical	Failure results in minor injury, exposure to harmful chemicals or radiation or fire or release of chemical to environment
4 - 6	Major	Failure results in low level exposure to personnel or activates facility alarm system
1 - 3	Minor	Failure results in minor system damage without injury or any kind of exposure of chemicals or otherwise

Table 2 – Severity Scale used for FMCEA with a complex mechanical system.

Once the severity and frequency for each failure mode has been analyzed, they can be categorized into a risk matrix, below in the Figure 6 is an example of a risk matrix.

Frequency/ consequence	1 Very unlikely	2 Remote	3 Occasional	4 Probable	5 Frequent
Catastrophic					
Critical					
Major					
Minor					

Figure 6 – Risk Matrix

Green indicates that no further action is required, yellow meaning acceptable risk but some further investigation may be required and the components involved should be carefully considered during design. Red means that the risk is not unacceptable and risk reducing measures are required.

An alternative to the risk matrix is to use the ranking of a risk priority number (RPN). This is calculated according to the rating of the failure mode. The smaller the RPN, the better.

$RPN = \text{Severity} \times \text{Frequency} \times \text{Likelihood of failure detection}$

Discussion of Method

FMECA is an effective, structured method in identifying and prioritizing risks on a complex system. The bottom up approach is much better suited to existing systems and second generation systems where the components are known. Bottom up is also the most thorough as it investigates all aspects of a system. Using the top down approach should only be used where the required components are reasonably unknown and the system is an original idea. If time and money permits, it would be advantageous to do a bottom up risk analysis after the top down method has been used to identify the required components as top down is more susceptible to overlooking aspects of design. There are perhaps better methods of devising a system solution than applying a top down FMECA approach.

Using a fault tree analysis to lay out the system structure illustrates well how components and their failure modes directly correlate. The only issue would be the event of multiple failures and how different subsystem failures can influence each other. In this respect, how failures of one component affect others is very limited but if effective mitigating steps have been taken on all high risks, the likelihood of failures occurring should be reduced as a result.

Use of a worksheet on each component allows designers to really gain a greater appreciation of the diversity of functions within a system. Although these can be time consuming to complete and on a complex system, this could become a tedious task that could lead to parts being overlooked. Human error is often overlooked

during analysis also.

Rating the severity of a failure is reasonably simple, depending on the system objective. More than one perspective would further aid the correct categorization of severity. Frequency of failure is a much more difficult quantity to estimate. It is highly dependent on the system under investigation. Whether the measurement of frequency is failures per year, failures per cycle or the number of failures expected during the lifetime of the system. Large assumptions have to be made about the operation manner of the systems. Most manufacturers should be able to produce life span data from testing but in the case where no such data is readily available, the only reference source is either previous designs or the expert opinion from someone with a lot of experience with the part or system in question.

The combination of severity and frequency give a fair indication of risk when displayed on a simple colour coded risk matrix like the one shown in Figure 7. The degree of acceptable risk can be adjusted to suit the system. For example, a failure mode of same nature is more likely to be deemed an acceptable risk on a single prop plane than in a commercial jet.

The problem with the RPN evaluation method is that it has no clear meaning and the ranks of severity, frequency and likelihood are all defined depending on the application and the FMECA standard that is used. This means that sharing RPN numbers between projects and companies is very difficult.

Document 2:

Risk Assessment Methodologies for Fracture Critical Components

This article attempted to predict failure and its associated probability in gas turbine engines, particularly in the aerospace industry. The probability of failure had to be acceptably small in order for the engine to be fit for flight.

Failure can be due to foreign objects, manufacturing errors, maintenance issues, environmental influences and the actual expected life of the components under normal running conditions.

At the simplest level, there are hazards that are ever present and unaffected by parameters associated with the engine itself. These can be summarized as external factors such as foreign object damage or extreme weather conditions. The calculated risk for this can be quite simple by dividing the number of occurrences across the entire fleet by an appropriate measure of exposure time, usually described by flight hours in this case.

To predict the point of failure for a complex system, data must be derived from component service life records and statistical models. Unfortunately different components often follow different statistical models and for an accurate risk assessment, it is important that a correct failure distribution is selected. This often is only possible to discover by rigorous testing.

The standard used in the aeronautical industry is that each component must be replaced once it reaches half its "safe life". An objects safe life is determined by component rig tests to failure. Others are based on component life's currently in service use. Usage is counted in number of hours rather than cycles. Failure due to fatigue of a general component is when crack initiation exceeds 0.75mm.

Straight line, low cycle fatigue in components is a known failure distribution and can be predicted with acceptable accuracy. It follows a log normal curve with log standard deviation. The only requirements are the log mean, which is deduced from test data. The only problem is that this distribution is only valid once crack initiation has occurred which is can be seemingly random occurrence.

The problem is the variation in the type of failure mode. When applying statistical failure distribution, it can be assumed that the lifetime of the system is large enough to reach the initial distribution. Components may already have flaws and cracks.

Manufacturing tolerances affect life; tolerances are set so the component has an expected life. Deviance from this is dependent on the population measured, the problem with all this is that it is highly case dependent.

The likelihood of a fault occurring also depends on the running conditions at the time of the fault. For example, if the aircraft is acting outside its comfort zone and the craft is undergoing a difficult maneuver then the likelihood of a fault is more likely. For example, takeoff engine failure is much more likely than during constant running due to the acceleration forces involved in takeoff. Consequence also depends on the situation, for example, if engine failure occurs while the aircraft is on the ground the consequence is much lower than if the engine failed while the aircraft was in flight. RAF hazard risk index is very similar to other systems where risks are categorized into either red, yellow or green categories. A risk is deemed acceptable if only 1 failure occurs for every 10^{-6} /aircraft flight hour, otherwise, the craft is deemed unsafe to fly. There is always an element of risk present. Per annum is another operational period commonly used. An improvement to the Hazard risk index is the addition of expected per annum as well as individual risk/per flight hour.

Discussion of Method

This method is potentially the most accurate of all risk assessment methodologies when done correctly using appropriate statistical models for each component. The downside is that to apply models to all components of a complex system can be very time consuming and costly exercise. Monte Carlo would be effective analysis tools to assist in producing an overall system reliability figure. An estimate of components with manufacturing flaws can be estimated and built into the analysis tool as well as many other factors but the result can only be as accurate as the data given. If one component is outside the normal that could lead to premature failure, the statistical data fed into the model will be false. If a number of critical

components do not have accurate lifetime data then the complexity of the analysis tool is not going to improve the uncertainty in the investigation.

Having a clear risk boundary of 10^{-6} /aircraft flight hour is helpful in dispensing of uncertainty with moderate risks.

Document 3:

Design Review Based on Failure Mode

Toyota have taken FMEA a step further by adapted their own system of risk analysis as well as employing traditional FMEA. They have developed a system called Design Review Based on Failure Mode, (DRBFM). This is specifically driven at identifying problem areas when an existing proven system is modified and or has components changed or added and what the consequences are on the other systems. Given Toyotas track record for reliability, and the extensive interchangeability of their parts, this method has been highly successful.

Document 4:

The Practical Application of Design Risk Assessment Models

This investigation explored a number of case studies, one involving the company, Rolls Royce. They were using a risk management strategy for the development of a new aerospace engine. Being a large company, the detail design involved 500 engineers. The development was of an existing engine, from concept through detail design, manufacture, build and test. Emphasis was placed on reliability and meeting certification dates. The method they used can be described as a mix of qualitative and quantitative.

Rolls Royce work on a 'performance bid procedure.' Where separate departments working on separate components and subsystems outline specific performance levels that they will strive to achieve in order for the entire engine to achieve it's performance goals. All bids are risk assessed to make sure that they are supportable and built into an entire engine risk model. Detail design leads each

component through an iterative process where if compromises are made to meet budget, physical and or performance requirements, other departments must attempt to make up for them so the overall system goals are not affected. If compromises cannot be mitigated then discussion with the client and potential negotiation and reconsideration of the projects goals may be required.

Targets are driven by market requirements and approximation of capabilities, which can be mitigated later.

The first stage of the risk assessment procedure is choosing labels, high, medium or low impact when applied to probabilities, (ie. low being for the 0-10%) to manufacturing cost impacts, time impacts and appropriate technical attribute impacts (per performance levels such as fuel consumption etc). At treatment stage, the risk is either accepted, mitigated against or transferred to another work package for mitigation.

Defining high med low for each project is an effective opportunity to prioritize risks and weigh cost against time and technical risk. All recorded in a risk register and at each project milestone top risks required a mitigation plan. 1600 - 2000 risks were identified. 400 were categorized as top risks. Significant risks were investigated in more detail, some having the risk negated or reduced, some were allowed to continue but were closely monitored from that point onwards.

Purpose of the investigation was to evaluate degree of confidence unit cost / weight performance targets would be met at component level.

Discussion of Method

This methodology is highly iterative and is best suited to when the design is pushing technological limits and attempting to achieve the most optimum level possible give a particular budget. This could also be a very expensive method as could lead to a large amount of rework and re design since it is conducted concurrently with design and production. It proved to be highly efficient when working under a strict time constraint.

This methodology is an effective way of evaluating deliverables on a project in the early stages of design. The bidding system also introduces competitiveness

between departments, each attempting to achieve the best they can so not to hinder other departments. Although expensive, some impressive innovation can result. Goals of a project have to be clearly defined and a client must be willing for compromise when using this type of approach. Although, compromise is always expected when attempting to develop state of the art products.

Document 5:

Independent Review of the Failure Mode of the F1 engine & propellant system

The F1 engine was the thrust provider for the Saturn 5 that propelled man to the moon in July 1969. It was the largest, most powerful liquid rocket engine ever built. It accelerated the shuttle to 10800kph out of earth's atmosphere.

After the mission was successful, some of the key engineers involved with the design of the F1 engine were asked to outline the failure modes and rate the risk for each. The system was divided into 8 systems; Fuel feed, oxidizer feed, igniter fuel, gas generator, vehicle pressurization, hydraulic control, electrical systems and instrumentation. These were split into inboard and outboard sets where there was one inboard and five outboard. All the components in each system were considered along with all their possible failure modes. Once identified, the consequences on other components and the system themselves were brought under scrutiny. The severity of each failure mode was highly dependent on amount, location and altitude. Once a sufficient list of failure modes were identified and fully understood a group of engineers that were involved in the initial development of the project were asked to scale each of the 8 systems for the likelihood of failure with a number of 1 -5, 5 being the highest risk. The scores from each engineer for each system was totaled and the systems were ranked in order of risk based on the hierarchy of scores. The results of this can be seen in Table 1 below.

Failure Modes	Gross	Pearson	Galuska	Tepool	Goetz	Hyde	Cornelius	Total
Combustion Instability	5	5	5	5	5	5	5	35
Fuel-Mix at injection Face	3	3	3	4	4	1	1	19
Propellant Leakage	2	3	3	2	1	2	2	15
Structural failures	4	2	2	2	2	3	3	18
Ignition at Start	4	2	2	2	4	3	3	20
Nozzle Tubes	3	2	2	2	3	2	2	16

Table 3 – Risk Ranking for F1 engine by engineers involved in the design

As can be seen from Table 3, combustion instability was rated as the highest risk by all the engineers.

Discussion of Method

Although this review was conducted well after the mission's success, it was interesting to learn about how different the perspective of risks by each engineer was and it showed how important it is that risk be evaluated as a collective. Apart from the highest risk system, the others were all rated very similarly. This shows that this method does not clearly define risk priorities, either a much larger group need to be considered or a different method needs to be practiced.

Document 6:

Industrial Engine Reliability & Maintenance

This article outlined the steps taken to develop a successful monitoring plan maximize the reliability of an engine using a risk assessment approach. It specified the data that should be collected and analyzed on every engine.

It involved defining failure modes which are described as something that either

Prevents the engine from working

Prevents the engine from performing at its intended performance level

Accelerates wear

Once failure modes are identified, indicators were outlined for when the engine was in operation that would preempt the failure mode. The necessary steps to avoid this failure were then outlined.

Discussion of Method

This article helped define common failure modes in engines and how these failures can be detected with common indicators. It also defined maintenance steps to prolong the life of the engine.

Document 7:

Relative Reliability Risk Assessment to original designs at conceptual stage

This explored predicting reliability without the aid of historical test data or where components may be unknown. It uses risk assessment to make design and concept decisions. First a system structure is created, using a top down approach, with function being the focus for the component possibilities. Then an analytical hierarchy process is developed (AHP).

Analytical Hierarchy Process (AHP)

This is a structured technique for organizing and analyzing complex decisions. With a goal in mind, a criteria is defined that constitute the goal. This is illustrated by the example shown in Figure 7 for when choosing a leader.

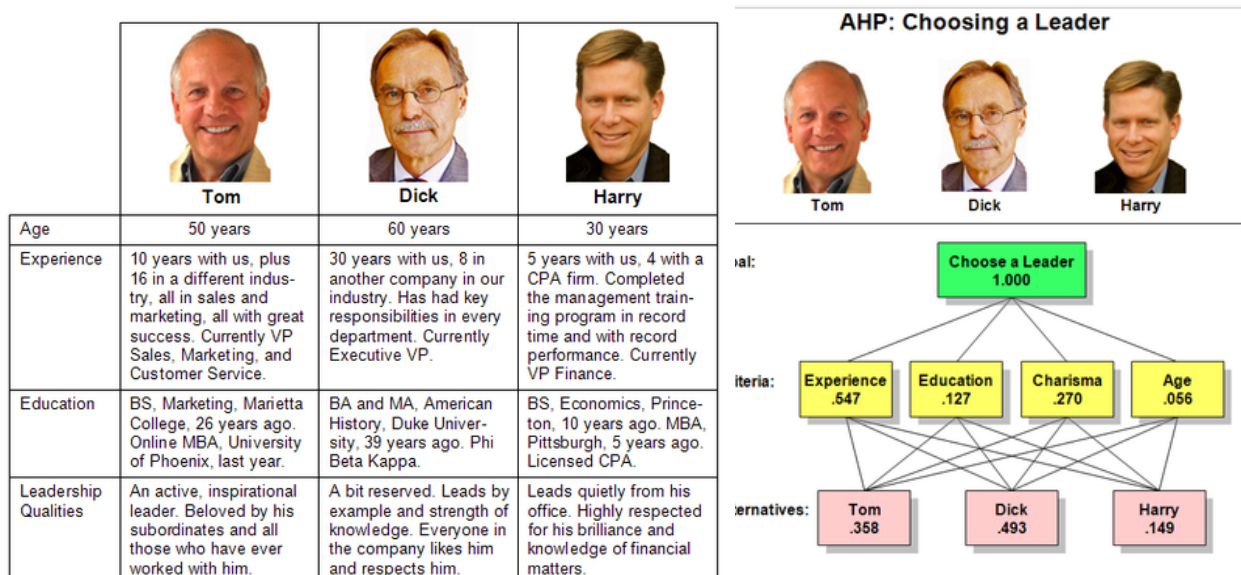


Figure 7 – AHP example showing how information is translated to an overall rating of each alternative.

The criteria that make up the goal is given an order of importance. As can be seen from Figure 7, experience was the desired criteria, age being the least. Each candidate is rated and ranked according to each of the criteria on a scale of 1 to 10. This rating is then multiplied by the respective criteria rating and the results are added to devise their final score out of 1. As can be seen by the final scores, Dick was the preferred choice. This was predominantly because of his larger amount of experience than the other two candidates whom may be better in the other criteria, experience was the weightiest.

This methodology can be used for selections of components in a system. Software selection can be made (depending on the size of the system) that can crunch numbers to select the optimum component selections based on the system requirements.

Discussion of Method

This method of analysis is quite lengthy and is susceptible to error. This error is from the way that attributes and qualities are rated. To work effectively, qualities would have to be rated by a group of people rather than a single person to avoid biases. If it is difficult to choose between alternatives in a system this is an

effective way of prioritizing decisions and helping making the best choice for task. If there are multiple alternative options, the use of a software package would be advantageous to help with the extensive number crunching.

Document 8:

Probability Risk Assessment Approach: A practical and cost effective approach

This investigation was into the Lunar Reconnaissance orbiter (LRO). It is intended for the moon, mars and beyond and this analysis was done concurrently with design to identify problem areas prior to the manufacturing phase. The design consisted of 14,000 piece parts, 120 of which would need to be purchased or contractor built. It was desirable to obtain the probability of failure for each component. FMEA and Fault tree analysis (FTA) were used extensively but within a tight budget.

The LRO was divided into seven subsystems and mission was deemed successful if the module ran for 14 months and completed all of its' primary objectives. Objectives were built into the module because there were certain functions that the LRO must conduct in order to complete these objectives.

Reliability predictions of components were predominantly gained from the manufacturer specifications and or predicted form previous similar designs. Reliability was measured as failures per 10^6 hours.

The following assumptions were made for the investigation:

- All components operate constantly at 100% duty cycle during the 14 months. (10,220 hours.)
- Only flight environment is taken into account.
- Reliability of parts/components/subsystems and systems is an exponential function of time.
- Failure rates of previously used systems are used if there are no manufacturing data available.

- Component failure rates at launch are assumed to be the same as during flight. A constant environmental factor is also built into reliability calculations.
- Since the LRO is a single string design, only major failures are considered to avoid a costly analysis.
- Only one failure mode exists at a time.
- Only direct connections between systems are considered. (ie. Electrical systems are assumed not to affect mechanical).

A top down approach was used to identify and assess risks and to apply appropriate mitigation. It began with a single page top level mission function block diagram (shown in Figure 8) that was adapted into a fault tree to show how the mission can fail to meet its mission success criteria. This fault tree was constantly updated during design.

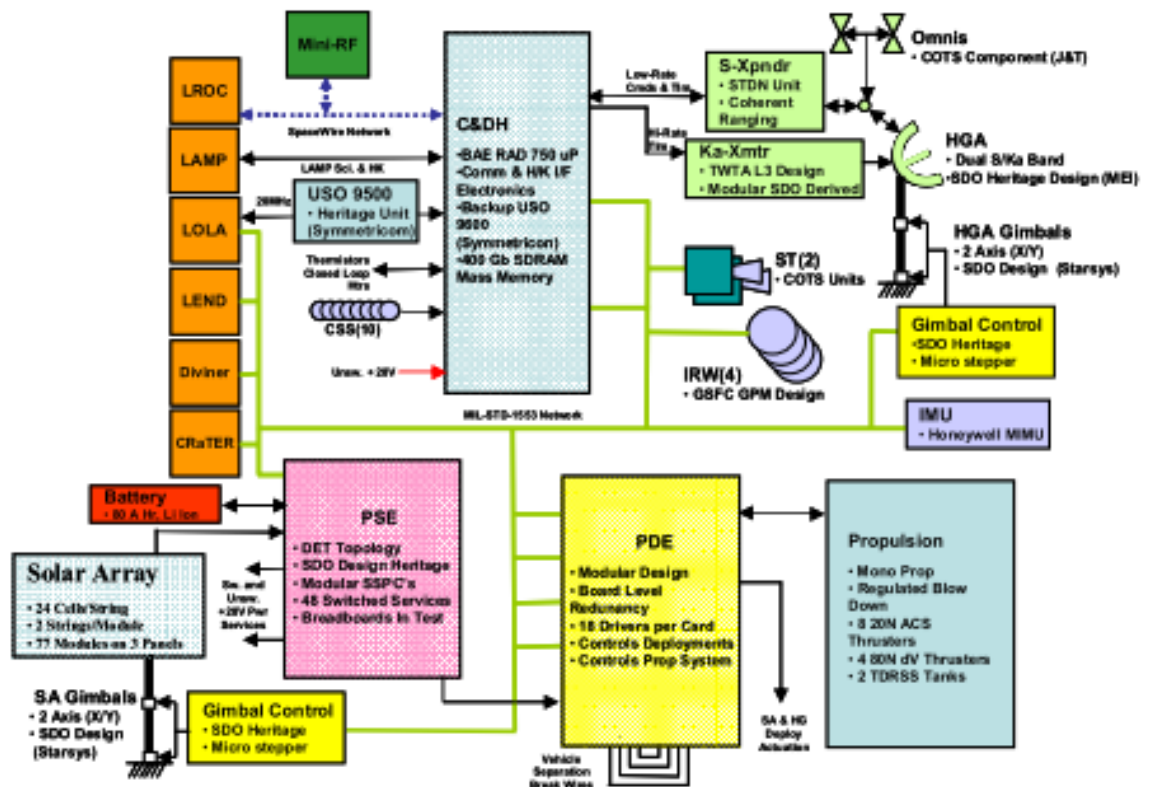


Figure 8 – Functional Block diagram showing how each component interacts with each other.

In total there were 159 critical/catastrophic failure modes identified, 13 with no compensating provisions. The top four with a reliability below 0.99 were deemed the main reliability driver and were heavily instrumented to be meticulously monitored. These are summarized in Table 2.

Subsystems	Reliability Drivers (Single Point Failures)	Reliability	Failure Modes	Mission Effects
GN&C	Gyro	0.97777	Loss of IMU output	Degraded ability to maintain attitude.
Communications	Transponder	0.98006	Loss of Telemetry, Tracking, and Control (TT&C) Transponder	Loss of mission.
C&DH	RAD 750 SBC	0.98784	Loss of processor functionality.	Loss of mission.
Power	PSE Monitor Card	0.98997	Loss of low voltage to PSE.	Loss of mission.

Table 4 – Summary of risk drivers for LRO system.

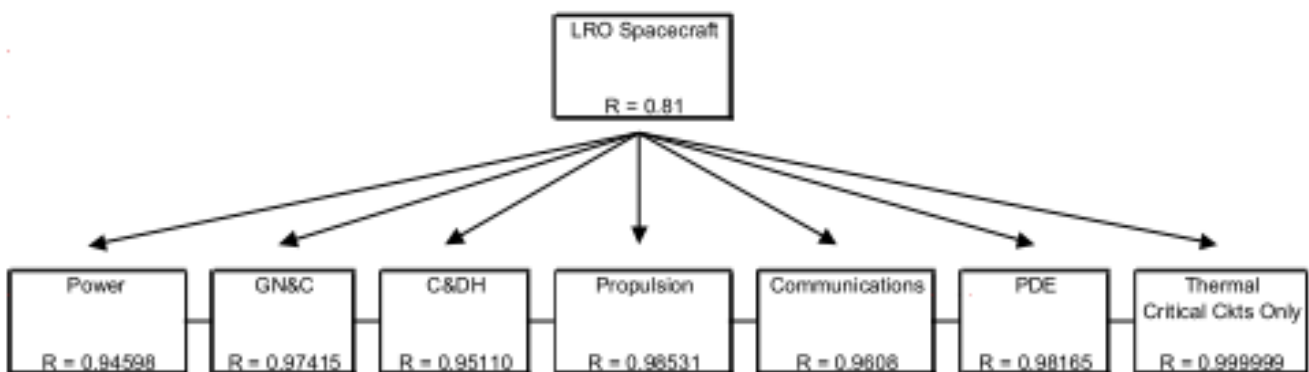


Figure 9 - The seven systems that made up the LRO Spacecraft had a reliability estimate assigned to them that collectively gave the Spacecraft a 81% chance of mission success.

Figure 9 illustrates the final failure probability of each respective sub systems. Power Systems were the least reliable and thermal systems were rated the best.

Discussion of Method

This illustrated the FMEA top down approach to estimate the overall reliability of an extremely complex system. Although the bottom up procedure would have been more accurate, top down was selected to save time and more importantly, money. This was a quick analysis and there were some very large assumptions made. No extra ordinary circumstances were considered. Mechanical systems were not considered in this investigation since the extensive testing of each and every component to levels well beyond that expected during flight meant that a mechanical reliability investigation was deemed unneeded. It is also worth noting that the majority of reliability data on the components were predominantly gathered from manufacturer's data. Due to the complexity of the system, it is likely that there is a lot of uncertainty associated with the final probability model.

METHOD SELECTION FROM REVIEW

It is apparent that the appropriate method selected is highly dependent on the system and the objectives of the project. The most beneficial outcome of a risk assessment would be to outline all possible failure modes and which of those modes are more susceptible to failure. Because the engine in the case study is not being mass produced and most of the components are either custom built or have been adapted straight from various sources, statistical data and distribution for individual components are not available. Therefore it is useless employing a complicated Monte Carlo or Fuzzy Theory analysis.

An AHP could be used but this early in the design phase, component alternatives are unknown. But since there is an existing prototype, the basic components and their functions are known so an in depth Bottom up investigation is possible.

The best data about failure frequencies of components can be estimated from components found in a typical internal combustion engine. A qualitative FMECA investigation is the most appropriate, using a risk matrix to rate and prioritize the risks. A fault probability tree will also be produced.

Risk Assessment Using FMECA

First, a system structure was devised, shown below in Figure 11 splitting the engine into 3 main subsystems, mechanical, external and electrical. External also covers inputs into the engine including fuel and air. Each branch shows each main component and sub component within that subsystem and the links indicate how each influences subsequent components. Each part was given a reference number for easy indication later in the investigation. Each box also shows the number components of that type are present where applicable.

Assumptions

Several assumptions are needed for the investigation

- The engine is expected to have a 10 year life cycle.
- All components operate at constant speed under constant load during lifetime.
- All components are assumed to run daily at 100% for the entire 10 year period.
- Failure rates are based on existing internal combustion engine component reliability estimates since there are no manufacturing data available.
- Only one failure mode exists at a time.
- Only direct connections between systems are considered. (ie. Electrical systems are assumed not to affect mechanical).
- That all parts were made to specification and flaws from manufacturing processes were neglected.

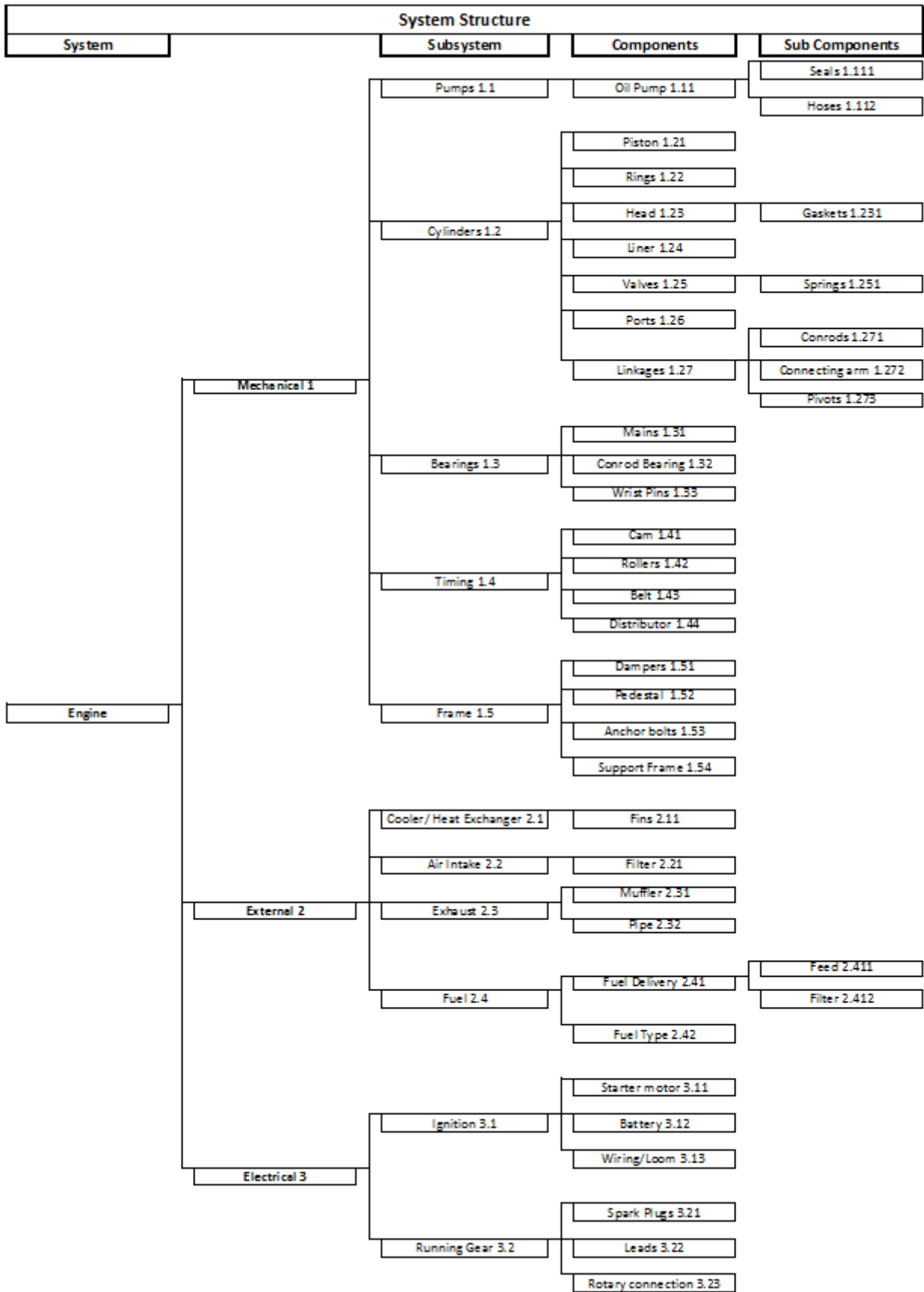


Figure 11 – System Structure and Parts Reference List

Next, each component was analyzed individually using a FMECA worksheet, defining its function, operational mode, possible failure modes, causes and failure detection methods. Their effects on the subsystem and the overall system were also considered. Finally failure rate, severity and possible failure mitigation procedures were suggested. Severity of failure was measured using a 1 -10 ranking system.

Rank	Severity Class	Description
10	Catastrophic	Failure results in complete engine failure, requiring entire engine replacement Possible damage to surroundings and personnel.
7 - 9	Critical	Failure results in a critical component failure, requiring expensive component replacements and engine rebuild. Large downtime.
4 - 6	Major	Failure results in moderate component damage, resulting in some downtime requiring minor repairs and part replacement.
1 - 3	Minor	Failure causes minor system damage and the engine to not function properly.

Table 5 – Severity Ranking System for Case Study

When evaluating the frequency of failure for each of the components a scale of 1 to 5 was given.

Rating	Description	Per Unit Comparison
1	Very unlikely	Once per 10000 units or more seldom
2	Remote	Once per 1000 units
3	Occasional	Once per 100 units
4	Probable	Once per 10 units
5	Frequent	Every Unit

Table 6 – Frequency Ranking System for Case Study

Per unit means that it is expected that one in that many units will fail if many were produced. This was based on typical component failures in traditional internal combustion engines. The simple scale of 1 to 5 was used since the uncertainty involved in the evaluation meant only low level resolution should be used.

For example, let's consider to failure modes. One is a fractured exhaust port that hot gases pass through. Because this has no moving parts and even though it is subject to high pressures and temperatures, it is a part of the block and is part of the head and is generally over engineered. Although they can be susceptible to wear from the valves, it is extremely uncommon for the port to crack, break or fracture under normal running conditions in an internal combustion engine. It is likely that only 1/10000 units or less should fail in this manner, which according to the scale in Table 4 corresponds to a frequency of 1. Alternatively, it is expected that during the engines 10 year life, it is likely that frame will fail at least 1 in 10 frames will need to be repaired, corresponding to a rating of 4.

The rating is very dependent on the component in question and some will sit between two rating levels, it becomes the designers discretion to decide how likely the component is to fail. An alternative scale that could be considered if the above scale is deemed inappropriate is how likely a failure is to occur during the engines life, 5 meaning the component will at some point need replaced during the engines 10 year life and 1 meaning that the part is not expected to fail at all.

Table 7 - Component and Sub Component Failure Modes

Description of Unit			Description of Failure			Effect of Failure		Risk Assessment		
Part. ref. no.	Function	Operational mode	Failure mode	Failure cause or mechanism	Detection of Failure	On the subsystem	On the system function	Failure rate	Severity ranking	Risk reducing measures
1	2	3	4	5	6	7	8	9	10	11
1.111 1.112	Lubrication	Running Not Running	Cracked,broken or fractured Corrosion	Pressure Environment	Oil P. Sensor or Inspection	Pump Failure	Major wear or failure of critical components	3 3	7 7	Monitor Pressure Sensor or Inspection
1.21	Absorbs force of fuel combustion	Running	Excessive Wear Cracked,broken or fractured	Improper Lubrication and Oil Degradation. Excessive Force Cyclic loading	Smoke Inspection Smoke Inspection Loud noise	Cylinder worn Cylinder Damage	Reduced performance Cylinder stops functioning	3 1	2 9	Inspection
1.22 1.23 1.231 1.24	Seals cylinder allowing power stroke	Running	Leaking Cracked,broken or fractured	Improper Lubrication and Oil Degradation. Excessive Force Cyclic loading	Smoke Inspection Smoke Inspection	Minimal Minimal	Reduced performance Cylinder stops functioning	2 3 3 2	1 4 4 1	Inspection
1.25 1.251	Controls intake and exhaust cycles	Running	Cracked,broken or fractured Excessive Wear Leaking	Improper Lubrication and Oil Degradation. Excessive Force Fatigue	Inspection Loud noise	Cylinder damage other components no longer function properly	System breaks down	1 1	9 8	Inspection
1.26	Let fuel and air mixture into cylinder	Running	Excessive Wear Cracked,broken or fractured	Improper Lubrication and Oil Degradation. Detonation	Premature detonation, smoke Premature detonation, smoke	Minimal damage Damage to other components	Reduced performance Severley reduced performance	3 1	4 7	Inspection
1.27 1.271 1.272 1.273	Activate rotation	Running	Cracked,broken or fractured	Excessive Force Cyclic loading Missalignment	Inspection Loud noise	No longer function	System breaks down	1 1 1 1	10 10 10 10	Inspection Vibrational test
1.31 1.32 1.33	Link motor to frame Link between conrod and cam roller Link between conrod and piston	Running	Cracked,broken or fractured	Improper Lubrication and Oil Degradation. Debris and excessive deposits	Inspection Loud noise	no longer function properly	Severley reduced performance	2	6	Inspection

1.41 1.42	Controls the stroke and timing within the cylinders also power and torque characteristics	Running	Cracked, broken or fractured Excessive Wear	Excessive Force Poor geometry	Inspection or changes in system performance	Timing changes, misfiring occurs	Gradual degradation in performance	4	5	Inspection
1.43	Controls valve operation	Running	Cracked, broken or fractured	Environment or external influence	Inspection or changes in system	Severe damage to other components	System breaks down	2	7	Inspection and periodic changing of part
1.44	Controls Ignition timing	Running	Excessive Wear	Environment or external influence	Performance change	Severe damage to other components	System breaks down	1	3	Inspection and timing gun
1.51 1.52 1.53 1.54	Supports engine and allows transmission of power	Running Not Running	 Corrosion	Cyclic loading Vibration from torsional and mechanical resonance Environment or external influence	Inspection	System instability	Potential system failure	4	5	Inspection
2.11	Keeps engine cool	Running	Cracked, broken or fractured	Overheat causes over expansion of critical metallic components Electrical system detrimentally affected	Temperature sensor in oil or with thermocouple	Severe Damage	Potential system failure	3	7	Monitor temperature sensor or inspection
2.21	Provides oxygen for combustion	Running	Cracked, broken or fractured Blocked	Environment or external influence	Air flow sensor or combustion fails	None	System Fails	1	1	Inspection Check sensor
2.31 2.32	Extracts hot combusted gases and reduces harmful noise	Running	Cracked, broken or fractured	Vibration Thermal cyclic loading Blockage	Inspection	Performance decrease, severe increase in noise	Performance may be reduced	3	4	Inspection
2.41 2.411 2.412	Delivers fuel to combustion chamber	Running	Cracked, broken or fractured Blocked Corrosion	Blockage Contamination Fuel or environment	Inspection	Minimal	System will run improperly or not at all	5	2	Inspection
2.42	Provides potential energy to system	Running	Combusted Incombustible	Premature explosion Contaminated	Visual signs of flame Engine fails to fire	Potential damage to components Components may need cleaning out	System may be damaged System will not run properly	2 4	9 2	Inspection

3.11	Starts motor	Running	Cracked, broken or fractured	Excessive wear	Whether it is able to rotate motor at sufficient torque for startup	Will not start	Will not start	1	2	Inspection
3.12	Provides chemical charge to power ignition	Running	Cracked, broken or fractured Worn out	Environment Reaction no longer sufficient to current	Voltmeter	Electrical components will not function	System fails	4	1	Voltmeter
3.13	Connects electrical components	Running	Cracked, broken or fractured	External or environmental influence or heat	Multimedia and check electrical responses	Electrical components will not function	System may not function correctly	4	1	Multimedia
3.21	Provides spark for ignition	Running	Don't spark	Carbon layer build up Deformed and require replacement	Inspection	Combustion fails to occur	System will not run properly	3	2	Inspection
3.22	Transports electrical charge to spark plugs	Running	Resistance too great	Heat and age causes increase in resistance restricting voltage delivery to spark plugs	Multimeter	Combustion fails to occur	System will not run properly	3	2	Inspection
3.23	Transports electrical charge from stationary point to rotating engine	Running	Connection worn	No longer transmits electrical current	System stops firing Multimeter	Electrical components will not function properly	System will not run properly or not at all	3	2	Inspection of connection Multimeter

Now that all failure modes have been evaluated, each mode requires further analysis and a reference for each failure is given in Table 8. A RPN number (risk x severity) has also been incorporated, neglecting the level of detection factor. This has been displayed a percentage, 100% being the highest risk. This percentage proved useful in defining the risk matrix. Failure rate was converted into an approximate reliability on any given day over the 10 year lifetime also by:

$$\text{Chance of failure} = 1 / (\text{Total Days} \times \text{Failure Rate}) \quad \text{and} \quad \text{Reliability Probability} = 1 - \text{Chance of Failure}$$

Rating	Chance of failure Mode Under normal conditions	Reliability Probability
1	2.73973E-06	0.99999726
2	2.73973E-05	0.99997260
3	0.000273973	0.99972603
4	0.002739726	0.99726027
5	0.032876712	0.96712329

Table 8 – Component Reliability

Table 8 - Failure Mode Analysis							
Fault Ref.	Failure	Part Ref. no.	Failure mode	Failure rate	Severity ranking	Risk Rate x Severity	Chance of Failure under normal running conditions
1.a 1.b	Seal Failure Hose Failure	1.111 1.112	Cracked,broken or fractured	3 3	7 7	42% 42%	0.9997260274 0.9997260274
1.c	Worn Piston	1.21	Excessive Wear	3	2	12%	0.9997260274
1.d	Broken Piston	1.21	Cracked,broken	1	9	18%	0.9999972603
1.e 1.f 1.g 1.h	Leaking Rings Leaking Head Leaking Gasket Leaking Liner	1.22 1.23 1.231 1.24	Leaking	2 3 3 2	1 4 4 1	4% 24% 24% 4%	0.9999726027 0.9997260274 0.9997260274 0.9999726027
1.i 1.j 1.k 1.l	Damaged Rings Damaged Head Damaged Gasket Damaged Liner	1.22 1.23 1.231 1.24	Cracked,broken or fractured	2 3 3 2	1 4 4 1	4% 24% 24% 4%	0.9999726027 0.9997260274 0.9997260274 0.9999726027
1.m 1.n	Faulty Valve Faulty Springs	1.25 1.251	Cracked,broken or fractured Leaking Excessive Wear	1 1	9 8	18% 16%	0.9999972603 0.9999972603
1.o	Worn Port	1.26	Excessive Wear	3	4	24%	0.9997260274
1.p	Damaged Port	1.26	Cracked,broken or fractured	1	7	14%	0.9999972603
1.q 1.r 1.s 1.t	Damaged Linkage Damaged Conrods Damaged Connecting arm Damaged Pivots	1.27 1.271 1.272 1.273	Cracked,broken or fractured	1 1 1 1	10 10 10 10	20% 20% 20% 20%	0.9999972603 0.9999972603 0.9999972603 0.9999972603
1.u 1.v 1.w	Damaged Main Bearing Damaged Conrod Bearing Damaged Wrist Pins	1.31 1.32 1.33	Cracked,broken or fractured	2	6	24%	0.9999726027
1.x 1.y	Damaged Cam Damaged Rollers	1.41 1.42	Cracked,broken or fractured Excessive Wear	4	5	40%	0.9972602740
1.z	Damaged Belt	1.43	Cracked,broken or fractured	2	7	28%	0.9999726027

2.a	Worn distributor needle	1.44	Excessive Wear	1	3	6%	0.9999972603
2.b 2.c 2.d 2.e	Failed Dampers Damaged Pedestal Damaged Anchor bolts Rusted Frame	1.51 1.52 1.53 1.54	Corrosion	4	5	40%	0.9972602740
2.f	Damaged Fins	2.11	Cracked,broken or fractured	3	7	42%	0.9997260274
2.g	Faulty filter	2.21	Cracked,broken or fractured Blocked	1	1	2%	0.9999972603
2.h 2.i	Faulty Muffler Cracked pipe	2.31 2.32	Cracked,broken or fractured	3	4	24%	0.9997260274
2.j 2.k 2.l	Fuel delivery problem Feed failure Faulty fuel filter	2.41 2.411 2.412	Cracked,broken or fractured Corrosion Blocked	5	2	20%	0.9671232877
2.m	Fuel explosion	2.42	Combusted	2	9	36%	0.9999726027
2.n	Contaminated fuel	2.42	Incombustible	4	2	16%	0.9972602740
2.o	Faulty starter motor	3.11	Cracked,broken or fractured	1	2	4%	0.9999972603
2.p	Dead battery	3.12	Cracked,broken or fractured Worn out	4	1	8%	0.9972602740
2.q	Wires damaged	3.13	Cracked,broken or fractured	4	1	8%	0.9972602740
2.r	Faulty spark plug	3.21	Don't spark	3	2	12%	0.9997260274
2.s	Worn out carbon leads	3.22	Resistance too great	3	2	12%	0.9997260274
2.t	Worn connection	3.23	Connection worn	3	2	12%	0.9997260274

Now that all fault modes have been identified and categorized, the system and its subsystems relative reliability can be estimated using a probability tree. The reliability probability of each component is multiplied by the amount of components and the probability of other failure modes to define the overall probability of that component.

Finally, each failure mode can be placed on the failure matrix. Using the Risk x severity RPN rating, I created the risk based on these percentages. Anything above 50% was deemed unacceptable (red) and below 20% risk was deemed acceptable. The corresponding RPN percentage can be seen on Figure 12 and the final risk matrix categorizing the failure modes can be seen on Figure 13.

Risk Matrix					
Frequency/ consequence	1 Very Unlikely	2 Remote	3 Occasional	4 Probable	5 Frequent
Catastrophic 9 to 10	20%	40%	60%	80%	100%
Critical 7 to 8	16%	32%	48%	64%	80%
Major 5 to 6	12%	24%	36%	48%	60%
Moderate 3 to 4	8%	16%	24%	32%	40%
Minor 1 to 2	1%	8%	12%	16%	20%

Figure 13 – Risk Matrix showing approximate RPN %










Risk Matrix											
Frequency/ consequence	1 Very Unlikely	2 Remote	3 Occasional	4 Probable	5 Frequent						
Catastrophic 9 to 10	1.d , 1.l , 1.m , 1.p 1.s , 1.q , 1.r	2.m									
Critical 7 to 8	1.p , 1.n	1.z	1.a , 1.b , 2.f								
Major 5 to 6		1.u , 1.v , 1.w		1.x , 1.y , 2.b 2.c , 2.d , 2.e							
Moderate 3 to 4	2.a		1.f , 1.g , 1.i , 1.j 1.o , 2.i , 2.h								
Minor 1 to 2	2.g , 2.o	1.e , 1.h , 1.i , 1.l	1.c , 2.r , 2.s , 2.t	2.p , 2.q , 2.n	2.j , 2.k , 2.l						
<table border="0"> <tr> <td></td> <td>Acceptable</td> </tr> <tr> <td></td> <td>Acceptable but consider further investigations</td> </tr> <tr> <td></td> <td>Unacceptable - risk reducing measures required</td> </tr> </table>							Acceptable		Acceptable but consider further investigations		Unacceptable - risk reducing measures required
	Acceptable										
	Acceptable but consider further investigations										
	Unacceptable - risk reducing measures required										

Figure 14 – Risk Matrix Categorizing Failure Modes for Case Study

DISCUSSION

It was found that if correct procedures are followed during design and manufacture, there are no serious risks of compromising the project. Although there are some priority risks, particularly in the 48% boxes, this indicates that careful consideration should be made to these components during design. The main reliability drivers that were identified during the case study were:

- The cam and rollers.
- The frame and supports of the engine.
- The air cooling system.
- Seals and hoses.

Fuel explosion was also had a large risk associated to it, mainly because of the large consequence in the event of this failure mode. When considering Figure 12, it can be seen that the external subsystem is more susceptible to failure, predominantly because of fuel problems as can be seen by the failure probability. The main contributor to mechanical system failure was due to the frame and electrical seemed the most reliable. This shows that it is beneficial to have both the fault tree to trace sources of failure as well as use of a risk matrix to prioritize individual failure modes.

REFERENCES

- System Reliability Theory (2nd ed), Wiley, 2004; Failure Mode & Effects Critical Analysis Marvin Rausand Department of Production and Quality Engineering Norwegian University of Science and Technology
- GU14,0LX, UK. Risk Assessment Method for Fracture of Critical Components
- A.D. Boyd-Lee and D.P. Shepherd Structures and Materials Centre, QinetiQ, Farnborough, Hants
- Design Review Based on Failure Mode <http://www.quality-one.com/services/fmea.php>
- Practical Application of Design Risk Assessment Models, R Crossland, J Sims Williams and C McMahan <http://pib.safepub.com/content/217/2/227>
- 2002 Nasa Faculty Fellowship Program, Marshall Space Flight Center, Independent Review of the Failure Mode of the F1 engine and Propellant System Associate Professor Paul Ray
- IT3C 0J7, Beta Machinery Analysis Independent Engine Reliability Maintenance, J.W.S. Grose, E.I.T., Calgary, AB, Canada
- Proceedings of the Institute of Mechanical Engineers, Part B: Journal of Engineering Manufacture 2006
- Relative Reliability Risk Assessment to Original Designs at Concept Stage & AHP, G Mamtani, G Green, SMcDonald
<http://pib.safepub.com/content/220/6/917>

- Probabilistic Risk Assessment Approach; A Practical and Cost Effective Approach, Lydia Lam Lee, NASA Goddard Space Flight Center, Antonino J. Ingegneri, SRS Technologies
- Dr. Ming Li, SRS Technologies, David F. Everett, NASA Goddard Space Flight Center
- Managing Risk and Reliability Fourth Edition 2011, Dirk Pons PhD CPEng MIPENZ MPMI, AS/NZS ISO 31000:2009 Standard of Risk Management
- Pinto Madness by Mark Dowie, Mother Jones Magazine, 1977
- <http://www.motherjones.com/news/feature/1977/09/dowie.html>
- Engine Fleet Reliability Data Management Optimization John R. Gebhard, Systems Engineer, Rolls-Royce Corporation.

